AD-A220 775

AFWAL-TR-89-4001

THERMAL ANALYSIS OF ACETYLENE TERMINATED SULFONE (ATS) RESIN

W. T. K. Stevenson
I. J. Goldfarb
E. J. Soloski

Polymer Branch
Nonmetallic Division

18 January 1990

Final Report for Period January 1981 to June 1983

Approved for public release; distribution unlimited

MATERIALS LABORATORY
WRIGHT RESEARCH AND DEVELOPMENT CENTER
AIR FORCE SYSTEMS COMMAND
WRIGHT-PATTERSON AIR FORCE BASE, OHIO 45433-6533

NOTICE

WHEN GOVERNMENT DRAWINGS, SPECIFICATIONS, OR OTHER DATA ARE USED FOR ANY PURPOSE OTHER THAN IN CONNECTION WITH A DEFINITELY GOVERNMENT-RELATED PROCUREMENT, THE UNITED STATES GOVERNMENT INCURS NO RESPONSIBILITY OR ANY OBLIGATION WHATSOEVER. THE FACT THAT THE GOVERNMENT MAY HAVE FORMULATED OR IN ANY WAY SUPPLIED THE SAID DRAWINGS, SPECIFICATIONS, OR OTHER DATA, IS NOT TO BE REGARDED BY IMPLICATION, OR OTHERWISE IN any MANNER CONSTRUED, AS LICENSING THE HOLDER, OR ANY OTHER PERSON OR CORPORATION; OR AS CONVEYING ANY RIGHTS OR PERMISSION TO MANUFACTURE, USE, OR SELL ANY PATENTED INVENTION THAT MAY IN ANY WAY BE RELATED THERETO.

THIS REPORT HAS BEEN REVIEWED BY THE OFFICE OF PUBLIC AFFAIRS (ASD/PA) AND IS RELEASABLE TO THE NATIONAL TECHNICAL INFORMATION SERVICE (NTIS). AT NTIS, IT WILL BE AVAILABLE TO THE GENERAL PUBLIC INCLUDING FOREIGN NATIONS.

THIS TECHNICAL REPORT HAS BEEN REVIEWED AND IS APPROVED FOR PUBLICATION.

R. C. EVERS
Polymer Branch
Nonmetallic Materials Division

T. E. HELMINIAK, Chief
Polymer Branch
Nonmetallic Materials Divison

FOR THE COMMANDER

MERRILL L. MINGES, Director
Nonmetallic Materials Divison

If your address has changed, if you wish to be removed from our mailing list, or if the addressee is no longer employed by your organization, please notify WRDC/MLBP, Wright-Patterson AFB, OH 45433-6533 to help us maintain a current mailing list.

Copies of this report should not be returned unless return is required by security considerations, contractual obligations, or notice on a specific document.

REPORT DOCUMENTATION PAGE

Form Approved
OMB No. 0704-0188

1a. REPORT SECURITY CLASSIFICATION Unclassified	1b. RESTRICTIVE MARKINGS
2a. SECURITY CLASSIFICATION AUTHORITY	3. DISTRIBUTION/AVAILABILITY OF REPORT Approved for public release; distribution unlimited
2b. DECLASSIFICATION/DOWNGRADING SCHEDULE	
4. PERFORMING ORGANIZATION REPORT NUMBER(S) AFWAL-TR-89-4001	5. MONITORING ORGANIZATION REPORT NUMBER(S)
6a. NAME OF PERFORMING ORGANIZATION Materials Lab, WRDC, AFSC 6b. OFFICE SYMBOL (If applicable) WRDC/MLBP	7a. NAME OF MONITORING ORGANIZATION
6c. ADDRESS (City, State, and ZIP Code) Wright-Patterson Air Force Base, Ohio 45433-6533	7b. ADDRESS (City, State, and ZIP Code)
8a. NAME OF FUNDING/SPONSORING ORGANIZATION same as 6a 8b. OFFICE SYMBOL (If applicable)	9. PROCUREMENT INSTRUMENT IDENTIFICATION NUMBER
8c. ADDRESS (City, State, and ZIP Code)	10. SOURCE OF FUNDING NUMBERS PROGRAM ELEMENT NO. 61102F; PROJECT NO. 2303; TASK NO Q3; WORK UNIT ACCESSION NO. 07

11. TITLE (Include Security Classification)

Thermal Analysis of Acetylene Terminated Sulfone (ATS) Resin

12. PERSONAL AUTHOR(S)

W.T.K. Stevenson, I.J. Goldfarb, E.J. Soloski

13a. TYPE OF REPORT	13b. TIME COVERED	14. DATE OF REPORT (Year, Month, Day)	15. PAGE COUNT
Final	FROM Jan 81 TO Jun 83	1990 February	231

16. SUPPLEMENTARY NOTATION

Resins, Thermal Analysis, Degradation

17 COSATI CODES		
FIELD	GROUP	SUB-GROUP
07	04	
11	04	

18. SUBJECT TERMS (Continue on reverse if necessary and identify by block number)

Polymers, Resins, Thermal Analysis, Degradation

19. ABSTRACT (Continue on reverse if necessary and identify by block number)

A number of new thermo-analytical techniques for the elucidation of kinetic and mechanistic aspects of the decomposition of thermally stable polymers under high vacuum conditions are described herein, with particular reference to their use in conjunction with more conventional techniques of organic structural analysis to gain a more comprehensive insight into the degradation process. In addition to general procedures, some approaches geared specifically to the thermal analysis of acetylene terminated sulfone (ATS) resins are also detailed. These techniques are applied to a study of ATS resin prepared for the Air Force by Gulf Chemicals, Inc., (ATS-G). A compositional analysis of volatiles "flashed" from thin films of ATS-G prepolymer is used to assess the purity of the feedstock used to prepare ATS-G, and to propose the existance of some preparative side reactions. A brief description of the cure process of ATS-G is followed by a more complete study of the post cure step and its overlap with low temperature degradations in the polymer. Finally, a fairly comprehensive mechanisms of accelerated high temperature thermal degradation of ATS-G and its component fractions,

20. DISTRIBUTION/AVAILABILITY OF ABSTRACT	21. ABSTRACT SECURITY CLASSIFICATION
☒ UNCLASSIFIED/UNLIMITED ☐ SAME AS RPT ☐ DTIC USERS	Unclassified
22a. NAME OF RESPONSIBLE INDIVIDUAL R. C. Evers	22b. TELEPHONE (Include Area Code) 513-255-9161 22c. OFFICE SYMBOL WRDC/MLBP

19. with particular reference to the influence of the sulfone linkage as a (relatively) unstable thermal weak link, and the polyene crosslink (or its thermal derivative) on the weight loss processes operative within the basic polyphenylether constituent of the polymer.

ACKNOWLEDGEMENTS

The authors would like to thank Mr J. Henes for his technical help and Mr R. Grant who fabricated most of the free-standing glassware described here. In addition, W. T. K. Stevenson would like to thank the National Research Council for its support in the provision of a Research Associateship for him at WPAFB.

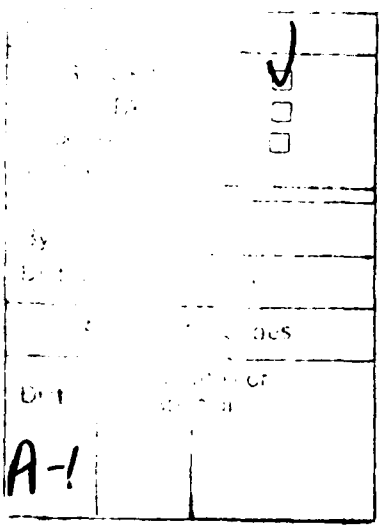

TABLE OF CONTENTS

LIST OF FIGURES

LIST OF TABLES

PART A

TECHNIQUES OF ANALYSIS

SECTION A.I

INTRODUCTION

The thermal degradation reactions of most polymers are complex in nature, with the result that their interpretation is often difficult and time consuming. The situation has been somewhat alleviated in recent years by the use of "on line" devices such as mass spectrometers and Fourier Transform Infrared spectrometers, often used in tandem with thermogravimetric analyzers to monitor the volatile flux or eluent mixture release from a polymer when it is heated in the absence of oxygen, usually under programmed conditions. Such devices, if used within their limitations, can, in a short space of time, generate useful information of a qualitative nature of the identification of potentially hazardous products of degradation or a comparison of polymer stability.

A better but more time consuming approach would be to employ a range of analytical techniques chosen for their complimentary nature and applicability to the system under study. In Part A of this study we describe some techniques of analysis which were developed to study thermal degradation processes in thermally stable polymers. Some of these techniques are applicable to the study of polymeric systems in general, while others, developed specifically for the study of acetylene terminated resins, may not be applicable elsewhere.

SECTION A.II

Thermal Volatilization Analysis (TVA)

(1). Products of Polymer Thermal Degradation

Polymeric materials, when subjected to thermal stress in the form of programmed heating under high vacuum conditions, are degraded by processes, the rates and mechanisms of which are structurally dependent. The products of polymer degradation may be grouped into four "fractions" depending upon their volatility.

The noncondensable volatile product fraction of degradation

This fraction is volatile at -196°C at pressures of up to a few torr in a high vacuum system. It may contain any of the permanent gases, for example, hydrogen, carbon monoxide, nitrogen, oxygen and methane.

The condensable volatile product fraction of degradation

This product fraction is composed of material which is volatile at room temperature and involatile at -196°C in a high vacuum manifold. It is usually composed of material of molecular weight up to (100-150) a. m. u.

The oligomeric (or "cold ring") product fraction of degradation

This fraction is composed of material in the molecular weight range (150-800) a. m. u. It is volatile at elevated temperatures such as would be encountered in a degradation assembly, but involatile at room temperature in a high vacuum manifold. As such, it usually condenses onto the degradation assembly immediately above the hot zone, hence the trivial label "cold ring fraction."

The residue of degradation

This product fraction is composed of material which is involatile at degradation temperatures and therefore remains in the oven assembly. It is often high in carbon content, heavily crosslinked, and"cnarred" - especially if the polymer was exposed to high temperatures during the degradation experiment.

For a proper mechanistic description of polymer degradation pathways it is essential that the complete product distribution of the polymer be elucidated. To do so, we must devise a (preferably

simple) method for product isolation and manipulation. To this end, we next discuss the Thermal Volatilization Analysis Experiment.

(2). The Basic Thermal Volatilization Analysis (TVA) Experiment

Consider a material in a container situated within an oven and connected to a high vacuum pumping system. As the oven warms, the material decomposes to produce the four product fractions of thermal degradation. If a Pirani (or other electronic pressure gauge) is placed between the oven and the pumping system it will measure a pressure, the magnitude of which is a balance between the rate of production and removal of condensable and noncondensable volatile products of degradation. This continuous pressure measurement forms the basis of the Thermal Volatilization Analysis or TVA experiment. If all TVA experiments are performed under the same conditions, the Pirani response can be used as a measure of the rate of volatile production in a material exposed to high oven temperatures. The nonlinearity of the Pirani response enables the technique to follow reactions which produce only small quantities of volatile material (<<1% of sample weight); processes often invisible to conventional thermogravimetric analysis (TGA). On the other hand, a Pirani gauge, situated between the oven and pumps, is sensitive only to those products which are volatile at room temperature under high vacuum conditions. It cannot, therefore, detect high molecular weight or oligomeric products readily detectable by TGA. The TVA and TGA experiments are, therefore, complimentary in this respect and often yield valuable information when used in tandem.

In the basic TVA experiment, Pirani output and sample temperature are recorded simultaneously to produce a trace which reproducibly depicts the onset temperatures, rate profiles, and rate maxima of those thermal processes which produce condensable and noncondensable products of polymer degradation[1].

(3). Differential Condensation TVA

In the differential condensation TVA experiment (Figure 1), a Pirani gauge (P1) is used to measure the volatile flux from the degrading polymer before it is forced through a cold trap held at a predetermined sub-ambient temperature. A second Pirani gauge (P2) is used to measure that portion of the gaseous flux which is volatile at the trap temperature. Differences between the two readings can often be used to completely or partially elucidate the nature of the gas flux.

The experiment is best illustrated by considering a single component gas flux, for example that of styrene from polystyrene or methylmethacrylate from polymethylmethacrylate (Figure 2). If the differential condensation TVA experiment is conducted using a trap

held at 0°C or -45°C, curve (i) is observed for both polymers. If the trap is held at -75°C, curve (ii) is observed for both polymers. This "limiting rate effect" is produced when the product of degradation is partially condensed in the cold trap and removed thereafter at a rate which is dependent upon its volatility at the trap temperature. The pressure (P_L) is characteristic of the material and reproducible within a given degradation assembly. If the trap is held at -100°C or -196°C, curve (iii) is produced as both styrene and methylmethacrylate are involatile at these temperatures.

Most polymers produce a mixture of volatile products when degraded under programmed conditions, with the result that a complete interpretation of the nature of the volatile flux cannot be made from the differential condensation TVA trace. A comparison of the two Pirani outputs is, however, usually sufficient to separate and identify processes of degradation, their rate/temperature profiles and volatility range of their associated products. In the TVA experiment devised by McNeill and co-workers, this problem was partially surmounted by forcing the gas stream through four parallel conduits each with a sub-ambient trap at a different temperature. By recording on one trace all Pirani gauge outputs a more detailed picture of the degradation process could be painted[2]. McNeill's approach is followed here.

SECTION A.III

Sub-Ambient Thermal Volatilization Analysis (SATVA)

In the basic SATVA experiment a glass "cold finger" is immersed in p-xylene which is contained in a pyrex flask. The assembly is cooled to -196°C and a mixture of condensable volatiles, usually produced in the TVA experiment, is transferred to the cold zone by close system distillation. The assembly is opened to the pumping system through a receiving trap also held at -196°C, and allowed to warm slowly to room temperature. The SATVA trap temperature and adjacent Pirani gauge output are recorded simultaneously as components of the mixture are evolved to the receiving trap according to their volatility[3]. The SATVA experiment may be considered as similar to programmed gas liquid chromatography of GLC, except that the mixture is separated purely on a basis of volatility with no interaction between the mixture and substrate (the glass tube).

A closed system distillation of an involatile liquid such as p-chloro styrene to the SATVA "cold finger" is a time consuming process even under high vacuum conditions. To alleviate this problem, the SATVA "cold finger" was replaced by a "U" tube which could be charged by through pumping.

P-xylene exhibits a heating and cooling discontinuity at its melting point of 7°C, with the result that involatile components of a condensable volatile mixture are often poorly resolved by the basic SATVA experiment. In addition, evaporation of p-xylene from the jacketing flask between experiments often changed warmup profiles, with the result that comparisons between SATVA curves were sometimes difficult. Both problems were solved by using high melting point paraffin wax ("canning wax") as a substitute jacketing material.

The SATVA trap constructed for this work is shown in Figure 3. Some SATVA curves are illustrated in Figure 4 to show how the warmup profile of the SATVA trap can be modified to effect a good separation of involatile liquids, volatile liquids, and condensable gases of similar volatility. A typical SATVA separation is illustrated in Figure 5. Materials evolved from the SATVA trap are subsequently expanded into a fractionating grid (Figure 6) where up to five individual components can be isolated for subsequent examination by the most appropriate ancillary techniques of analysis.

SECTION A.IV

Adsorption TVA (ATVA)

It has been known for some time that synthetic zeolites, at subambient temperatures, are able to concentrate noncondensable gases under equilibrium conditions[4], and pump noncondensable gases under nonequilibrium conditions[5]. In fact, zeolites now form the basis of a number of commercial "clean" high vacuum systems. The ATVA experiment makes use of synthetic zeolites to selectively adsorb, concentrate, and manipulate small quantities of noncondensable gas in a high vacuum manifold without the complications associated with the use of a Toepler pump, and with a higher efficiency (approaching 99%) for product transferal. Mention of this technique is made elsewhere[6,7].

In the ATVA experiment, Pirani pressure gauges are placed before and after a preactivated 5Å molecular sieve trap situated between the oven and pumping assemblies. A noncondensable gas flux from the oven is first freed of condensable impurities by passage through a liquid nitrogen trap then directed through the sieve containing trap held at -196°C. Differences in the Pirani recorder outputs are interpreted to elucidate the composition of the gas flux[7]. It was found that noncondensable gases are adsorbed with increasing efficiency in the order $H_2 << O_2 < N_2 << CH_4 < CO$. Under the conditions of the ATVA experiment, CH_4 and CO are efficiently adsorbed by the sieve trap unlike H_2 which is not adsorbed to any extent. At

the end of the experiment, condensed material can be evolved by warming the sieve trap to room temperature, and transferred quantitatively to a molecular sieve trap containing infrared gas cell for spectroscopic analysis. The ATVA assembly constructed for this work is shown in Figure 7.

SECTION A.V

Combined TVA/ATVA (CATVA) Experiment

The TVA[2] and ATVA[7] experiments were combined in an experiment able to quantitatively analyze both the condensable and noncondensable product fractions of polymer thermal degradation (Figure 8). Briefly, the sample to be degraded is placed in the oven assembly which is evacuated and heated under programmed conditions to degradation temperatures. The total volatile flux from the sample is recorded by the Pirani gauge 1. Pirani gauge 2 measures that portion of the flux which is volatile at -75°C under high vacuum conditions. Differences in the two outputs may be related to the quantity of involatile liquid in the gas mixture. Pirani gauge 3 is used to measure that portion of the gas flux which is volatile at -196°C. Differences in output between Pirani gauges 2 and 3 may be related to the quantity of volatile liquid and condensable gas (C_2H_{2-6}, CO_2, etc.) in the product mixture. Differences in output between Pirani gauges 3 and 4 may be related to the quantity of (usually) carbon monoxide and/or methane in the gas flux while that recorded by gauge 4 provides a measure of hydrogen as a degradation product. The output from a typical CATVA experiment is shown in Figure 9. Note the small sample size (which can be reduced by an order of magnitude without sacrificing any information). At a glance, we can see that this resin evolves some solvent during cure and thereafter degrades, under programmed conditions, by a three step process. The first product fraction consists mainly of condensable volatile material, and the second and third product fractions, of noncondensable volatiles. A more complete description of these processes is made later in the text.

SECTION A.VI

Instrumentation for the Combined TVA/ATVA (CATVA) Experiment

Four Edwards™ PR10-C Pirani gauge heads, powered by two Edwards™ Pirani 11 gauges, were connected to pen 2 of a Linear Instruments™

model 585, two pen flat bed recorder, via a Dataplex^{tm} 10 signal switching clock. Pen 1 of the recorder was connected to the oven thermocouple to achieve a system able to record simultaneously oven temperatures and Pirani outputs over the complete range of the CATVA experiment.

(1). Pirani Gauge Alignment

The vacuum assembly was pumped to about 10^{-4} torr, as measured by a swivel McCloud gauge, and each Pirani gauge head "set vac" variable resistor adjusted to achieve a recorder output of 0mv. The manifold was opened to the atmosphere and each individual Pirani gauge head output adjusted to 10mv using the gauge head "set atmos" variable resistor. A range of intermediate pressures was achieved by pumping on the system then isolating the manifold. Each time the "set atmos" resistor was incremented to achieve reasonable coincidence over the complete pressure range.

(2). Coincidence Check

As expected, the pressure registered by a Pirani gauge is inversely proportional (nonlinearly) to its distance from the volatile source or oven assembly. As such, even if no material is condensed in the trapping system, the pressure registered by Pirani gauge 1 will always be greater than that registered by Pirani gauge 2, and so on. An approximate relationship between the pressures registered by Pirani gauges 1, 2, 3, and 4 for the degradation experiment is shown in Figure 10. It will be shown that ATS polymers produce only noncondensable products of degradation above 750°C. The relationship between gauges 1, 2, and 3 was, therefore, directly accessible from the CATVA experiment. The relationship between gauges 3 and 4 was obtained by monitoring a hydrogen flux produced by the thermal decomposition of calcium hydride. This relationship is somewhat arbitrary due to the large physical gas "hold up" effect engendered by the molecular sieve trap[7], and should be used on a qualitative basis only.

SECTION A.VII

Degradation Vacuum Manifold

A vacuum manifold of minimum complexity, able to combine the CATVA and SATVA experiments was designed and built (Figure 11). Its use is detailed below. The "gas manipulation manifold" mentioned in Figure 11 consisted of a mercury manometer for pressure measurement, two gas storage bulbs, and a port for the connection of such as an

Infrared gas cell. The "oxidation assembly" mentioned also in the figure will be discussed in a forthcoming publication.

(1). The CATVA Experiment

The bypass manifold or "line" is isolated and volatiles from the oven are forced through the main manifold, through traps T_1, T_2, and "A", and past Pirani gauges 1, 2, 3, and 4 to effect the CATVA experiment. At the end of the experiment, noncondensable material is evolved from the ATVA trap ("A") and transferred to the Infrared gas cell depicted in Figure 7 for spectroscopic examination.

(2). The SATVA Experiment

At the end of the CATVA experiment the SATVA trap ("S") is cooled to -196°C, traps T_1 and T_2 are warmed to room temperature, and the condensable volatile product fraction pumped into "S". Trap S is then warmed to room temperature and evolved material is monitored by Pirani gauge 3 as it is back pumped through the bypass manifold and trapped in the fractionating manifold for subsequent analysis. Multiple SATVA experiments were performed by trapping "packets" of condensable volatile material, produced in the CATVA experiment, in the fractionating grid (up to four at a time), transferring them individually to, and volatilizing them from the SATVA trap as required.

SECTION A.VIII

Oven Assembly

The basic TVA oven head assembly consists of a flat bottomed Pyrex degradation tube which is charged with a polymer sample in the form of a solvent cast film or a fine powder. The degradation tube is placed in a modified programmable GLC oven, and connected to a vacuum manifold by a glass oven head adaptor, protected from oven heat by a glass water cooled "cold ring." This type of assembly possesses a maximum use temperature of 500°C[8].

The basic oven assembly was modified here to raise its maximum use temperature to 1000°C, that it may be used to study high temperature materials. This assembly is shown in schematic form in Figure 12. Samples for analysis are weighed into the quartz crucible which is then placed in the quartz degradation tube. The tube is lowered into a Marshal™ 2000F programmable tubular muffle furnace and connected to the vacuum manifold by an oven head adaptor protected from oven heat by water cooled copper cooling coils. The degradation

experiment was conducted isothermally at any temperature below 1000°C, or under programmed conditions to 1000°C at a nominal heating rate of 5°C/min.

At the end of the experiment the residue of degradation was estimated gravimetrically and removed from the crucible for chemical and spectroscopic analysis. The oligomeric product fraction of degradation was then removed from the internal cold finger and treated in a similar manner.

(1). Oven Calibration

(i) Under programmed conditions

The oven head assembly internal cold finger was removed and replaced with the oven calibration assembly (see Figure 12). The oven thermocouple was connected to pen 1 of the two pen strip chart recorder as before and the calibration thermocouple connected to pen 2 of the same recorder. The degradation tube was positioned 20cm into the muffle furnace which as usual was sealed top and bottom with sliding plates of furnace cement. The tube was then connected through the oven head adaptor to the TVA manifold and pumped to a rough vacuum. The whole assembly was then heated to 1000°C at a nominal heating rate of 5°C/min to obtain the plot of oven vs sample temperature shown in Figure 13. From this chart, "true" sample temperatures could be calculated for any "oven temperature" as recorded in the CATVA experiment.

(ii) Under isothermal conditions

The oven head assembly described in Section (i) above was placed in the furnace, warmed to a predetermined temperature, and held there for at least 30 min to establish thermal equilibrium. The oven and sample temperatures were then recorded. The isothermal calibration curve for the oven in the temperature interval (310-380)°C, of particular importance to this work, is shown in Figure 14. The high thermal inertia of the Marshal™ 2000F muffle furnace made it an ideal tool for isothermal work. For example, fluctuations of less than ± 5°C at a sample temperature of 328°C were detected over a 10.5 hour period of operation. In normal use the oven would be temperature equilibrated then raised to enclose the degradation tube to minimize the warmup period with its temperature ambiguity.

(2). Sample Preparation

A programmed warmup of an uncured ATS resin can be divided into two stages, a region of "cure" and "post cure" covering the temperature interval between room temperature and about 350°C, and one of degradation occurring above 350°C. To study the "cure" and "post

cure" reactions in ATS polymers, we introduced material to the degradation tube in small pieces to avoid complications induced by the concurrent evaporation of casting solvent. Such samples melt flowed to thin films during cure. A study of the degradation processes occurring above 350°C is complicated by material which evolves from the polymer during lower temperature cure (ATS monomer in the cold ring fraction, solvent in the condensable volatile product fraction of degradation), and so samples for this purpose were precured as solvent cast thin films into the sample "boats" under an atmosphere of nitrogen prior to the TVA experiment.

Sample sizes were determined by the objectives of the experiment and ranged from 100mg to 250mg. The sample crucibles used in this work were all of surface area (10.7 ± 0.5) cm^2. Film thicknesses, therefore, ranged from 90um to 235um. It must be noted that as a result of their large surface areas the film thicknesses of even the most bulky samples (250mg) are comparable to those encountered in a typical TGA experiment.

SECTION A.IX

The Residue of Degradation

(1). Gravimetric Analysis

At the end of the CATVA experiment the oven head assembly is dismantled and the crucible with its residue of degradation carefully removed from the quartz tube with spring loaded pincers. The preweighed crucible is reweighed to estimate the mass of residue which may be expressed as a percentage of the original sample mass.

(2). Elemental Analysis

The carbon, hydrogen, sulfur, and oxygen contents of residues of partial degradation were estimated by elemental analysis, and used in conjunction with total residue weights to construct element loss curves for the polymer.

(3). Infrared (IR) Spectroscopy

Residues of partial degradation were incorporated into KBr disks and examined by IR spectroscopy. In general, a good dispersion of residue throughout the disk was difficult to achieve because of the intractable nature of the material. Spectra obtained by this method were, therefore, often highly attenuated and distorted, and open only to qualitative interpretation. Better spectra were obtained by

degrading polymer samples which were cured onto NaCl salt plates. The disadvantage of this method is that exact temperatures of degradation are often difficult to achieve, especially under programmed conditions, due to the unique thermal lag across each salt plate.

SECTION A.X

The Oligomeric or Cold Ring Product Fraction of Degradation

(1). Gravimetric Analysis

A removable pyrex jacket was wedged onto the end of the oven assembly internal cold finger as shown in Figure 12. The degradation experiment was performed, after which the jacket was removed, weighed, washed clean with solvent, and reweighed to estimate the mass of oligomeric product material. Recovered material was stored for subsequent analysis.

This method will, for example, weigh a 15mg product mixture with an accuracy of $\pm$ 1mg. It will, however, not efficiently condense a large flux of oligomeric material such as would be volatilized from a thin film of resin during cure. In this instance some material "escapes" the cold finger to condense onto the surface of the degradation tube above the oven assembly. For this reason the oligomeric product fraction of a curing experiment was estimmated by the difference between the loss of sample weight and the mass of volatilized solvent.

(2). Infrared (IR) and Nuclear Magnetic Resonance (NMR) Spectroscopy

The oligomeric product fractions of degradation were analyzed by IR spectroscopy as thin films cast from chloroform onto salt plates, using a Beckman^{tm} 33 grating spectrometer. The same materials were analyzed by proton NMR spectroscopy, in deuterochloroform at room temperature, using a Varian^{tm} EM360, 60MHz spectrometer.

(3). Thin Layer Chromatography(TLC)

The oligomeric product fraction of degradation of all the polymers studied in this work could be separated into four subfractions by TLC using SiO_2 (F_{254}) as the stationary phase and methylene chloride as the mobile phase. On the basis of IR and NMR studies of the four fractions and TLC separations of reference materials under the same conditions (Table 1), the gross composition of each sub-fraction was ascertained.

TABLE I THIN LAYER CHROMATOGRAPHY OF SOME REFERENCE COMPOUNDS

Compound	R_f
Diphenyl	0.7
Phenylether	0.7
ATS Monomer	0.3
ATS Dimer	0.2
Phenol	0.2
P-phenoxyphenol	0.2
m,m-phenoxyphenoxyphenol	0.2
Resorcinol	0
Catechol	0
Hydroquinone	0

(4). Preparative Thin Layer Chromatography

(i). Gravimetric Analysis

Preparative TLC separations of oligomeric product fractions of degradation were performed on (20x20)-cm SiO_2 F_{254} plates using methylene chloride as a developing agent. Separated bands were stripped from the plate using tetrahydrofuran (THF) solvent, evaporated to dryness, and weighed to estimate their weight percent of the original mixture. The absolute quantity of each TLC sub-fraction was estimated by a simple calculation relating its weight percentage of the original product mixture to its weight percentage in the original polymer.

(ii). IR and NMR Spectroscopy

Materials isolated by preparative TLC were examined by IR and NMR spectroscopy in the manner outlined in Section A.X (2) above to provide information relating to chemical functionality.

(iii). Chemical Ionization Mass Spectrometry (CIMS)

TLC sub-fractions were introduced to the sample probe of a Finnegan™ 4021 mass spectrometer at 30°C. The probe was warmed as required to evaporate material and identify the most abundant parent ions in each mixture.

(iiii). Joint Application of the Above Techniques

Microstructural information from IR and NMR spectroscopy was combined with parent ion molecular weights obtained using CIMS and

polarity measurements by TLC to elucidate the structures in sub-fractions which were isolated by the preparative TLC method. A gross compositional analysis is outlined below. A more precise analysis is reported later in the text.

Sub-fraction 1 R_f : 0.7

This fraction is composed of a mixture of benzene end capped polyphenol residues.

Sub-fraction 2 R_f : 0.3

This fraction is composed of a mixture of polyphenol residues which contain one sulfone end group.

Sub-fraction 3 R_f : 0.2

This fraction is composed of a mixture of polyphenol residues which contain one hydroxylic end group.

Sub-fraction 4 R_f : 0.0

This fraction is composed of a mixture of mono and polyphenol residues which contain two hydroxylic end groups. Some components of this mixture also contain one sulfone group.

Microdot TLC was used to quickly detect the presence or absence of each of the aforementioned sub-fractions in the oligomeric product fractions of degradation of ATS polymers through different temperature intervals. Preparative TLC, in conjunction with the techniques outlined above, was then used for a more precise analysis.

SECTION A.XI

The Condensable Volatile Product Fraction of Degradation

(1). Gravimetric Analysis of Condensable Volatile Products of Degradation

The condensable volatile product fraction of degradation was directed to, and condensed into, a limb of the fractionating grid. The limb was isolated, the cold trap was rigorously heated with a hot air blower, and trapped material was quantitatively transferred

to a small glass storage vessel. The vessel was removed from the vacuum line, weighed, and returned to the vacuum line. The vessel was reweighed and the weight of trapped condensable volatile material was estimated by difference. Using this procedure a 30mg sample mixture could be weighed with an accuracy of ± 2mg.

(2). Gas Phase Infrared (IR) Spectroscopy

(i). Qualitative Gas Phase IR Spectroscopy

The condensable volatile product mixture or a component of that mixture was directed to, and condensed into, a "limb" of the fractionating grid sketched in Figures 6 and 11. The limb was isolated, the cold trap was warmed to room temperature, and material was flash distilled to the cold finger of a gas phase IR cell. The cell was sealed and removed from the vacuum line, the cold finger was warmed to room temperature and a gas phase IR spectrum obtained of the cell contents. The condensable gas and volatile liquid components of an organic mixture contribute most to its gas phase IR spectrum. These materials often produce unique IR spectra which can be used in their identification.

(ii). Quantitative Gas Phase IR Spectroscopy

To be examined by quantitative gas phase dispersive IR spectroscopy a material must produce strong and distinctive IR absorbance bands which by virtue of their position in the spectrum are free of additive interference from other components of the mixture. It must also exist as an ideal gas within the pressure limits of its confinement in the IR cell. Sulfur dioxide and carbon dioxide, two products of degradation of ATS polymers, meet these requirements and were studied quantitatively by this method.

(a). Cell calibration

The gas phase IR cell was connected to a vacuum manifold which was pumped to a high vacuum. The system was isolated from the pumps and a pure reference gas was introduced from a storage cylinder. Non-condensable impurities were removed by repeated degassing cycles, after which the gas was introduced to the IR cell over a range of pressures. The quantity of gas "n" corresponding to each pressure was obtained by a simple application of the ideal gas law.

$$n = PV/RT$$

Where:

n = quantity of gas in cell (Moles)
P = gas pressure in cell (cm Hg)
V = cell volume (in this instance 7.96cm^3)
R = gas constant (6240cm^3 cm Hg $(M.K)^{-1}$)
T = absolute temperature of gas manipulation manifold (K)

Infrared calibration curves for sulfur dioxide (Figure 15) and carbon dioxide (Figures 16 and 17) were obtained by this method. These graphs were used to measure quantitatively both gases in product fractions of degradation of ATS monomer.

(b). Spectrum interpretation

The condensable volatile product fraction of degradation is condensed into one of the limbs of the fractionating manifold. The limb is isolated and the condensable volatile product fraction distilled to the cold finger of the IR cell. The mixture was warmed to room temperature and its IR spectrum recorded. A representative spectrum is reproduced in Figure 18. Absorbances were related to quantities of gas using the appropriate calibration curve. Weight percentage yields of gas were obtained by relating the absolute gas yield to the sample size.

In theory, water, a condensable volatile product of ATS thermal degradation, is able to remove carbon dioxide and sulfur dioxide from the gas phase to form the corresponding acids. If water is present in product fractions of degradation, then, in theory at least, the apparent concentration of both materials in the gas phase will be reduced. In practice, apparent percentage yields of both gases were reproducible in mixtures which contained water, and did not change when water was removed by SATVA fractionation. In addition, the apparent weight percentage yield of carbon dioxide in mixtures which contained water was shown to be constant over a five fold range of ATS-G sample size.

(3). Proton Magnetic Resonance (NMR) Spectroscopy

(i). Qualitative Proton NMR Spectroscopy

The condensable volatile product mixture, or a component of that mixture, was directed to, and condensed into, a limb of the fractionating grid. The limb was isolated, the cold trap was warmed above room temperature, and materials were flash distilled to a small glass "cold finger" on the vacuum line. The finger was removed from the vacuum manifold and its frozen contents were quickly dissolved in deuterated chloroform or acetone. The mixture

was then transferred to an NMR tube for subsequent examination. This technique of examination was found to be particularly useful for the examination of involatile liquid components of the condensable volatile product fraction of degradation.

(ii). Quantitative Proton NMR Spectroscopy

Three of the condensable volatile products for degradation of ATS polymers; benzene, water, and phenol, cannot be measured quantitatively by gas phase spectroscopy because of their low volatility. The most logical alternative method of analysis, gas liquid chromatography (GLC), being unavailable at the time, an alternative procedure was devised making use of gravimetry in conjunction with proton NMR spectroscopy.

The condensable volatile product fraction of degradation was condensed into the SATVA assembly. The SATVA tube was surrounded by a vacuum flask and slowly warmed to room temperature. As depicted in Figure 19, benzene, water, and phenol were efficiently separated from more volatile components of the mixture and directed to a limb of the fractionating grid where they were weighed by the procedure discussed in (1) above. The mixture from the storage vessel was volatilized to a second limb of the fractionating grid, then to a second storage vessel precharged with 0.5ml of carefully dried deuterated acetone as depicted in Figure 20. The mixture was quickly transferred to an NMR tube for quantitative analysis. A typical spectrum is reproduced in Figure 21 showing resonances produced by water, phenol, and benzene.

If the relative peak areas produced by benzene protons are represented by the letter "C", aromatic phenol protons by the letter "B", and combined water and phenol hydroxyl protons by the letter "A", then the mole ratio of benzene/water/phenol can be expressed in the form:

$$C/6 : (A-B/5)/2 : B/5$$

The absolute abundance of each component in the mixture can, therefore, be obtained by combining its relative abundance with the absolute mass of the mixture.

SECTION A.XII

The Noncondensable Volatile Product Fraction of Degradation

Carbon monoxide and methane were shown to be important high temperature products of ATS thermal degradation. As such, a procedure was devised to estimate them quantitatively in ATS product frac-

tions of degradation by gas phase IR spectroscopy, that a better estimate of the degradation pathway of the polymer be made.

(1). Cell Calibration

The transfer of noncondensable gas from one molecular sieve trap to another is not a process of simple distillation, being complicated by the ability of molecular sieve to concentrate gas even at room temperature. As such, it is not possible to assume a transfer efficiency of 100% at all times. If a calibration procedure for noncondensable gas analysis is to be devised, it must parallel the approach used to manipulate material after the CATVA experiment as closely as possible. It must be noted in passing that any calibration information is unique to the particular batch of molecular sieve used in the ATVA trap and in the ATVA gas phase IR cell. If either are changed, for example, after a breakage of the manifold, the calibration procedure must be repeated. The calibration procedure is outlined below.

A volume calibrated storage vessel was connected to the gas manipulation manifold described in Section A.VII. A second storage vessel was charged with 5A molecular sieve and connected to the same manifold. The molecular sieve was activated by heating to 200°C under high vacuum conditions. Carbon monoxide or methane was introduced from a storage cylinder and condensed onto the molecular sieve at -196°C. The manifold was opened to the pumping system until a pressure of 10^{-2} torr was achieved, isolated, and the molecular sieve was warmed to room temperature. The process was repeated to produce a sample of gas, freed of condensable and noncondensable impurities. Oxygen and nitrogen, unlike carbon monoxide and methane, are inefficiently condensed onto molecular sieve at -196°C and are removed by pumping on the system. On the other hand, carbon dioxide and water, the other likely major impurities, are efficiently trapped by molecular sieve under high vacuum conditions even at room temperature, and remain in the sieve when it is warmed to transfer material to the "second" storage bulb.

The volume calibrated storage bulb was filled with gas to a predetermined pressure as measured by a mercury manometer. The contents of the bulb were completely transferred to the ATVA trap on the degradation manifold. The sieve trap was warmed and material transferred to the adjacent IR gas cell for analysis. The quantity of gas in the IR cell was obtained by a simple application of the ideal gas law:

$$n = PV/RT$$

Where:

n = quantity of gas in calibrated container (M)
P = gas pressure in calibrated container (cm Hg)
V = volume of calibrated container (in this instance 57.9cm^3)
R = gas constant (6240cm^3 .cm Hg $(MK)^{-1}$)
T = absolute temperature of gas manipulation manifold (K)

Plots of % absorbance vs n for carbon monoxide and methane are shown in Figures 22 and 23 respectively.

(2). Spectrum Interpretation

Noncondensable material collected in the CATVA experiment was examined by gas phase IR spectroscopy in the manner outlined above. A representative spectrum is reproduced in Figure 24.

In theory, at room temperature, carbon monoxide and methane will compete for binding sites within the molecular sieve contained in the gas phase IR cell. This, in effect, would exclude material from the sieve and increase the effective gas phase concentration of both species as measured by IR spectroscopy. To test this assumption, the combined yield of carbon monoxide and methane from a degradation experiment was obtained gravimetrically by difference and compared with the apparent yield as measured by gas phase IR spectroscopy. The two estimates differed by approximately 2% to show that, in practice, this effect does not complicate the analysis procedure.

SECTION A.XIII

Conclusions

(1). The TVA, ATVA, and SATVA experiments were combined, for the first time, to form an analytical system able to monitor the composition and rate profiles of formation of condensable and noncondensable product fractions of polymer thermal degradation.

(2). The basic TVA oven assembly was modified, by the use of quartz glassware and a more powerful heat source, to raise its upper temperature limit of operation from 500°C to 1000°C. The removal, for quantitative analysis, of the oligomer and residual product fractions of degradation was facilitated by incorporating into the TVA oven assembly an internal cold finger and a quartz sample crucible respectively.

(3). A combination of analytical procedures was devised to efficiently analyze the oligomer and residual product fractions of ATS thermal degradation.

(4). The technique of quantitative gas phase IR spectroscopy was successfully applied to the analysis of condensable volatile product mixtures containing sulfur dioxide and carbon dioxide. It was shown to be insensitive to the presence of water in those mixtures.

(5). It was shown, for the first time, that the condensable volatile products of polymer degradation can be separated by SATVA and estimated gravimetrically. This procedure was used in conjunction with NMR spectroscopy to produce an experiment able to quantitatively analyze benzene, water, and phenol as products of polymer thermal degradation.

(6). The technique of gas phase IR spectroscopy was, for the first time, successfully applied to a quantitative analysis of carbon monoxide and methane as products of polymer thermal degradation. Both gases were shown to behave independently within the limits of their confinement in an IR cell in the presence of 5A molecular sieve at room temperature. As such, their individual concentrations in the cell could be estimated by reference to the appropriate individual IR cell calibration curve.

PART B

SOME CURE AND POST CURE REACTIONS OF ATS POLYMERS

SECTION B.I

Introduction

Acetylene terminated resins have generated much interest as candidate high performance matrix resins for aerospace applications. This interest has hinged upon several attractive features of the material including a chain addition mechanism of cure which promised void free laminates[9], a thermally initiated cure without added catalyst or hardener which holds open the possibility of long shelf lives and batch to batch homogeneity approaching that of the thermoplastics[10], high glass transition temperatures[11,12], and thermal stabilities[13] made possible by the incorporation of wholly aromatic precursors into a heavily crosslinked polyene network. As part of an extensive thrust in this area, the Air Force commissioned Gulf Chemicals[tm] Inc. to produce a pilot plant quantity of acetylene terminated sulfone resin (more properly, bis[4-(3-ethynylphenoxy) phenyl] sulfone and its higher oligomers)[14]. In an earlier study[15], we began a systematic examination of this material, designated ATS-G, before and after fractionation into molecular weight homologues. In this study we use the technique of thin film flash distillation in conjunction with the TVA technique to isolate low molecular weight impurities in ATS-G resin in an attempt to better characterize the synthetic process used by Gulf Chemical[tm] Inc. We move on to an analysis of the cure and post-cure reactions of this material by Infrared spectroscopy and Differential Scanning Calorimetry, concentrating mainly on the high temperature post cure stage, which we show to overlap the first stages of thermal degradation of the material. Fortunately, this overlap is shown to be associated with decomposition of sulfone linkages in the polymer and not with reactions of the acetylene derivative, and is, therefore, a shortcoming of ATS itself and not of the AT concept.

SECTION B.II

Gravimetric Analysis of Materials Evolved on Heating ATS Under High Vacuum Conditions

It is common knowledge that the extent of vaporization of a substrate (all other parameters being equal) is a function of ambient pressure. For this reason it came as no surprise that solvents and some higher molecular weight materials are evolved on heating a thin film of ATS prepolymer prior to its vitrification. As stated previously, we intended to characterize this evaporated fraction in

an attempt to gain some fresh insight into the composition of the ATS-G mixture and reasonably pure fractions of ATS monomer, dimer, and trimer previously isolated from that mixture by column chromatography[15]. As a preliminary, we first ascertained the proportions of material evaporated from well defined thin films of uncured resin by programmed heating under high vacuum conditions. In this type of analysis we were confident that solvents would be efficiently removed under high vacuum conditions, as earlier work had shown an efficient removal of the same even under a nitrogen blanket[15].

Gravimetric product distributions for the programmed cure cycles of ATS-G, ATS monomer, and ATS dimer are shown in Table 2. As expected, ATS monomer with its lower molecular weight, is more efficiently evaporated from a thin film than higher molecular weight dimer, trimer or ATS-G itself (which contains a proportion of dimer and trimer)[15]. Perhaps as a result of its room temperature "tack and drape," ATS monomer was also shown to contain more solvent than the other fractions. ATS dimer and trimer, both recovered after fractionation and lyophilization as stable fine powders, did not contain any appreciable quantity of solvent, nor did they themselves evaporate to any extent on heating.

TABLE 2 GRAVIMETRIC PRODUCT DISTRIBUTIONS FOR THE PROGRAMMED CURE CYCLES OF ATS-G, ATS MONOMER, AND ATS DIMER UNDER HIGH VACUUM CONDITIONS

Material	Film Thickness (um)	Weight % Volatilization	Weight % High Molecular Weight Material	Weight % Solvent
ATS-G	95	7.2	5.7	1.5
ATS Monomer	95	17.4	12.3	5.1
ATS Dimer	95	=1	Negligible	Negligible
ATS Trimer	95	Negligible	Negligible	Negligible

It must be noted that the extent of evaporation from ATS-G or ATS monomer is inversely related to the film thickness used in the experiment. For example, 3.7 wt% and 5.7 wt% of high boiling point material was evolved from ATS-G upon heating, under otherwise identical conditions, as films approximately 240um and 95um thick respectively.

SECTION B.III

Condensable Volatile Materials Evolved on Heating ATS Under High Vacuum Conditions

An analysis of solvents evolved from ATS-G on programmed heating has already been reported[15]. Not unexpectedly, toluene, the solvent used in the last stage of synthesis, constituted the bulk of this fraction together with minor amounts of diethynyl benzene, a well understood by-product of synthesis. Solvent evolved from ATS monomer was shown to be benzene by Nuclear Magnetic Resonance (NMR) spectroscopy. Although less material was removed from ATS dimer, the SATVA technique proved sensitive enough to confirm the presence of benzene as the major component. The corresponding SATVA trace for this material is reproduced in Figure 25. Benzene was identified on the basis of comparison with reference compounds. These results were expected, as benzene was the solvent from which all fractions were recovered by "freeze drying" after column fractionation[15].

As expected, noncondensable volatile products were absent from this product distribution.

SECTION B.IV

Oligomeric Materials Evolved on Heating ATS Under High Vacuum Conditions

The oligomeric product fractions evolved from ATS-G and ATS monomer on heating under high vacuum conditions were collected in the experiment described in Section B.II above. These fractions were separated into three sub-fractions by the technique of preparative Thin Layer Chromatography (TLC) described in Section A.X[4] of this report. Sub-fractions were characterized by gravimetry, Gel Permeation Chromatography (GPC), by Infrared (IR) and Nuclear Magnetic Resonance (NMR) Spectrometry, and Chemical Ionization Mass Spectrometry (CIMS) as outlined below.

(1). Gravimetric Analysis of Preparative TLC Sub-Fractions

Preweighed sub-fractions were isolated by preparative TLC, recovered in high yield (>90 wt%), and examined by gravimetry to yield the results reproduced in Table 3. A number of similar reference compounds separated under identical conditions, as out-

lined in Section A.X[3], provided a data base for indentification of the gross composition of solute fractions. By such comparisons, sub-fraction 1 was shown to be composed of polyphenylethers sub-fraction 2 to consist of polyphenylethers containing one sulfone group, and sub-fraction 3 to be composed of polyphenylethers, end capped by two hydroxyl groups, which in addition may also contain one or more sulfone linkage.

TABLE 3 GRAVIMETRIC ANALYSIS OF SUB-FRACTIONS ISOLATED BY PREPARATIVE TLC FROM THE HIGH BOILING POINT FRACTION EVOLVED FROM ATS-G AND ATS MONOMER ON PROGRAMMED CURING UNDER HIGH VACUUM CONDITIONS

Sub-Fraction	$R_f(CH_2Cl_2/SiO_2)$	Weight % of Uncured Polymer	
		ATS-G	ATS Monomer
1	0.7	0.4	≈0.1
2	0.3	2.7	11.9
3	0.0	2.7	<0.1

As indicated in Table 3, high boiling point material volatilized from ATS-G on curing consists of an approximately 50/50 mixture (by weight) of sub-fractions 2 and 3 while that volatilized from ATS monomer was shown to be composed predominantly of sub-fraction 2 (>99 wt%) with trace quantities of sub-fractions 1 and 3.

(2). GPC Analysis of Preparative TLC Sub-Fractions

The effective hydrodynamic radii (EHR) in tetrahydrofuran (THF), of components of sub-fractions 1-3, isolated by preparative TLC from oligomers from ATS-G, were obtained by GPC using a Waters Associates liquid chromatograph equipped with microstyrogel columns. The results of this analysis are reproduced in Table 4. As with the TLC experiments discussed above, some information could be gleaned from this experiment on the basis of comparisons with reference compounds, in this instance, of hydrodynamic radii.

TABLE 4 GPC ANALYSIS OF SUB-FRACTIONS ISOLATED BY PREPARATIVE TLC FROM THE HIGH BOILING POINT FRACTION EVOLVED FROM ATS-G ON PROGRAMMED CURING UNDER HIGH VACUUM CONDITIONS

Sub-Fraction	$R_f(CH_2Cl_2/SiO_2)$	Effective Hydrodynamic Radius (EHR) Angstromes
1	0.7	120
2	0.3	310
3	0.0	55 (Major) 120 (Minor) 310 (Minor)

On the basis of this type of comparison, sub-fraction 1 (120A) is probably composed of simple aromatics which contain two benzene rings. By a similar analysis[15], sub-fraction 2 is almost certainly shown to contain relatively pure ATS monomer (310A). The major component of sub-fraction 3 contains one benzene ring (55A), a smaller component contains two benzene rings (120A), and an even smaller component (310A) is probably residual ATS monomer, incompletely fractionated by the TLC experiment.

(3). Infrared (IR) Analysis of Preparative TLC Sub-Fractions

Sub-fractions, isolated by preparative TLC from oligomers evolved from ATS-G and ATS monomer during programmed cure under high vacuum conditions were examined by IR spectroscopy as thin films on sodium chloride salt plates. Band assignments are given below.

TLC Sub-Fraction 1 from ATS-G, $R_f = 0.7$

The IR spectrum of this sub-fraction, reproduced in Figure 26, shows it to contain aromatic material ($3080cm^{-1}$) terminal acetylenes ($330°cm^{-1}$), saturated material ($2940cm^{-1}$ and $2860cm^{-1}$) and phenyl ethers ($1260cm^{-1}$).

TLC Sub-Fraction 2 from ATS-G Monomer, $R_f = 0.3$

Infrared spectra of these sub-fractions from ATS-G and ATS monomer are reproduced in Figures 27 and 28 respectively. Both fractions were shown to contain small concentrations of saturated material ($2960cm^{-1}$, $2930cm^{-1}$, and $2860cm^{-1}$), terminal acetylenes ($330°cm^{-1}$), aromatic material ($\simeq 3080cm^{-1}$), phenyl ethers ($1250cm^{-1}$), and sulfone bridges ($\simeq 1300cm^{-1}$ [doublet], $1125cm^{-1}$ [doublet]).

TLC Sub-Fraction 3 from ATS-G, R_f = 0.0

The IR spectrum of this sub-fraction (Figure 29) indicates that it contains aromatic material (3070cm^{-1}), hydroxyl groups (3400cm^{-1},[broad]), a small concentration of terminal acetylenes (3300cm^{-1}), and phenoxy linkages (1190cm^{-1}, 1120cm^{-1}).

(4). Proton Nuclear Magnetic Resonance (NMR) Analysis of Preparative TLC Sub-Fractions

Sub-fractions isolated by preparative TLC from material evaporated during curing of ATS-G and ATS monomer were examined by proton NMR spectroscopy. Data relating to "sub-fraction" 1 from both materials is not reported due to a lack of sufficient material for analysis.

TLC Sub-Fraction 2 from ATS-G and ATS Monomer, R_f = 0.3

The proton doublets (8s "A"), multiplets (7.5 - 7.0s, "B"), and singlets (3.1s, "C"), produced by both sub-fractions and indicated in Figures 30 and 31, are characteristic of those produced by uncured ATS molecules. The A/B/C proton ratios for both sub-fractions are 1.0 : 3.2 : 0.5. This ratio is characteristic of ATS monomer as produced by Gulf Chemicals™ Inc.[15]. The sub-fraction from ATS-G also contains a small concentration of unidentified saturated material.

TLC Sub-Fraction 3 from ATS-G, R_f = 0.0

The broad multiplet at about 7.8s and the sharp multiplet centered on 7.6s (ratio 1:3) are characteristic of those produced by resorcinol or m-hydroxyphenol. Other components of the mixture are present in quantities too small for detection by the continuous wave spectrometer used in this work.

(5). Chemical Ionization Mass Spectrometry (CIMS) of Preparative TLC Sub-Fractions

CIMS spectra of preparative TLC sub-fractions were obtained as described in Section A.X of this report. Parent ion masses from a programmed warmup of the sample probe are reported in Table 5. (It must be noted in passing that some components of these mixtures may escape detection by this technique. For example, more volatile components may be lost on pump down while less volatile material, especially if present in small quantity, may evolve between scans. In addition, the possibility exists that a fraction of material may crosslink on the probe to form an involatile residue.)

TABLE 5 CHEMICAL IONIZATION MASS SPECTROSCOPY (CIMS) OF SUB-FRACTIONS ISOLATED BY PREPARATIVE TLC FROM THE HIGH BOILING POINT FRACTION EVOLVED FROM ATS-G AND ATS MONOMER ON PROGRAMMED CURING UNDER HIGH VACUUM CONDITIONS

Sub-fraction	R_f (CH_2Cl_2/SiO_2)	Parent Ion Masses (a.m.u.)	
		ATS-G	ATS Monomer
1	0.7	218	218
2	0.3	---	386 (Minor) 450 (Major
3	0.0	110 (Major) 278 (Minor	---

(6). Structural Assignments

Structural assignments of sub-fractions isolated by preparative TLC were made using the results of sub-sections (2-5) above. These assignments are illustrated in Table 6.

TABLE 6 COMPOSITION OF SUB-FRACTIONS ISOLATED BY PREPARATIVE TLC FROM THE HIGH BOILING POINT FRACTIONS EVOLVED FROM ATS-G AND ATS MONOMER ON PROGRAMMED CURING UNDER HIGH VACUUM CONDITIONS

Sub-fraction	R_f (CH_2Cl_2/SiO_2)	Most Probable Structure	
		ATS-G	ATS Monomer
1	0.7	*-ϕOϕ-* (a)	*-ϕOϕ-*
2	0.3	*-ϕOϕSO_2ϕOϕ-*	*-ϕOϕSO_2ϕOϕ-*
			-ϕOϕϕOϕ- (f)(Minor)
3	0.0	HO-ϕ-OH	(b)(Major)
		HO-ϕϕ-OH	(c)(Minor)
		HO-ϕϕOϕ-OH	(d)(Minor)
		-ϕOϕSO_2ϕOϕ-	(e)(Minor)

Legend

*	Terminal Acetylene
ϕ	Phenyl Ring
OH	Hydroxyl Group
ϕ-O-ϕ	Phenyl Ether Linkage
(a)-(e)	Items for Comment (Structural assignments not immediately obvious from the preceding text)

Comments on Table 6

(a). The major component of this sub-fraction was shown by GPC to possess a backbone containing two benzene rings. The only parent ion detected by CIMS suggested diethynyldiphenylether (DEDPE) as the major component of the mixture. Although saturated material was detected in some quantity by infrared spectroscopy, we must conclude that such is not included with a polyphenylether backbone, as such would possess a volatility similar to that of DEDPE and would have evaporated from the probe at a similar time to be detected in the same scan.

(b). The presence of this component was confirmed by a joint application of IR and NMR spectroscopy, GPC, and CIMS in conjunction with TLC retention index (R_f).

(c). The presence of this component was confirmed through its hydrodynamic volume as measured in the GPC experiment, and by its TLC retention index.

(d). This component was confirmed by its parent ion mass and retention index in the TLC experiment.

(e). This component was identified through GPC and IR spectroscopic analysis.

(f). This component was identified through its parent ion mass as measured by CIMS.

SECTION B.V

Some Comments on the Synthesis of ATS-G

The objective of this work was to complete a careful compositional analysis of ATS-G, begun and recorded in an earlier report[15], and to use such as a basis for the identification of possible side reactions of synthesis. Some trace components of the ATS-G mixture were anticipated as logical consequences of the synthetic pathway [14,15], while the identification of others provoked some thought. For example, component (b) probably originated from an Ullman ether condensation of m-dibromobenzene with two waters (present as an impurity in the reaction mixture)[16]. Component (c) most probably was introduced to ATS-G as an impurity in the sulfonyldiphenol feedstock, (a statement open to confirmation or denial by a simple analysis of such by High Pressure Liquid Chromatography). In a similar vein, component (d) could have been produced by reaction of m-dibromobenzene, then water, with component (c), both by Ullman ether condensation; while component (f) would be the product of acetylation of (c) after symmetric reaction with m-dibromobenzene and water, in a manner analogous to the preparation of ATS monomer

from sulfonyldiphenol. Component (a) could have been produced by the double condensation of m-dibromobenzene onto water, followed by acetylation as with ATS.

Although it may appear from this and a preceding report[15] that ATS-G is an exceedingly complex resin mixture, in reality it is less complex than most commercial resin "prepregs." Based on a careful comparison of the thermal stabilities of ATS-G and pure resin components, previously isolated by column chromatography, it can be stated with some confidence, that none of the minor products discussed here significantly detract from resin performance in that sphere.

SECTION B.VI

Infrared Spectroscopy of Partially and Fully Cured ATS

Thin films of ATS were deposited onto freshly polished salt plates, then heated at a rate of 5°C/min to an approximate end temperature of 300°C. The salt plate with its resin coating was cooled to room temperature under high vacuum conditions and its IR spectrum recorded. It must be noted here that the thermal lag across each salt plate is unique with the result that end or upper temperature limits of the cure process could be estimated, at best, with an accuracy of ±10°C.

An IR spectrum of fully cured ATS monomer is shown in Figure 33. This spectrum is reproducible and representative of that produced by fully cured ATS-G, ATS dimer, and ATS trimer. As expected, the terminal acetylenes are completely consumed, as indicated by the absence of the associated C-H stretch at 330°cm^{-1}, to form structures which absorb in the region (3200-2800)cm^{-1}. The appearance of a small but measurable population of free hydroxylic material was not expected on the basis of known cure mechanisms of ATS polymers[9]. On the other hand, similar features were observed in the IR spectra of thermally cured phenyl acetylenes[13]. Although not commented upon, the same authors recognized the possibility of reaction of the growing polyene with oxygen. A logical extension of this rationale would be subsequent breakdown of the peroxide so formed to the corresponding alcohol.

This feature was further investigated by partially curing ATS-G under high vacuum conditions. The results, recorded in Figure 34, indicate that hydroxylic material is formed at approximately 200°C in the ATS mixture. As normal peroxide groups are known to decompose in this temperature range[17], this rationale would appear to carry weight, although the authors have some difficulty in explaining their appearance under high vacuum conditions, except as

products of post oxidation of trapped polyene radicals. Further work is needed to clarify this point.

SECTION B.VII

Differential Scanning Calorimetry (DSC) of ATS Dimer

The cure reactions of ATS polymers have been examined by DSC[15] and by Torsion Impregnated Cloth Analysis (TICA)[11] in earlier communications. The glass transition temperature (T_g) of ATS monomer which had been precured to 450°C at a heating rate of 10°C/min was shown by DSC to occur at approximately 320°C. On the other hand, the T_g of ATS-G attained by a ramped warmup of uncured resin at a heating rate of 2°C/min in the TICA experiment was shown to be 366°C. The discrepancy between the two measurements (46°C) appears a little large to be accounted for by structural differences between the two samples, by differences in warmup rate (although T_g is a rate dependent transition), or in the phenomena measured by the techniques themselves (even though forced oscillation DMA techniques do often suggest a T_g (or tans max) different from that obtained by DSC). One possible simple solution to this discrepancy would be that the ATS network undergoes some thermal degradation in the temperature interval (400-500)°C. Although not destined for use at these temperatures, this observation does warrant some follow up work, on the basis that a post cure in this temperature interval is thought to be required to fully develop the physical properties of ATS resin. A knowledge of possible degradation in this temperature interval would alert the operator to a more precise control of the post cure process.

More detailed DSC measurements were performed to test these assumptions using ATS dimer which had been isolated from the ATS mixture. ATS dimer was chosen for these measurements because of its easily detectable and well defined glass transition temperature[15]. To test the effect of thermal history on T_g, ATS dimer was subjected to repeated ramped heating experiments in the DSC cell to yield the thermograms illustrated in Figure 35.

Scan 1 (Room Temperature - 300°C)

The uncured resin on heating through its "glass transition temperature" underwent a sharp hysteresis endotherm at 69°C then a polymerization exotherm which achieved a rate maximum at 229°C.

Scan 2 (Room Temperature - 350°C)

A glass transition in the sample was not observed during this experiment. A small exothermic process which could be associated with residual cure or with a post cure process was shown to commence at approximately 300°C. The first explanation would appear the more likely, as such would explain its onset at the upper limits of the first scan and the absence of the glass transition which would be obscured by exothermic heat flow. On the other hand, the T_g of ATS dimer is less than 300°C, suggesting that said exotherm may correspond to a post cure process. A more definitive statement cannot be made on the basis of this evidence alone.

Scan 3 (Room Temperature - 400°C)

A broad, poorly defined change of baseline slope was observed during the temperature interval (200-300)°C in place of a well defined T_g transition. This indicated that the network, at that point, was composed of a mixture of dissimilar structures. An exothermic process was shown to commence at approximately 325°C. With respect to the cure history of the sample, it can be stated with some certainty that terminal acetylenes are not involved in this process.

Scan 4 (Room Temperature - 450°C)

A sharp, well defined T_g transition was observed at 258°C, indicating that the process of network unification or "homogenization" occurred toward the end of Scan 3.

Scan 5 (Room Temperature - 450°C): T_g = 242°C

Scan 6 (Room Temperature - 450°C): T_g = 237°C

Scan 7 (Room Temperature - 450°C): T_g = 237°C

Scan 8 (Room Temperature - 490°C): T_g = 220°C

Setting aside the puzzle posed by the small but measurable exotherm witnessed towards the end of the initial DSC experiments, it can be clearly seen that repeated scans to 450°C degrade the resin network with consequent lowering of glass transition temperature. To provide corroborating evidence, a sample of ATS dimer was heated to 450°C under high vacuum conditions, and the condensable volatile product fraction examined by SATVA. An analysis by quantitative gas phase IR spectroscopy, as outlined in Part A of this discussion, indicated the production of sulfur dioxide or SO_2 at a 1.2

wt% yield of the original sample weight, or 8.3 mole% of the ultimate SO_2 yield from the polymer at a heating rate of 5°C/min. (Part 2 of this discussion.)

The observation of SO_2 as a product of degradation is strong evidence for the deterioration of the ATS network, as such would result in the production of some pendent phenyl ethers in the resin with a concomitant lowering of glass transition temperature. To complete the link it was, therefore, necessary only to demonstrate that repeat scans in the TVA apparatus produced SO_2 as a product of degradation to further lower T_g in agreement with the DSC measurements. The same sample of ATS dimer, was, therefore, reheated to 450°C in the TVA apparatus and the condensable volatile products of degradation separated by SATVA as before. The sulfur dioxide yield in this instance was shown to constitute 0.6 wt% of the original sample, or 4.2 wt% of the maximum sulfur dioxide yield from the polymer.

The relatively small changes in T_g induced by these relatively large yields of SO_2 from ATS dimer, constitute strong circumstantial evidence to indicate that initial sulfone scissions in ATS polymers are often followed by recombination of radical centers to form the diphenyl linkage. This hypothesis is elaborated upon in Part C of this discussion.

SECTION B.VIII

Isothermal Aging of ATS in the Absence of Oxygen

In an earlier report[15] we showed that ATS-G and fractions from that mixture were stable with respect to weight loss in air at 260°C over extended periods of time but unstable at 316°C under the same conditions. It is of more than academic interest to determine the nature of this instability at 300+°C, more precisely, whether or not it is oxidative in nature. To this end, a sample of ATS monomer was cured to a final temperature of 270°C under vacuum at a heating rate of 5°C/min. The polymer sample was removed from the oven assembly, weighed (481.5mg), returned to the oven assembly, pumped to high vacuum, and carefully heated to 328±5°C to avoid temperature overshoot. This temperature was maintained for 10.5 hours with constant monitoring of vacuum quality via recorded Pirani gauge output. Condensable volatile products of degradation of the polymer during this time period were collected in a liquid nitrogen trap for subsequent separation by SATVA. The polymer was then cooled to room temperature and reweighed (479.8mg). The weight lost by the polymer during the experiment was, therefore, 1.7mg or 0.4 wt% of the initial sample. Assuming the rate of weight loss to be linked to sample conversion (a) through a numerical function f(1-a), then such

should be constant provided that (a) be sufficiently small. This being the case, by extrapolation, we can assume that close to 4 wt% of the sample should be volatilized after 100 hours at 328°C in the absence of oxygen. In contrast, approximately 25 wt% of this polymer is lost in air at the lower temperature of 316°C. The weight loss process in ATS polymers is, therefore, shown to be predominantly oxidative in nature.

Volatiles trapped during the 10.5 hour duration of the experiment were separated for analysis by SATVA to yield the trace shown in Figure 38. It will be shown in Part C of this work that sulfur dioxide and phenol constitute the initial condensable volatile products of thermal degradation of ATS polymers at a programmed heating rate of 5°C/min. It is interesting to note that benzene and especially water represent a considerable fraction of this product mixture. Benzene is, of course, the solvent from which ATS monomer was freeze dried in the last stage of its separation from ATS-G, while the presence of water in a vacuum line is always suspect. Their significance in this experiment is, therefore, difficult to judge. On the other hand, the presence of sulfur dioxide and phenol is firmly linked to the initial stages of degradation of the polymer.

The T_g of the aged sample was shown to be 336°C by Differential Scanning Calorimetry (DSC). It must be concluded that the high temperature post-cure process referred to in Section B.VII operates also at the relatively low temperature of 328°C if given sufficient time. The high T_g of this sample indicates that the process has been driven almost to completion at a temperature where thermal degradation has been shown to be minimal. This would tend to indicate that a prolonged period of post cure at relatively low temperature may be the most efficient way to complete the ATS network without degradation. It remains to be seen whether or not such an approach could gain commercial acceptance.

The aged sample was shown in the same DSC experiment to produce a relatively large and well defined exotherm beginning at approximately 360°C. This exotherm is not associated with the polymerization of terminal acetylenes because none are present in the sample at this stage of the cure process. It is also probably not associated with the post cure process because such must be close to completion. It may be, as first suggested[15], a result of thermal isomerizations of the polyene crosslink to a more stable configuration. It may also be a result of a partial cyclization of the polyene network. It is unlikely that such an exotherm could result from the relatively slow processes of thermal degradation operative in this temperature range.

SECTION B.IX

Conclusions

(1). The basic cure reaction of ATS polymers, as expected, does not produce any volatile products other than components of the reacting mixture which simply evaporate at the high cure temperatures before the onset of vitrification.

(2). Solvents are efficiently removed from thin films of ATS on programmed heating under high vacuum conditions. Higher molecular weight oligomers are evolved in lower yields which are inversely proportional to their molecular weight and the film thickness used in the experiment.

(3). Diphenol and materials based on diphenol were detected in the ATS-G resin mixture. It was postulated that this class of material may have been introduced to the resin mixture as a feedstock impurity. If this is the case then an alternative explanation of the anomalous aromatic proton ratios of ATS polymers prepared by the Gulf Chemicals^{tm} synthetic route may be advanced as a simple incorporation of this class of material into the resin fraction through coupling with sulfonyldiphenol via m-dibromobenzene, followed by acetylation. The simplest test of this hypothesis would consist of a simple compositional analysis of reactant feedstock (if such is still available).

(4). Infrared (IR) spectra of fully and partially cured ATS-G and pure ATS monomer, dimer, and trimer which had been prepared by Gulf Chemicals^{tm} method all developed a relatively weak absorbance at about 3600cm^{-1} indicative of the presence of small quantities of free and involatile hydroxylic material. IR spectra of partially cured ATS-G indicated that such is introduced to the resin at about 200°C. We do not at this point possess definitive evidence pointing toward any specific mechanism of formation, although similar spectral features in the IR spectra of fully and partly polymerized phenyl acetylenes suggest that these impurities may be found in other AT polymers. Reaction of the growing polyene chain with oxygen followed by hydrogen abstraction and subsequent decomposition of the hydroperoxide so formed could form the basis of a plausible explanation if supporting evidence were found.

(5). Simple consumption of terminal acetylenes was found to be insufficient for the formation of a cohesive network in ATS polymers as evidenced by a distinct glass transition temperature. A well defined T_g transition was observed only after prolonged exposure to higher "post cure" temperatures. Evidence is not available at this point to allow us to speculate on the mechanisms of this "post cure" process.

(6) Evidence was presented to indicate that the ATS network is significantly deteriorated by processes of thermal degradation when heated to 450°C. On this basis it must be concluded that the "final" glass transitions of ATS polymers obtained after curing in this temperature range may be in error. Earlier estimations of glass transitions obtained using "overcured" samples[15] may, therefore, reflect this discrepancy.

(7). The cure cycles of AT polymers containing relatively unstable linkages such as SO_2 or bisphenol A must be carefully evaluated to maximize the influence of the (apparently) indispensable post cure reactions whilst minimizing the deleterious effect of low temperature thermal scissions on the network. This post cure process was shown to be operative at relatively low temperatures over prolonged periods of time.

(8). ATS polymers are stable in air at 260°C but unstable at 316°C with respect to weight loss[15]. Although processes of thermal degradation were shown to be operative in ATS polymers to a small but measurable extent at 328°C, a quantitative analysis showed that the bulk weight loss process operative in this temperature interval can only be oxidative in nature.

PART C

THERMAL DEGRADATION OF ATS POLYMERS

SECTION C.I

Introduction

A number of acetylene terminated (AT) resins have been synthesized in this laboratory with a view to their evaluation as improved matrices for the fabrication of high performance composites. A relatively low cost synthetic route to acetylene terminated sulfone or ATS resin was devised by Gulf Chemicals[tm] Inc. under contract to this laboratory[14]. A 50lb pilot plant batch of ATS (which will henceforth be designated as ATS-G) was prepared by the same company for detailed evaluation by the Air Force. In this report we evaluate the thermal stability of this high performance resin, concentrating upon mechanistic and kinetic aspects of its high temperature decomposition under anaerobic conditions. The goal of this work was, first of all, to define environmental parameters for the use of this material, and secondly, and perhaps more importantly, to establish mechanistic pathways for degradation of this material that such knowledge aid in the identification of structural "weak links" to be eliminated in future syntheses for the improvement of resin properties.

In simple terms, we consider the ATS polymer to consist of polysulfone bridges and polyene crosslinks or "tie points." The ultimate stability of the resin rests firmly upon the stability of both constituents along with any synergistic stabilization or destabilization. Any such analysis of this type is always hampered when a constituent is incompletely defined, for example, when dealing with a mixture. By comparison with most commercial resin systems with hardener, the ATS-G mixture is relatively pure. The statistical nature of the synthesis reactions have, however, resulted in a product with an average molecular weight. Fortunately, such mixtures are amenable to separation by column chromatography, which was used previously to prepare relatively pure fractions containing the ATS homologues[15]. A comparison here of the mechanisms and rates of degradation of these homologues has helped us resolve this difficulty.

Enough indirect evidence has been accumulated to suggest that AT polymers cure by the formation of a linear polyene structure with a maximum chain length of about 6 units[9]. The polyene crosslink is not observable in the cured resin because of its intractable nature. However, an analysis of degradation products from the ATS polymer has been used, through a process of backward deduction, to gain some insight into the polyene structure and its interaction with the resin backbone during the process of thermal degradation.

In short, we have applied the chemical and thermo-analytical procedures developed in Parts A and B of this discussion to a study of the rates and mechanisms of thermal degradation of ATS polymers.

These techniques were applied to a study of ATS-G and its component fractions to study the effect of resin chain length, impurities introduced during synthesis, and polyene structure, on ATS stability.

SECTION C.II

Carbonyl Sulfide (COS)

A low yield condensable volatile product of the high temperature decomposition reactions of ATS polymers was identified as carbonyl sulfide on the basis of its gas phase IR spectrum and high volatility in the vacuum line. We were intrigued by the appearance of this unusual product and decided to prepare a batch for comparison in the SATVA experiment, and for the calibration of a gas phase IR cell; that yields from the degradation of ATS polymers be measured quantitatively.

(1). Preparation of Carbonyl Sulfide

We decided to prepare carbonyl sulfide using a simpler modification of an established technique[18]. The apparatus involved is outlined in Figure 39. Essentially, carbon monoxide was allowed to react with sulfur at 650°C in the absence of moisture or oxygen, and the product purified by trap to trap distillation in the vacuum line.

Purification of Elemental Sulfur

Sublimed sulfur (1.6g) was introduced to the base of a quartz tube. The sulfur was heated to approximately 50°C under high vacuum conditions to remove volatile impurities. The oven was lowered and the sulfur was allowed to cool to room temperature in the quartz tube.

Purification of Carbon Monoxide

Research grade carbon monoxide (1.68g) was condensed into a 5A molecular sieve trap held at -196°C in the gas manipulation manifold. The manifold was opened to the pumping system and residual oxygen (which is less strongly bound to the molecular sieve at -196°C) was removed from the cold trap. On the other hand, carbon dioxide and water, which are more strongly bound to molecular sieve than carbon monoxide, were removed simply by warming the first trap

to room temperature and transferring its contents to a second sieve trap held at -196°C. The water and CO_2 were left behind.

Purification of the Carbonyl Sulfide

Product receiving traps (Figure 39) were cooled to -196°C and the molecular sieve trap containing the carbon monoxide was slowly warmed to achieve a pressure of about 50cm Hg of CO in the vacuum line. The sieve trap was isolated and recooled to -196°C and the oven raised to initiate the reaction. After about 10 min, the oven was lowered and the system reconnected to the molecular sieve trap through the receiving traps. The molecular sieve trap efficiently removed residual CO aiding the transfer of carbonyl sulfide product to the receiving traps.

Product Analysis

A small proportion of the carbonyl sulfide product mixture was routed to a vacuum trap and separated according to volatility by the SATVA experiment to yield the trace shown in Figure 40. As such it can be seen to be very pure, containing no sulfur dioxide and only traces of water. In Figure 41 we reproduce the SATVA curves produced by some relevant reference compounds, from which it can be seen that carbon dioxide with its similar volatility cannot be detected as an impurity in the COS product mixture by SATVA. Fortunately the former is easily detectable by gas phase IR spectroscopy. The gas phase IR spectrum of the COS product mixture, shown in Figure 42, was identical to that of the "unknown" product of polymer degradation, and devoid of any of the very characteristic absorbances associated with gaseous CO_2.

(2). Quantitative Gas Phase Infrared (IR) Spectroscopy of Carbonyl Sulfide

A quantitative gas phase IR calibration curve for carbonyl sulfide was obtained using its 2040cm^{-1} absorption band. The corresponding curve for the weaker but still prominent band at 2900cm^{-1} was recorded for possible future studies. Both curves are reproduced in Figures 43 and 44 respectively.

SECTION C.III

A Justification for the Use of the Combined CATVA/TGA Experiment

The Combined Thermal Volatilization Analysis/Adsorption Thermal Volatilization Analysis (CATVA) experiment described in Part A of this work is complimentary to, and can yield valuable information when used in conjunction with, programmed thermogravimetric analysis (TGA). When the TGA experiment is performed under high vacuum conditions the two can be directly compared. Problems do, however, arise when the TGA experiment is performed under an inert atmosphere of usually hydrogen or helium. A blanketing atmosphere, can, and often does, suppress the evolution of high molecular weight products of thermal degradation which are efficiently volatilized under high vacuum conditions. This effect is particularly noticeable at low temperatures at which high boiling point material may be expected to possess limited volatility. Fortunately all the polymers under investigation are reasonably stable and begin to decompose only at relatively high temperatures at which oligomers may be expected to be volatile even under an atmospheric blanket. Further complications may arise when the two experiments are performed at different heating rates. In this instance, the TGA experiment is performed at a heating rate of exactly 5°C/min while the corresponding CATVA experiment is performed at a "nominal" heating rate of 5°C/min. Differences between the two may also conspire to invalidate the comparison.

The problems associated with a comparison between the two techniques can only be quantified by experiment. To this end, an ATS polymer was examined by TGA under helium to yield the weight loss curve depicted in Figure 45 (broken line). Polymer samples were also reweighed after interrupted CATVA experiments to yield the data points reproduced on the same curve. The close agreement between the two indicates that, in practice, the two experiments are, indeed, complimentary when applied to an analysis of the degradation of ATS polymers.

SECTION C.IV

Combined CATVA/TGA of ATS and Related Polymers

ATS-G, some of its component fractions isolated by preparative column TLC[15], ATP monomer (kindly supplied by B. A. Reinhardt of the Polymer Laboratory, WPAFB), and Radel™ - a commercially available polyphenylether-sulfone thermoplastic, were examined by CATVA

(as outlined in Part A of this report) and by programmed Thermogravimetry. The results of these experiments are discussed below. Structural trends are inferred by internal comparison of CATVA/TGA traces. To this end, extensive comparisons are made especially with ATS monomer as a reference material.

(1). CATVA/TGA of ATS Monomer

The combined CATVA/TGA trace for uncured resin is reproduced in Figure 46. Solvent and some higher boiling point material is removed from this resin in the early stages of the experiment. (For an analysis of this product fraction, the reader may refer to Part B of this discussion.) Volatile products of degradation begin to be formed in small quantities at approximately 320°C as the resin passes through its fully cured glass transition, and in larger quantities at approximately 420°C.

The first detectable process of thermal degradation produces a low temperature "shoulder" on the third process of degradation which achieves a rate maximum at 632°C (at this particular heating rate). The first process produces a mixture of condensable volatile products. The third and fourth processes, which achieve rate maxima at 632°C and 732°C respectively, produce mixtures of noncondensable products containing hydrogen.

A SATVA analysis of the condensable volatile products of degradation of this and other ATS polymers (Section C.X), indicated the presence of a "second" process of degradation which is "sandwiched" between the first and third processes of degradation. The second process was shown to remove from the polymer a mixture of condensable volatile products. A schematic representation of the temperature range of operation of these four processes is made in Figure 47.

A comparison of CATVA and TGA traces for this material indicate that the bulk of the weight loss is associated with the action of processes 1 and 2 on the resin or (perhaps more correctly) its thermal derivative. As such, it can be seen that the products of processes 3 and 4 produce Pirani gauge responses out of all proportion to their gravimetric yields from the polymer - a characteristic of noncondensable gases.

(2). CATVA/TGA of ATS Dimer

The CATVA/TGA trace for this polymer is reproduced in Figure 48. As expected, only a small quantity of solvent is evaporated from this resin prior to its vitrification. Condensable volatile products of thermal degradation are first detected in small quantities at approximately 250°C, again possibly related to passage of the polymer through its final glass transition temperature. Larger quantities of condensable volatile material begins to be produced at about 400°C.

The CATVA/TGA trace is similar to that produced by ATS monomer with a few exceptions. For example, more weight is lost from ATS dimer than from ATS monomer in processes 1 and 2 of degradation. In fact, this increased weight loss is sufficient to produce a small rate maximum in the CATVA/TGA trace for ATS dimer. In addition, the temperatures which correspond to the rate maxima of processes 3 and 4 of degradation of ATS dimer are lower than the corresponding temperatures for ATS monomer. As stated previously, both processes 3 and 4 of degradation of ATS polymers produce noncondensable products. A comparison of the noncondensable volatile emission curves produced by ATS monomer and ATS dimer indicate that a smaller quantity of permanent gas is produced upon thermolysis of ATS dimer than of ATS monomer. It would, therefore, be reasonable to suggest that ATS dimer or its thermal derivative contains a smaller concentration than ATS monomer of those structural entities which participate in these processes. Of course an alternate explanation could be based simply upon the fact that a smaller proportion of ATS dimer remains in the hot zone at the temperatures at which processes 3 and 4 are operative.

(3). CATVA/TGA of ATS-G

The CATVA/TGA trace for this polymer is reproduced in Figure 49. As expected, a solvent mixture is released from the polymer prior to its vitrification (an analysis of which is reported in Part B of this work). Products of thermal degradation begin to be detected at approximately 350°C, a temperature close to the expected final glass transition temperature of the material[15].

The CATVA/TGA traces for ATS monomer and ATS-G are again similar with a few notable exceptions. For example, ATS-G is more extensively volatilized than ATS monomer in processes 1 and 2 of degradation. In common with the behaviour of ATS dimer, process 3 of degradation operates to a smaller extent in ATS-G than in ATS monomer. In contrast, the temperature which corresponds to the rate maximum of process 4 of degradation of ATS-G (744°C) is slightly higher than that which corresponds to the rate maximum of process 4 of degradation of ATS monomer (732°C).

(4). CATVA/TGA of ATS Trimer

The CATVA/TGA trace for ATS trimer, as isolated from the ATS mixture, is significantly different from that of ATS monomer. This confirmed earlier observations which suggested the presence of structural abnormalities in this fraction[15]. The CATVA/TGA trace for ATS trimer, reproduced in Figure 50, indicates the presence of a low temperature process of degradation which achieves a rate maximum at 450°C. This process was shown to volatilize a small quantity of condensable and noncondensable volatile products (but

not hydrogen) from the polymer. In common with ATS dimer and ATS-G, more material is thermolysed from ATS trimer than from ATS monomer.

(5). CATVA/TGA of F4

As explained in an earlier report, F4, or the fourth fraction isolated from ATS-G in ascending order of column retention, is a mixture of anomalous monomeric species which resisted definitive analysis. As expected, the CATVA/TGA trace for F4, as depicted in Figure 51, is substantially different from that produced by ATS monomer, dimer, or by ATS-G.

A comparison of the CATVA/TGA traces produced by ATS trimer and F4 shows that both fractions degrade by an initial process which achieves a rate maximum at (450-460)°C. This provided us with the clue that perhaps ATS trimer was simply contaminated with small amounts of F4 from which it was separated by column chromatography. This was fortuitous in that, if this were the case, a kinetic analysis of the cure reaction of ATS trimer would then allow us to measure the effect of small concentrations of F4 on the cure process of an ATS resin, an important topic when one remembers that F4 is present in, and therefore contributes to, the cure process of ATS-G itself. This analysis was performed to show that F4 (if indeed present as an impurity in ATS trimer) does indeed accelerate the polymerization of ATS resin[15].

Polymers usually contain trace amounts of solvent which is volatilized under high vacuum conditions at temperatures in the range (50-200)°C, usually at temperatures above the glass transition temperature of the material. Even relatively unstable polymers do not usually decompose at these temperatures in the absence of oxygen. Using this criterion, the small rate maximum of volatile formation in F4 at 180°C is not of any particular significance. On closer inspection however, it can be seen that trace quantities of noncondensables are formed in the polymer at temperatures as low as 100°C. Noncondensable volatile products of degradation are usually formed in polymers at very high temperatures. Oxygen, a noncondensable gas is, however, a product of anaerobic peroxide decomposition in polymers at temperatures as low as 100°C[19]. It is possible, therefore, that F4 may contain some peroxides. If so, then its accelerative effect on the polymerization of ATS trimer would be a simple consequence of peroxidic free radical initiation of the acetylene polymerization process[15].

(6). TVA/TGA of F5

Fraction 5, or the fifth fraction to be isolated from the ATS-G mixture, in order of ascending retention on chromatographic silica gel, was previously identified as the partly hydrolysed "acetone adduct" of ATS monomer[15]. Only small amounts of F5 were avail-

able for analysis. This precluded its examination by the normal CATVA experiment. Instead, it was examined by a modified TVA experiment producing the volatile emission curve depicted in Figure 52.

It can be seen that there is operative in this material a low temperature process of degradation which achieves a rate maximum at approximately 473°C. The temperature profile of this process is close enough to those observed in ATS trimer and fractions 4 and 5 to suggest that the anomalous pathways of degradation in all those fractions may be attributed to simple contamination by "acetone adduct" type material.

(7). CATVA/TGA of ATP Monomer

ATP monomer possesses a structure similar to that of ATS monomer except for the omission of the bridging sulfone linkage. A comparison of the CATVA/TGA traces of ATS and ATP monomers, therefore, affords a simple test of the effect of the bridging sulfone group on the thermal stability of the basic polyene crosslinked polyphenylether based resin.

The CATVA/TGA trace for ATP monomer, as depicted in Figure 53, is similar to that produced by ATS polymers with a few significant differences which may be summarized as follows. First of all, the proportion of weight lost on thermolysis of ATP is less than that lost by the ATS polymers. Secondly, the low temperature rate "shoulder" on the first rate maximum of volatile production in ATS polymers is absent from the CATVA trace produced by ATP monomer. This indicates that such is associated with the decomposition of sulfone links in the ATS polymer. (A subsequent analysis of the volatile products of ATP degradation by the SATVA technique indicated qualitatively the operation of process 2 of degradation as associated with ATS polymers but the absence of the associated process 1.) This would tend to suggest, albeit tentatively, that process 1 of degradation of ATS be somehow linked to the presence of sulfones in the polymer.

In a similar vein, it can be seen that process 3, as is associated with the degradation of ATS polymers, is operative to a larger extent in ATP than in any of the ATS polymers we examined.

(8). CATVA/TGA of Radel

Radel^{tm}, a commercially available thermoplastic polyphenylethersulfone polymer possesses a structure very similar to that of the ATS polymers with the simple omission of the polyene crosslink. Its structure may be depicted as [-(-ϕ-ϕ-O-ϕ-SO_2-ϕ-O-)-]. The CATVA/TGA trace for Radel^{tm} is similar to that produced by the ATS resins with some notable exceptions which are summarized below.

Process 1 of degradation of ATS polymers it would appear operates also in Radel[tm] thermoplastic but lacks the pronounced low temperature "tail" associated with the ATS resins. Presumably the Radel[tm] thermoplastic contained fewer impurities than the resin systems. Processes 1 and 2 of degradation of this type of polymer together volatilize a larger proportion of Radel[tm] than of the ATS resins. On the other hand, the volatile emission peak associated with process 3 of degradation is much reduced in Radel[tm] with respect to the ATS resins. With the exception of the acetylenic end groups of the ATS monomer molecule it would appear that the base structure of ATS monomer and Radel[tm] are very similar. The higher thermal stability of ATS resin is, therefore, probably associated with the presence of the polyene crosslink.

(9). Noncondensable Emission Curves for ATS and Related Polymers

A comparison of temperatures corresponding to the rate maxima of formation of noncondensable gases in ATS and related polymers is reproduced in Table 7. Such a comparison proves not to be particularly informative. In contrast, a comparison of the rate profiles of formation of noncondensables, as depicted in Figure 55, proved more so. It can be seen that the quantity of noncondensable material produced in the third process of degradation, associated with the first "noncondensable" rate maximum in ATS polymers, increases with the polyene concentration in the polymer. It must be noted in passing that the Radel[tm] sample under investigation weighed 108.4mg - approximately 5% more than other polymers in this comparison. It must also be noted that the ATS monomer sample under investigation weighed approximately 10% less than other polymers in this study as a result of evaporation from the sample prior to its vitrification.

TABLE 7 TEMPERATURES WHICH CORRESPOND TO THE RATE MAXIMA OF PRODUCTION OF NONCONDENSABLE VOLATILE MATERIAL IN ATS AND RELATED POLYMERS AT A HEATING RATE OF 5°C/MIN

Polymer	First Rate Maximum (°C)	Second Rate Maximum (°C)
ATS-G	637	744
ATS Monomer	632	732
ATS Dimer	584	703
Radel[tm]	602	703
ATP Monomer	602	685

SECTION C.V

Gravimetric Analysis of the Product Fractions of Thermal Degradation of ATS Polymers

The residue of degradation, along with the high boiling point and condensable volatile product fractions of thermal degradation to 1020°C of ATS polymers were estimated gravimetrically as outlined in Part 1 of this report. The magnitude of the noncondensable volatile product fraction of degradation was then established by difference. Results are summarized in Table 8.

TABLE 8 GRAVIMETRIC ANALYSIS OF THE PRODUCT FRACTIONS OF THERMAL DEGRADATION TO 1020°C OF ATS POLYMERS

	Wt% of Cured Polymer		
Product Fraction	ATS Monomer	ATS-G	ATS Dimer
The Residue of Degradation	54.5	53.2	49.6
The High Boiling Point Product Fraction of Degradation	4.4	5.4	11.3
The Condensable Volatile Product Fraction of Degradation	30.4	32.2	31.4
The Noncondensable Volatile Product Fraction of Degradation	10.8	9.3	7.7

Monomeric acetylene terminated sulfone, by virtue of its higher initial acetylene concentration, will exhibit a higher concentration of polyenes after polymerization than ATS dimer. By the same argument it can be shown that ATS-G will exhibit a polyene concentration, after polymerization, intermediate between ATS monomer and dimer. It can be seen from Table 8 that the yields of residual material follow this trend with the highest yield corresponding to the material with the highest polyene concentration. The presence of polyene crosslinks in ATS would, therefore, appear to constitute a stabilizing, or high char promoting influence on the material. In a similar vein, the yields of noncondensable volatile product from ATS polymers follows a similar trend with the highest yield corresponding to the most heavily crosslinked polymer of the series, in this instance ATS monomer. This result is in good agreement with qualitative observations based on the relative magnitudes of the noncondensable volatile emission curves discussed in Section C.IV above.

The yields of condensable volatile and oligomeric products follow opposite trends, with the highest yields originating in the polymer with the lowest polyene concentration, in this instance ATS dimer. The trend is best illustrated using the high boiling product fractions of degradation. It will be shown later in this discussion that this product fraction finds its origin essentially through random scissions of the ATS backbone (somewhat aided by the destabilizing influence of the sulfone linkage). As the resin backbone length increases so also does the probability of random scission of that chain segment, which is in addition, on average, further from stabilizing polyene crosslink.

SECTION C.VI

The Residues of Thermal Degradation of ATS Polymers

The residues of thermal degradation to 1020°C of ATS and related polymers were estimated gravimetrically. Results are reported in Table 9.

TABLE 9 RESIDUES OF THERMAL DEGRADATION TO 1020°C OF ATS AND RELATED POLYMERS

	: Heating Rate 5°C/min: : Sample Size 100mg:
Polymer	Weight % Residue of Cured Polymer
ATP Monomer (for Comparison)	60.1
ATS Monomer	54.5
ATS-G	53.2
ATS Dimer	49.6
Radel (for Comparison)	35.2

It can be seen from Table 9 that a very high proportion of ATP monomer is converted to involatile "char" on thermolysis. This is not surprising in the light that this material contains a high proportion of polyene crosslinks which are known to promote char formation in the closely related ATS polymers[15]. In addition, it does not contain any sulfone groups which have been shown in Part B of this communication to promote (relatively) low temperature bond

scissions in AT polymers. Radel, in contrast, contains the same basic polyphenylether sulfone moieties as the ATS resins but does not contain the polyene crosslinks common to all AT polymers. As expected, it is less efficiently converted to char than the ATS resins. As an aside, it should be noted that the yield of noncondensables from Radel is less than from the ATS resins, presumably because less of the sample remains in the hot zone at the temperatures at which heteroatoms are expelled from the growing polyaromatic condensates which constitute the final char.

(1). Infrared (IR) Spectroscopy

The residues of partial degradation of ATS-G under high vacuum conditions were examined by IR spectroscopy yielding spectra as depicted in Figure 56. The intractable nature of the cured resin limited its dispersion in the KBr matrix with the result that spectroscopic analyses could be made only on a qualitative basis. Even so, it can be observed from this work that sulfone and phenyl ether linkages are progressively removed from the resin on heating and are completely absent from the residue of programmed degradation at 576°C. Aromatic material is still detectable in large quantity at 576°C, in small quantity at 661°C, but not at all in the residue of degradation at 1020°C, presumably as a result of progressive ring fusions which increase the symmetries and decrease the IR extinction coefficients of this class of material.

(2). Elemental Analysis

The carbon, hydrogen, oxygen, and sulfur contents of residues of partial degradation of ATS-G were examined by elemental analysis, from which element loss curves were constructed for each element as illustrated in Figure 57. Carbon, as you would expect, constitutes the bulk of ATS-G. As such, its loss curve more or less parallels that of the corresponding TGA weight loss curve for the polymer.

Sulfur, which is initially contained in sulfone linkages in ATS-G, was shown earlier (Part B) to be volatilized from and to promote isothermal low temperature weight loss in ATS polymers. The early precipitous loss of sulfur fron ATS-G heated under programmed conditions indicates that the sulfone linkage behaves similarly under programmed heating conditions. A change of slope in the sulfur loss curve at approximately 500°C suggests a possible change in its mode of volatilization from the polymer - an observation confirmed later in this report by quantitative gas phase IR spectroscopy. A small amount of sulfur is retained by the residue of degradation to 1020°C presumably within fused ring heterocycles.

The loss of elemental oxygen from ATS-G closely parallels that of sulfur up to about 530°C. In common with sulfur, oxygen loss profile changes curve shape but at the higher temperature of 550°C. Above 550°C oxygen is removed from the polymer as carbon monoxide

and carbon dioxide as is discussed later in this report. The residue of degradation to 1020°C contains a little stable oxygen, presumably within fused ring heterocycles.

Hydrogen is removed from ATS-G in a manner similar to that of oxygen except with a profile which is skewed to higher temperatures. Above 600°C it is removed from the polymer as methane and hydrogen gas.

In general terms the changes of slope of the sulfur, oxygen, and hydrogen emission curves may be linked to the "watershed" transition between processes 1 and 2 of degradation and the later processes 3 and 4 as depicted in Figure 47.

SECTION C.VII

Infrared (IR) Spectroscopy of the Oligomeric Product Fraction of Degradation of Pre-Cured ATS Polymers

(1). Material Produced in the Temperature Interval: (RT-1020)°C

The Infrared spectra of high boiling point products, evaporated from ATS-G, ATS monomer, ATS dimer, and ATS trimer on heating to 1020°C all possessed similar features. A representative spectrum is reproduced in Figure 58. Major structural features are numbered in the figure and identified in the associated "Key." Spectral features are somehwat similar to those exhibited in the IR spectrum of the cured resin. The presence of sulfone and polyphenylether links suggest a product mixture similar in composition to the base resin backbone, presumably produced by evaporation of those products of chain scissions falling into the correct molecular weight range. In addition, the presence of hydroxylic material in this product fraction indicates that a proportion of the polyphenylether linkages in the polymer succumb to thermal scissions.

Bands observed in the carbon-hydrogen stretching region of fractions from each polymer mentioned above are reproduced in Figure 59, from which it can be seen that the relative concentration of saturated material in those fractions from sulfone containing polymers increases with the polyene concentration in the original polymer. The apparent low concentration of saturated material in the high boiling point product fraction of degradation of ATP monomer presumably reflects the absence of sulfones in the original resin, which with their associated low temperature decompositions encourage the chain fragmentations producing this type of material.

(2). Material Produced in the Temperature Interval: (RT-532)°C

The end or upper temperature of this experiment (532°C) can be thought of as an intermediate between processes 1 and 2 of thermal degradation of ATS polymers as depicted in figure 47. As the oligomeric products of degradation of ATS polymers are produced by these two processes, it was felt that an examination of products essentially released by the first, or low temperature process, could prove potentially informative.

The Infrared spectrum of high boiling point material evolved from ATS monomer on heating to this upper temperature limit is shown in Figure 60. By comparing it to the IR spectrum of material evolved from the corresponding polymer on heating to 1020°C, it can be seen to possess most or all of the structures contained in the latter.

(3). Material Produced in the Temperature Interval: (532-1020)°C

Having established the major structures contained in oligomeric products of process 1 of degradation of ATS polymers, the study was completed by an examination of those products associated with process 2 of degradation. Experimental design in this context proved no problem. We simply heated samples of ATS monomer and dimer to the intermediate temperature of 532°C, cooled the degradation tube, removed oligomers produced in process 1 of degradation from the oven cold finger, then reheated the oven assembly to 1020°C. As processes 3 and 4 of degradation of this class of material do not produce oligomeric products, those collected could be unambiguously identified with the second process of degradation.

The IR spectra of high boiling point products of thermal degradation of ATS monomer and dimer in the temperature interval (532-1020)°C were similar in appearance. The IR spectrum of material evolved from ATS monomer in this temperature interval is shown in Figure 61. The major features of this spectrum are similar to those produced by the oligomeric product fraction of degradation to 1020°C of precured ATS polymers as depicted in Figure 58 except for the absence of absorbance bands associated with the presence of sulfone linkages in the product fraction.

(4). Summary

Infrared spectra of the high boiling point product fractions of degradation of ATS polymers are similar to those of the polymers from which they were evolved. This indicates that the former is produced by bond scissions rather than by rearrangements in the polymer. The pronounced concentrations of hydroxylic end groups in these oligomer fractions indicate that a proportion of these bond scissions involve the polyphenylether linkage.

Oligomers produced above 532°C do not contain sulfone linkages. This was expected in view of the fact that 532°C is close to temperatures which correspond to the end of process 1 of degradation of ATS polymers - a process which has been shown by elemental analysis to quantitatively remove sulfur from the polymer in the form of sulfur dioxide.

SECTION C.VIII

Thin Layer Chromatography (TLC) of the Oligomeric Product Fraction of Degradation of Precured ATS Polymers

(1). Thin Layer Chromatography (TLC) of Material Evolved from ATS and Related Polymers

We discussed in Part A of this report the use of TLC to identify the four structural types which together comprise the oligomeric product fraction of degradation of ATS polymers. Having established its utility, we endeavored to use the technique to establish the presence or absence of the major structural types in the oligomeric product fractions of degradation of ATS and structurally related polymers between well defined temperature intervals. The results of a number of simple spot tests we performed for this purpose are related in Table 10. The TLC system used in this work and the precise nature of the material which forms "spots" with retention indices equal to 0.7, 0.3, 0.2, and 0.0 has been discussed in Part B of this report.

TABLE 10 TLC OF THE OLIGOMERIC PRODUCT FRACTION OF THERMAL DEGRADATION OF ATS AND RELATED POLYMERS

Polymer	Temperature Interval (°C)	Sub.F^n.1 R_f 0.7	Sub.F^n.2 R_f 0.3	Sub.F^n.3 R_f 0.2	Sub.F^n.4 R_f 0.0
ATS-G	RT-1020°C	P	P	P	P
ATS Monomer	RT-1020°C	P	P	P	P
ATS Dimer	RT-1020°C	P	P	P	P
ATS Trimer	RT-1020°C	P	P	P	P
F4	RT-1020°C	P	P	P	P
F5	RT-1020°C	P	P	P	P
VAA	RT-1020°C	P	P	P	P
Radel	RT-1020°C	P	P	P	P
ATP Monomer	RT-1020°C	P	*A*	P	P

Polymer	Temperature Interval (°C)	Sub.F^n.1 R_f 0.7	Sub.F^n.2 R_f 0.3	Sub.F^n.3 R_f 0.2	Sub.F^n.4 R_f 0.0
ATS Monomer	RT-532°C	P	P	P	P
ATS Dimer	RT-532°C	P	P	P	P
ATS Monomer	RT-1020°C	P	*A*	P	P
ATS Dimer	RT-1020°C	P	*A*	P	P

Key:
P: Sub-Fraction is Present
A: Sub-Fraction is Absent
VAA: Vinyl Acetone Adduct of ATS

In qualitative terms, the high boiling point product fractions of degradation to 1020°C of all ATS polymers contained the same structural types. This implies, of course, that similar pathways of degradation are operative in all the ATS polymers. The high boiling product fraction of degradation from Radel[tm] thermoplastic contained similar structural types, reinforcing our belief that the bulk of this product fraction originates in the backbone of the ATS resin and not in its polyene crosslink. Material which separates to a retention index of 0.3 has been shown to contain one sulfone group per residue. As expected, therefore, the high boiling point product fraction evolved from ATP monomer did not express this fraction.

The high boiling point product fractions evolved from precured ATS monomer and ATS dimer in the temperature intervals (RT-532)°C and (532-1020)°C were examined by TLC in an attempt to further elucidate the structures produced in processes 1 and 2 of degradation of ATS polymers. In qualitative terms, processes 1 and 2 of thermal degradation of ATS polymers were shown to produce similar high boiling point products by, presumably, bond scissions within the polyphenylether backbone of the resin. As expected (in view of the Infrared measurements discussed in the previous section) the former contained structures which possessed sulfone links while the latter did not. It can be seen from the element loss curves reproduced in Figure 57 that ATS polymers still contain some elemental sulfur at 532°C. Its absence, in the form of sulfone, from the oligomeric products of process 2 of degradation is strong circumstantial evidence for the transformation of sulfone to another structural type such as sulfide.

(2). Gravimetric Analysis of Preparative TLC Sub-Fractions

In a previous section we measured by gravimetry the yields of high boiling point product of thermal degradation to 1020°C of ATS polymers. Those measurements we summarized in Table 8. We now set

out to measure by gravimetry the yields of each individual fraction as isolated by preparative TLC from the original product mixture using procedures outlined in Part A of this discussion. Our results, expressed as a percentage of the inital sample weight, may be examined in Table 11.

TABLE 11 GRAVIMETRIC ANALYSIS OF SUB-FRACTIONS, ISOLATED BY PREPARATIVE TLC FROM THE HIGH BOILING POINT PRODUCT FRACTION OF THERMAL DEGRADATION TO 1020°C OF ATS POLYMERS

TLC Fraction	R_f	Wt % of Resin		
		ATS Monomer	ATS-G	ATS Dimer
1	0.7	1.4	1.6	2.6
2	0.3	0.6	0.7	1.9
3	0.2	1.1	1.6	3.6
4	0.0	1.3	1.5	3.2

As expected, in view of the results summarized in Table 8, the yield of each sub-fraction increased from ATS monomer through ATS-G to ATS dimer. Concentrating on products from ATS monomer and ATS dimer we can see that sub-fractions 3 and 4 are present in higher proportions in the product fraction from the latter. These sub-fractions, on average, contain higher molecular weight material than the other two, and so become relatively more prominent in the product fraction from the resin with the longer chain backbone.

SECTION C.IX

Composition of Sub-Fractions, Isolated by Preparative Thin Layer Chromatography from the High Boiling Point Fractions of Thermal Degradation to 1020°C of ATS Polymers

Having estimated the gravimetric yields of sub-fractions isolated by preparative Thin Layer Chromatography (TLC) from the high boiling point product fractions of degradation to 1020°C of ATS polymers, we next performed a structural analysis to ascertain the most probable compositon of each sub-fraction using Infrared (IR) spectroscopy, Nuclear Magnetic Resonance (NMR) spectroscopy, and Chemical Ionization Mass Spectroscopy (CIMS) in tandem. The results of our investigations are reproduced below. Repetition for the sake of clarity was found to be necessary here.

(1). Sub-Fraction 1

(a). Infrared (IR) Spectroscopy

The IR spectra of high boiling products of degradation of ATS monomer, ATS-G, and ATS dimer as reproduced in Figures 62, 63, and 64 respectively show those fractions to be similar in composition. All fractions contain aromatic material, phenylether linkages, and some saturated material. As expected in view of prevous discussions, the proportion of saturated material in these product fractions increases with the polyene concentration in the resin from which it was volatilized (Conc. in ATS Monomer> Conc. in ATS-G> Conc. in ATS dimer).

(b). Proton Nuclear Magnetic Resonance (NMR) Spectroscopy

The NMR spectra of material from ATS monomer, ATS-G, and ATS dimer are shown in Figures 65, 66, and 67 respectively. In common with the IR measurements, the technique of NMR spectroscopy shows all three product fractions to be similar in composition. The bulk of the saturated functionality was clearly shown to be methyl groups by virtue of the sharp singlet observed in all three spectra at about 1.24ppm. By comparing the relative proportions of protonated aromatics to aliphatics, we again show that the concentration of saturated material increases with the crosslink density in the initial polymer. The aromatic signals produced by the sub-fraction from ATS monomer are rather featureless. On the other hand, some sharp signals characteristic of m-polyphenylethers are observable in the NMR spectra of fractions from ATS-G and ATS dimer. Their concentration in the appropriate sub-fraction increases from that produced by ATS-G to that produced by ATS dimer, presumably reflecting the longer polyphenylether segments initally present in the latter polymer.

(c). Chemical Ionization Mass Spectroscopy (CIMS)

Chemical Ionization Mass Spectra of material which originated in ATS monomer, ATS-G, and ATS dimer were obtained by procedures outlined in Part A of this report. Parent ion masses so obtained by this method are listed in Table 12.

TABLE 12 CIMS OF SUB-FRACTION 1, ISOLATED BY PREPARATIVE TLC FROM THE HIGH BOILING POINT PRODUCT FRACTION OF DEGRADATION TO 1020°C OF ATS POLYMERS

Parent Ions (a.m.u.)		
ATS Monomer	ATS-G	ATS Dimer
184		
246	246	246
		260
262	262	262
338		338
352		352

(d). Structural Assignments

Information contained in the Infrared and Nuclear Magnetic Resonance spectra was combined with results from Thin Layer Chromatography and Chemical Ionization Mass Spectrometry to propose structures for components of Sub-Fraction 1. These most probable structures are depicted in Table 13.

TABLE 13 STRUCTURAL ASSIGNMENTS FOR THE COMPONENTS OF SUB-FRACTION 1

From ATS Monomer	From ATS-G	From ATS Dimer
$\phi O \phi CH_3$		
$\phi\phi O\phi$	$\phi\phi O\phi$	$\phi\phi O\phi$
		$\phi\phi O\phi CH_3$
$\phi O\phi O\phi$	$\phi O\phi O\phi$	$\phi O\phi O\phi$
$\phi\phi O\phi O\phi$		$\phi\phi O\phi O\phi$
$\phi O\phi\phi O\phi$		$\phi O\phi\phi O\phi$
$\phi O\phi\phi O\phi CH_3$		$\phi O\phi\phi O\phi CH_3$

Key :
ϕ : Phenyl group
$\phi o \phi$: Phenyl ether group

(2). Sub-Fraction 2

(a). Infrared (IR) and Proton Nuclear Magnetic Resonance (NMR) Spectroscopy

The proton NMR spectra of material from ATS monomer, ATS-G, and ATS dimer are shown in Figures 68, 69, and 70 respectively. The corresponding IR spectra of products from all three polymers were similar. As such, only one is reproduced here. We have chosen as an example, the spectrum produced by products from ATS-G as representative of this class of material (Figure 71).

Both the IR and NMR spectra indicate that the material in this sub-fraction contains sulfone linkages in a polyphenylether backbone. The broadening of the aromatic resonances toward 8ppm in the NMR spectra suggest (albeit tentatively) that some diphenyl type linkages are present in all three sub-fractions. The sub-fraction from ATS monomer contained practically no saturated material and the corresponding sub-fraction from ATS dimer contained only a little saturated material in quantities too small for accurate analysis. On the other hand, the corresponding sub-fraction from ATS-G was shown to contain a complex mixture of saturates, presumably from some of its anomalous constituents such as F4 etc. A low concentration of hydroxylic material was detected by IR spectroscopy but not by NMR spectroscopy, presumably because of the greater sensitivity of the former towards this functionality.

(b). Chemical Ionization Mass Spectrometry (CIMS)

Chemical Ionization Mass Spectra of each sub-fraction were obtained as outlined in the previous section. Parent ion masses are listed in Table 14.

TABLE 14 CIMS OF SUB-FRACTION 2, ISOLATED BY PREPARATIVE TLC FROM THE HIGH BOILING POINT PRODUCT FRACTION OF DEGRADATION TO 1020°C OF ATS POLYMERS

Parent Ions (a.m.u.)		
ATS Monomer	ATS-G	ATS Dimer
186	186	186
262	262	262
		278

ATS Monomer	ATS-G	ATS Dimer
310	310	310
		354
402		402
		416

(c). Structural Assignments

As before, information contained in the IR and NMR spectra was combined with TLC retention indices and parent ion information from CIMS to propose most probable structures for compnents of sub-fraction 2. Structural assignments are given in Table 15.

TABLE 15 STRUCTURAL ASSIGNMENTS FOR THE COMPONENTS OF SUB-FRACTION 2

(*designates a minor component)

ATS Monomer	ATS-G	ATS Dimer
$\phi o \phi o H$*	$\phi o \phi o H$*	$\phi o \phi o H$*
$\phi o \phi \phi o H$*	$\phi o \phi \phi o H$*	$\phi o \phi \phi o H$*
$\phi o \phi SO_2 \phi$	$\phi o \phi SO_2 \phi$	$\phi o \phi SO_2 \phi$
		$\phi o \phi o \phi \phi o H$
$\phi o \phi SO_2 \phi o \phi$		$\phi o \phi SO_2 \phi o \phi$
$\phi o \phi SO_2 \phi o \phi CH_3$		$\phi o \phi SO_2 \phi o \phi CH_3$

(3). Sub-Fraction 3

(a). Infrared (IR) and Proton Nuclear Magnetic Resonance (NMR) Spectroscopy

The procon NMR spectra of material from ATS monomer, ATS-G, and ATS dimer are shown in Figures 72, 73, and 74 respectively. The IR spectrum of material from ATS-G is shown in Figure 75.

By a joint examination of the IR and NMR spectra it can be seen that each fraction contains some diphenyl linkages (broadening of the NMR spectra towards 8ppm), massive amounts of hydroxylic material, probably as a result of polyphenylether scission in the

polymer, and small quantities of sulfone, most probably as a result of incomplete separation of this type would explain also the presence of hydroxyls in sub-fraction 2.

All three sub-fractions were shown to contain m-polyphenylethers, as evidenced by the NMR signal pattern below 6.5ppm, in quantities which increased from ATS monomer (barely detectable) through ATS-G to ATS dimer. This trend is probably a simple reflection of the relative average resin backbone lengths in the three polymers.

(b). Chemical Ionization Mass Spectroscopy (CIMS)

Parent ion masses as obtained by CIMS are listed in Table 16.

TABLE 16 CIMS OF SUB-FRACTION 3, ISOLATED BY PREPARATIVE TLC FROM THE HIGH BOILING POINT PRODUCT FRACTION OF DEGRADATION TO 1020°C OF ATS POLYMERS

Parent Ions (a.m.u.)		
ATS Monomer	ATS-G	ATS Dimer
170	170	170
	186	186
262		262
		278
		310
312		312
		402

(c). Structural Assignments

Information contained in the IR and NMR spectra was combined with parent ion masses from CIMS and polarities from TLC measurements to propose most probable structures from components of Sub-Fraction 3. Structural assignments are outlined in Table 17.

TABLE 17 STRUCTURAL ASSIGNMENTS FOR THE COMPONENTS OF SUB-FRACTION 3

(*designates a minor component)

ATS Monomer	ATS-G	ATS Dimer
ϕϕoH	ϕϕoH	ϕϕoH
	ϕoϕoH	ϕoϕoH
ϕoϕϕoH		ϕoϕϕoH
		$\phi o \phi SO_2 \phi$*
$HoS=o[(o\phi)(\phi)_2]$		$HoS=o[(o\phi)(\phi)_2]$
		$\phi o \phi SO_2 \phi o \phi$*
		HoϕϕoϕoH*

Key :

ϕ : Phenyl Ring
o,O : Oxygen

(4). Sub-Fraction 4

(a). Infrared (IR) and Proton Nuclear Magnetic Resonance NMR Spectroscopy

The proton NMR spectra of material from ATS monomer, ATS-G, and ATS dimer are shown in Figures 76, 77, and 78 respectively. The IR spectrum of material from ATS-G is shown in Figure 79.

An examination of the corresponding IR and NMR spectra showed that each sub-fraction contained sulfone linkages in some quantity, a relatively large amount of hydroxyls and polyphenylethers, some saturated material, and some diphenyls. The large amount of resorcinol in the fraction from ATS-G is not reflected in the composition of the other purer fractions, namely from ATS monomer and dimer. Most probably, this material was trapped in ATS-G on vitrification of the resin and was simply released upon decomposition of the resin network. (Confirmation of the presence of resorcinol in the ATS-G mixture can be had from Table 4 and supporting text.) Upon separation of the oligomers from ATS-G by Gel Permeation Chromatography, as shown in Figure 80, we can see that resorcinol constitutes only a small proportion of that product mixture.

(b). Chemical Ionization Mass Spectrometry (CIMS)

Parent ion masses are listed in Table 18.

(c). Structural Assignments

Information contained in the IR, NMR, TLC and CIMS measurements were combined to propose most probable structures for components of sub-fraction 4 of the high boiling point products of ATS degradation. These "most probable" structures are reproduced in Table 19.

TABLE 18 CIMS OF SUB-FRACTION 4, ISOLATED BY PREPARATIVE TLC FROM THE HIGH BOILING POINT PRODUCT FRACTION OF DEGRADATION TO 1020°C OF ATS POLYMERS

Parent Ions (a.m.u.)		
ATS Monomer	ATS-G	ATS Dimer
	110	
186	186	186
250		
262		
	278	278
326	326	326
	418	418
		510

TABLE 19 STRUCTURAL ASSIGNMENTS FOR THE COMPONENTS OF SUB-FRACTION 4

(*designates a minor component)

ATS Monomer	ATS-G	ATS Dimer
	HoϕoH	
HoϕϕoH	HoϕϕoH	HoϕϕoH
$Ho\phi SO_2\phi oH$		

ATS Monomer	ATS-G	ATS Dimer
Ho$\phi\phi$oϕ*		
	Ho$\phi\phi$oϕoH	Ho$\phi\phi$oϕoH
ϕo$\phi$$SO_2$$\phi$oH	ϕo$\phi$$SO_2$$\phi$oH	ϕo$\phi$$SO_2$$\phi$oH
	ϕoϕo$\phi$$SO_2$$\phi$oH	ϕoϕo$\phi$$SO_2$$\phi$oH
		Ho$\phi\phi$oϕo$\phi$$SO_2$$\phi$oH

SECTION C.X

The Condensable Volatile Product Fraction of Degradation to 1020°C of ATS and Related Polymers

To complete our knowledge of the mechanisms of thermal degradation of ATS polymers, it was essential that we gain some understanding, both qualitatively and quantitatively, of the volatile product fractions from those polymers. In this section we deal with the condensable volatile products of degradation, and in the next we deal with the noncondensable product fractions of degradation.

(1). Sub-Ambient Thermal Volatilization Analysis (SATVA) and Identification of Condensable Volatile Products of Degradation

This section may be considered in two parts. We first of all set out to identify condensable volatile products of degradation of ATS and related polymers. We next sought to estimate quantitatively the proportions of each measurable component of the condensable volatile product fractions from each polymer under investigation.

In order to obtain large enough quantities of condensable volatile material for definitive spectroscopic analysis, large quantities of polymer were degraded under vacuum in the TVA oven assembly, usually to end or upper temperatures of 1020°C. For example, we commonly degraded quantities up to 500mg or 1g of ATS-G (the polymer most often used in these qualitative investigations). It must be noted in passing that the large surface area of the sample "boats" used in the TVA experiment ensured a low sample thickness even with the biggest of samples. The experimental arrangement used here was simple. We first of all degraded the polymer by programmed heating in the TVA oven assembly. The condensable volatile products of degradation were trapped in a "U"

tube on the vacuum line and transferred at the end of the experiment to the SATVA tube for separation on a volatility basis. A SATVA curve produced by volatiles from a small sample of ATS-G is reproduced in Figure 81. The SATVA curves produced by the bigger samples used here were less well defined but retained the same general curve shape. Fractions 1-5 as discussed below refer to those five fractions "eluted" from the SATVA trap as annotated in Figure 81.

Fraction 1

This fraction was identified by gas phase Infrared spectroscopy as reproduced in Figure 82. The major identifiable constituents of this fraction were shown to be carbon dioxide, carbonyl sulfide, and sulfur dioxide. The presence of hydrogen sulfide in this product fraction was confirmed by difference gravimetry as outlined later in this discussion.

Fraction 2

This fraction was shown by Infrared spectroscopy to contain only sulfur dioxide (see Figure 83).

Fraction 3

The IR (Figure 84) and NMR (Figure 85) spectra of this fraction showed it to consist of benzene contaminated with traces of sulfur dioxide (Fraction 2), and phenol (Fraction 5).

Fraction 4

The gas phase IR (Figure 86) and proton NMR (Figure 87) spectra of this fraction prove it to be composed of water containing trace quantities of phenol.

Fraction 5

The proton NMR spectrum of this fraction as depicted in Figure 88 is identical to that of phenol. The slight possibility that said fraction may instead be composed of diphenylether (DPE) which produces a spectrum similar to that of phenol was dispelled by fractionating DPE on the vacuum line in the SATVA experiment as a reference compound as depicted in Figure 42. By virtue of its low volatility as expressed in this experiment, DPE may be present at most, in trace quantities in Fraction 5.

Having established the major components of the condensable volatile product fractions of ATS polymers as carbon dioxide,

carbonyl sulfide, hydrogen sulfide, sulfur dioxide, benzene, water, and phenol; we next initiated a program of work to estimate their proportions in each product mixture. We first of all, simply compared SATVA traces of product mixtures from the different polymers under investigation. Due to the nature of the Pirani response, peak heights or areas are not directly proportional to the quantity of material which is transferred from the SATVA trap to the receiving trap on the vacuum line. Pirani outputs also vary from material to material due to differences in thermal conductivity, with the result that peak heights or areas produced by differing materials cannot be directly compared. On the other hand, the SATVA trace for a polymer is very reproducible and qualitative comparisons can be made of corresponding peak heights within a class of polymers which produce the same product of degradation. A comparison of SATVA outputs at the peak maxima of fractions 1-5 for ATS and related polymers is made in Table 20 which also contains a key to the relevant Figure numbers. Owing to the small amount of F5 on hand, we could only degrade a small sample for subsequent SATVA fractionation. A SATVA curve produced by products of degradation of F5 is reproduced in Figure 89. The similarity between this product mixture and those produced by the other ATS polymers (allowing for the difference in sample size and therefore SATVA curve shape) suggest a similar degradation pathway.

TABLE 20 SATVA RATE MAXIMA PRODUCED BY ATS AND RELATED POLYMERS

(Sample size : 100mg)

Polymer	Fraction 1	Fraction 2	Fraction 3	Fraction 4	Fraction 5	Figure #
ATS Monomer	2.9	6.5	4.9	6.4	5.6	90
ATS-G	2.9	6.4	4.9	6.7	5.2	81
ATS Dimer	3.3	6.6	4.4	6.5	5.3	91
ATS Trimer	5.5	6.4	4.1	6.5	5.0	92
F4	6.1	6.3	4.6	7.1	5.2	93
Radel^{tm}	3.3	6.5	4.2	6.1	4.5	94
ATP Monomer	3.2	...	3.3	6.4	3.9	95

ATS-G, ATS monomer, ATS dimer, Radel^{tm}, and ATP monomer all produce similar amounts of the product mixture designated as Fraction 1, as measured by SATVA. F4 produces larger amounts as does ATS trimer, possibly because of contamination of this fraction by F4. It must be emphasized that the Pirani response "flattens out" at higher pressure readings with the result that small differ-

ences as may be evident between yields from ATS-G - ATP monomer are not visible here. In fact, this comment may be applied, where applicable, to each of the following discussions.

With the obvious exception of ATP monomer which does not contain any sulfone, all the other polymers produced similar amounts of sulfur dioxide (Fraction 2) product as measured by this technique.

ATS-G and ATS monomer both were shown within the limits of this experiment, to produce similar amounts of benzene or Fraction 4, as isolated by the SATVA technique. ATS dimer and Radel^{tm} thermoplastic produce smaller quantities of benzene, presumably for the simple reason that a smaller proportion of these materials are left in the hot zone at the temperatures at which this class of reaction becomes important.

ATS monomer, dimer, trimer, and ATP monomer all produce similar amounts of water. F4 produces more water (or Fraction 4), presumably by decompositons of its hydroxyl content. ATS-G also produces more water, most probably as a result of decompositions of abnormal components of the mixture such as F4 and F5. Radel^{tm} produces less water, possibly in part due to the fact that a smaller proportion of this polymer is present in the hot zone at the high temperatures at which water is formed in quantity by the sequency of reactions designated as "Process 2 of degradation."

ATS-G, ATS monomer, ATS dimer, ATS trimer, and F4 produce similar amounts of phenol or Fraction 5 of the SATVA separation. Radel^{tm} and ATP monomer on the other hand produce smaller quantities of this component. This observation may be rationalized by the following discussion. Phenol is produced by sulfone promoted phenoxy bond scissions in Process 1 of thermal degradation of ATS polymers, as illustrated in Figure 47 of this report. Phenol is also produced in Process 2 of thermal degradation of ATS polymers by less discriminate phenoxy bond scissions. As mentioned earlier, a smaller proportion of Radel^{tm} is present in the hot zone at the commencement of Process 2 of degradation. As such, the combined yield of phenol from Radel^{tm} is less than from the ATS polymers. By a similar argument it follows that as Process 1 appears to be inoperative within the resin from ATP monomer, the combined yield of phenol from this polymer is less than from the sulfone containing resins.

It is obvious from the preceding discussion that although adequate for qualitative comparisons of the condensable volatile product distributions from ATS polymers, this technique is not sufficiently sensitive to distinguish between yields of most product fractions from most of the polymers of interest here. As such, we were required to make a quantitative estimate of each volatile component by the more exacting techniques of Infrared and proton Nuclear Magnetic Resonance Spectroscopy. Before this was attemped, we first gained a more detailed picture of the temperature profiles of condensable volatile formation, by a comparison of

SATVA separations of volatile product fractions produced by ATS and related polymers over defined temperature intervals.

(2). A Comparison by SATVA of the Rate Profiles of Formation of the Condensable Volatile Product Fractions of Degradation of ATS-G and ATS Dimer

The condensable volatile product fractions of degradation of ATS-G and ATS dimer over defined temperature intervals of interest were examined by SATVA. The details of this experiment are contained in Table 21. Figures relevant to this discussion range from numbers 96 to 106.

It can be seen that the rate profiles of formation of condensable volatile products within the two polymers are similar within the limits of precision afforded by the SATVA experiment. It can also be seen that Process 1 of degradation, as depicted in Figure 47, is operative over a very wide temperature interval approximated by the limits (284-567)°C, producing sulfur dioxide, phenol, and small amounts of water. Process 2 of thermal degradation as identified also in Figure 47, appears to operate over a more narrow temperature range approximated by the interval (496-625)°C, producing water, benzene, and phenol.

TABLE 21 KEY TO SATVA SEPARATIONS

ATS-G		ATS Dimer	
Temperature Interval (°C)	Figure Number	Temperature Interval (°C)	Figure Number
238 - 424	96	238 - 355	97
		355 - 424	98
426 - 461	99	426 - 461	99
461 - 496	100	461 - 496	100
496 - 532	101	496 - 532	101
532 - 567	102	532 - 567	102
567 - 625	103	567 - 625	103
625 - 661	104	625 - 661	104
661 - 851	105		
851 - 1020	106		

It is interesting to note that proportionately large amounts of benzene and especially water are produced in the very early stages of degradation of both polymers as indicated in Figures 96-98. This would suggest that small amounts of phenolic chain ends may be formed in both polymers at abnormally low temperatures, an observation agreeing with results contained in Part B of this communication.

As we "scan" through volatile "packets" produced over progressively higher temperature intervals it becomes apparent that the same two major overlapping processes operate in ATS-G and ATS dimer to produce condensable volatile products. At lower temperatures, the major condensable products are sulfur dioxide and phenol. The production of sulfur dioxide, the definitive "marker" of the first process, achieves a rate maximum somewhere in the temperature range (461-532)°C. At progressively higher temperatures the production of sulfur dioxide decreases to cease above 567°C. Phenol, a co-product of the first process, on the other hand, continues to be produced at higher temperatures along with water and benzene. In quantitative terms, by using benzene as product marker for the second process, we can see that the rate profile of this second process is more narrow than that of the first, covering the temperature interval (532-625)°C. Even so, very small amounts of benzene, water, and phenol continue to be produced at temperatures up to 1020°C.

(3). SATVA of the Condensable Volatile Product Fractions of Thermal Degradation of F4

The ultimate goal of this work was to gain some understanding of the mechanisms of degradation of ATS polymers in general, and, on a more mundane level, to accumulate data to aid in the evaluation of the ATS-G resin mixture as a potential high stability/high performance matrix resin for aerospace applications. To this end, we felt obligated to examine the degradative pathways of some of the low yield impurities which we had separated from the resin mixture by column chromatography. One such component, F4, displayed characteristics sufficiently removed from the basic ATS system to warrant further study on the basis of its possible influence on the mixture as a whole.

The condensable volatile products of thermal degradation of F4 in the temperature intervals (234-307)°C, (307-450)°C, and (450-485)°C, as depicted in the TVA trace of Figure 51, were examined by SATVA fractionation to gain some idea of the temperature profiles of volatile product formation.

(234-307)°C

Water, as indicated in Figure 107, appears to be the major product of degradation in this temperature range. It is presumably formed by decompositions of hydroxyl groups within F4.

(307-450)°C

Large amounts of water and carbon dioxide are produced in this temperature interval along with some sulfur dioxide, phenol, and the noncondensables methane and carbon monoxide (both detected by gas phase IR spectroscopy of the noncondensable product fraction of degradation in this temperature interval). Carbon dioxide is usually formed by decompositions of di- or multi-oxygenated groups such as acids, esters, anhydrides, and the like. However, an Infrared spectroscopic examination of F4 indicated an absence of carbonyls. An alternate mechanism for the formation of carbon dioxide in normal ATS resins at higher temperatures will be postulated in a later section. Briefly, this route hinges on the attack of carbon monoxide, an expulsion product of ring fusion reactions, on polymeric oxygen, presumably in the form of phenoxy radical from scissions of the polyphenylether backbone of the polymer. The transient dioxide would subsequently be removed from the polymer as carbon dicxide. We now postulate here that the same process is operative within F4 except at lower temperatures, due to its accelerated decompositions. Water is formed in large quantities, presumably via the same phenoxy radicals, after termination to form the phenol. Methane is probably produced in this temperature interval by decompositions of saturated material within the polymer.

(450-485)°C

An analysis of SATVA, as depicted in Figure 109, shows that sulfur dioxide and phenol are the major products of degradation in this temperature interval, along with large amounts of water. Both materials are products in bulk of Process 1 of degradation of normal ATS polymers as defined in Figure 47 of this report. Their mechanisms of formation will be discussed here in the final or "Discussions" section. Water, on the other hand, is a minor product of this process. In contrast, water constitutes a large portion of the product fraction from F4 in this temperature interval. The absence of appreciable amounts of carbon dioxide from this product mixture possibly reflects a decline in the production of carbon monoxide as reflected in the CATVA/TGA trace for the polymer (Figure 51).

(4). Analysis by Quantitative Gas Phase IR Spectroscopy

(a). Product Yields

The condensable volatile product fractions of degradation of ATS and related polymers were examined by quantitative gas phase IR spectroscopy using protocols outlined in Part A of this report. By this method, quantitative yields of carbon dioxide, sulfur dioxide, and carbonyl sulfide were obtained for all polymers of interest. This information is listed in Table 22. From this data, the

percentage conversions of each polymer to sulfur dioxide and carbonyl sulfide were estimated as reproduced in Table 23.

To generalize, it may be stated that no broad trends emerged from this work - although some relationships could be discerned; for example, the absolute yields of carbon dioxide were shown to increase with the oxygen content of the polymer and to be high in those polymers which initially contained hydroxylic material. In a similar vein, it can be seen that the percentage yields of sulfur dioxide from Radel^{tm}, ATS trimer, and F4 are lower than expected, possibly because sulfone groups contained in those polymers are efficiently removed from the hot zone within the high boiling point product fractions of degradation prior to their conversion to sulfur dioxide. The yields of carbonyl sulfide appeared to increase from ATS monomer through ATS dimer to ATS trimer with the yield from ATS-G as intermediate between the first two. The yields of this material, therefore, appeared to be inversely related to the polyene concentration in the polymer (or to be directly proportional to the weight fraction of resin backbone in the polymer).

TABLE 22 CONDENSABLE VOLATILE PRODUCT GAS ANALYSIS BY QUANTITATIVE GAS PHASE INFRARED SPECTROSCOPY

	Product as a Weight % of the Cured Polymer		
Polymer	CO_2	SO_2	COS
ATS-G	1.2	10.7	0.31
ATS Monomer	1.2	11.4	0.14
ATS Dimer	1.8	14.4	0.37
ATS Trimer (s)	2.1	10.1	0.41
F4	2.3	7.0	0.64
VAA (s)	3.7	11.7	0.22
Radel^{tm} (s)	1.5	11.7	0.14
ATP Monomer (s)	0.9	....	....

Key : (s) : Single Measurement

From Table 23 it can be seen that the conversions of sulfur to sulfur dioxide and carbonyl sulfide, two mutually exclusive pro-

ducts of degradation, were not found to be inversely related. In fact, the yields of carbonyl sulfide from these polymers may be more closely related to the yields of carbon monoxide from the polymer.

TABLE 23 PERCENTAGE CONVERSIONS OF SULFUR, IN ATS AND RELATED POLYMERS TO SULFUR DIOXIDE AND CARBONYL SULFIDE

Polymer	Wt% Sulfur in Cured Polymer	% Conversion to SO_2	%Conversion to COS
ATS-G	6.6 (i)	81.1	2.5
ATS Monomer	6.9 (ii)	82.6	1.1
ATS Dimer	7.6 (ii)	95.4	2.6
ATS Trimer (s)	8.0 (ii)	62.7	2.7
F4	6.4 (iii)	54.7	5.3
VAA (s)	6.0 (ii)	96.7	1.9
Radel^{tm} (s)	8.0 (iv)	73.1	0.9

Key :
(s) : Single measurement
(i) : By elemental analysis of the cured polymer
(ii) : Based on an experimentally derived resin molecular weight (for method consult Reference 15)
(iii) : Based on an estimated molecular weight (for method consult Reference 15)
(iv) : Based on the concentation of sulfur in the polymer repeat unit

(b). Conversion Curves

Having established the final yields of low boiling point condensable volatile products from ATS and related polymers, we next determined to establish their rate profiles of formation using ATS-G as a typical model resin. The experimental procedure used to this end was simple. Samples of resin weighing 100mg were degraded in the TVA apparatus and the "packets" of volatile products formed over defined temperature intervals were examined by quantitative gas phase Infrared spectroscopy. Cumulative conversion curves to the products of interest; namely sulfur dioxide, carbon dioxide, and carbonyl sulfide; were then constructed as shown in Figure 110. From this curve it can be seen that sulfur dioxide is produced in a one step process. On the other hand, carbon dioxide and carbonyl sulfide are shown to be produced in two step processes of degradation.

Below 600°C, the rate profile for the formation of carbon dioxide parallels that for sulfur dioxide, possibly because the former (if our reasoning is correct), being produced by attack of carbon monoxide (a low yield product of thermal degradation in this temperature

interval) on phenoxy radicals, is maximized when those same phenoxy radicals attain peak concentrations in the polymer. As the rate profile of formation of those radicals parallels the production of sulfur dioxide in this temperature interval, then the production of carbon dioxide should parallel that of sulfur dioxide. Above 600°C, carbon dioxide is probably formed by attack of carbon monoxide on phenoxy radicals which are formed by random scissions of phenyl ethers remaining in the polymer after completion of the sulfur dioxide forming process.

The mechanism(s) of formation of carbonyl sulfide in ATS polymers will be discussed in a later section of this report. In brief, we suggest that a portion of the sulfone links in ATS polymer are reduced to sulfides by removal of oxygen. A proportion of these sulfide links then undergo homolytic scissions to produce the sulfide radical which may be attacked by carbon monoxide to form an unstable end-cap which breaks off to form carbonyl sulfide. Its formation in a two step process may, therefore, reflect either a double rate maximum in the formation of carbon monoxide or of sulfide radicals in the polymer.

(5). Hydrogen Sulfide by Difference Gravimetry

Hydrogen sulfide was detected by smell in the condensable volatile product fractions of degradation of ATS polymers. By virtue of its volatility and associated evolution profile in the SATVA experiment, as reproduced in Figure 42, we can state with some certainty that it would be volatilized from the SATVA trap along with carbonyl sulfide and carbon dioxide in the first eluent fraction. Being unable to make a positive identification of the material with Infrared spectroscopy, we resorted to the technique of difference gravimetry to infer the presence of hydrogen sulfide in the product mixture. We first measured the distribution of elemental sulfur in the product fractions of degradation as illustrated in Table 24. From this measurement we could see that about 10 percent of the initial sulfur content or about 0.7 weight percent of the polymer could not be accounted for. We next weighed the first two fractions evolved in the SATVA experiment by procedures outlined in Part A of this text, arriving at the measurements reproduced in Table 25. Subtracting from this weight the known amounts of sulfur dioxide, carbon dioxide, and carbonyl sulfide as measured by quantitative gas phase Infrared spectroscopy, we arrived at a discrepancy of about 0.6 weight percent of the cured polymer. Taking into account the cumulative errors involved in these measurements, the close agreement of these two measurements, (0.6 - 0.7) wt %, would appear to lend some credence to our argument that hydrogen sulfide is indeed a volatile product of degradation of ATS polymers.

(6). Analysis by Quantitative Proton Nuclear Magnetic Resonance (NMR) Spectroscopy

Liquid components of the condensable volatile product fractions of degradation of ATS polymers were examined by quantitative NMR spectroscopy as outlined in the first part of this discussion. As expected, phenol was shown to be a high yield, and benzene and water to be low yield products of the thermal degradation of ATS polymers, possibly as a result of decompositions of abnormal components of the ATS-G mixture. Most importantly, the relative yields of benzene from the three polymers did not vary in any manner which would suggest that it is formed by decompositions of the polyene crosslink. (If this were the case then the yield of benzene from ATS monomer would be considerably higher than the corresponding yield from ATS dimer.)

TABLE 24 DISTRIBUTION OF SULFUR IN THE PRODUCTS OF THERMAL DEGRADATION TO 1020°C OF PRECURED ATS-G

Product	Wt % Sulfur
SO_2	81.1
COS	2.5
Sulfur in the Residue of Degradation	6.1
Sulfur in the Oligomeric Products of Degradation	0.1
Total	89.8
Total Unaccounted for	10.2 (about 0.7 wt% of the Cured Polymer)

TABLE 25 GRAVIMETRY OF THE CONDENSABLE VOLATILE PRODUCTS, OF THERMAL DEGRADATION TO 1020°C OF ATS-G, CONTAINED IN SATVA FRACTIONS 1 AND 2

Product	Wt% of Cured Polymer
SO_2	10.7
CO_2	1.2

Product	Wt% of Cured Polymer
COS	0.3
Total	12.2
SATVA Fractions 1 and 2 by Gravimetry	12.8
Total Unaccounted for	0.6 Wt% of the Cured Polymer

TABLE 26 CONDENSABLE VOLATILE PRODUCT ANALYSIS BY QUANTITATIVE PROTON NUCLEAR MAGNETIC RESONANCE (NMR) SPECTROSCOPY

Polymer	Wt% of Cured Polymer		
	Benzene	Phenol	Water
ATS-G	2.1	11.6	4.9
ATS Monomer	1.7	10.2	1.3
ATS Dimer	2.1	11.1	2.0

SECTION C.XI

The Noncondensable Volatile Product Fraction of Degradation of ATS Polymers

(1). Product Yields

The noncondensable volatile product fractions of thermal degradation to 1020°C of ATS monomer, ATS-G, ATS dimer, and Radel™ were examined by quantitative gas phase Infrared spectroscopy using the method developed in Part A of this discussion, to yield the results reproduced in Table 27. It can be seen that the yield of both methane and carbon monoxide increase from Radel™ through ATS dimer then ATS-G to ATS monomer, in other words, with the polyene concentration in the original polymer. The product mole ratios of methane to carbon monoxide shown in Table 28 did not appear to vary much between the three ATS polymers under investigation but differed from that of material from Radel™.

TABLE 27 NONCONDENSABLE PRODUCT GAS ANALYSIS BY QUANTITATIVE GAS PHASE IR SPECTROSCOPY

	Wt% of Cured Polymer		
Polymer	CO	CH_4	Total
ATS Monomer	7.4	3.6	11.0
ATS-G	6.2	3.0	9.2
ATS Dimer	5.1	2.6	7.7
Radel^{tm}	4.9	0.6	5.5

TABLE 28 METHANE/CARBON MONOXIDE PRODUCT RATIOS

Polymer	CH_4/CO Mole Ratio
ATS-G	0.85
ATS Monomer	0.85
ATS Dimer	0.89
Radel^{tm}	0.21* 0.83**

Key :
* : Overall Yield
** : Yield in Process 2 of Degradation

(2). Product Distribution Within Processes 3 and 4 of Degradation

Noncondensable volatile products of degradation are formed in the thermolysis of ATS polymers by a two stage process, which we previously designated as Processes 3 and 4 of degradation of ATS polymers (Figure 47). In this attempt to separate out the products of Processes 3 and we chose ATS-G as a model system with fairly average characteristics. We chose also the thermoplastic polysulfone polymer "Radel^{tm}" for these measurements to allow us to compare polymers with like structures with and without the polyene cross-link.

To separate out the two noncondensable producing reactions we simply heated the polymer to a temperature intermediate between the two noncondensable producing reactions and held it there to drive

the first process to completion. We then heated the sample to 1020°C to drive the second reaction to completion. Noncondensable products from both processes could, therefore, be trapped separately for quantitative analysis by gas phase Infrared spectroscopy as outlined in Section A of this report. Radel[tm] was heated at 5°C/min under high vacuum conditions to 614°C and held there for 20 min to drive the first volatile producing reaction to completion. The same sample was then heated to 1020°C to drive the second noncondensable volatile producing reaction to completion. ATS-G was examined in a similar manner except that it was heated to an intermediate temperature of 661°C. Yields of carbon monoxide from Processes 3 and 4 of degradation may be inspected in Table 29.

TABLE 29 DISTRIBUTION OF CARBON MONOXIDE BETWEEN PROCESSES 3 AND 4 OF DEGRADATION

	% of Combined Carbon Monoxide Yield	
Polymer	Process 3	Process 4
ATS-G	76	24
Radel[tm]	26	74

It can be seen from Table 29 that carbon monoxide is predominantly formed in ATS-G by Process 3 of degradation. Carbon monoxide from Radel[tm] is predominantly formed in the higher temperature interval usually designated as "Process 4." Methane was shown by quantitative gas phase Infrared spectroscopy to be the major product of Process 4 of degradation of ATS polymers but to be only a minor product of the degradation of Radel[tm] in the same temperature interval.

This information is used by the authors to propose the existence of two processes which are operative within high temperature stable phenylether containing polymers to produce carbon monoxide. A low temperature process predominates in ATS polymers to produce carbon monoxide and form material which subsequently decomposed with approximately 90% efficiency to produce methane. This low temperature process is promoted by the presence of polyene crosslinks within the polymer. It will be postulated in Section C.XII of this report that this process (Process 3 of degradation) is a ring fusion reaction which converts the polymer (via Process 4 of degradation) to a thermally stable polyaromatic "char" residue.

Process 3 of degradation is operative to only a small extent in Radel[tm]. At higher temperatures, approximating the temperature range designated as "Process 4" of degradation of ATS polymers, a second process of degradation is operative within the Radel[tm] thermoplastic, to form a residue which is stable to further

decomposition. No further information is available as to the nature of this decomposition reaction.

SECTION C.XII

Discussion

Most of the relevant features of the mechanisms of decomposition of ATS polymers have been touched upon in previous sections. Here we draw those ideas together to discuss and comment upon the major degradation pathways which operate in this class of material. For brevity, we have divided this seciton into sub-sections, each of which presents information relating to one or a related group of reactions involved in the degradation of this class of polymer.

To recap on earlier discussions, we have established four major overlapping processes which operate consecutively in ATS polymers. The first detectable process removes sulfur dioxide, phenol, a little water, and some sulfur containing high boiling point material from ATS polymers. The second process removes benzene, water, and some more high boiling point material (differentiated from that removed by the first process by the presence of some diphenyl linkages and the absence of sulfones). The third and fourth processes of decomposition then remove carbon monoxide, methane, and some hydrogen from the polymer in differing ratios.

Some individual reactions not attributable to one of the four major processes of degradation were also identified. These are discussed on an individual basis.

(1). Production of Sulfur Dioxide and Phenol in Process 1 of Degradation

The rate profiles of formation of sulfur dioxide and phenol (at low temperatures) appear to coincide, indicating a somewhat concerted mechanism of formation. Of course such is essential to an understanding of the formation of phenol in this temperature range, as such, in the absence of neighbouring sulfone, as is found with ATP monomer, is formed only at much higher temperatures. We propose here that sulfur dioxide be formed by two processes. The first process we envisage as simple scission of SO_2 from the resin backbone leaving behind two phenyl radicals which may combine to form the diphenyl linkage, or which may terminate by hydrogen abstraction to form pendent groupings on the polyene. The second process, we postulate as a phenoxy bond scission "alpha" to the sulfone to form the phenoxy radical which is stabilized by resonance into the sulfone group, and which is subsequently removed from the

polymer as phenol in concert with sulfur dioxide, (after hydrogen abstraction to form the phenolic chain end). Phenol is, therefore, a co-product of a proportion of the sulfone bond scissions. It must be noted that if this second process does indeed occur in ATS polymers, then the residual free radical products of that process would probably terminate by hydrogen abstraction to form pendent groupings on the polyene chain. The first process is visualized in Figure 111 and the second in Figure 11..

(2). *Formation of Some High Boiling Point Products of Process 1 of Degradation*

High boiling point products of degradation which were unambiguously identified as products of Process 1 of degradation on the basis of work contained in earlier sections, are listed in Table 30. It must be emphasized here that these, in all probability, represent only a proportion of the high boiling point products produced in Process 1 of degradation.

TABLE 30 SOME HIGH BOILING POINT PRODUCTS OF PROCESS 1 OF DEGRADATION OF ATS POLYMERS

	Polymer		
Product	ATS Monomer	ATS-G	ATS Dimer
1	$\phi o \phi SO_2 \phi$	$\phi o \phi SO_2 \phi$	$\phi o \phi SO_2 \phi$
2	$\phi o \phi SO_2 \phi o \phi$		
3	$\phi o \phi SO_2 \phi o \phi CH_3$		$\phi o \phi SO_2 \phi o \phi CH_3$
4	$Ho \phi SO_2 \phi oH$		
5	$\phi o \phi SO_2 \phi oH$	$\phi o \phi SO_2 \phi oH$	$\phi o \phi SO_2 \phi oH$
6		$\phi o \phi o \phi SO_2 \phi oH$	$\phi o \phi o \phi SO_2 \phi oH$
7			$Ho \phi \phi o \phi o \phi SO_2 \phi oH$
8	$HoS=O[(o\phi)(\phi)_2]$		$HoS=O[(o\phi)(\phi)_2]$

Before mechanisms can be postulated to account for the formation of products numbered 1 through 7, it becomes necessary to propose the existence of a thermal derivative of the polyene crosslink and two subsequent degradation pathways. This derivative and a likely mechanism for its formation from the parent polyene and subsequent decomposition, are discussed below.

We, first of all, propose that a double bond migration takes place within the polyene chain to form a cyclic six membered ring with diene functionality. This transition state may then aromatize by the expulsion of adjacent substituents (hydrogen and phenyl) as H-ϕ. This type of reaction would, of course, account for the presence of long chain phenoxy's such as those containing the residue $\phi o \phi o \phi$ in the product mixture. Alternatively, the cyclic transition state could decompose at the saturated linkage prior to aromatization. A proportion of the products from this reaction could carry with them a methyl end cap, thus accounting for those high boiling point products designated as R-CH_3. The first decomposition pathway we designate as "Reaction 2 of the polyene crosslink." The common initial step is illustrated in Figure 113, the first decomposition pathway in Figure 114, and the second degradation pathway in Figure 115.

In order to complete our description of the origin of these products, we must propose a new class of reaction operative within ATS polymers, that of diphenyl promoted phenoxy bond scissions. Diphenyl linkages would most probably be formed within ATS polymers by coupling of phenyl radicals, for example, after expulsion of sulfur dioxide. These diphenyls could subsequently promote phenoxy bond scissions in much the same manner as the sulfone linkage itself by resonance stabilization of the resulting free radical products of scission. This reaction is illustrated in Figure 116.

Having accepted these arguments, we are able to rationalize the mechanisms of formation of most of the high boiling point products cited in Table 30. Most of these materials are produced by at least two reactions on the base resin. We of course make no attempt here to precisely sequence those reactions except to make the observation that all rearrangements should be complete prior to volatilization of the segment from the hot zone. Using this pragmatic approach, it becomes possible to suggest a most probable ordering of reactions. A recount of the types of reactions responsible for the formation of products designated as #'s 1-7 in Table 30 is made in Table 31.

TABLE 31 MECHANISMS OF FORMATION OF SOME HIGH BOILING POINT PRODUCTS OF PROCESS 1 OF DEGRADATION OF ATS POLYMERS

Product #	Reaction #'s (in most probable order)
1	3, 4, 1
2	1 (twice)
3	1, 2
4	3 (twice)

Product #	Reaction #'s (in most probable order)
5	3, 1
6	3, 8, 5
7	3, 8, 6, 7

Table 31, Key to Reaction #'s

#1: Reaction 1 of the polyene crosslink

#2: Reaction 2 of the polyene crosslink

#3: Sulfone promoted bond scissions

#4: Removal (as water) of hydroxylic chain ends generated by sulfone promoted phenoxy bond scissions

#5: Radical abstractions, after the removal of sulfur dioxide, to form inactive chain ends

#6: Radical recombinations, after the removal of sulfur dioxide, to form diphenyl linkages

#7: Diphenyl promoted phenoxy bond scissions

#8: Sulfone bond scissions to form sulfur dioxide

(3). Production of Benzene, Water, and Phenol in Process 2 of Degradation

Process 1, we have shown, quantitatively removes sulfur dioxide from ATS polymers, leaving behind polyene clusters which contain phenylether substituents. A portion of these "clusters" are linked by diphenyl bridges to other such clusters to form an involatile network throughout the material. Process 1 of degradation also produced sulfur dioxide and phenol by a concerted reaction. The involatile products of this reaction would be further separated in space, and therefore less likely to terminate by combination to the diphenyl, and more likely to terminate by hydrogen abstraction to form pendent residues on the polyene derivative. Some possible pendent residues are listed in Table 32 along with most probable mechanisms of formation (such mechanisms as defined in Table 31).

These residual structures can decompose by a number of routes forming a wide range of products. For example, simple chain end scissions of groups pendent on the polyenes would produce phenol, benzene, and water as is shown in Figure 117 Part (a). The ability of the polyene residue to delocalize and, therefore, stabilize

radicals would favor the production of phenol over that of water and benzene. In a similar vein, if we accept that the diphenyl linkage promotes neighbouring phenoxy bond scissions, then a mechanism becomes available for the production of water (but not benzene due to the stability of the diphenyl linkage), as is outlined in Figure 117, Part (b). The reaction which produces phenol we designate as #9 while the sequence producing equal amounts of water and benzene we designate consecutively as #'s 10 and 11. The diphenyl promoted phenoxy bond scission we, of course, have previously designated as reaction #7. The consecutive process to crack water off the diphenyl we now designate as reaction #11.

If these rationalizations are correct, then some qualitative estimations may be made as to the relative yields of condensable volatile products of degradation. For example, phenol should be a high yield product of reaction #9. Water and benzene should be produced in equal molar yields by processes #10 and 11, while water should be the sole product of reactions 7 then 11 as depicted in Figure 117. If these assertions are valid, then the molar yield of water should be higher than that of benzene. This was confirmed by experimentation which yielded the results reproduced in Table 33.

TABLE 32 MOST PROBABLE MECHANISMS OF FORMATION OF PENDENT RESIDUES ON THE POLYENE CROSSLINK

Residue Structure	Reaction #'s (in most probable order)
From ATS Monomer	
H-ϕ	3, 5
H-ϕoϕ	8, 5
H-ϕoϕϕoϕ-H	8, 6
From ATS Dimer	
H-ϕ	3, 5
H-ϕoϕ	8, 5
H-ϕoϕϕoϕ	3, 5, 8, 6
H-ϕoϕϕoϕoϕ	8, 8, 6, 5
H-ϕoϕϕoϕoϕϕoϕ-H	8 (twice), 6 (twice)

TABLE 33 WATER/BENZENE PRODUCT MOLE RATIOS FOR ATS POLYMERS

: (Samples heated to 1020°C) :

Polymer	Water/Benzene Product Mole Ratio
ATS Polymer	3.3
ATS Dimer	4.1

(4). Formation of Some High Boiling Point Products of Process 2 of Degradation of ATS Polymers

Some high boiling point products which could be unambiguously identified with the second process of degradation of ATS polymers are listed in Table 34. To avoid ambiguity, products are listed from #9 upwards to avoid any confusion with those listed in Table 30.

TABLE 34 SOME HIGH BOILING POINT PRODUCTS OF PROCESS 3 OF DEGRADATION OF ATS POLYMERS

Product #	From ATS Monomer	From ATS-G	From ATS Dimer
9	ϕoϕCH_3		
10	ϕϕoϕ	ϕϕoϕ	ϕϕoϕ
11	ϕoϕoϕ*	ϕoϕoϕ	ϕoϕoϕ
12	ϕoϕϕoϕ		ϕoϕϕoϕ
13	ϕϕoϕoϕ		ϕϕoϕoϕ
14			ϕϕoϕCH_3
15	ϕoϕϕoϕCH_3		ϕoϕϕoϕCH_3
16	ϕϕoH	ϕϕoH	ϕϕoH
17	ϕoϕoH*	ϕoϕoH	ϕoϕoH
18	ϕoϕϕoH	ϕoϕϕoH	ϕoϕϕoH
19			ϕoϕϕoϕoH
20			ϕoϕoϕoH*
21	Hoϕϕ oH	Hoϕϕ oH	Hoϕϕ oH
22	Hoϕϕoϕ oH*	Hoϕϕoϕ oH	Hoϕϕoϕ oH

Each of these products can be formed by phenoxy bond scissions of the type described in this section. A full list of processes involved in the formation of each product would serve no particular purpose. Instead, we chose a few at random to illustrate the degradation process. These "examples" are depicted in Table 35.

TABLE 35 MECHANISMS OF FORMATION OF SOME HIGH BOILING POINT PRODUCTS OF PROCESS 2 OF DEGRADATION OF ATS MONOMER

Product #	Reactions (in most probable order)
9	8, 5, 2
10	8, 6, 7, 11, 1
12	8, 6, 1, 1
15	8, 6, 1, 2
16	8, 6, 7, 11, 7

It is interesting to note that those products numbered 9 through 22 in Table 34 and identified by the symbol * can only be formed by decompositions of ATS species which contained extra phenoxy material of a type discussed in a previous publication[15].

(5). Production and Decomposition of Sulfide Linkages in ATS Polymers

Product 8 of the high boiling point product fraction of degradation of ATS polymers, as outlined in Table 30, can only be formed by attack of a phenoxy radical on the sulfone linkage. If such a reaction is possible then the sulfide linkage may be formed in ATS polymers by attack of phenyl radicals on the sulfone to eventually reduce that link to the corresponding sulfide. We showed in Figure 110 and associated discussion that carbonyl sulfide is formed in ATS polymers by a two step process. It has been shown elsewhere by a combined Thermogravimetric Analysis/Mass Spectrometric technique that hydrogen sulfide is formed in ATS polymers by a two step process with a very similar rate profile[20]. This would appear strong circumstantial evidence for the formation of carbonyl sulfide and hydrogen sulfide from a common precursor.

The double rate maximum for the formation of carbonyl sulfide and hydrogen sulfide may, in fact, result from a double rate maximum for the formation of sulfide linkages in the polymer. The first rate maximum would be achieved by attack on the sulfone linkage by phenyl radical generated in Process 1 of degradation, while the

second rate maximum would be achieved by attack on residual sulfone linkages by phenyl radicals generated in Process 2 of degradation.

This entire decomposition pathway is illustrated in Figure 118. The first step we envisage as attack of a radical on the sulfone linkage to form the corresponding ester which decomposes to remove an oxygen atom from the group. This occurs a second time to reduce the sulfone to the corresponding sulfide which undergoes homolytic scission to form the sulfide radical. The sulfide radical may hydrogen abstract to form the mercaptan end cap which is subsequently cracked off the resin to form hydrogen sulfide. Alternatively, the sulfide radical may react with carbon monoxide as it permeates through the resin, forming an unstable intermediate which decomposes to form carbonyl sulfide.

(6). Production of Carbon Dioxide in ATS Polymers

It was shown earlier in this discussion that small amounts of carbon dioxide are formed during the course of thermolysis of normal ATS polymers. A plausible explanation of the mechanism of formation of this product may be formulated by postulating that carbon monoxide, as it permeates through the resin, may react with phenoxy radicals in much the same manner as carbonyl sulfide is formed by reaction of carbon monoxide with sulfide radicals. The dioxygenated end cap so formed would then decompose to form carbon dioxide.

As illustrated in Figure 110, the rate profile of formation of carbon dioxide parallels that of sulfur dioxide in the early stages of degradation of ATS, presumably because a large quantity of phenoxy radicals are generated in this temperature interval by sulfone promoted bond scissions. Carbon dioxide is also produced at higher temperatures in ATS polymers by attack of carbon monoxide on phenoxy radicals which are produced by the more random scissions which characterize Process 2 of degradation.

(7). Processes 3 and 4 of Degradation

Any mechanistic explanation of the reactions involved in Processes 3 and 4 of degradation of ATS polymers must satisfy all of the following criteria. First of all, hydrogen and carbon monoxide must be explainable as products of Process 3 of degradation. Secondly, hydrogen and methane must be shown to be products of Process 4 of degradation. Both the methane and carbon monoxide yields and the proportion of "char" residue must increase with the polyene concentration in the AT polymer. The methane/carbon monoxide product ratio must be close to 1 and must not vary appreciably with the polyene concentration in the polymer. Finally, the polyene crosslink must be transformed in Process 3 of degradation to a derivative which is stable to fragmentation reactions to ensure a high "char" yield polymer.

We envisage the first step in "Process 3 of degradation" to consist of ring fusions of the polyene chain with pendent phenyls to form napthalenes and of pendent phenoxy ring fusions to form three ring furan containing heterocycles. Both processes, of course, produce hydrogen as a volatile by-product. These reactions are listed in Figure 119. In Figure 120 we visualize the subsequent expulsion of oxygen as carbon monoxide from the fused ring heterocycle to form a four membered bridged condensate; while in Figure 121, we visualize a polyene crosslink with its attendent array of fused heterocycle substituents. In a similar vein, we propose that "Process 4 of degradation" entails the rearrangement of the condensate products of Process 3 to the more stable anthracenes with concurrent expulsion of methane as shown in Figure 122. In Figure 123, we give our impression of the polyene derivative at this stage of degradation, while in Figure 124 we depict the product of successive ring fusions with expulsion of hydrogen, to form the polyaromatic cluster that is the polyene derivative at this point.

(8). High Temperature Decompositions of Radel^{tm} Thermoplastic

Although a lower char yield polymer than ATS, Radel^{tm} thermoplastic does express a somewhat similar degradation profile with respect to volatile emission in the temperature interval at which Processes 3 and 4 are operative in ATS polymers. We propose that similar processes are operative in this material, albeit to a lesser extent, due to the absence of the polyene which acts as a nucleus for polycondensation: *vis condensation across the phenoxy* linkage to form the corresponding tricyclic heterocycle with consecutive expulsion of carbon monoxide to form the four membered bridge (Process 3), then rearrangement to the corresponding napthalene (Process 4). These processes are illustrated in Figure 125. A tentative mechanism for the production of carbon monoxide in Radel^{tm} at high temperatures is illustrated in Figure 126.

(9). Parting Comments

We have shown in this report that acetylene terminated polymers indeed constitute a family of high use temperature resins. The thermal "weak link" in the ATS family of polymers is the sulfone bridge and not the polyene crosslink, which instead encourages the formation of highly stable aromatic polycondensates. Were it not for the high price of the AT system, we would urge that such polymers be evaluated as possible alternatives to the phenol formaldehyde resols as matrix materials for the formation of carbon/carbon composites.

REFERENCES

(1). I. C. McNeill, J. Polym. Sci., A4, 2479 (1966).
(2). I. C. McNeill, Europ. Polym. J., 6, 373 (1970).
(3). I. C. McNeill, L. Ackerman, S. N. Gupta, M. Zulfigar, and S. Zulfigar, J. Polym. Sci., Polym. Chem. Ed., 15, 2381 (1977).
(4). D. W. Breck, W. G. Eversole, R. M. Milton, T. B. Reed, and T. L. Thomas, J. Am. Chem. Soc., 78, 5963 (1956).
(5). C. V. G. Nair and P. Vijendran, Vacuum, 27(1), 549 (1977).
(6). I. C. McNeill and W. T. K. Stevenson, Polym. Deg. and Stab., 10, 247 (1985).
(7). W. T. K. Stevenson, Ph.D. Thesis, "Degradation of Polymers Based on Styrene and Butadiene," University of Glasgow, Scotland, U. K. (February 1981).
(8). I. C. McNeill, Europ. Poly. J., 3, 409 (1967).
(9). J. L. Koenig and C. M. Shields, J. Polym. Sci. Polym. Phys. Ed., 23, 845 (1985).
(10). P. M. Hergenrother, J. Macromol. Sci. Rev. Macromol. Chem., C19(1), 1 (1980).
(11). C. C. Kuo and C. Y-C Lee, AFWAL-TR-82-4037.
(12). C. Y-C Lee and E. J. Soloski, AFWAL-TR-82-4049.
(13). J. J. Ratto, P. J. Dynes, and C. L. Hamermesh, J. Polym. Sci. Polym. Chem. Ed., 18, 1035 (1980).
(14). J. J. Harrison and C. M. Selwitz, AFWAL-TR-79-4183.
(15). I. J. Goldfarb and W. T. K. Stevenson, AFWAL-TR-83-4011.
(16). M. Unroe, M. S. Thesis, Wright State University, Ohio (1982).
(17). I. C. McNeill and W. T. K. Stevenson, Polym. Deg. and Stab., 11, 123 (1985).
(18). T. G. Pearson and P. L. Robinson, J. Chem. Soc., p660, (1932).
(19). I. C. McNeill and W. T. K. Stevenson, Polym. Deg. and Stab., 11, 123 (1985).
(20). E. G. Jones, Personal communication to the authors.

FIGURES

KEY

P1 Pirani Gauge Before Sub Ambient Trap

P2 Pirani Gauge After Sub Ambient Trap

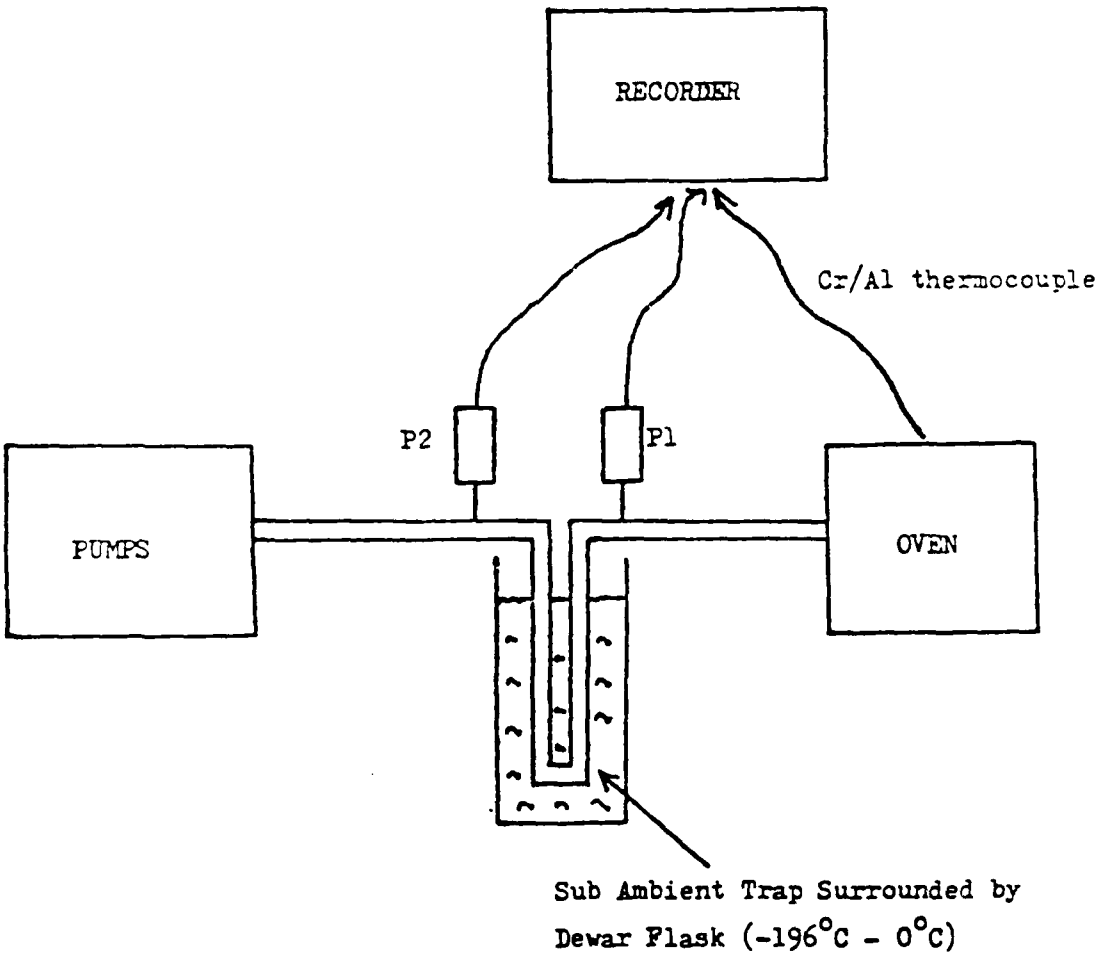

FIGURE 1 DIFFERENTIAL CONDENSATION TVA EXPERIMENT

(Styrene From Polystyrene : Methylmethacrylate From Polymethylmethacrylate)

(i) Trap Held at $0^{\circ}C$ or $-45^{\circ}C$

KEY

Pirani Gauge Before Trap

Pirani Gauge After Trap

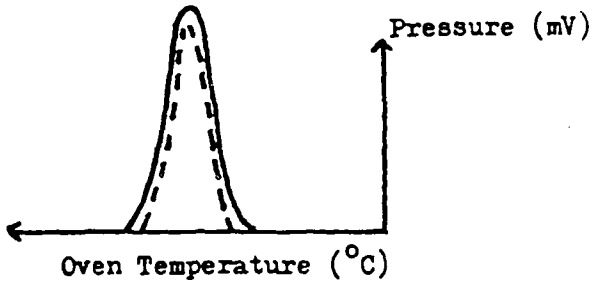

(ii) Trap Held at $-75^{\circ}C$

(limiting rate effect)

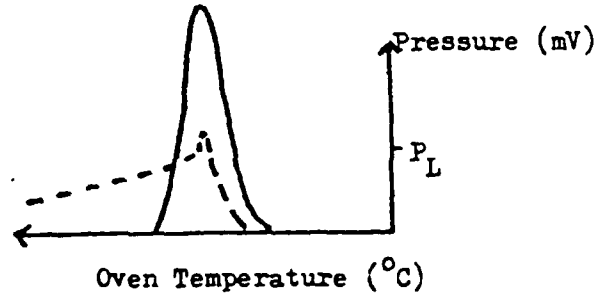

(iii) Trap Held at $-100^{\circ}C$ or $-196^{\circ}C$

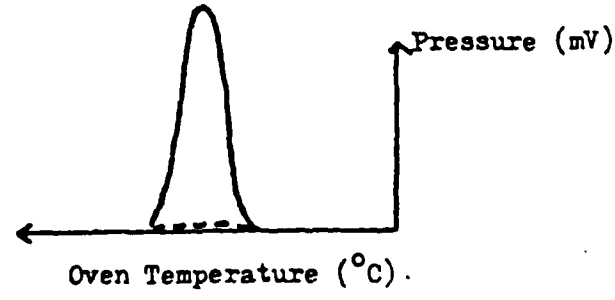

FIGURE 2 SOME POSSIBLE TVA CURVES FOR A SINGLE COMPONENT GAS FLUX

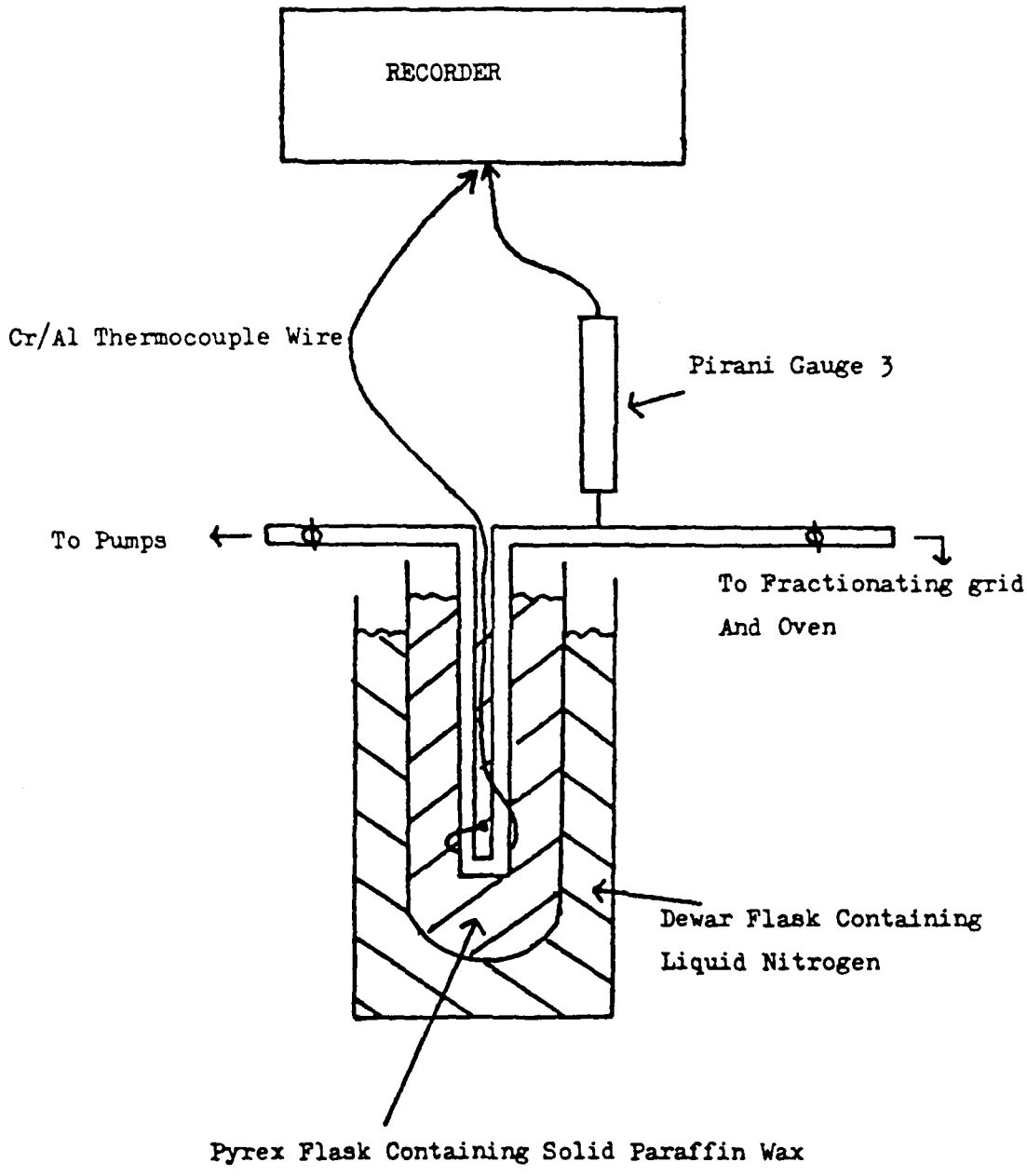

FIGURE 3 SUBAMBIENT THERMAL VOLATILIZATION (SATVA) ASSEMBLY

KEY

1 No Dewar Flask - Best for Separations in the Temperature Range (1.0 - 0) mV- Involatile Liquids

2 Warm Dewar Flask - Best for Separations in the Temperature Range (3.0 - 1.0) mV - Volatile Liquids

3 Cold Dewar Flask - Best for Separations in the Temperature Range (5.8 - 3.0) mV - Condensable Gases

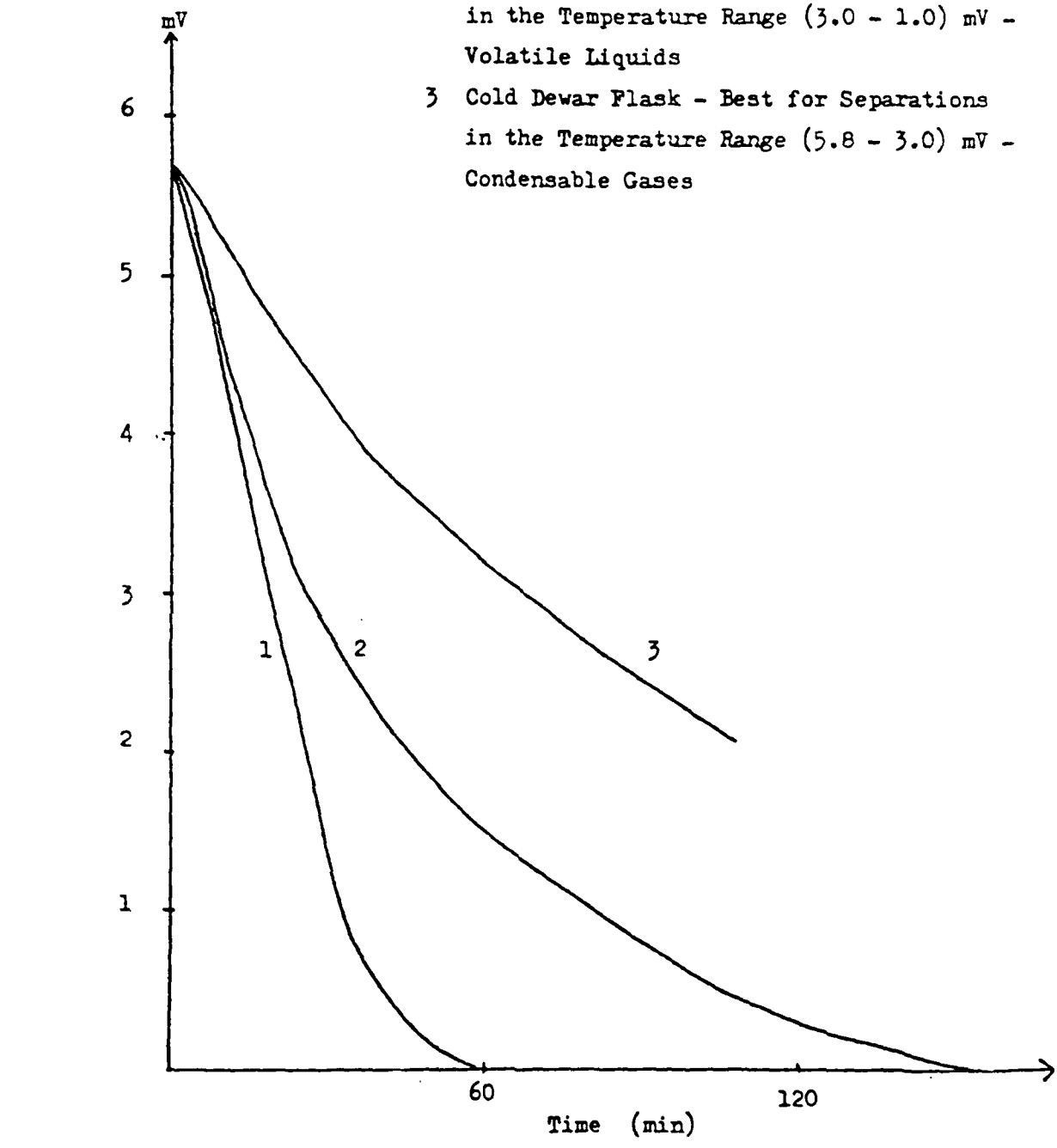

FIGURE 4 TYPICAL SATVA WARM-UP CURVES

Sample Size 101.6 mg

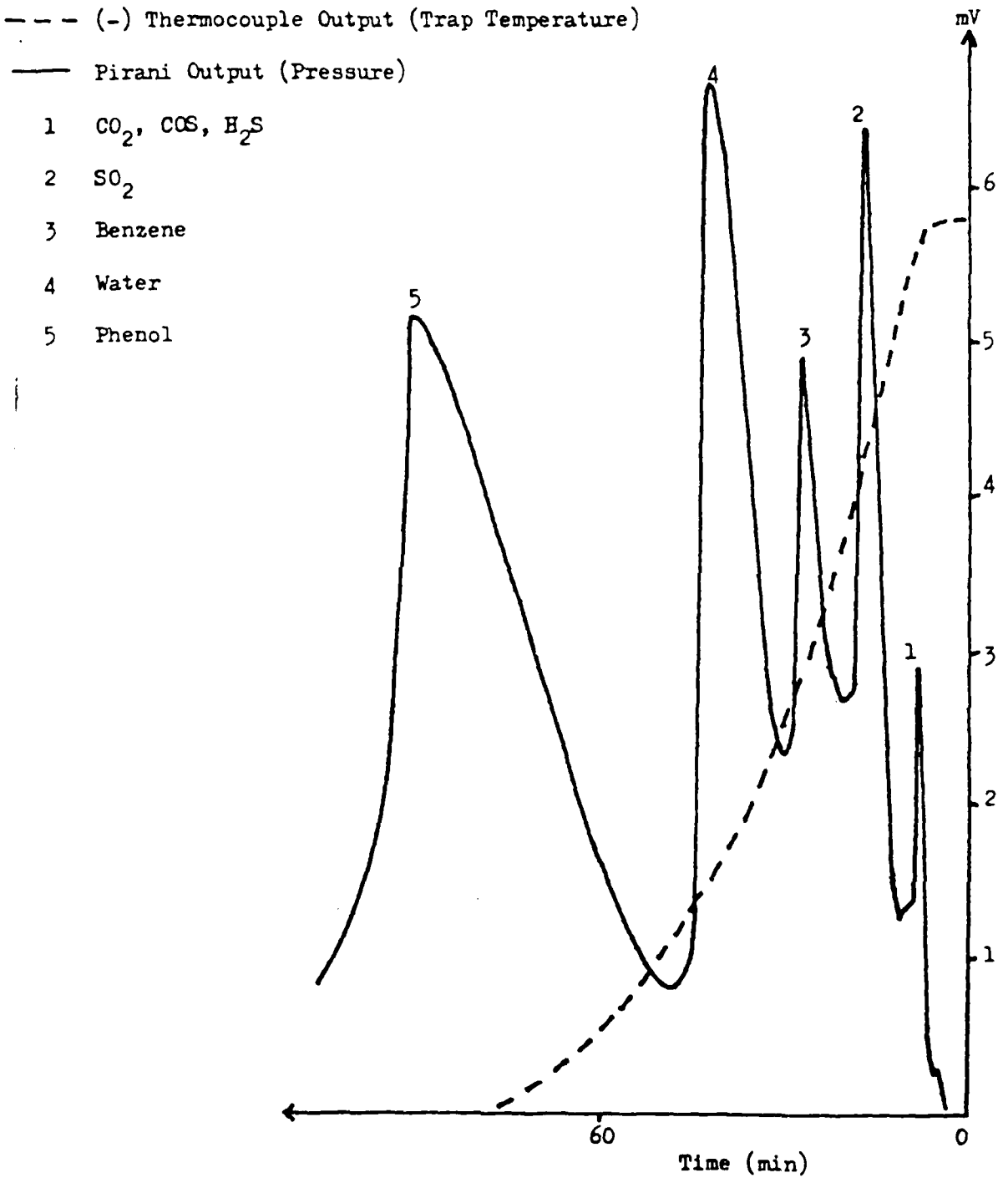

FIGURE 5 SATVA OF THE CONDENSABLE VOLATILE PRODUCT FRACTION OF DEGRADATION TO 1020°C OF ATS-G

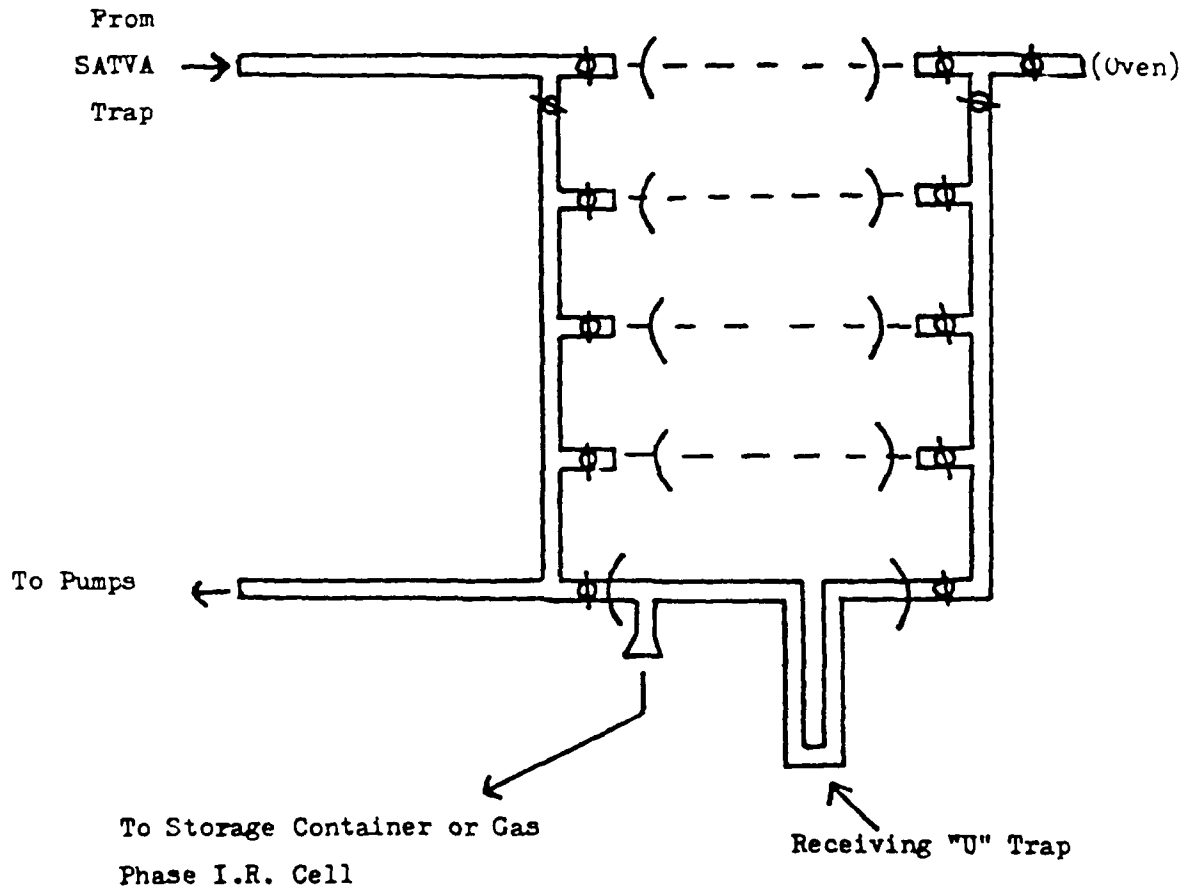

FIGURE 6 SATVA FRACTIONATING GRID

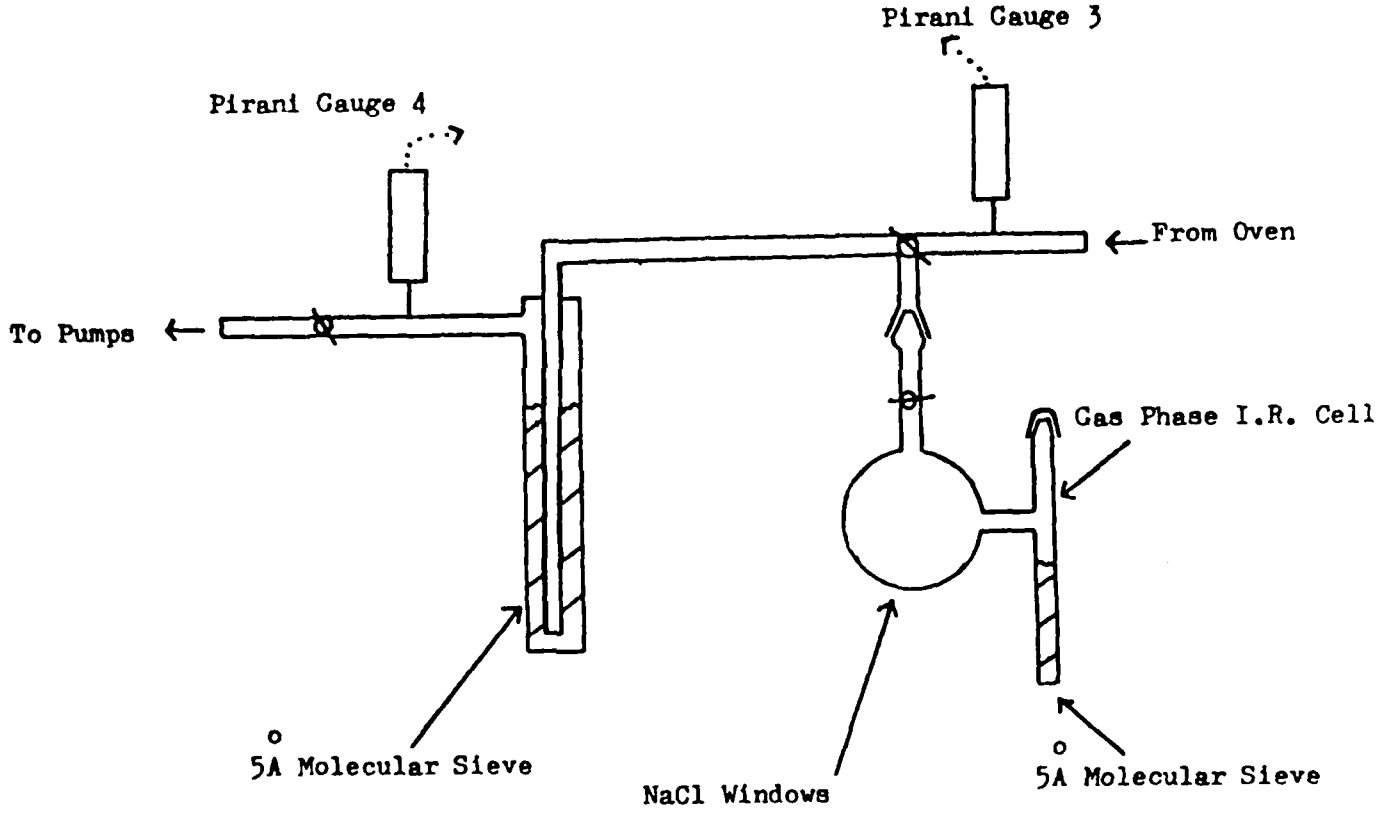

FIGURE 7 ADSORPTION THERMAL VOLATILIZATION ANALYSIS (ATVA) ASSEMBLY

KEY

P1 Pirani Gauge 1(Total Volatiles)

P2 Pirani Gauge 2(Material Volatile at -75°C)

P3 Pirani Gauge 3(Noncondensable Material)

P4 H_2

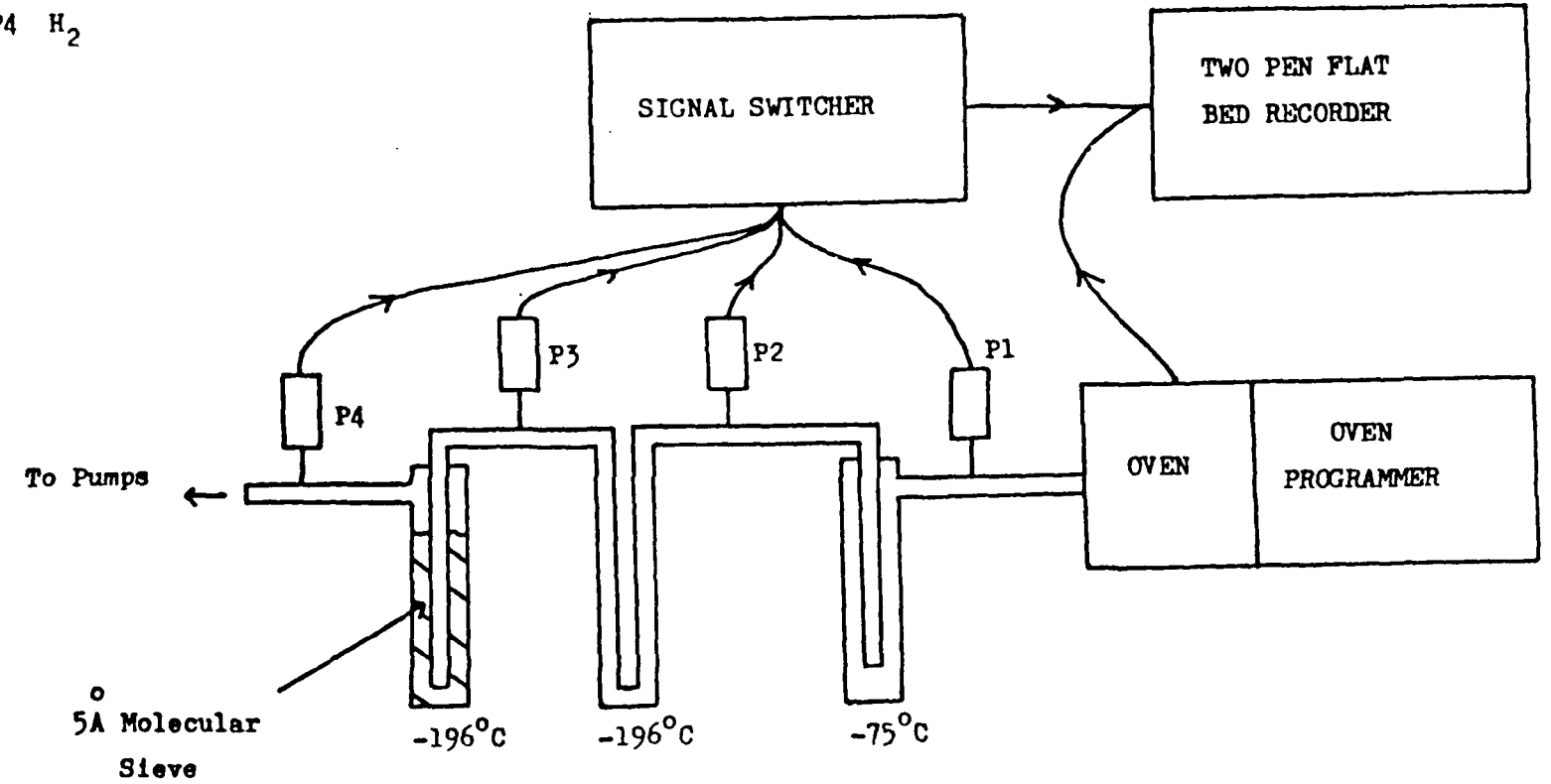

FIGURE 8 COMBINES TVA/ATVA (CATVA) EXPERIMENT

Heating Rate 5°C/min
Sample Size 100.0mg

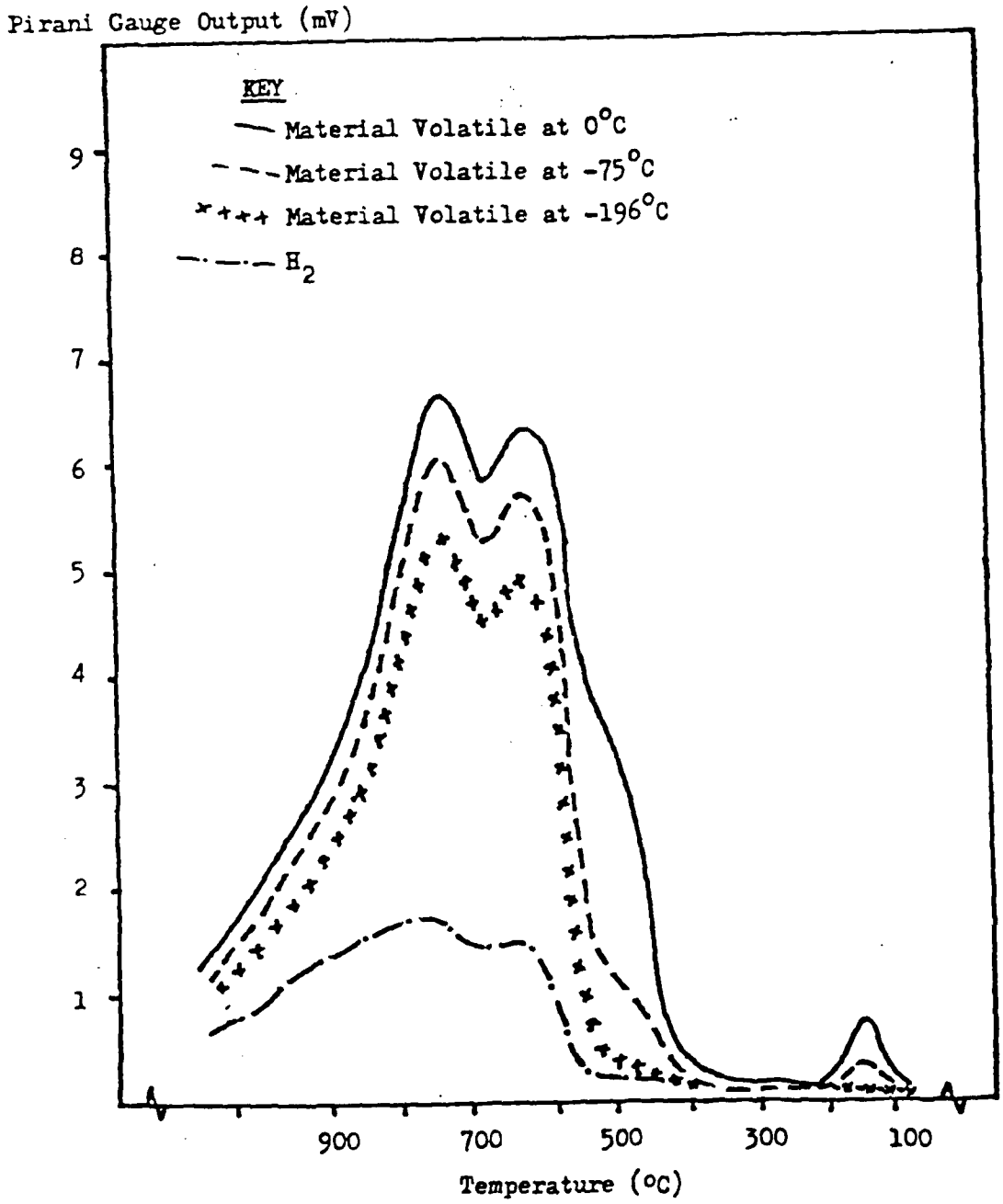

FIGURE 9 CATVA OF ATS-G

KEY

—— Pirani 1 Output (Total Volatiles)

– – – Pirani 2 Output (Material Volatile at $-75^{\circ}C$)

× × × × Pirani 3 Output (Material Volatile at $-196^{\circ}C$)

—·—· Pirani 4 Output, H_2

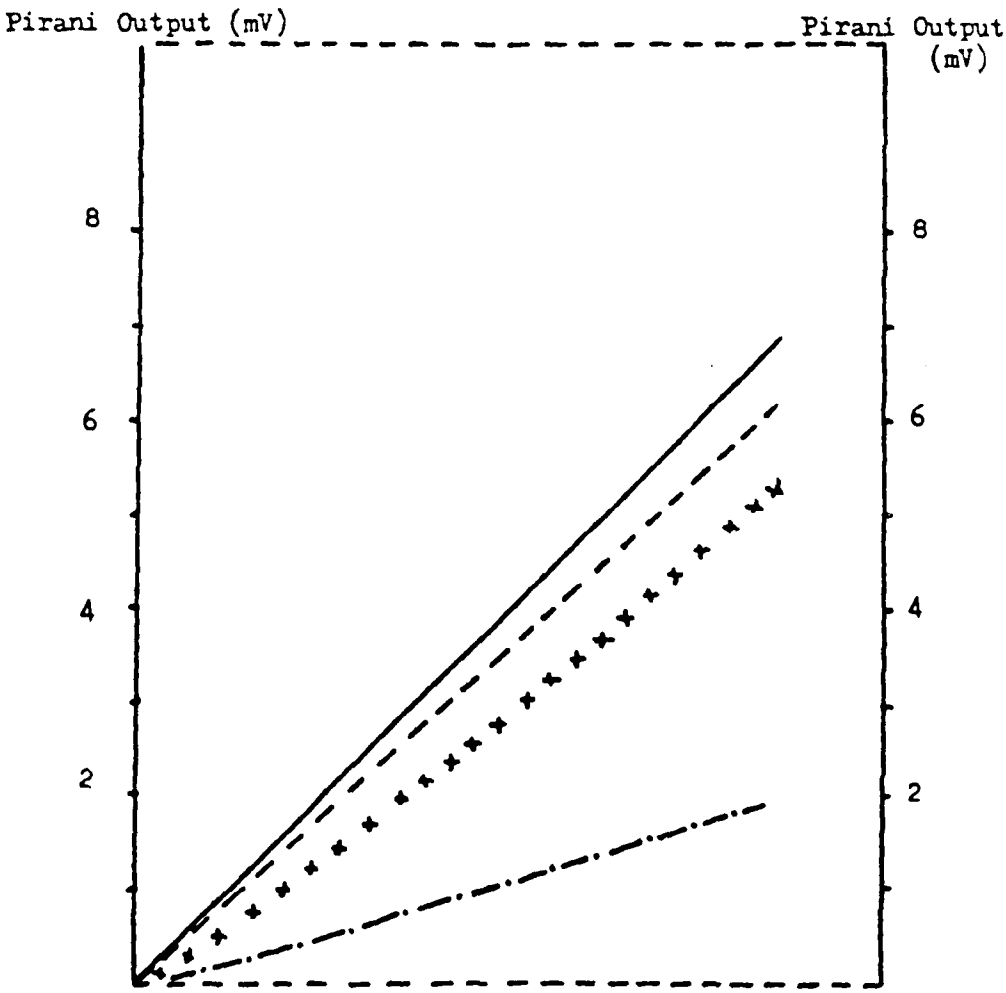

FIGURE 10 PIRANI GAUGE OUTPUTS FOR A NONCONDENSABLE GAS FLUX

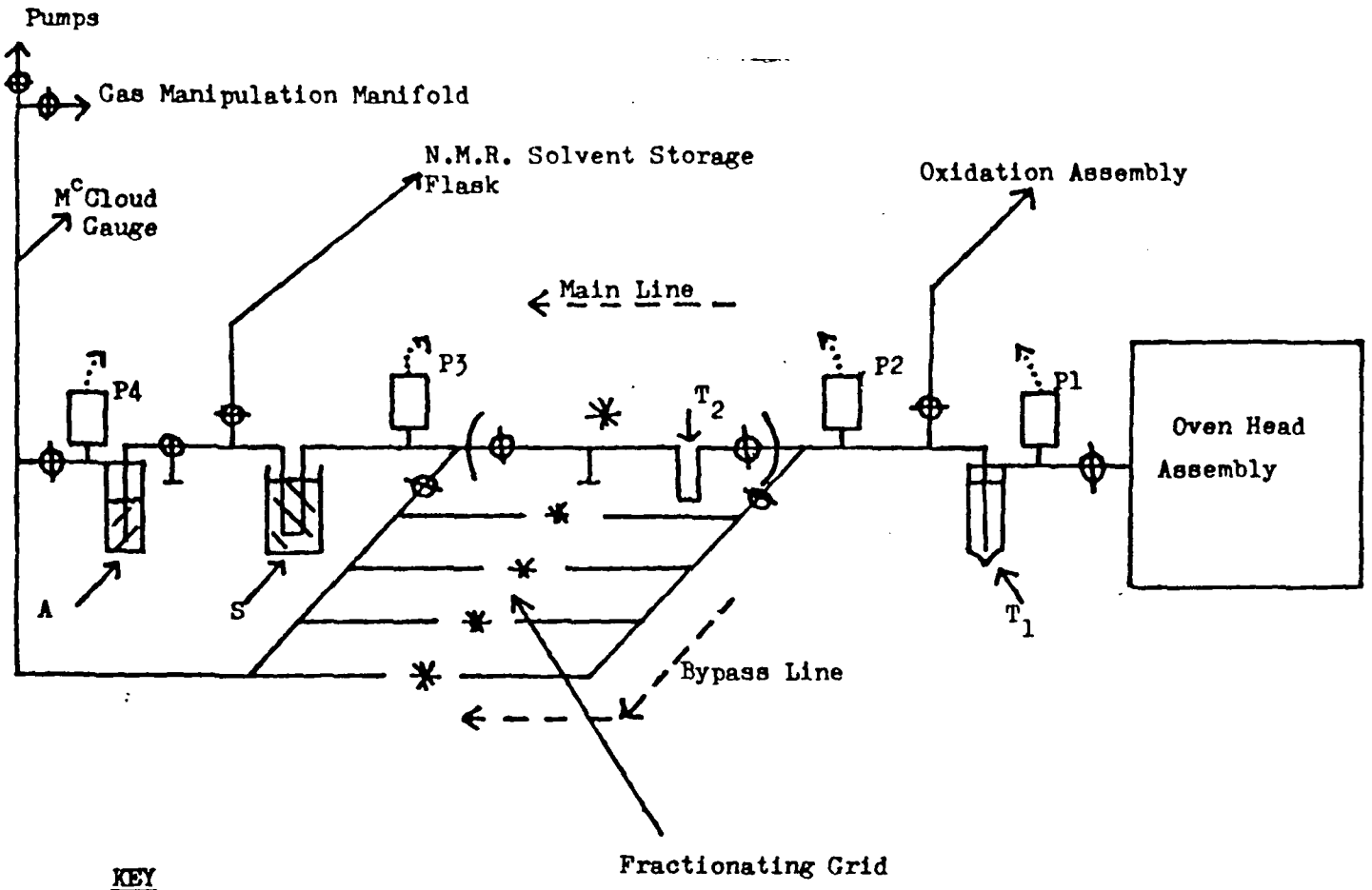

KEY

P1, P2, P3, P4	Pirani Gauge Heads
⊥	Product Removal Point
A	ATVA Trap
S	SATVA Trap
T_1,T_2	Cold Traps Used In The CATVA Experiment

FIGURE 11 CATVA/SATVA VACUUM MANIFOLD

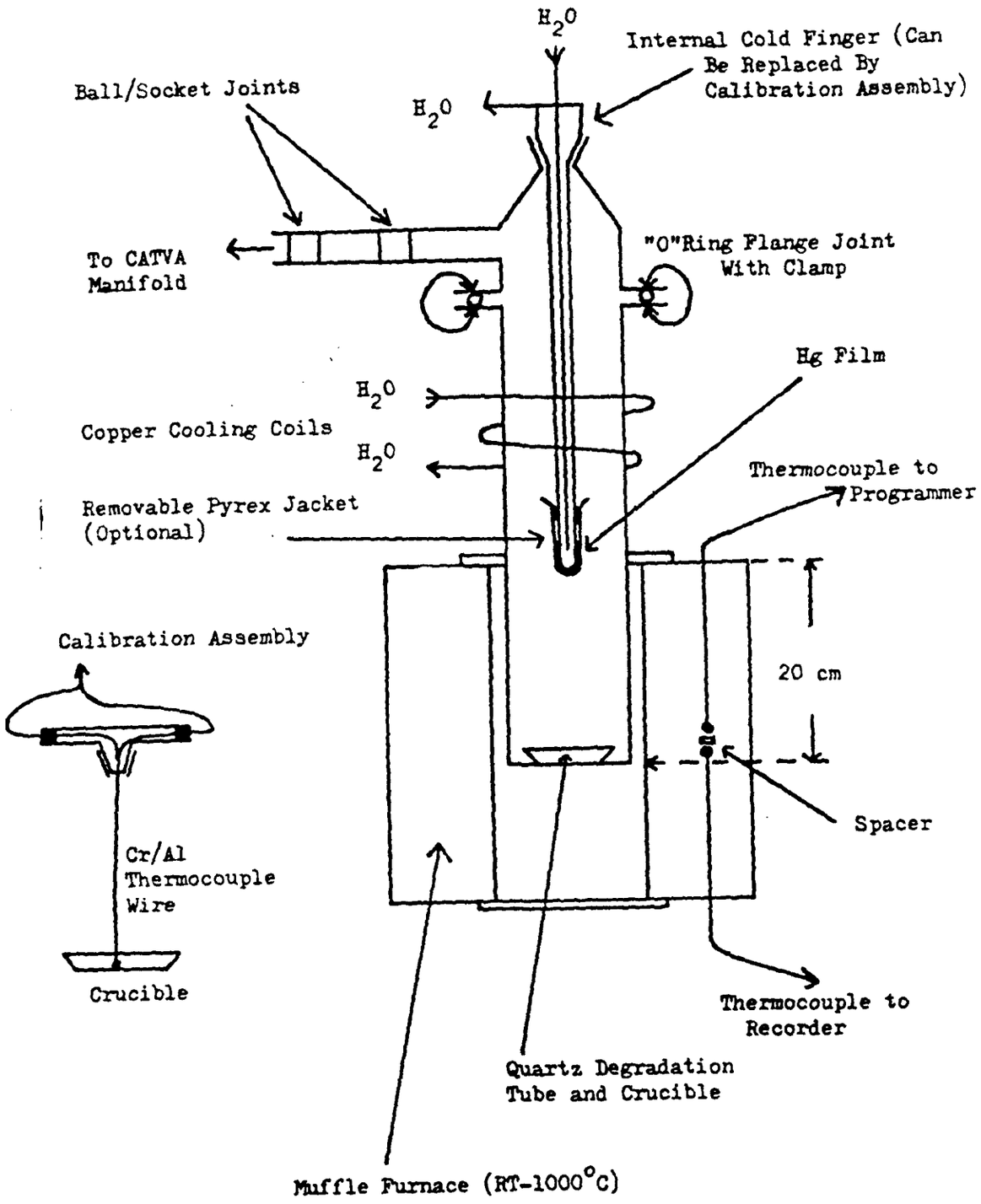

FIGURE 12 OVEN ASSEMBLY

Heating Rate 5°C/min

Crucible 20 cm into Oven

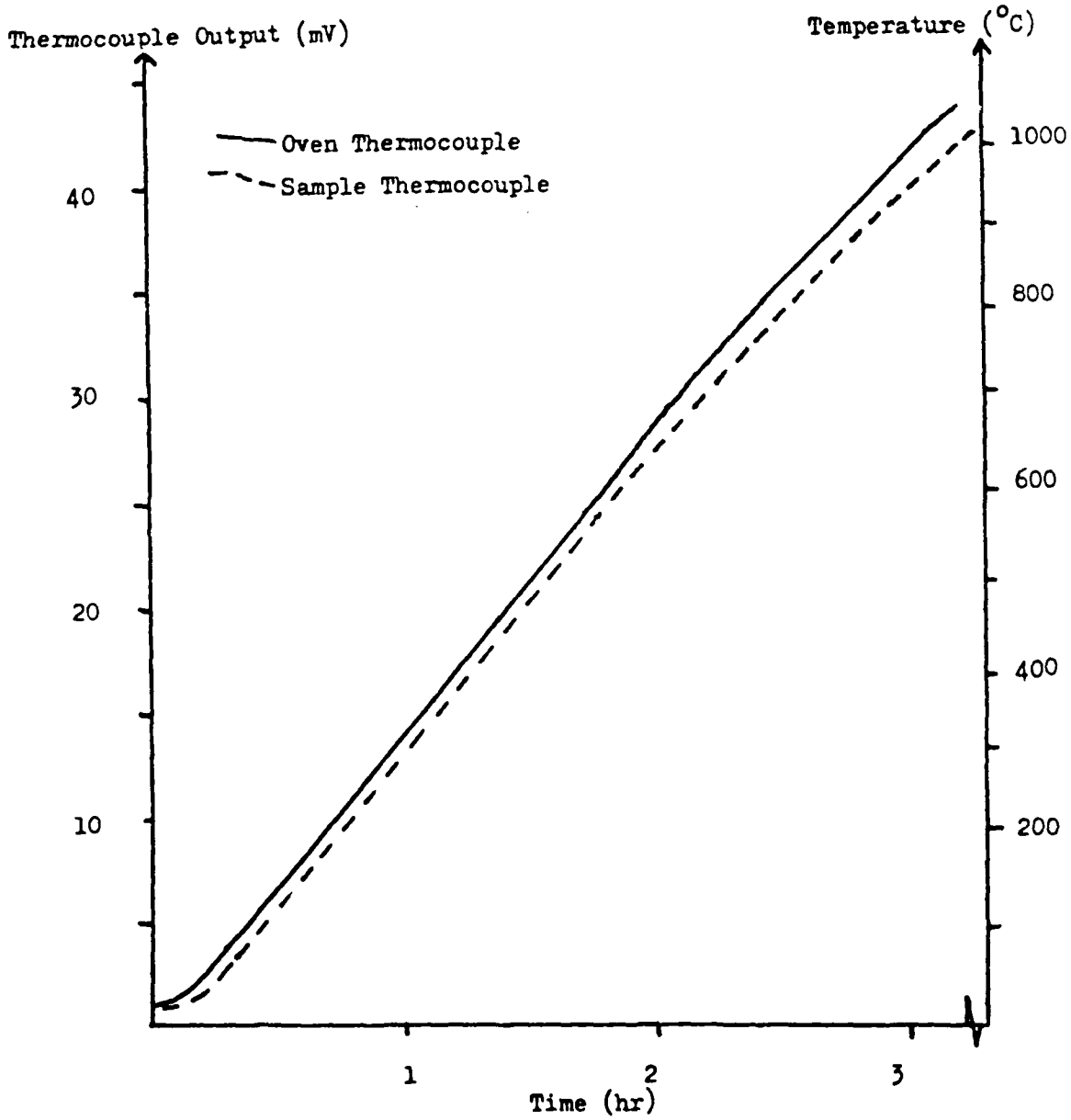

FIGURE 13 OVEN CALIBRATION CURVE FOR PROGRAMMED TVA EXPERIMENT

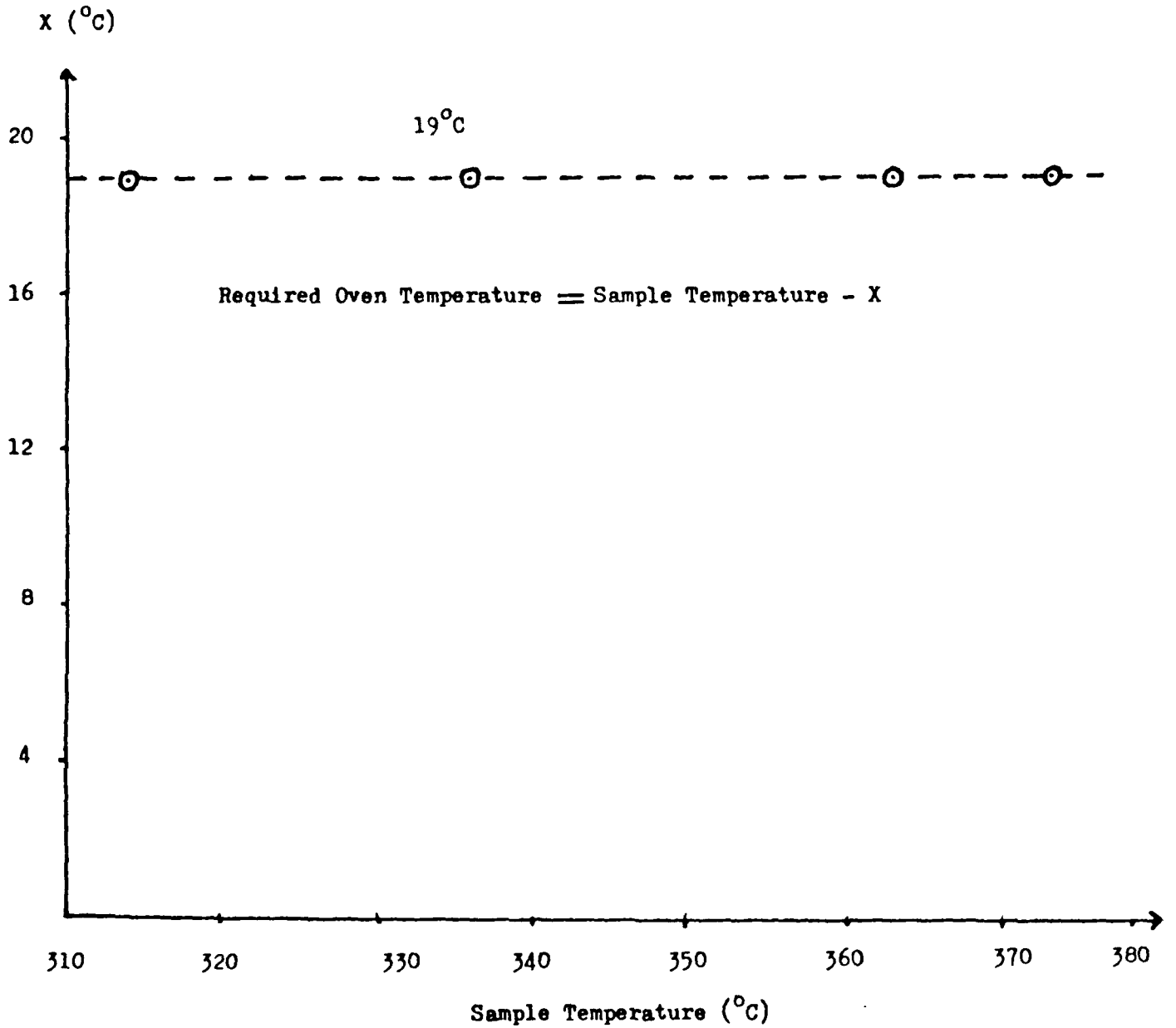

FIGURE 14 ISOTHERMAL TVA OVEN CALIBRATION CURVE

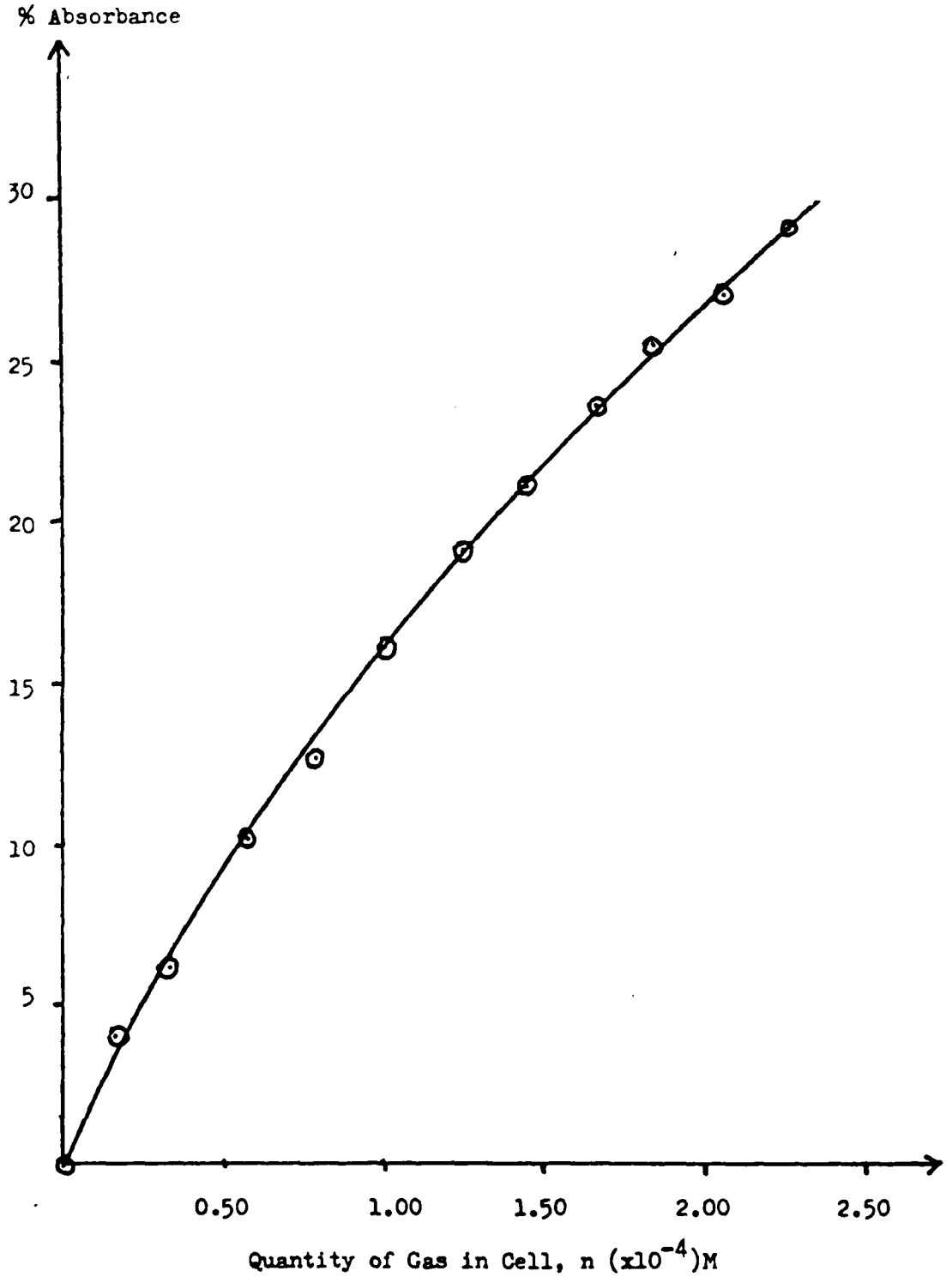

FIGURE 15 GAS PHASE I.R. CALIBRATION CURVE FOR SO_2 USING ITS 2490 cm^{-1} ABSORBANCE BAND

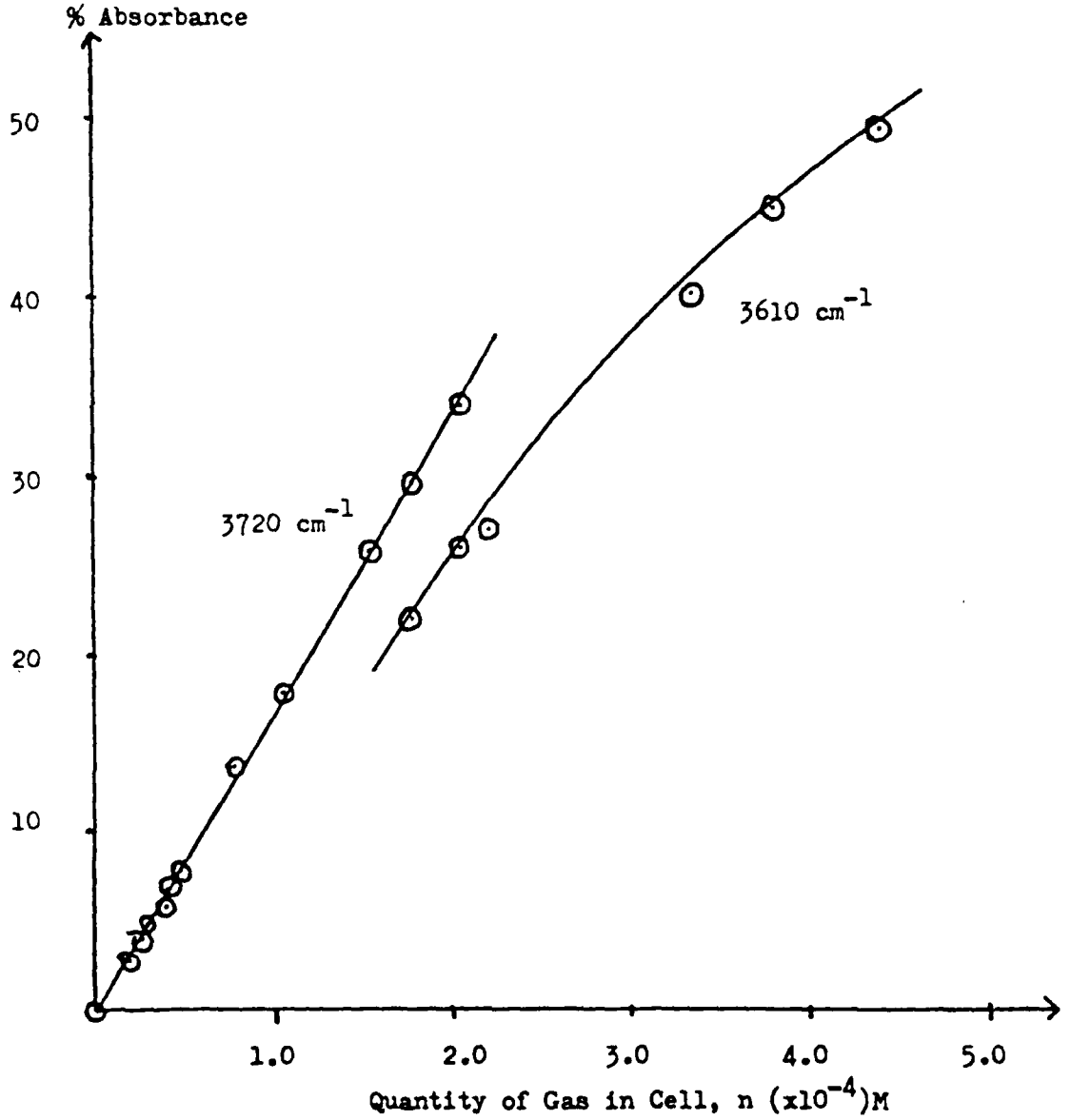

FIGURE 16 GAS PHASE I.R. CALIBRATION CURVES FOR CO_2 USING ITS 3720 cm^{-1} AND 3610 cm^{-1} ABSORBANCE BAND

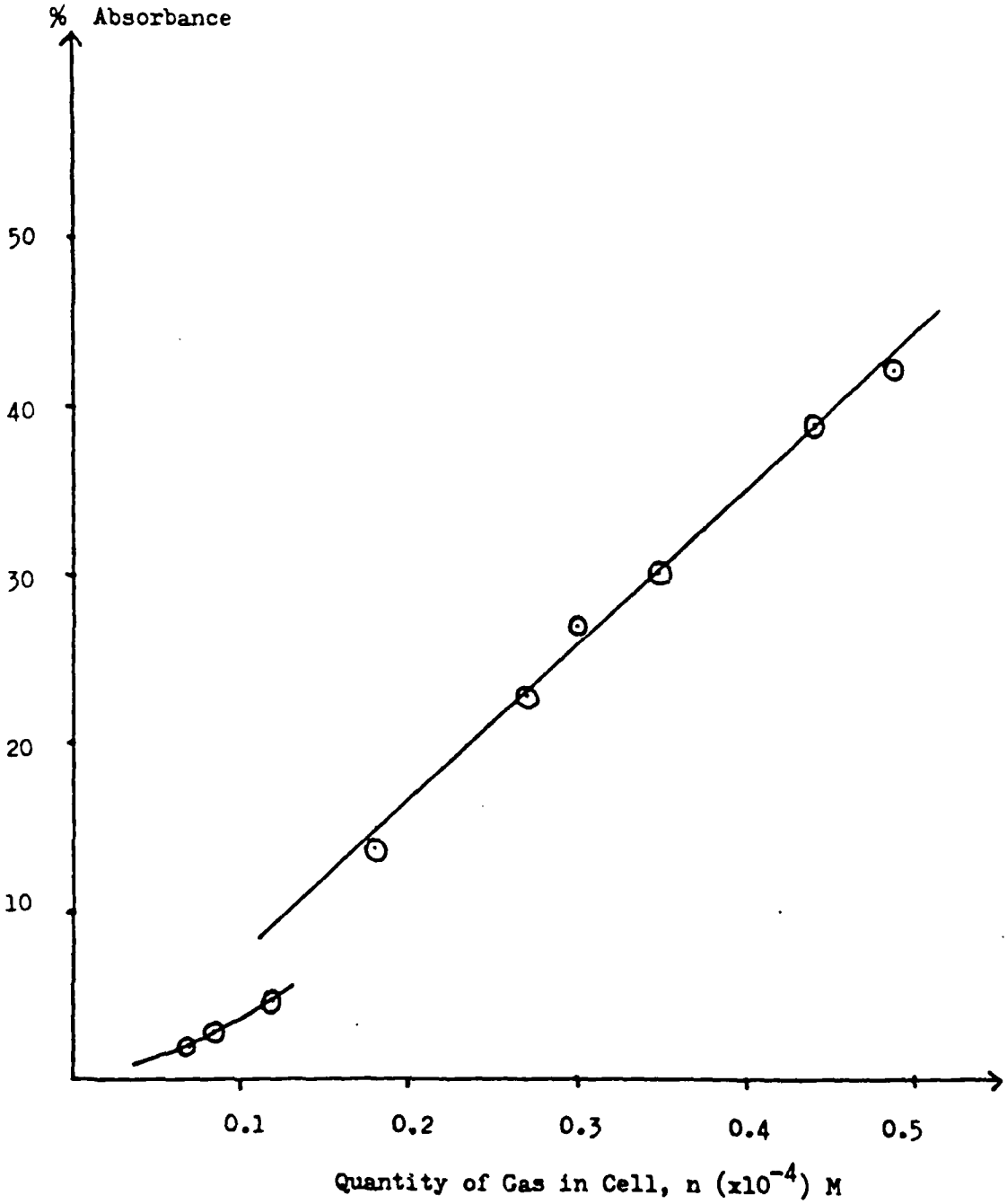

FIGURE 17 GAS PHASE I.R. CALIBRATION CURVE FOR CO_2 USING ITS 2300 cm^{-1} ABSORBANCE BAND

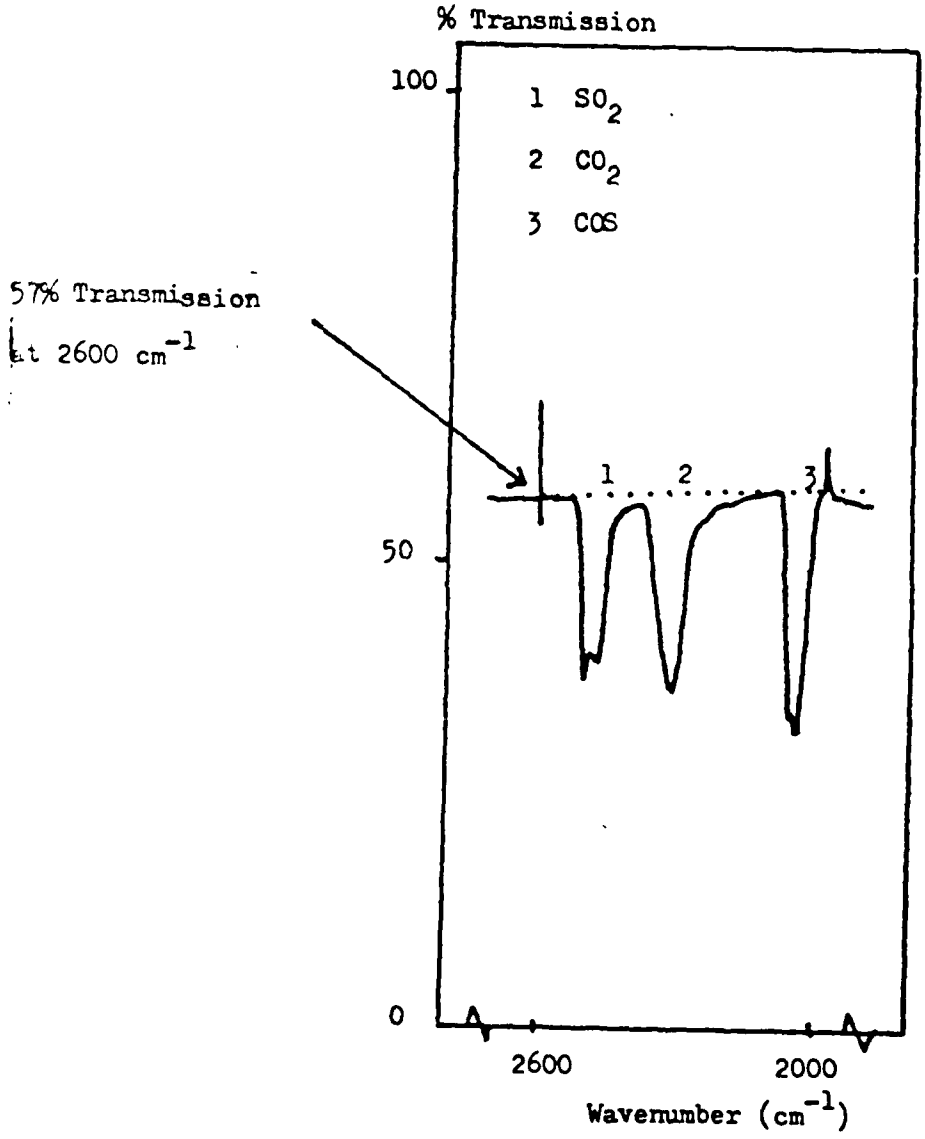

FIGURE 18 QUANTITATIVE GAS PHASE I.R. SPECTRUM OF THE CONDENSABLE VOLATILE PRODUCT FRACTION OF THERMAL DEGRADATION TO 1020°C OF ATS-G

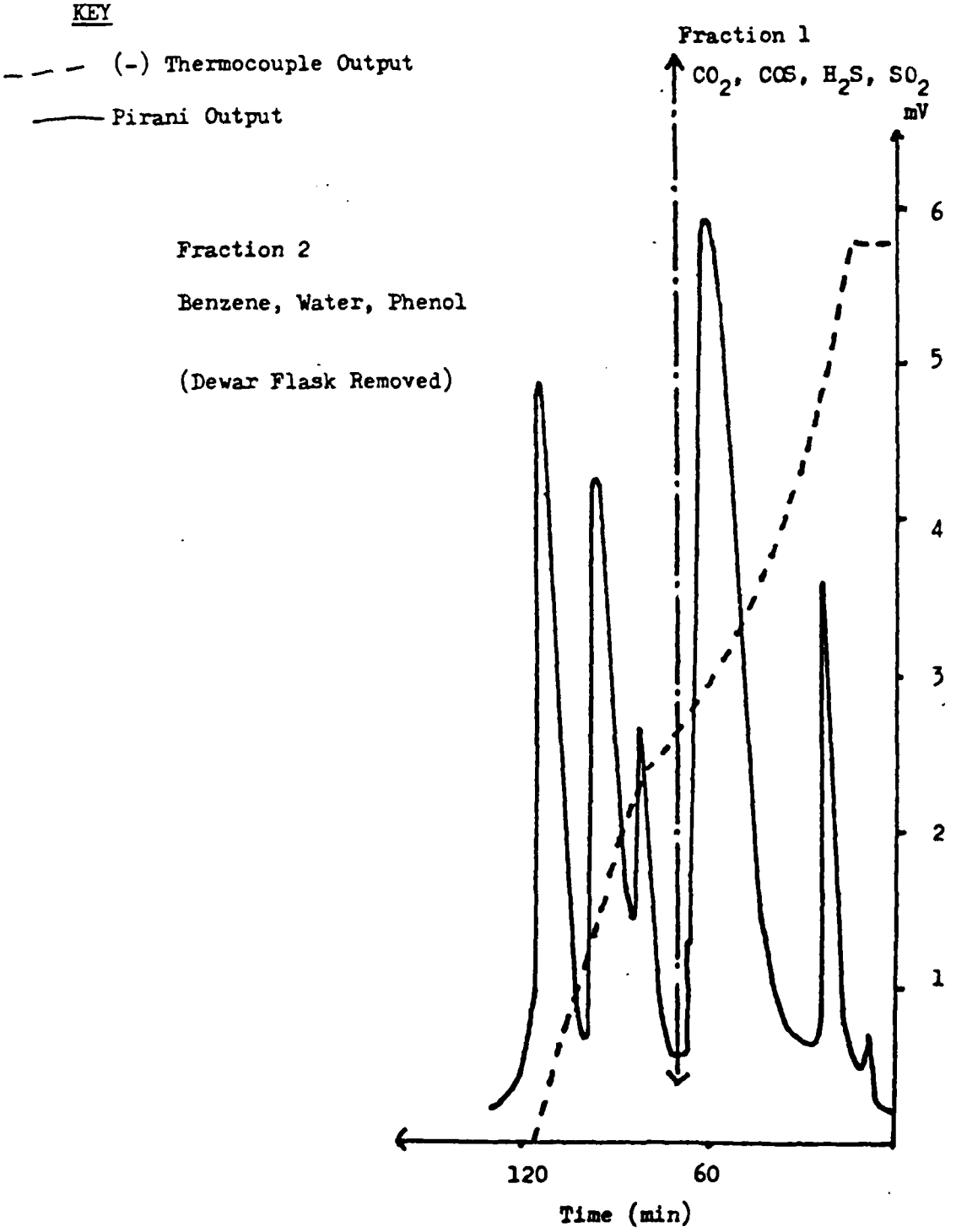

FIGURE 19 SATVA OF THE CONDENSABLE VOLATILE PRODUCT FRACTION OF DEGRADATION TO 1020°C OF ATS-G, SLOW WARM-UP

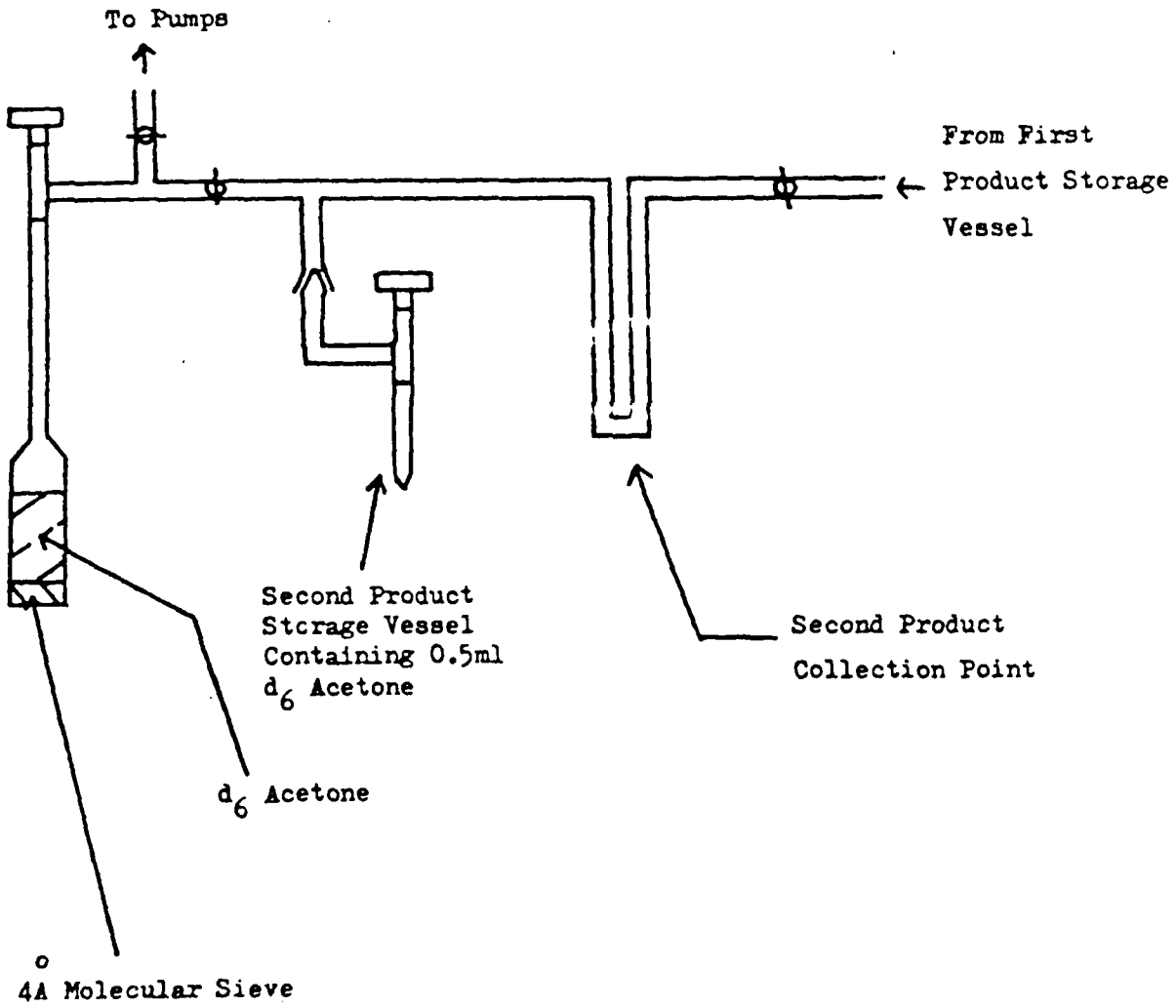

FIGURE 20 APPARATUS FOR COMBINES GRAVIMETRIC AND N.M.R. ANALYSIS OF CONDENSABLE VOLATILE PRODUCTS OF DEGRADATION

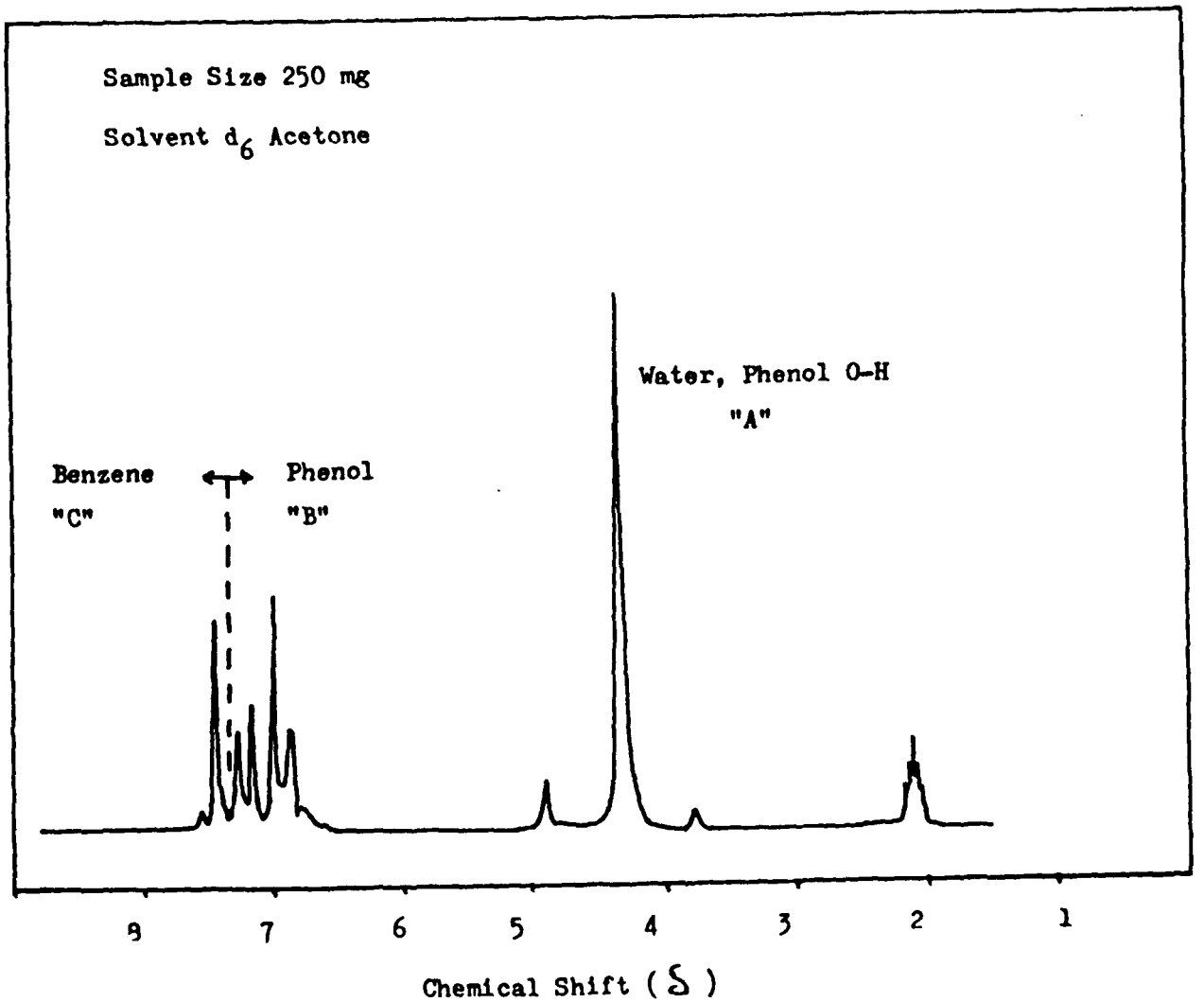

FIGURE 21 QUANTITATIVE PROTON N.M.R. SPECTRUM OF THE CONDENSABLE VOLATILE PRODUCT FRACTION OF THERMAL DEGRADATION TO 1020°C OF ATS-G

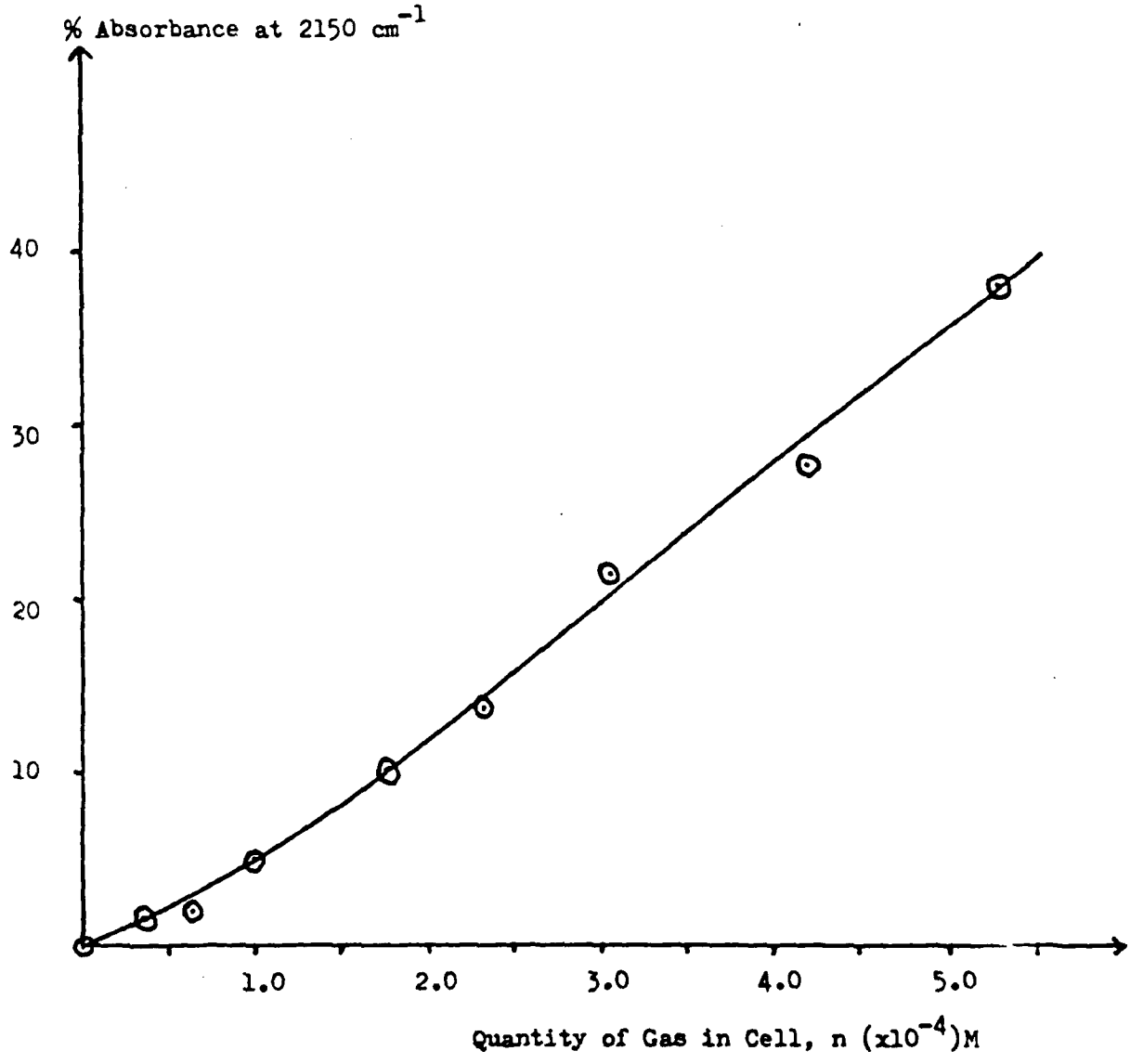

FIGURE 22 GAS PHASE I.R. CALIBRATION CURVE FOR CO USING ITS 2150cm^{-1} ABSORBANCE BAND

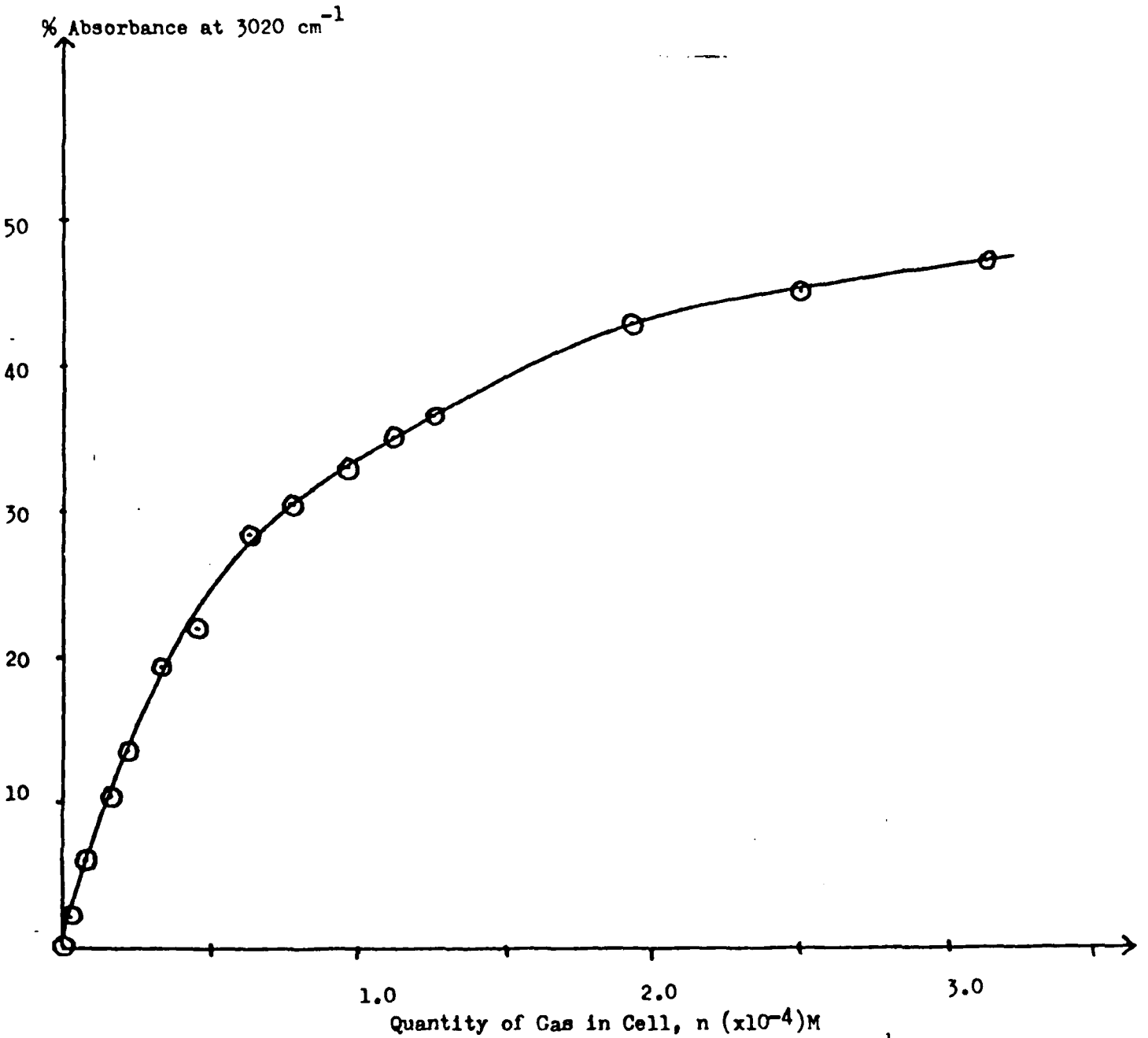

FIGURE 23 GAS PHASE I.R. CALIBRATION CURVE FOR CH_4 USING ITS 3020cm^{-1} ABSORBANCE BAND

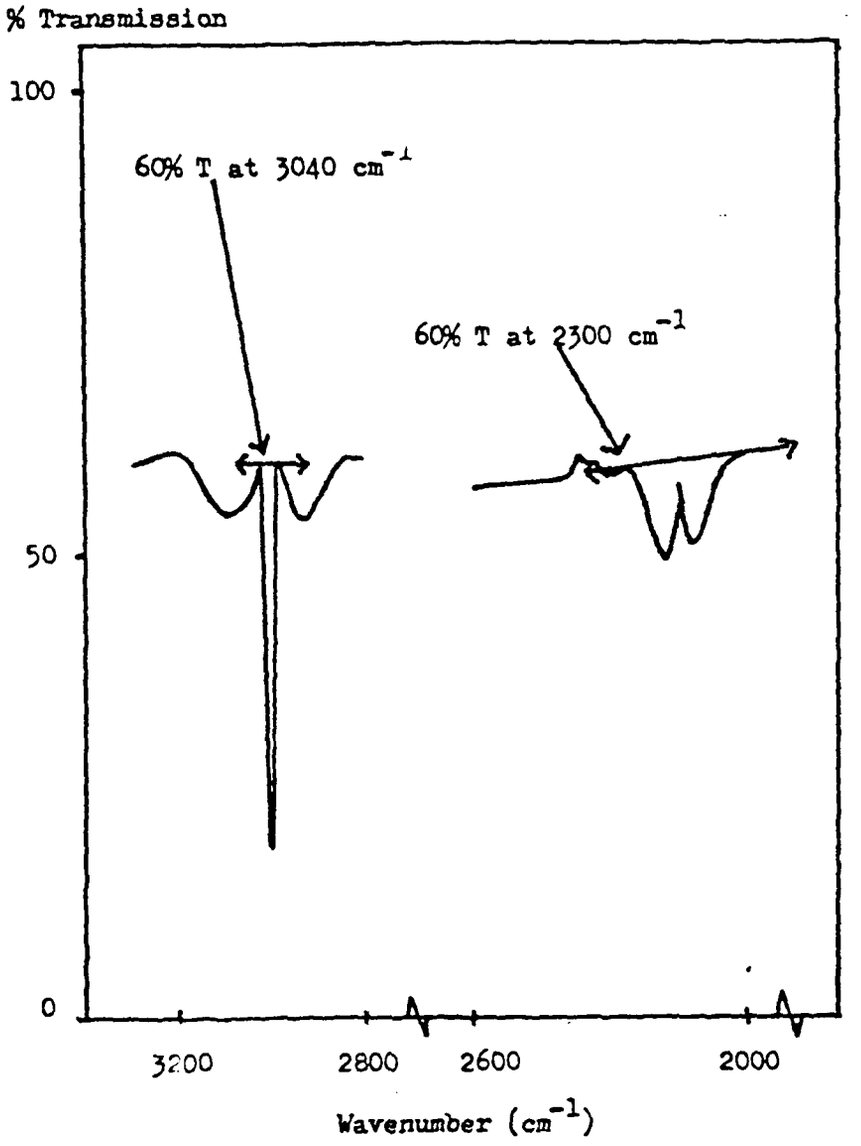

FIGURE 24 GAS PHASE I.R. SPECTRUM OF THE NONCONDENSABLE PRODUCT FRACTION OF THERMAL DEGRADATION TO 1020°C OF ATS DIMER

Sample Size 150 mg

Heating Rate 5°C/min

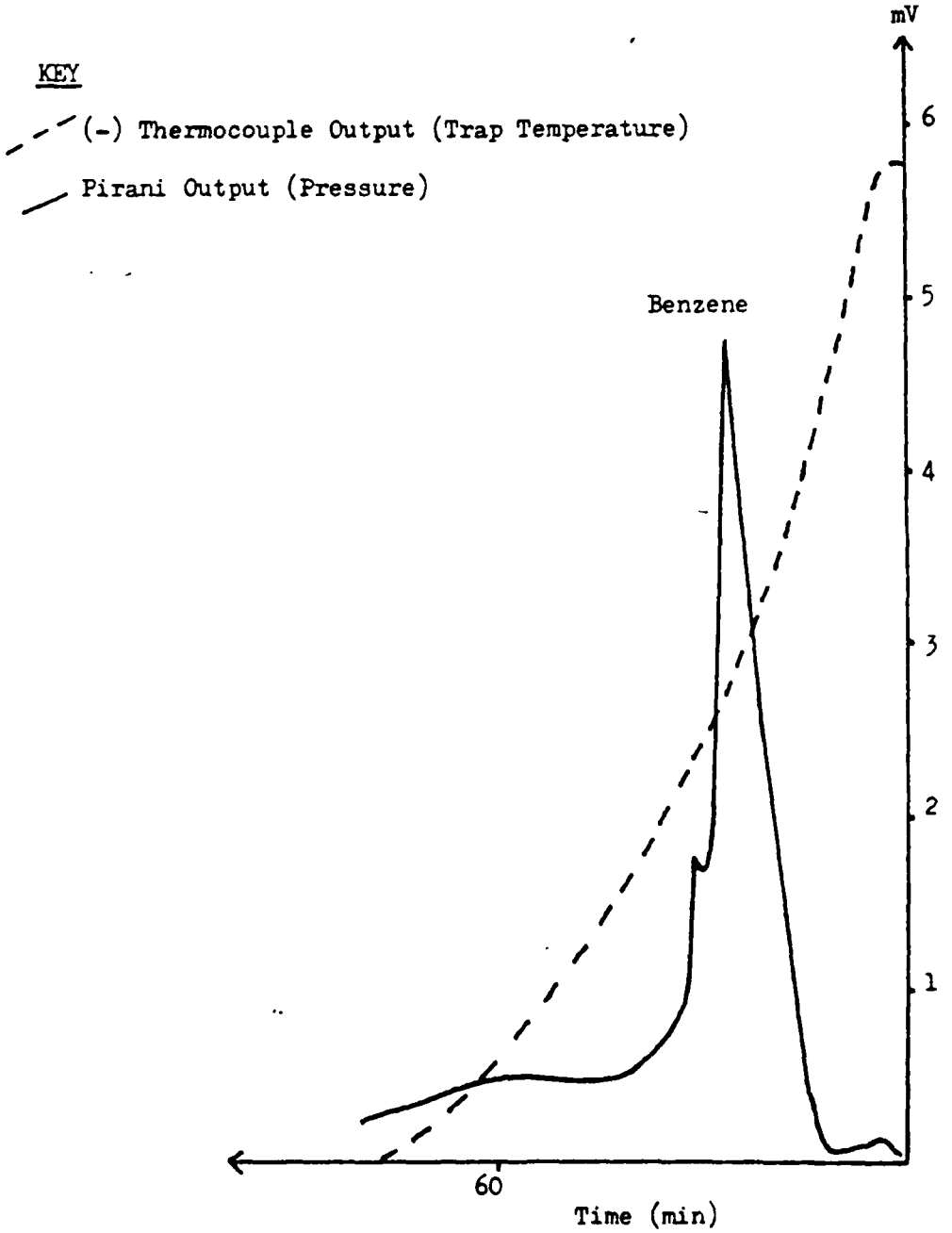

FIGURE 25 SATVA OF SOLVENTS EVOLVED FROM ATS DIMER ON PROGRAMED CURING UNDER HIGH VACUUM CONDITIONS

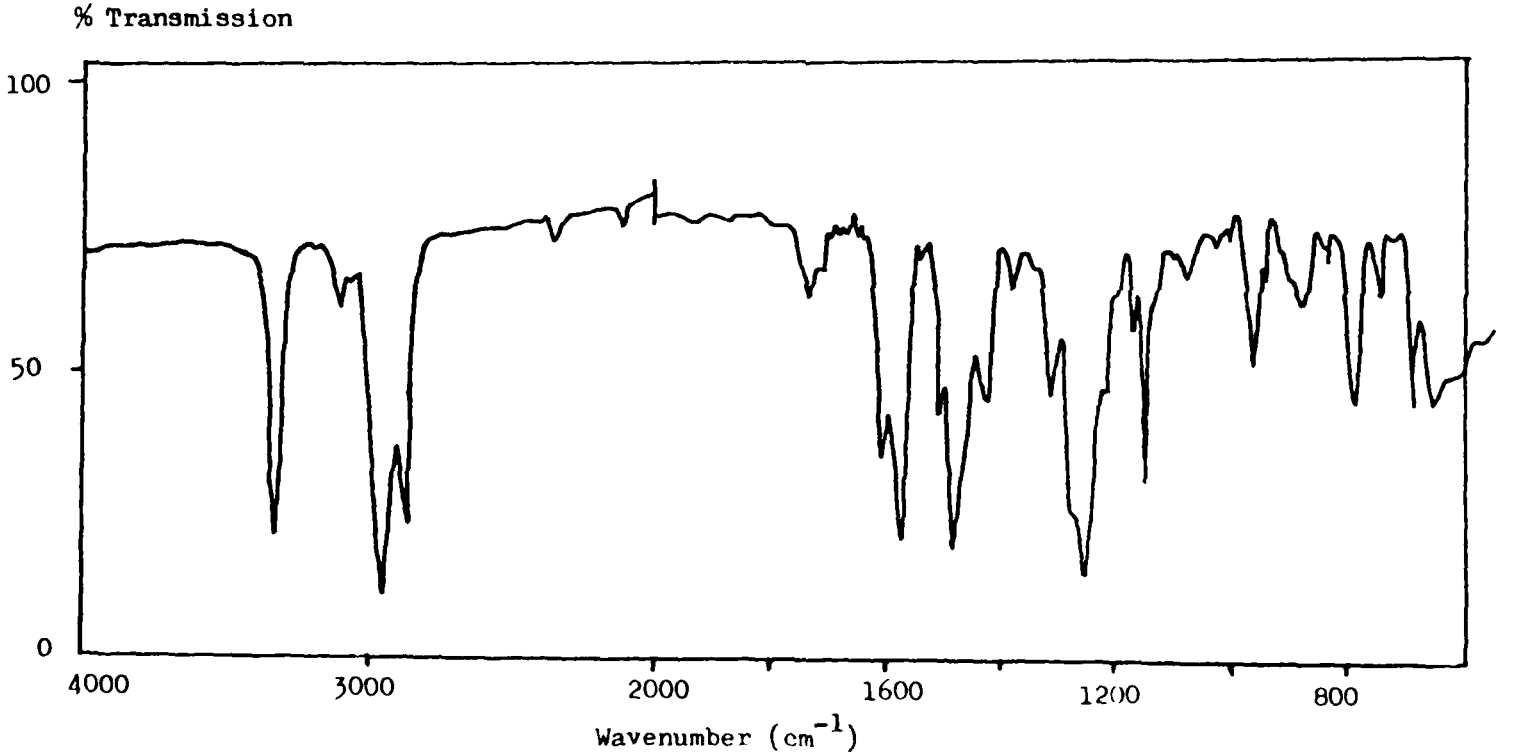

FIGURE 26 I.R. SPECTRUM OF SUB-FRACTION 1, ISOLATED BY PREPARATIVE T.L.C. FROM THE HIGH BOILING POINT FRACTION EVAPORATED FROM ATS-G ON CURING UNDER HIGH VACUUM CONDITIONS

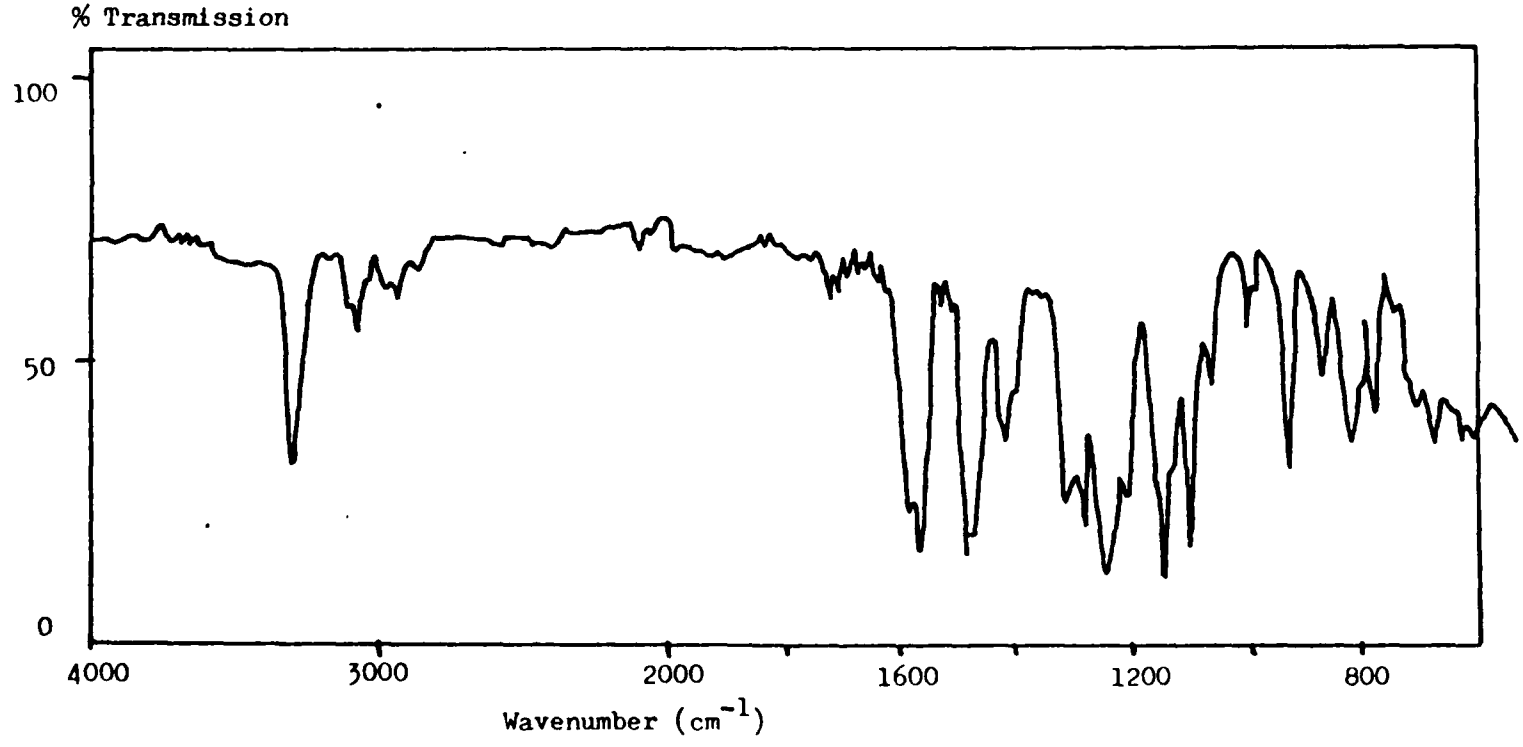

FIGURE 27 I.R. SPECTRUM OF SUB-FRACTION 2, ISOLATED BY PREPARATIVE T.L.C. FROM THE HIGH BOILING POINT FRACTION EVAPORATED FROM ATS-G ON CURING UNDER HIGH VACUUM CONDITIONS

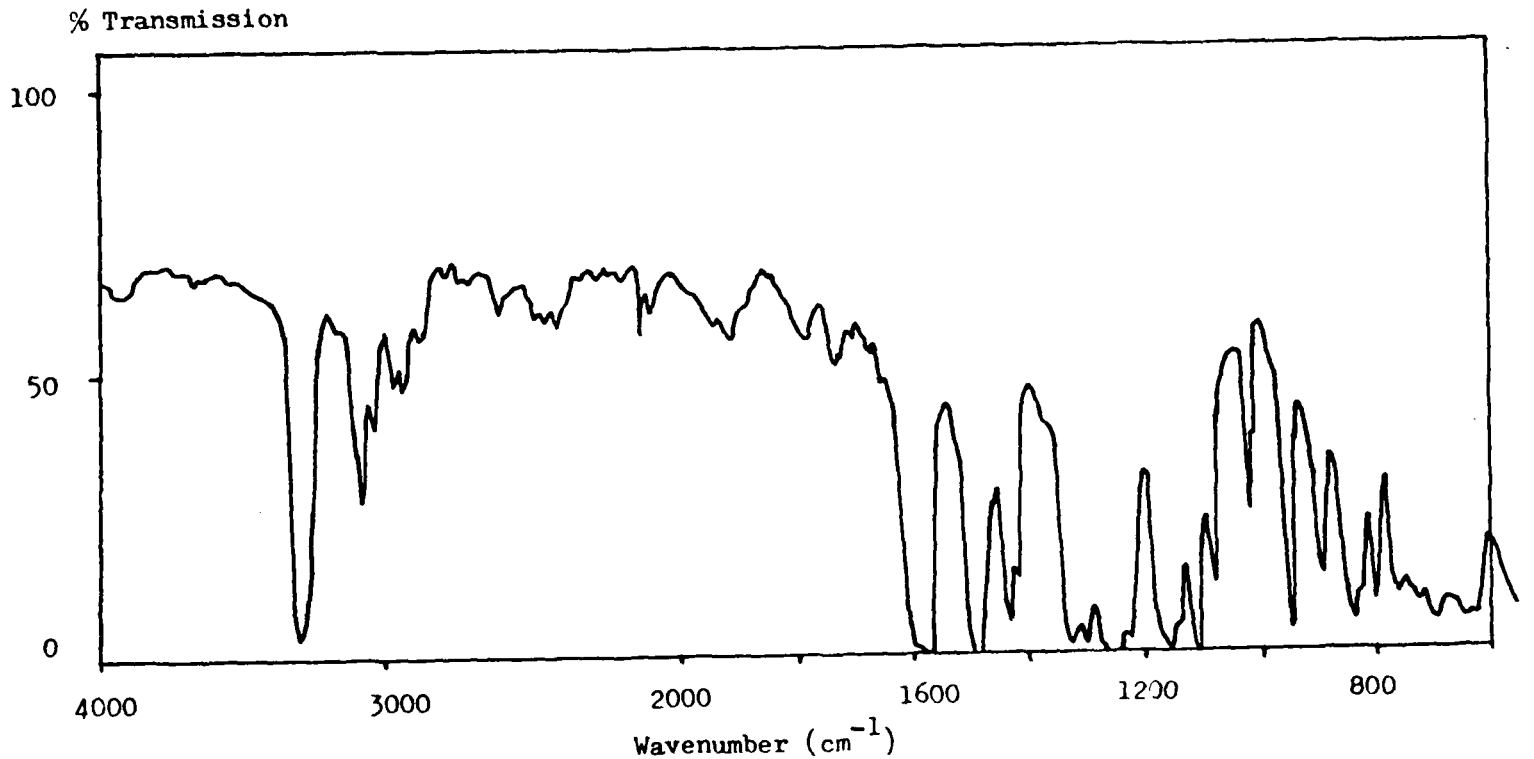

FIGURE 28 I.R. SPECTRUM OF SUB-FRACTION 2, ISOLATED BY PREPARATIVE T.L.C. FROM THE HIGH BOILING POINT FRACTION EVAPORATED FROM ATS MONOMER ON CURING UNDER HIGH VACUUM CONDITIONS

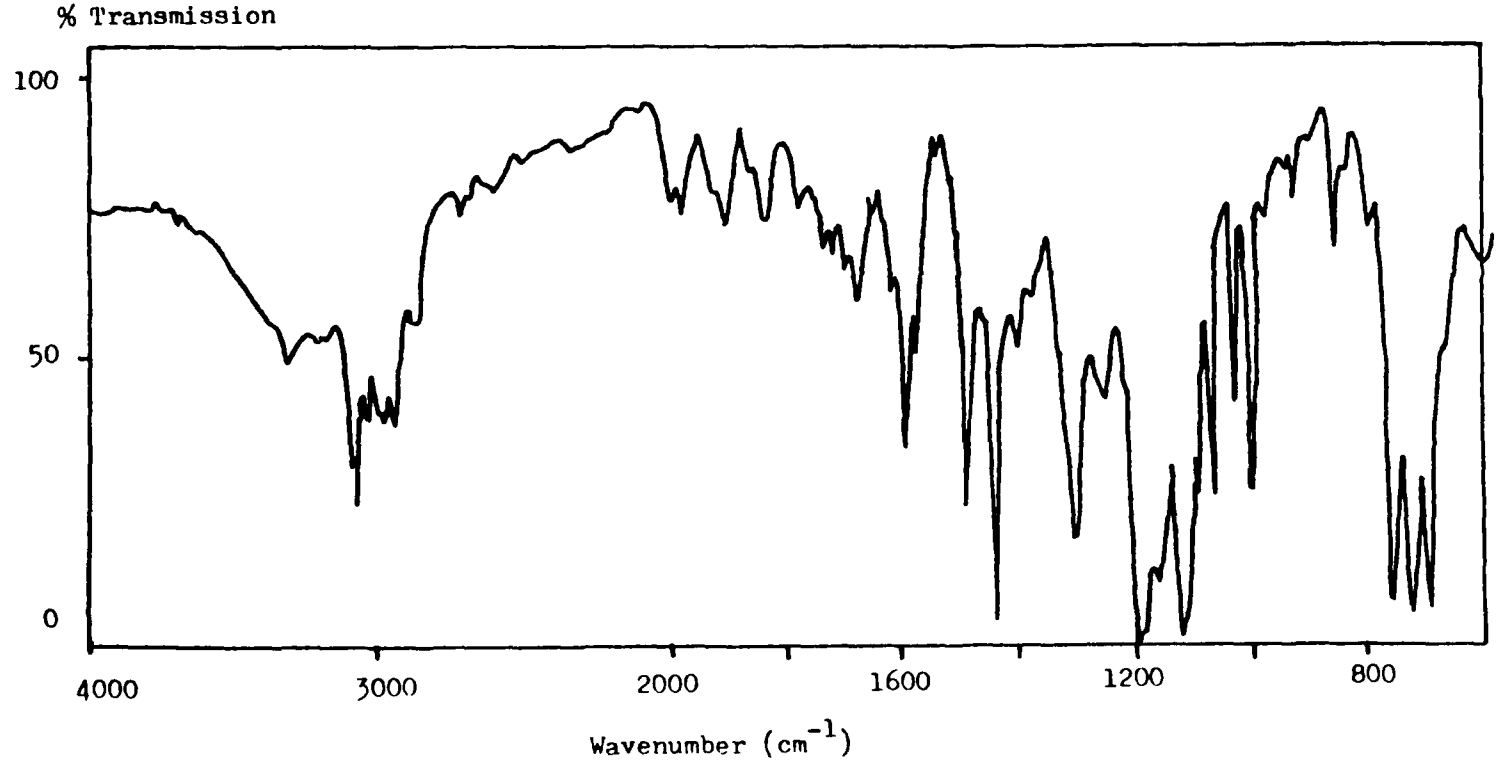

FIGURE 29 I.R. SPECTRUM OF SUB-FRACTION 3, ISOLATED BY PREPARTIVE T.L.C. FROM THE HIGH BOILING POINT FRACTION EVAPORATED FROM ATS_G ON CURING UNDER HIGH VACUUM CONDITIONS

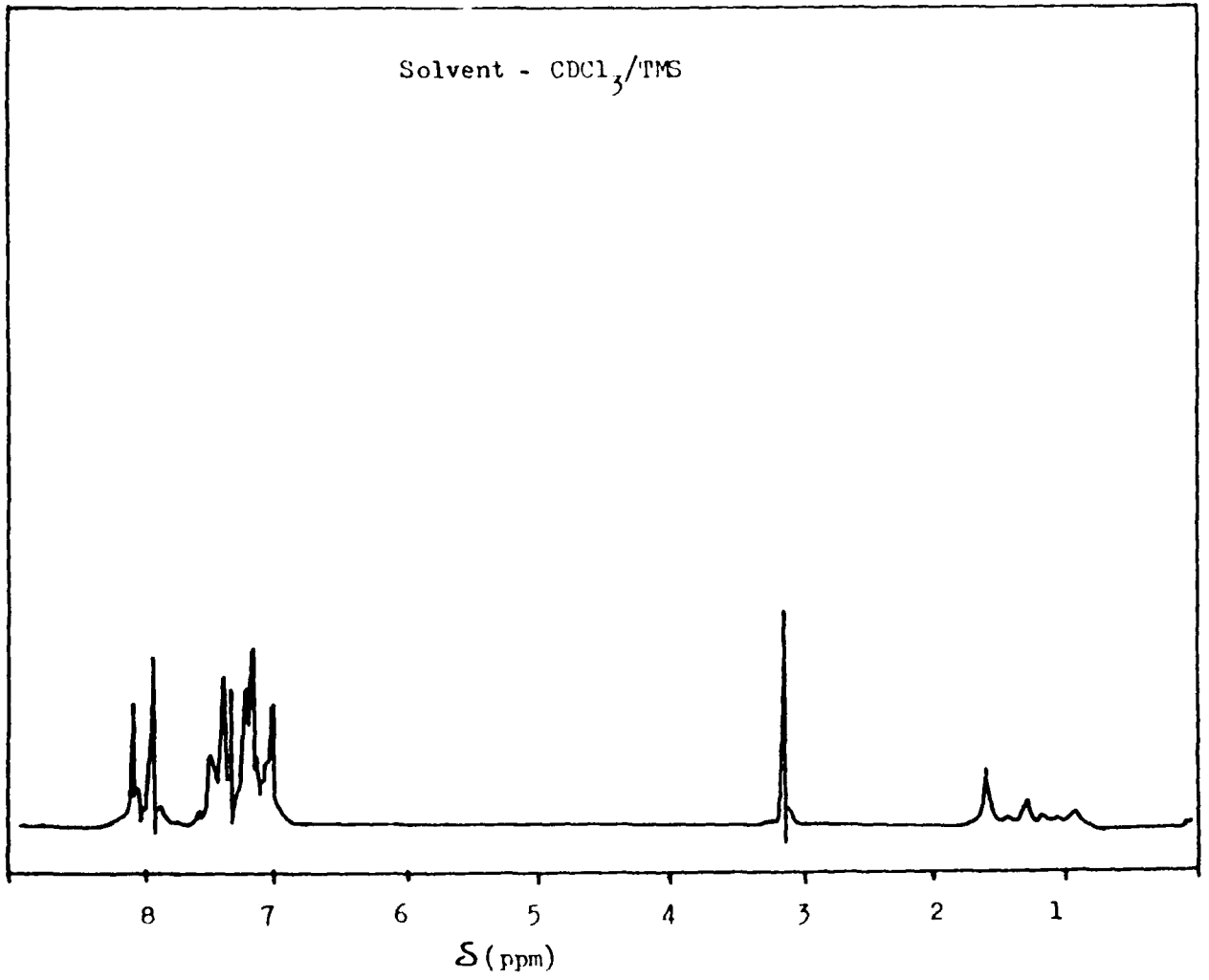

FIGURE 30 PROTON N.M.R. SPECTRUM OF SUB-FRACTION 2, ISOLATED BY PREPARATIVE T.L.C. FROM THE HIGH BOILING POINT FRACTION EVAPORATED FROM ATS-G ON CURING UNDER HIGH VACUUM CONDITIONS

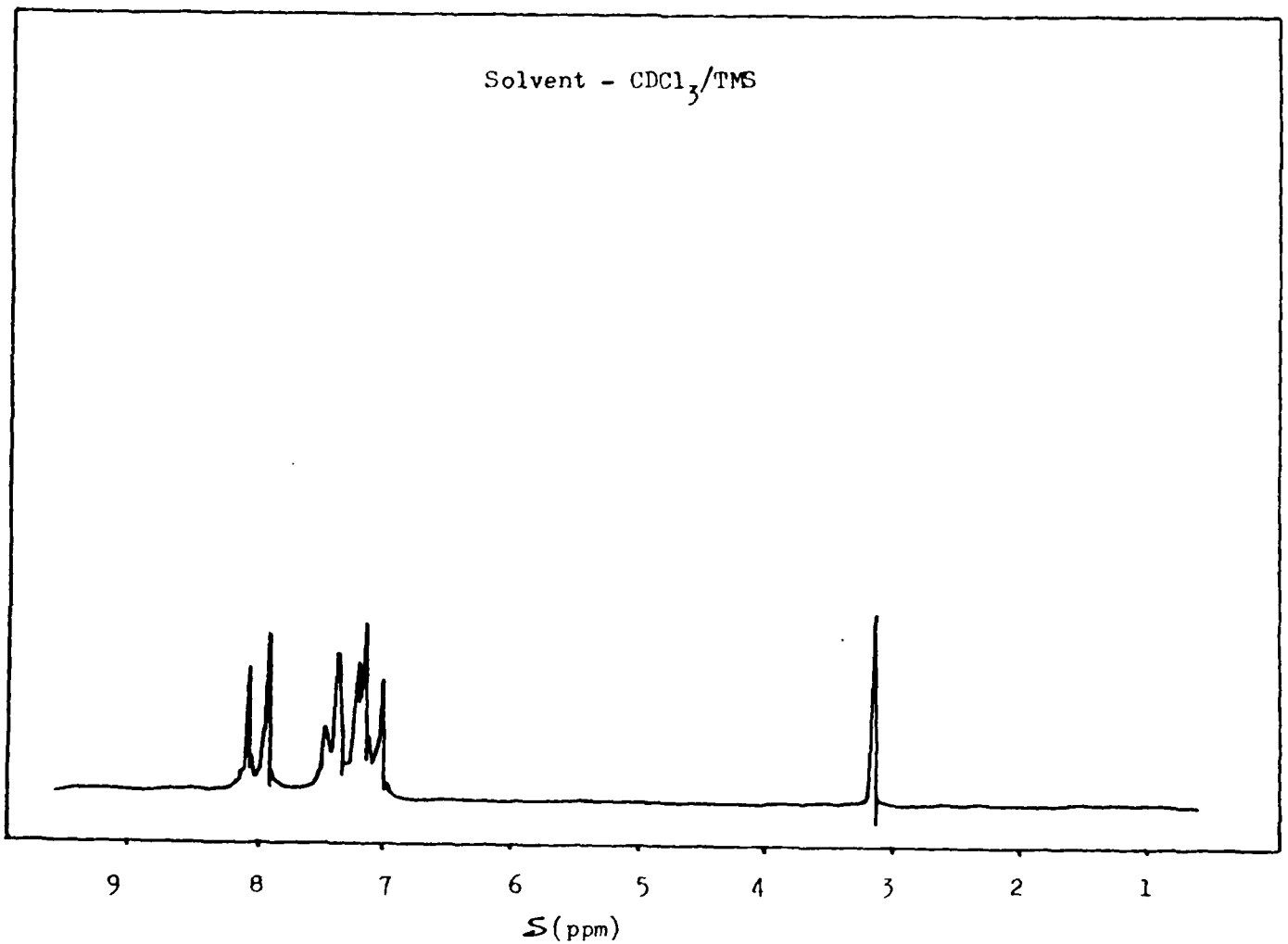

FIGURE 31 PROTON N.M.R. SPECTRUM OF SUB-FRACTION 2, ISOLATED BY PREPARATIVE T.L.C. FROM THE HIGH BOILING POINT FRACTION EVAPORATED FROM ATS MONOMER ON CURING UNDER HIGH VACUUM CONDITIONS

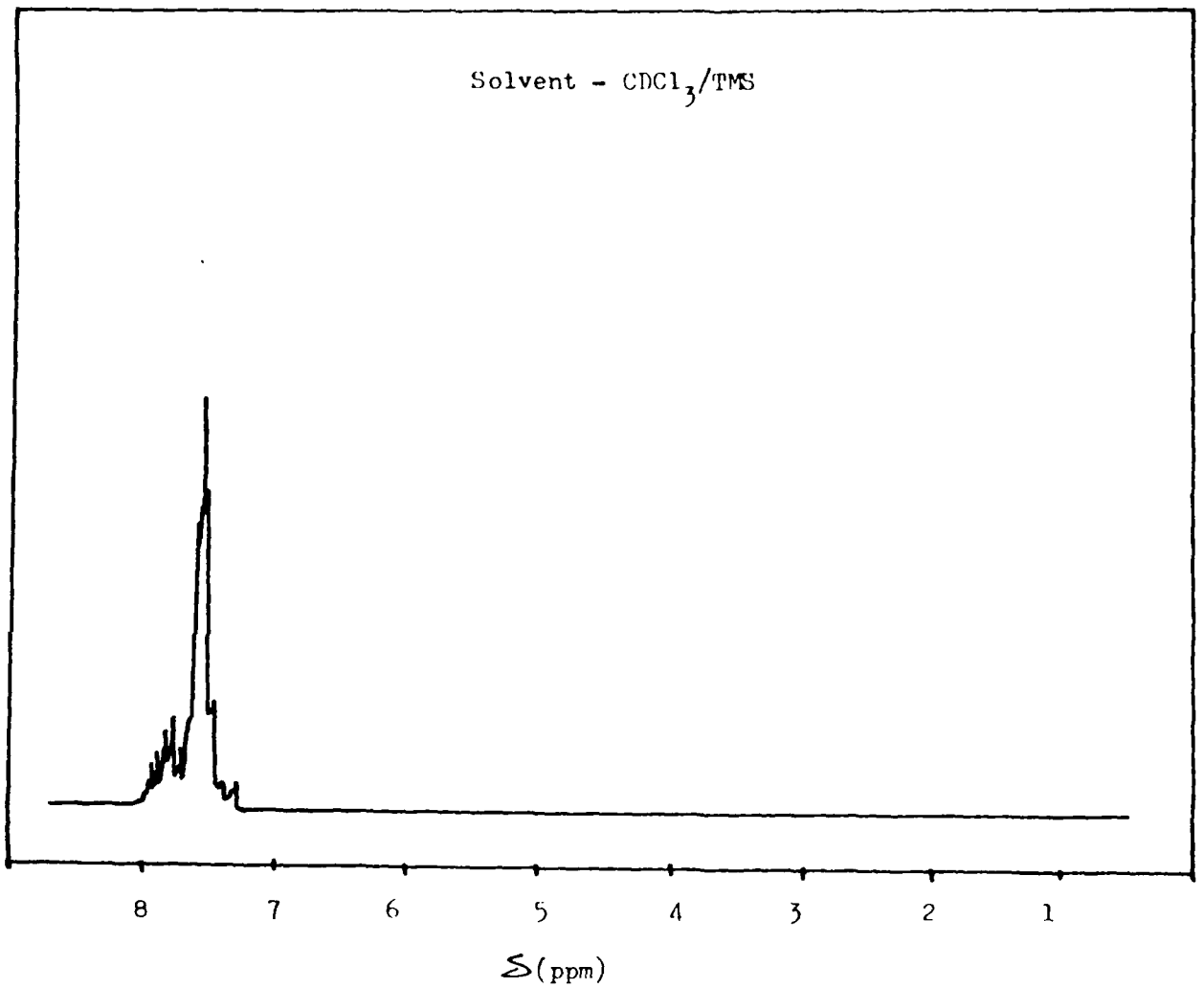

FIGURE 32 PROTON N.M.R. SPECTRUM OF SUB-FRACTION 3, ISOLATED BY PREPARATIVE T.L.C. FROM THE HIGH BOILING POINT FRACTION EVAPORATED FROM ATS-G ON CURING UNDER HIGH VACUUM CONDITIONS

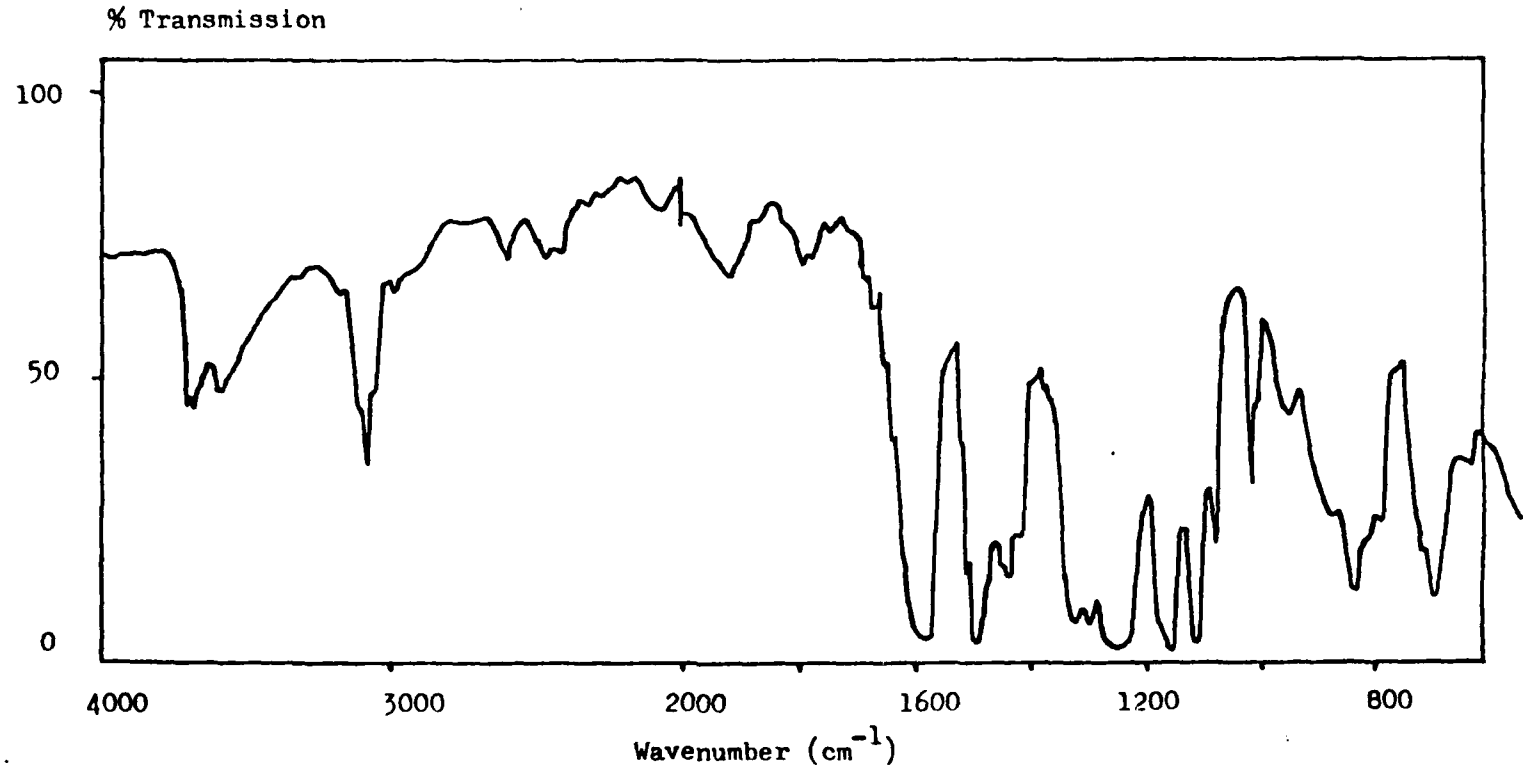

FIGURE 33 I.R. SPECTRUM OF ATS MONOMER, HEATED TO APPROXIMATELY 300°C AT 5°C/min, THEN COOLED TO ROOM TEMPERATURE UNDER HIGH VACUUM CONDITIONS

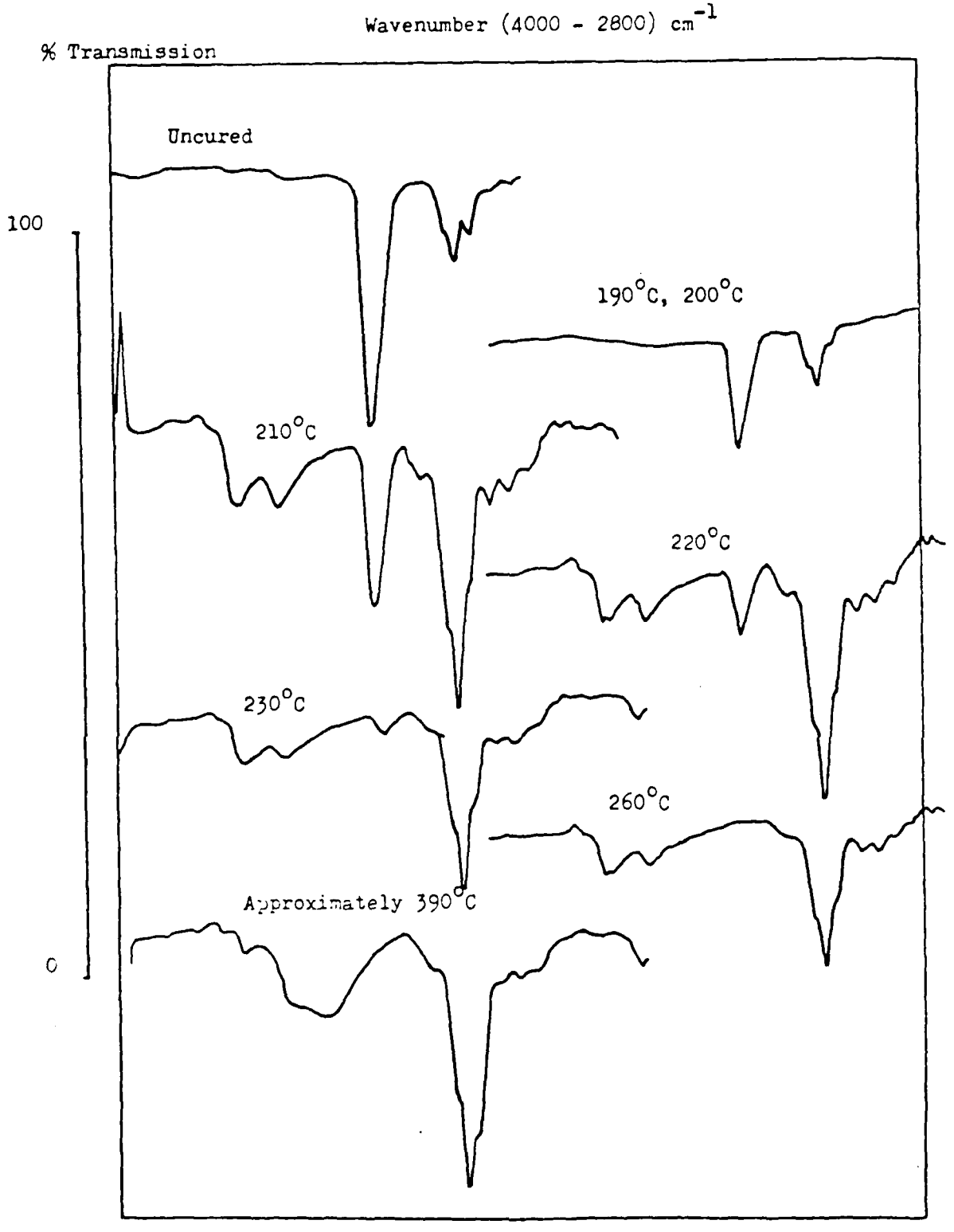

FIGURE 34 I.R. SPECTRA OF ATS-G, PARTIALLY AND COMPLETELY CURED BY HEATING AT 5°C/min UNDER HIGH VACUUM CONDITIONS

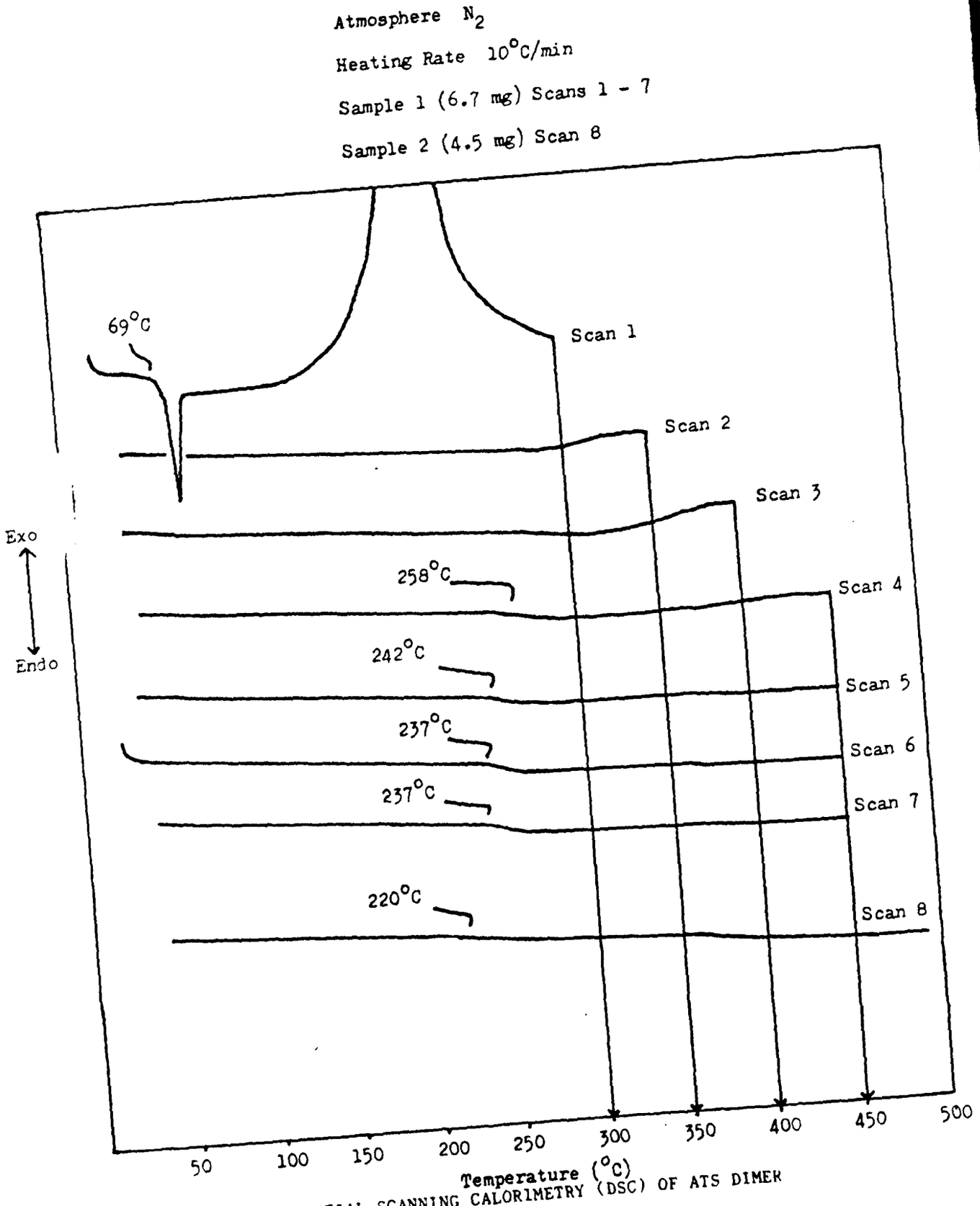

FIGURE 35 DIFFERENTIAL SCANNING CALORIMETRY (DSC) OF ATS DIMER

Sample Size 109.1 mg

Heating Rate 5°C/min

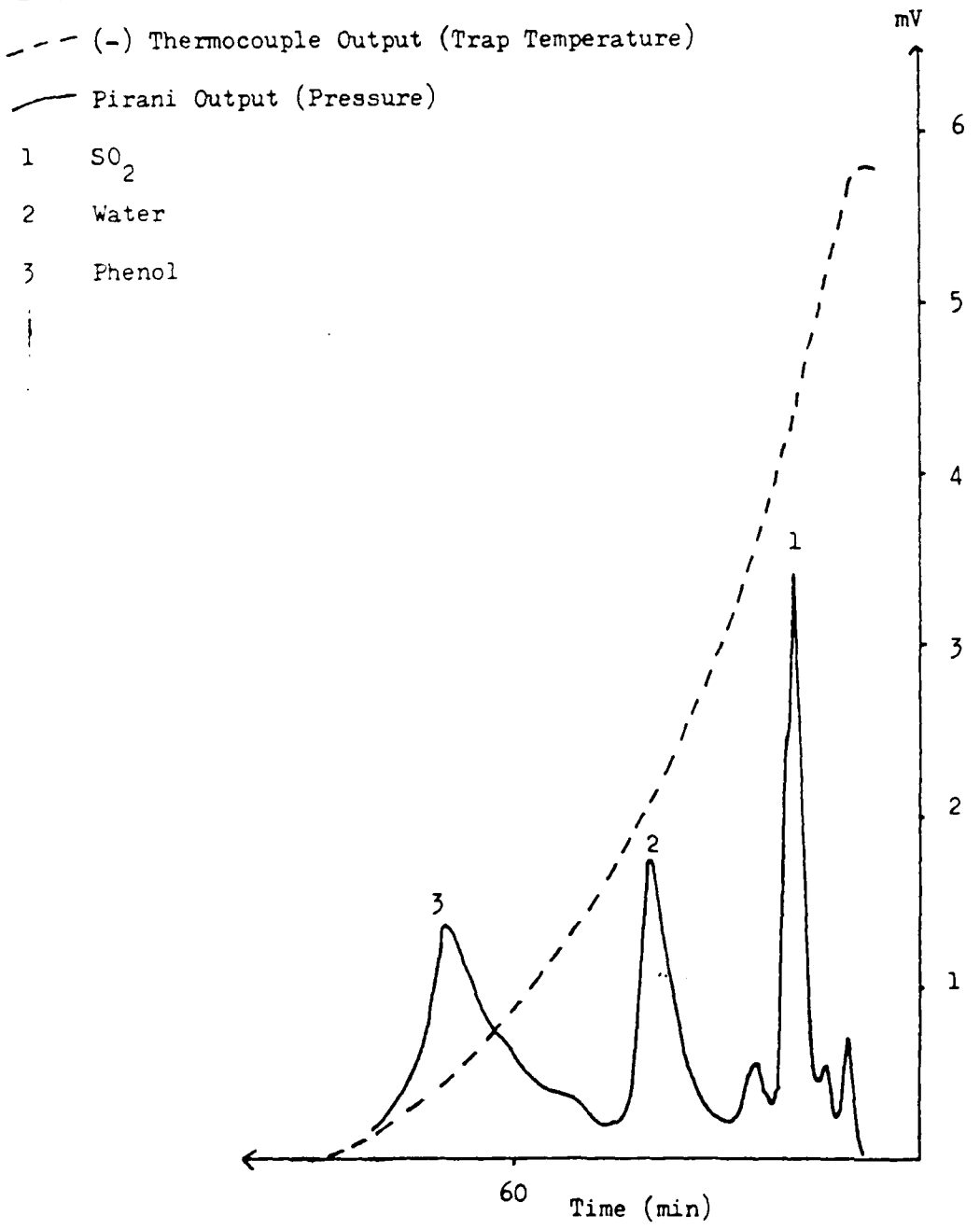

FIGURE 36 SATVA OF THE CONDENSABLE VOLATILE PRODUCT FRACTION OF THERMAL DEGRADATION TO 450°C OF ATS DIMER

Original Sample Size 109.1 mg

Heating Rate 5°C/min

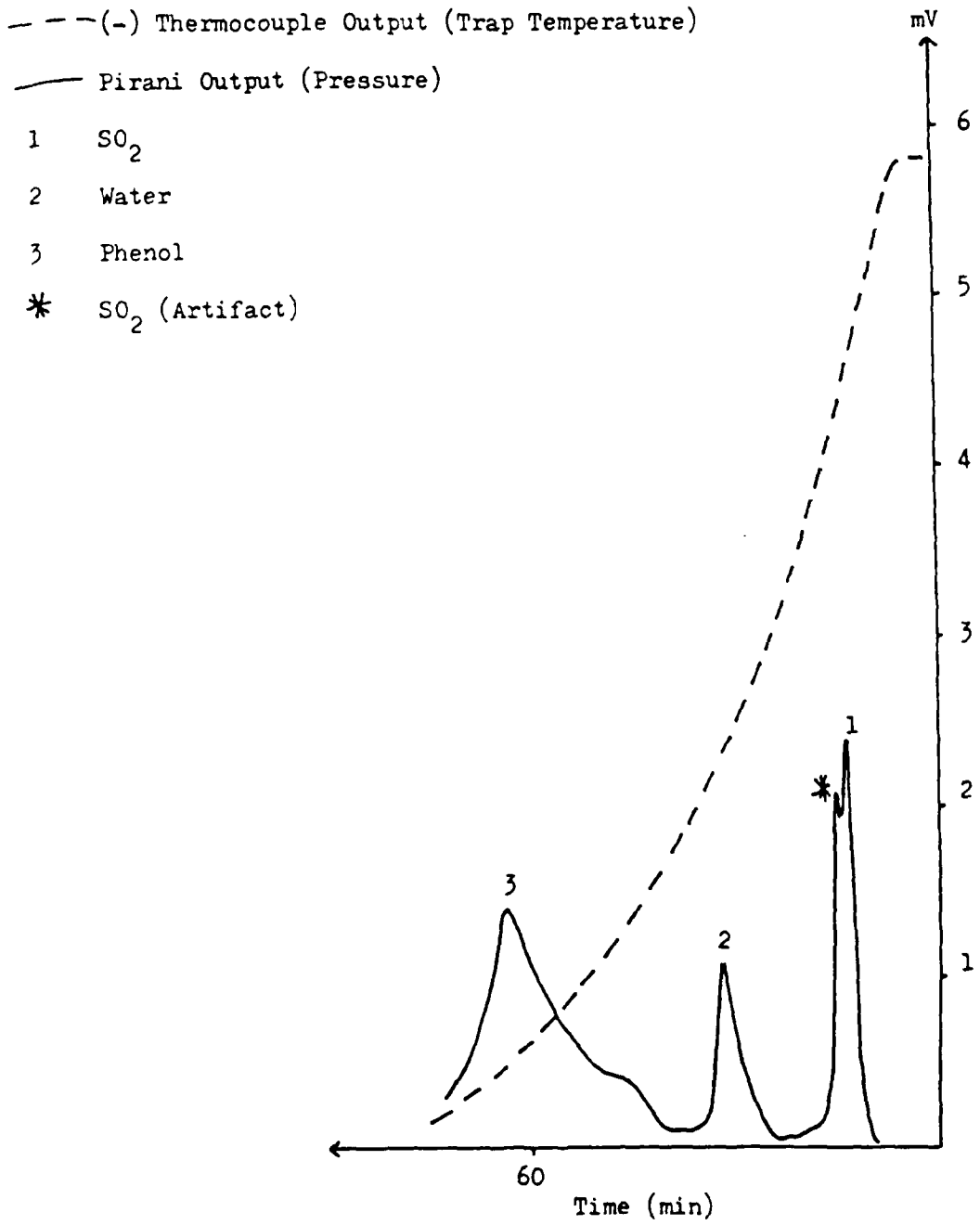

FIGURE 37 SATVA OF THE CONDENSABLE VOLATILE PRODUCT FRACTION OF THERMAL DEGRADATION TO 450°C OF ATS DIMER PREDEGRADED TO 450°C

Sample Size 481.5 mg

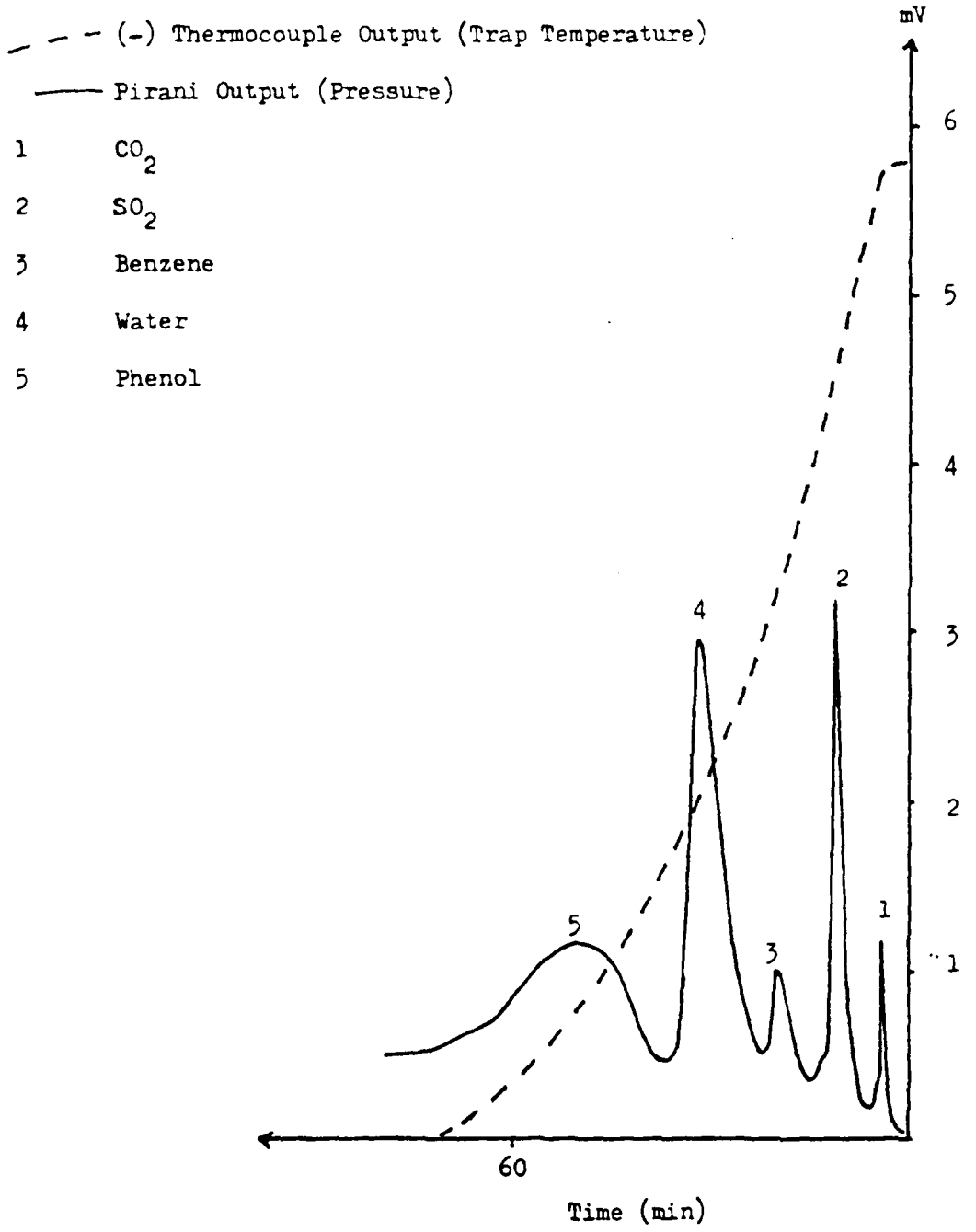

FIGURE 38 SATVA OF THE CONDENSABLE VOLATILE PRODUCT FRACTION OF ISOTHERMAL DEGRADATION OF PRECURED ATS MONOMER AT 328°C FOR 10.5 hrs UNDER HIGH VACUUM CONDITIONS

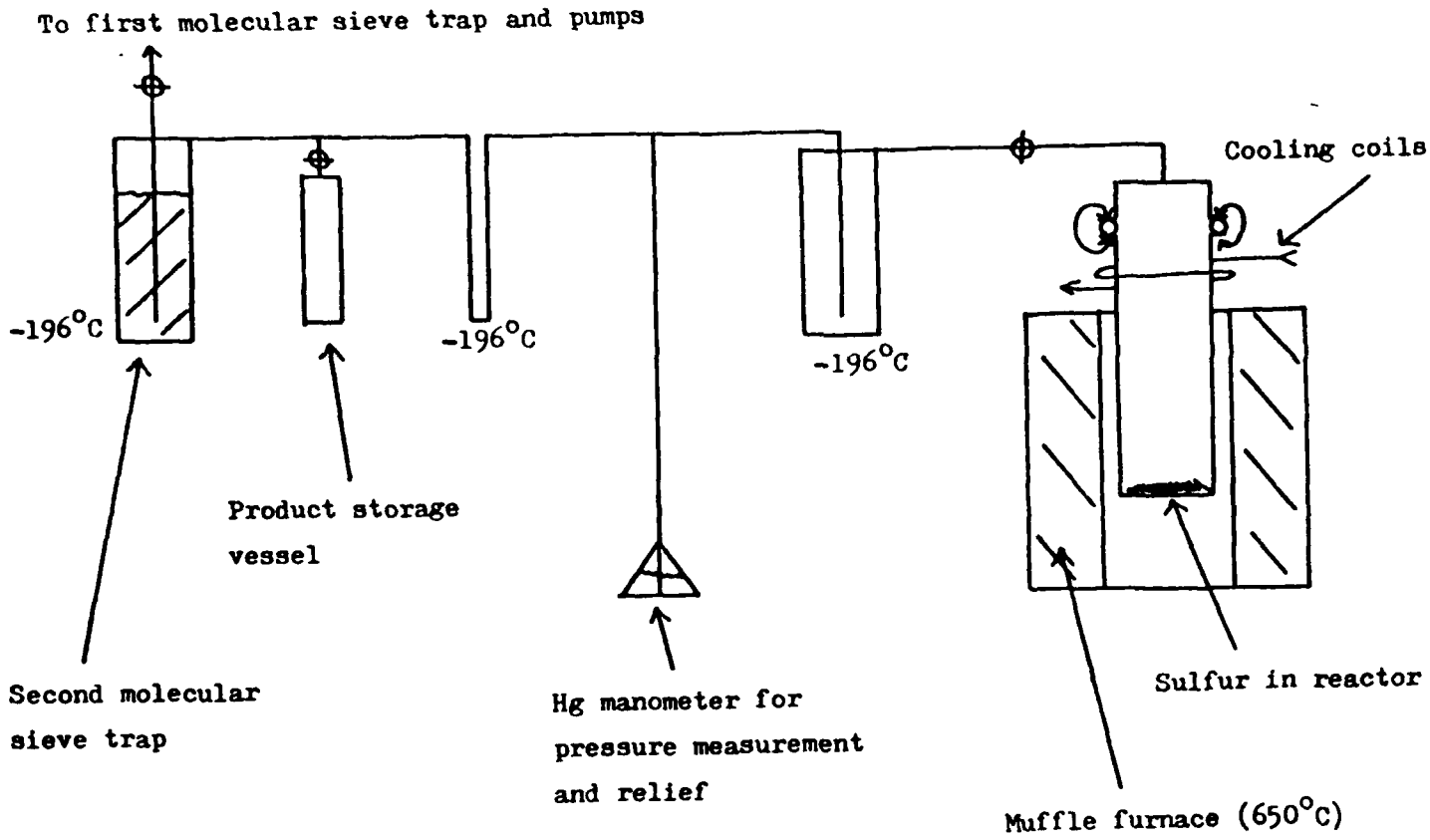

FIGURE 39 APPARATUS USED IN THE PREPARATION OF CARBONYL SULFIDE

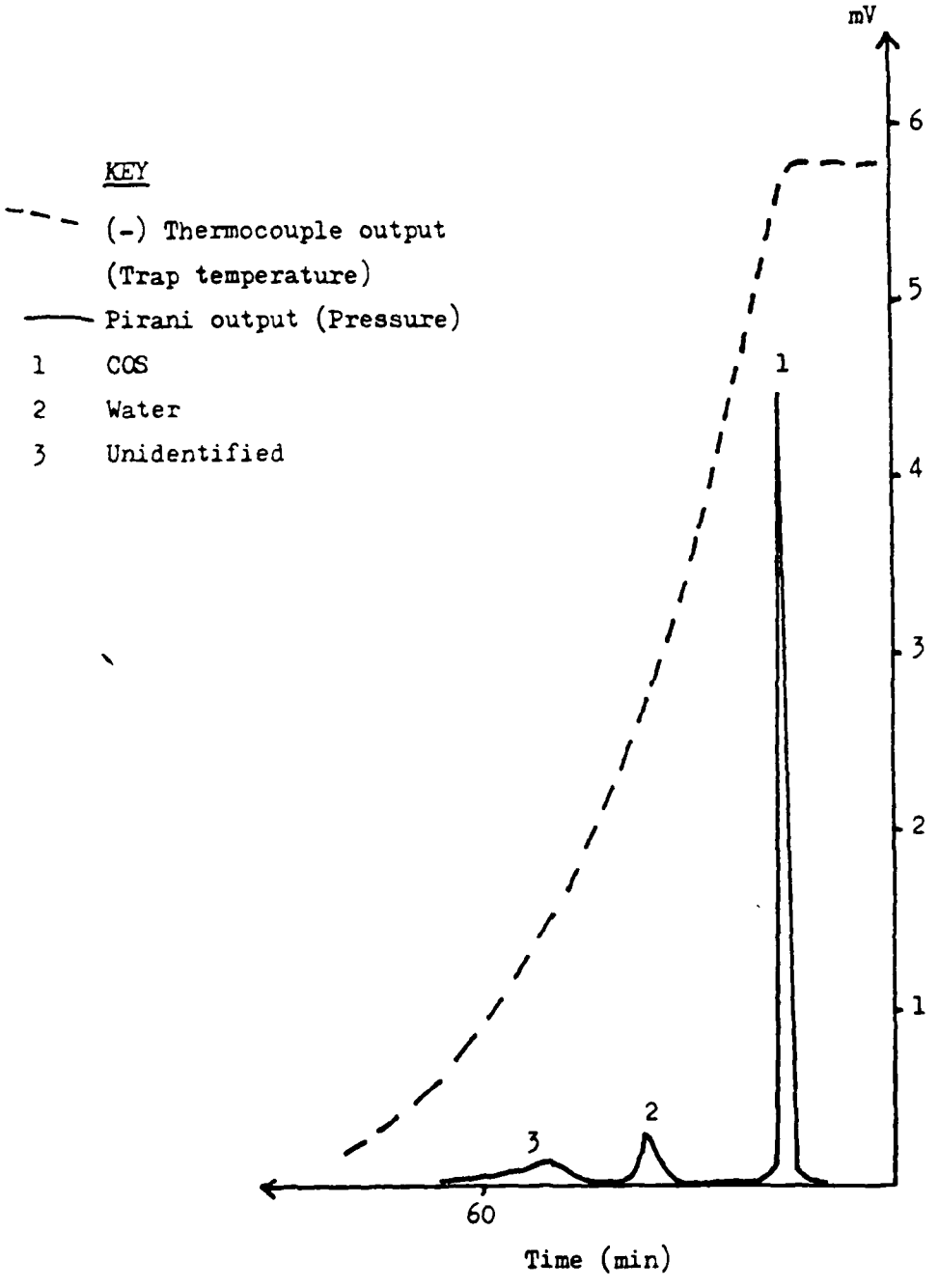

FIGURE 40 SATVA OF THE CARBONYL SULFIDE PRODUCT MIXTURE

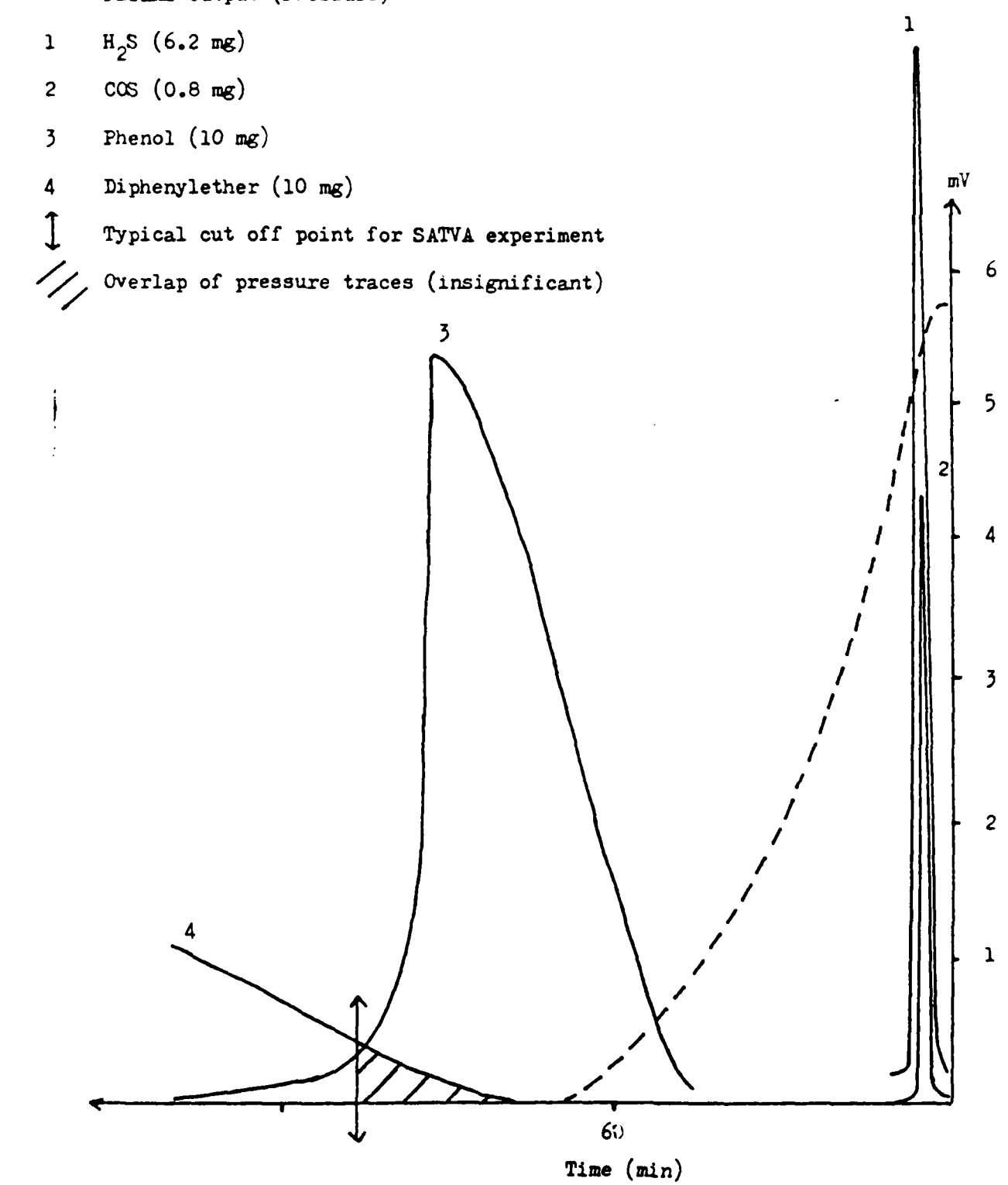

FIGURE 41 SATVA OF SOME REFERENCE COMPOUNDS

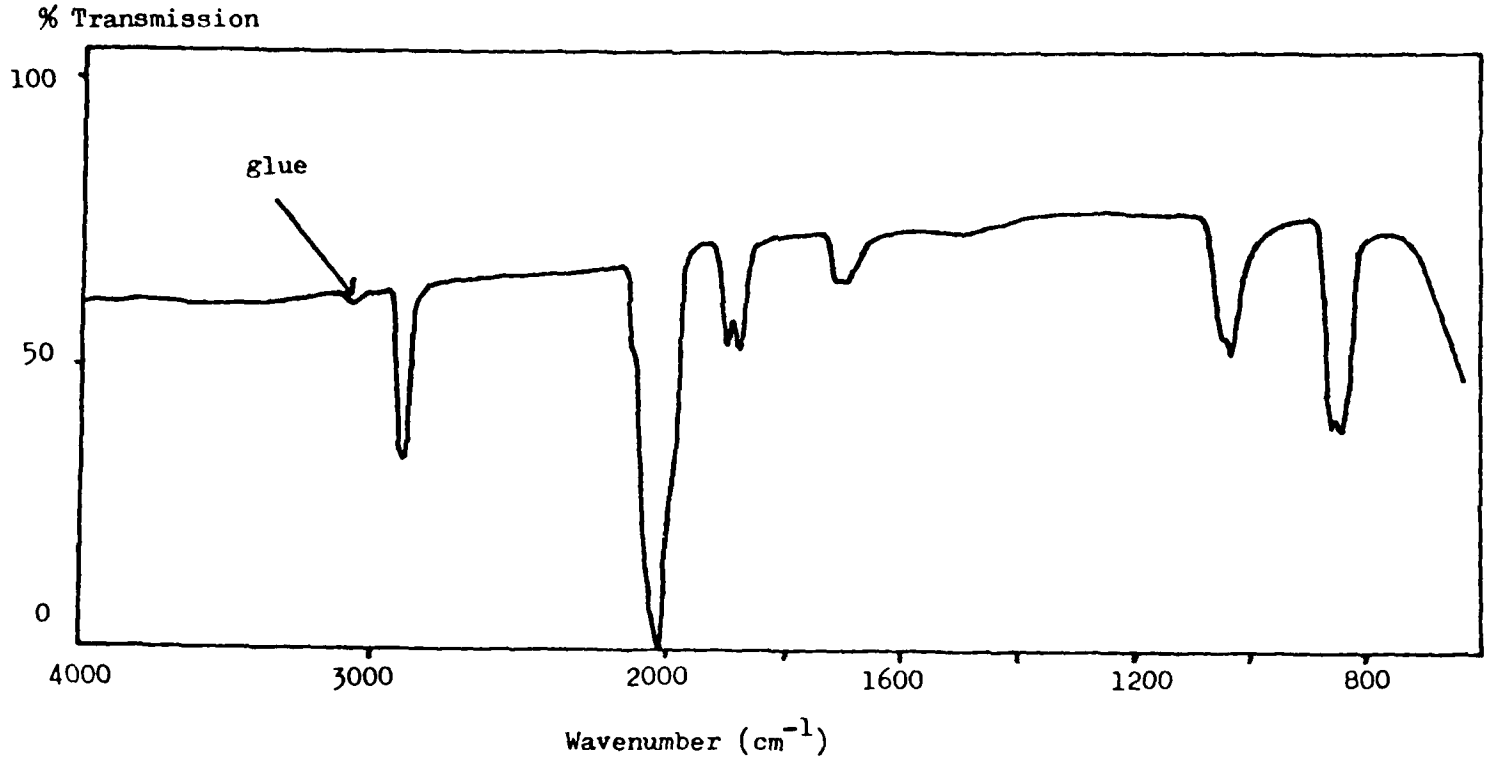

FIGURE 42 GAS PHASE I.R. SPECTRUM OF THE CARBONYL SULFIDE PRODUCT MIXTURE

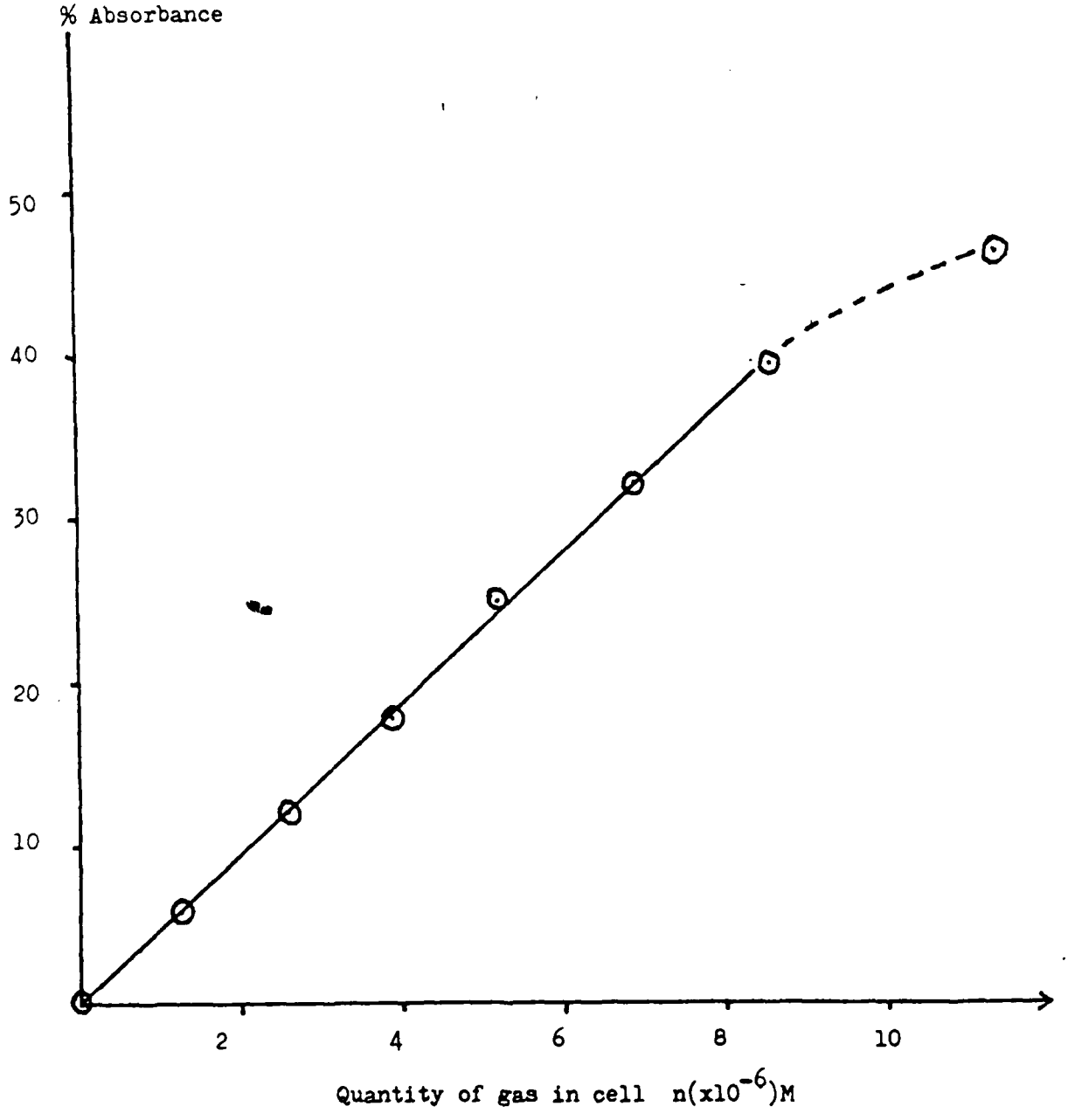

FIGURE 43 GAS PHASE I.R. CALIBRATION CURVE FOR CARBONYL SULFIDE USING ITS 2040 cm^{-1} ABSORBANCE BAND

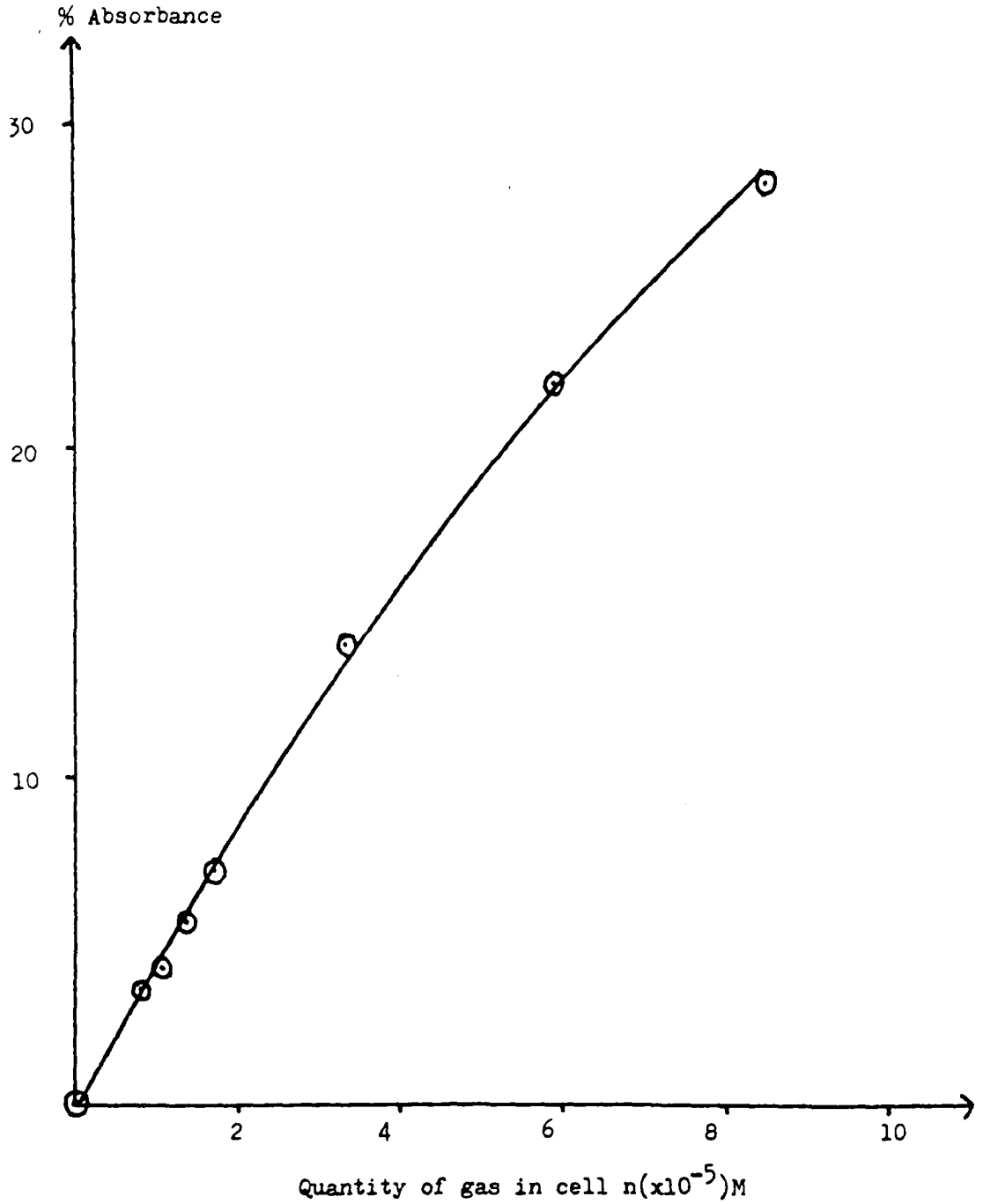

FIGURE 44 GAS PHASE I.R. CALIBRATION CURVE FOR CARBONYL SULFIDE USING ITS 2900 cm^{-1} ABSORBANCE BAND

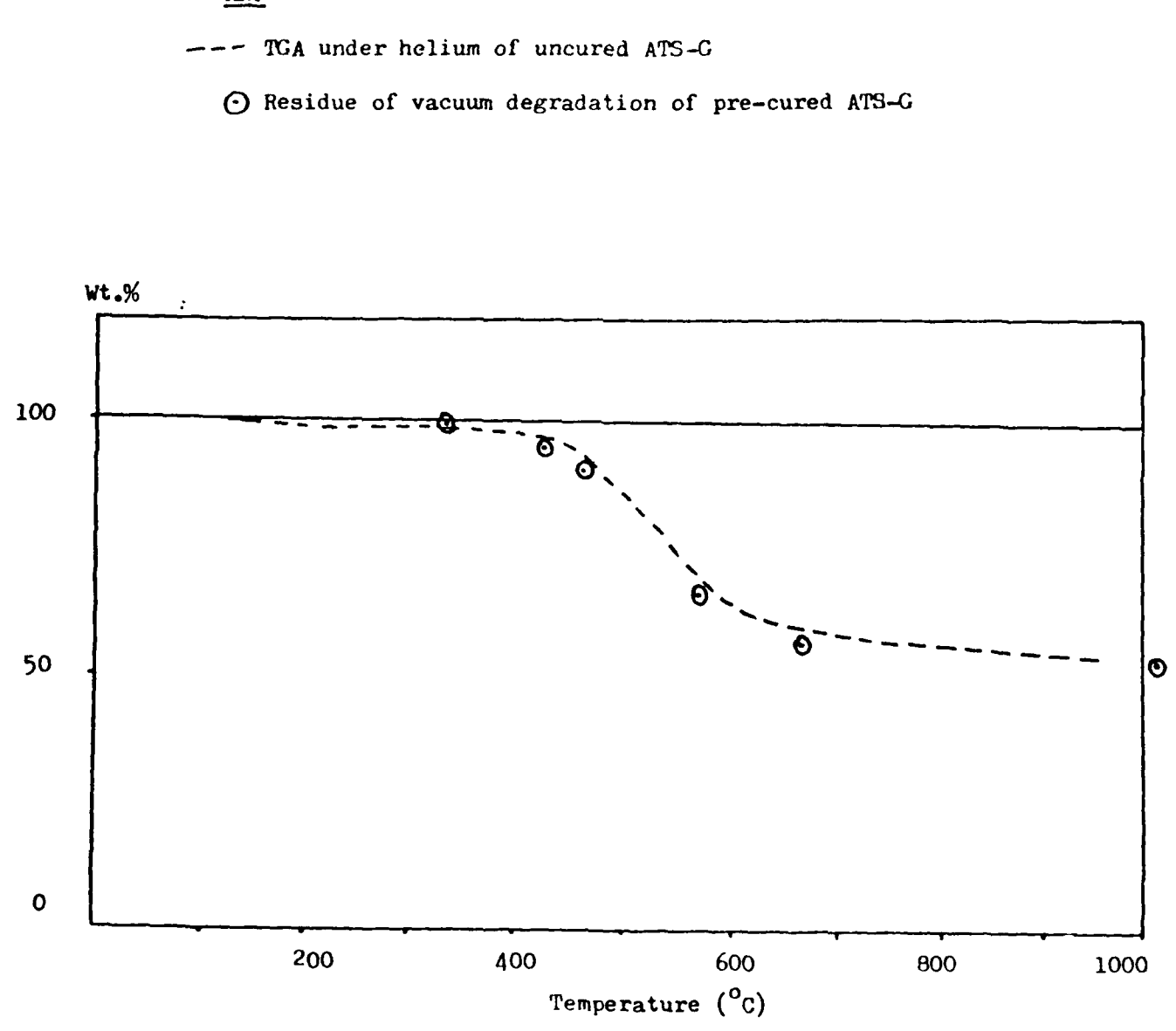

FIGURE 45 ATS-G, A COMPARISON BETWEEN WEIGHT LOST UNDER HELIUM AND UNDER HIGH VACUUM CONDITIONS

Heating rate 5°C/min

CATVA sample size 100 mg

TGA sample size 12.1 mg

KEY

—— Material volatile at 0°C

— — — Material volatile at -75°C

××× Material volatile at -196°C

·—·— H_2

····· TGA under helium

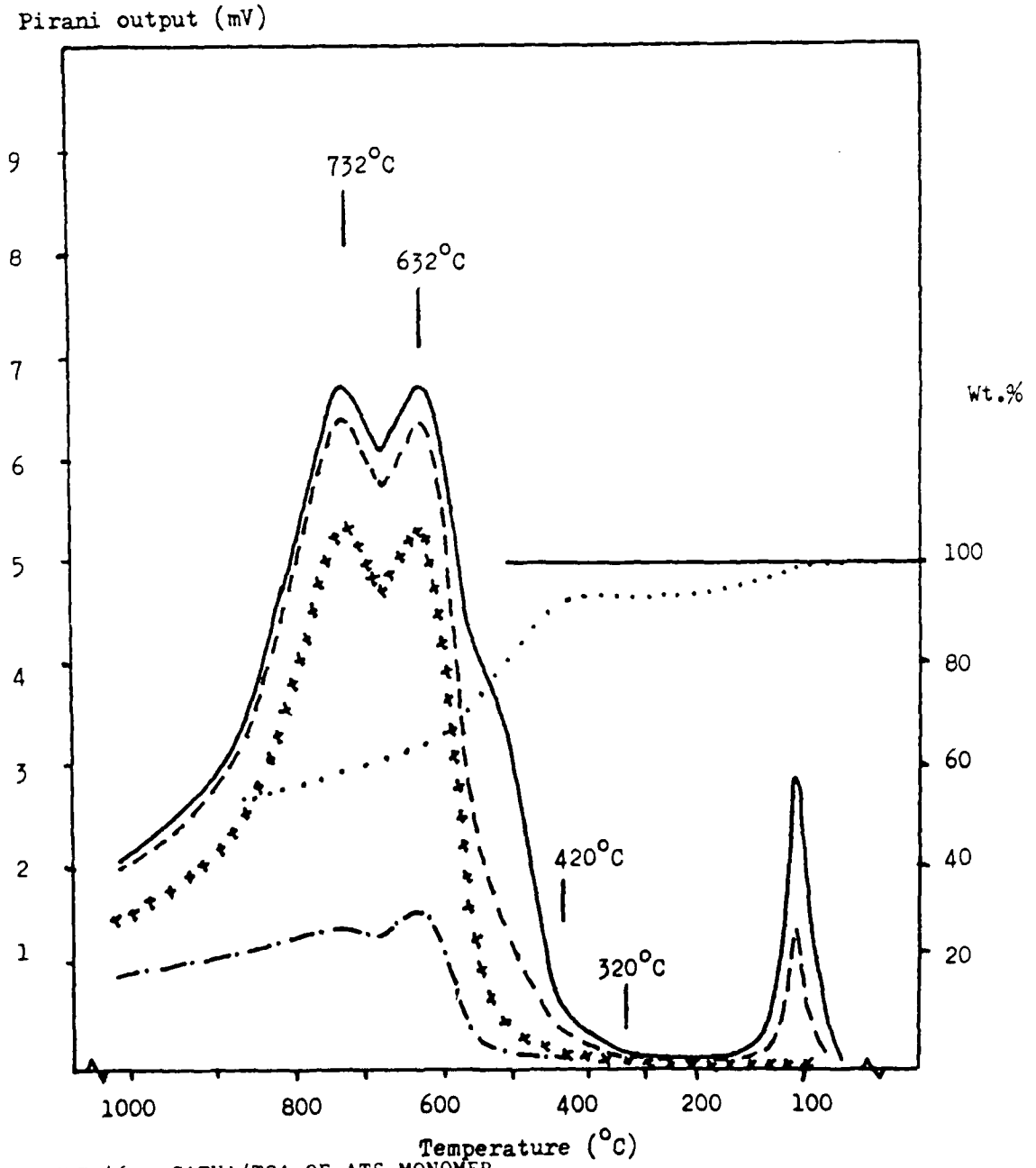

FIGURE 46 CATVA/TGA OF ATS MONOMER

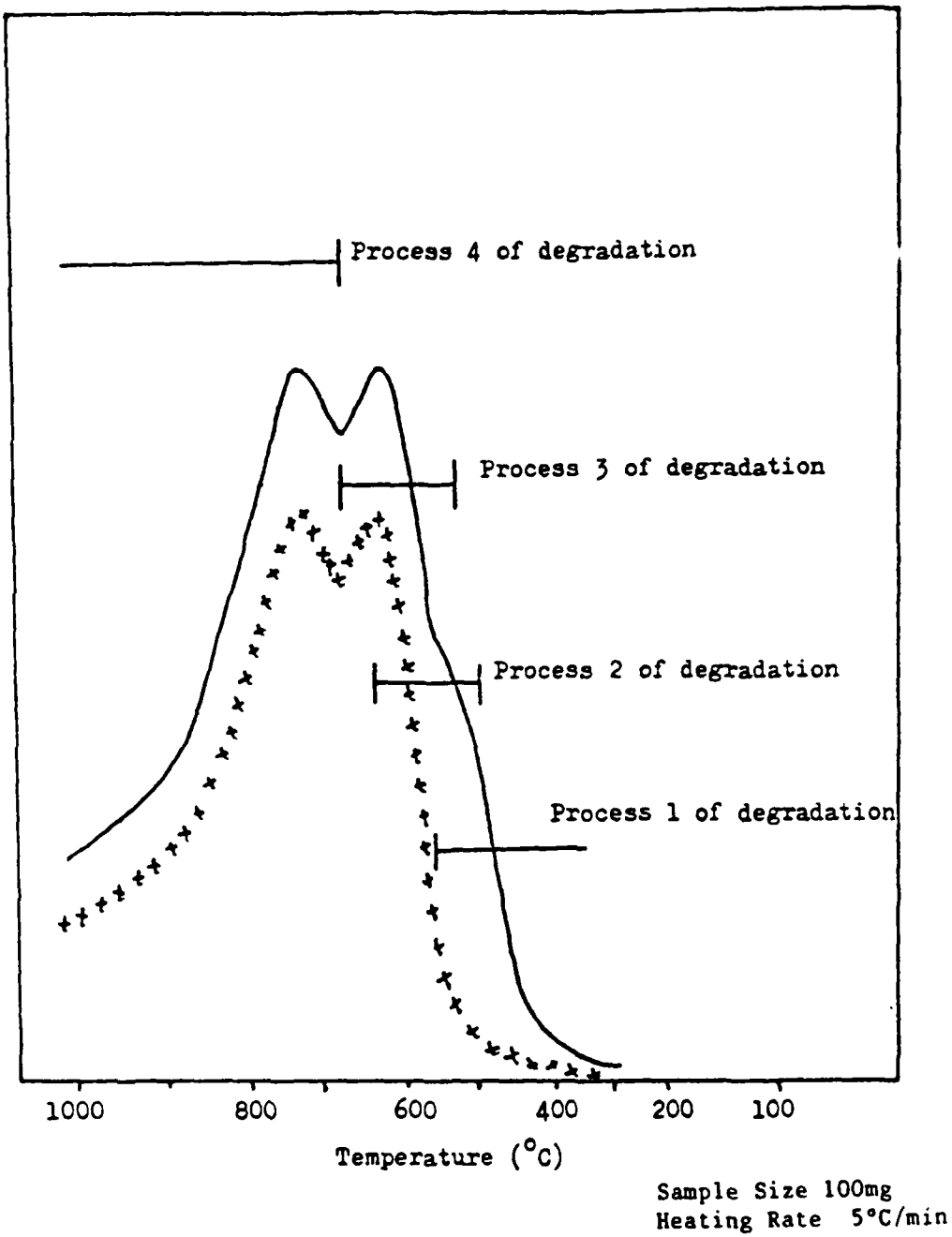

FIGURE 47 PROCESSES OPERATIVE IN THE THERMAL DEGRADATION OF ATS POLYMERS

Heating rate 5°C/min

CATVA sample size 100 mg

TGA sample size 12.0 mg

KEY

—— Material volatile at 0°C

– – – Material volatile at -75°C

×××× Material volatile at -196°C

.—.—. H_2

..... TGA under helium

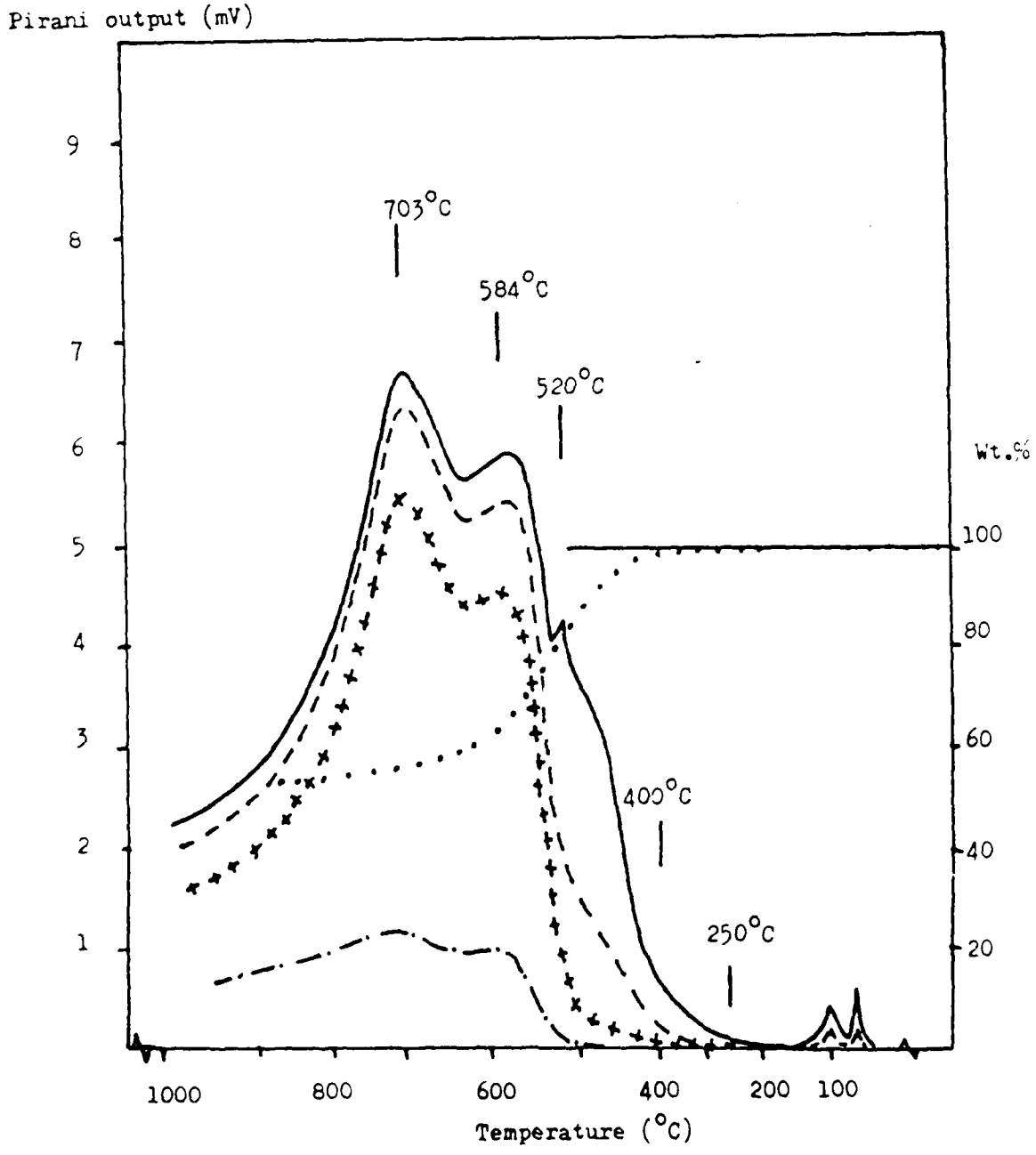

FIGURE 48 CATVA/TGA OF ATS DIMER

Heating rate 5°C/min

CATVA sample size 100 mg

TGA sample size 10.6 mg

KEY

—— Material volatile at 0°C

– – – Material volatile at -75°C

×××××× Material volatile at -196°C

-·-·- H_2

····· TGA under helium

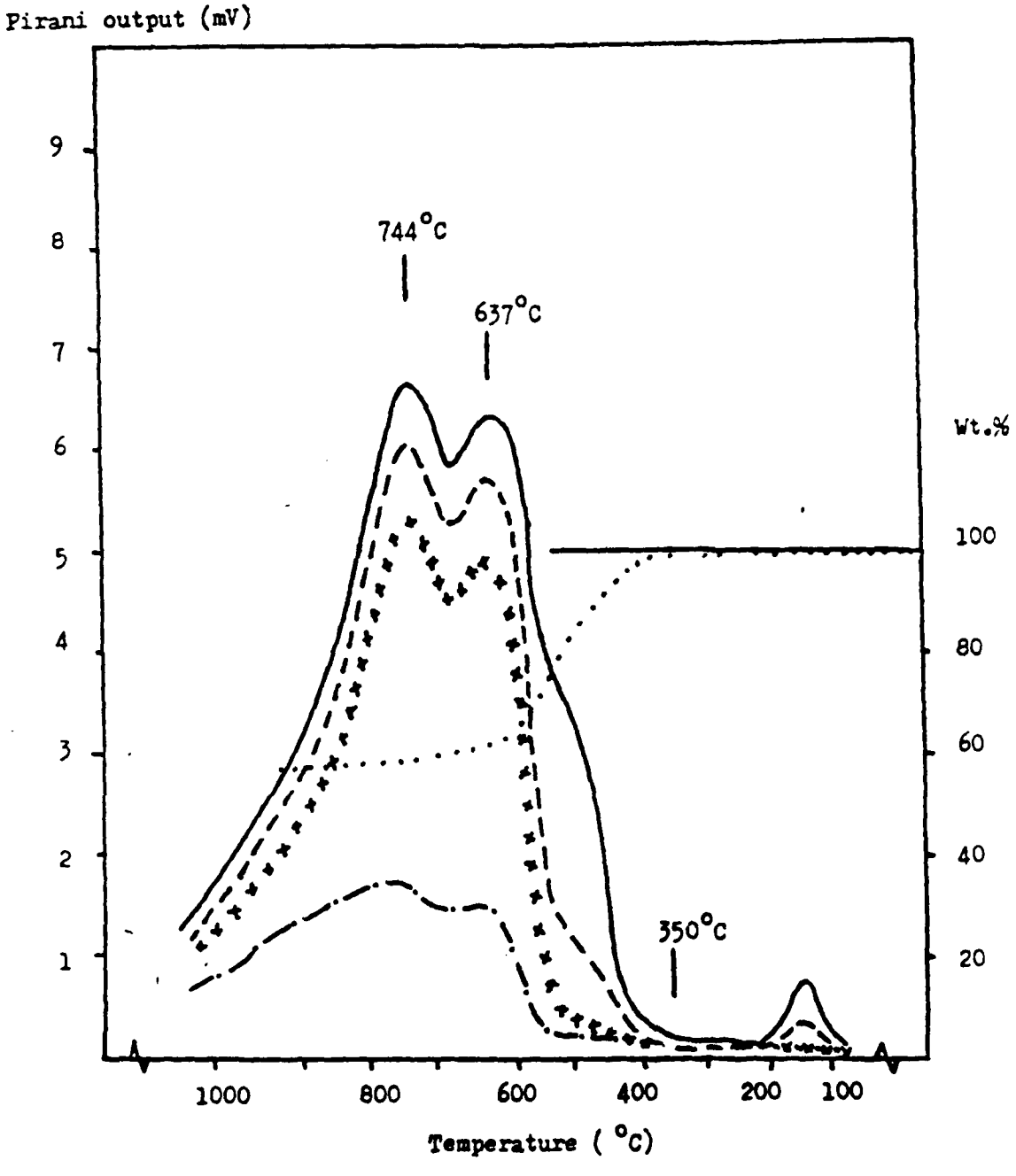

FIGURE 49 CATVA/TGA OF ATS-G

Heating rate 5°C/min

CATVA sample size 100 mg

TGA sample size 13.5 mg

KEY

—— Material volatile at 0°C

– – – Material volatile at -75°C

×××× Material volatile at -196°C

·—·—· H_2

•••• TGA under helium

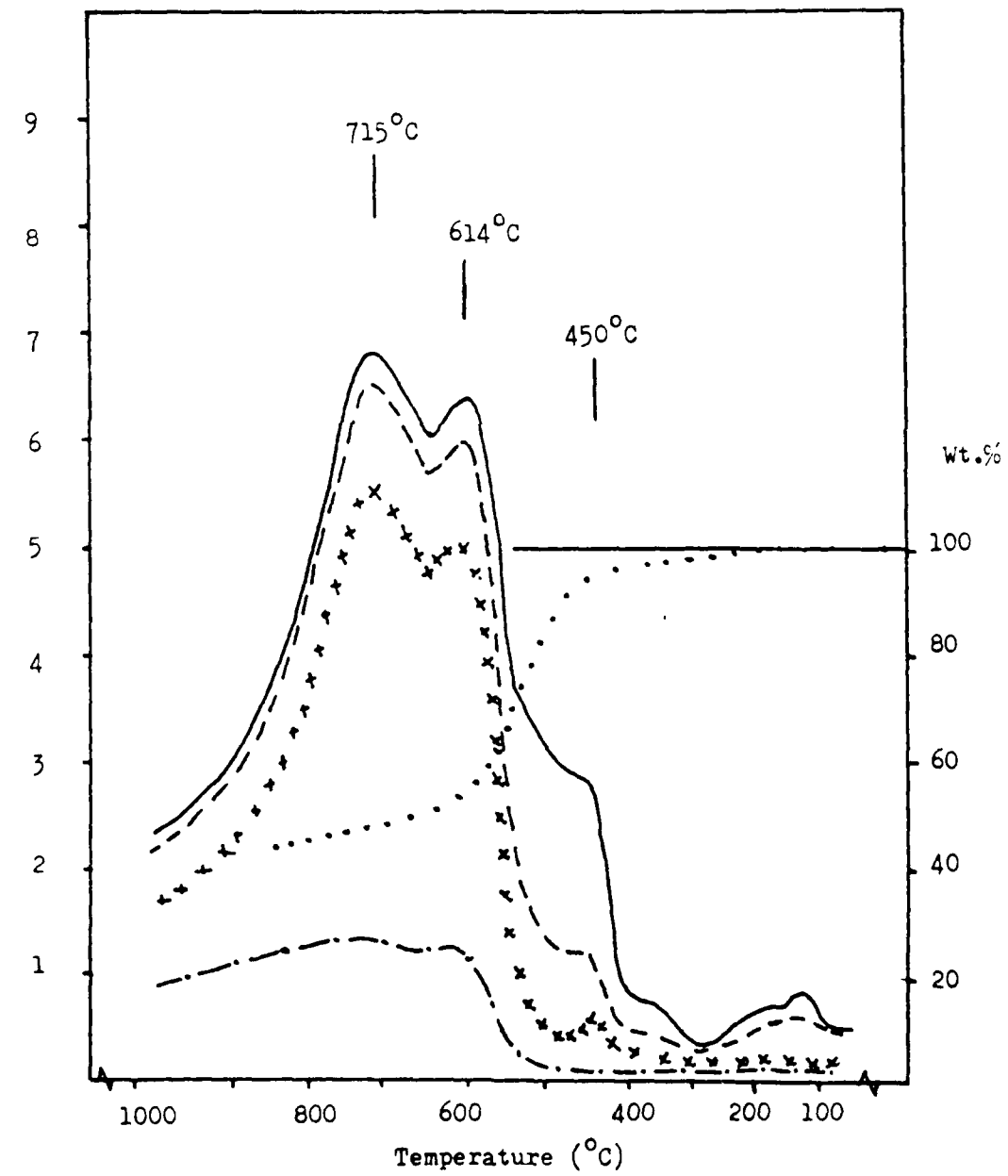

FIGURE 50 CATVA/TGA OF ATS TRIMER

Heating rate 5°C/min

CATVA sample size 100.2 mg

TGA sample size 10.65 mg

KEY

—— Material volatile at 0°C

– – – Material volatile at -75°C

**** Material volatile at -196°C

·—·— H_2

····· TGA under helium

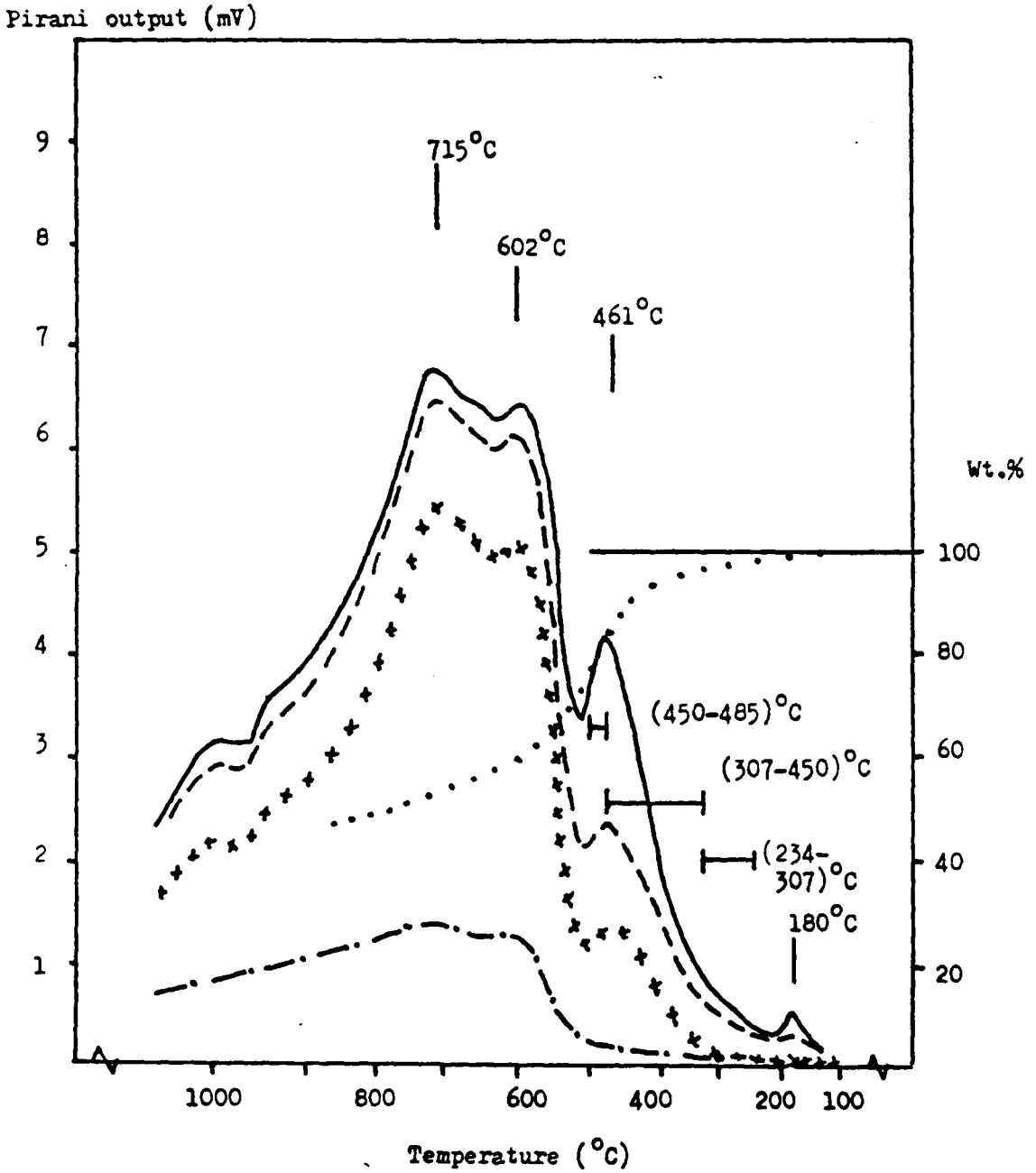

FIGURE 51 CATVA/TGA OF F4

Heating rate 5°C/min

TVA sample size 8.8 mg

TGA sample size 11.1 mg

KEY

—— Material volatile at 0°C

– – – Material volatile at -196°C

····· TGA under helium

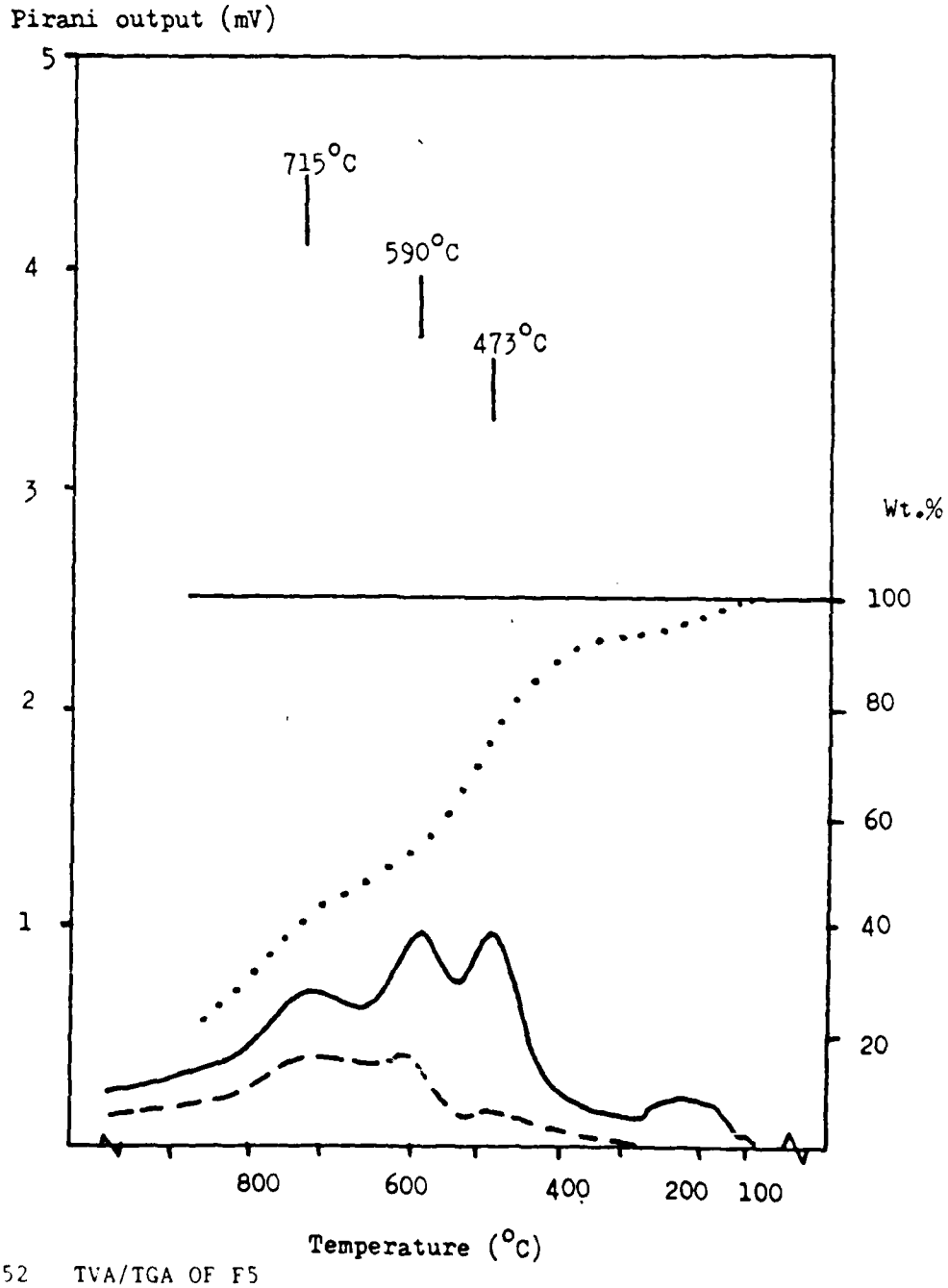

FIGURE 52 TVA/TGA OF F5

Heating rate 5°C/min

CATVA sample size 105.3 mg

TGA sample size 10.5 mg

KEY

—— Material volatile at 0°C

– – – Material volatile at -75°C

×××××× Material volatile at -196°C

.-.-.- H_2

..... TGA under helium

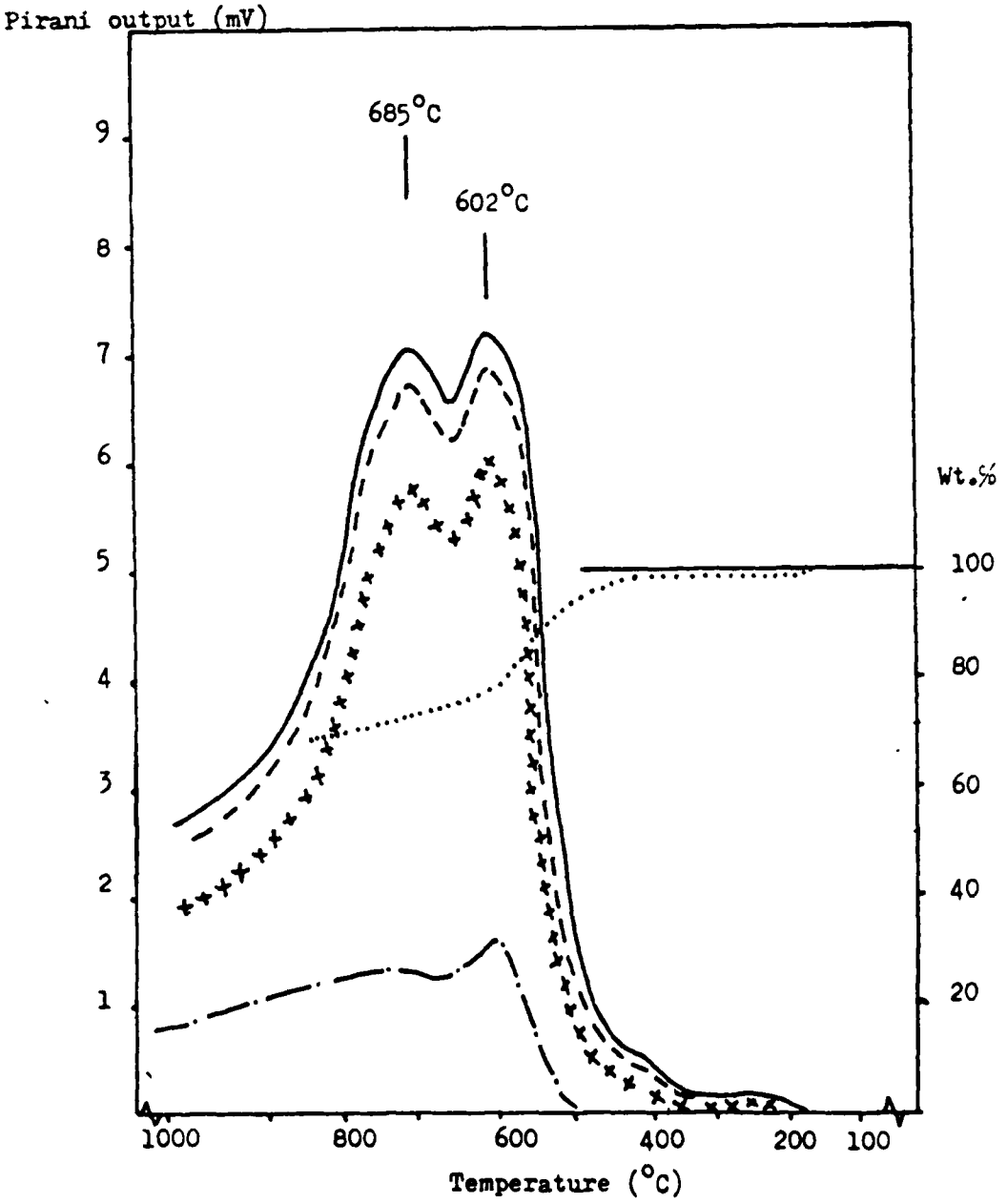

FIGURE 53 CATVA/TGA OF ATP MONOMER

Heating rate 5°C/min

CATVA sample size 108.4 mg

TGA sample size 9.1 mg

KEY

—— Material volatile at 0°C

– – – Material volatile at -75°C

×××× Material volatile at -196°C

·—·— H_2

····· TGA under helium

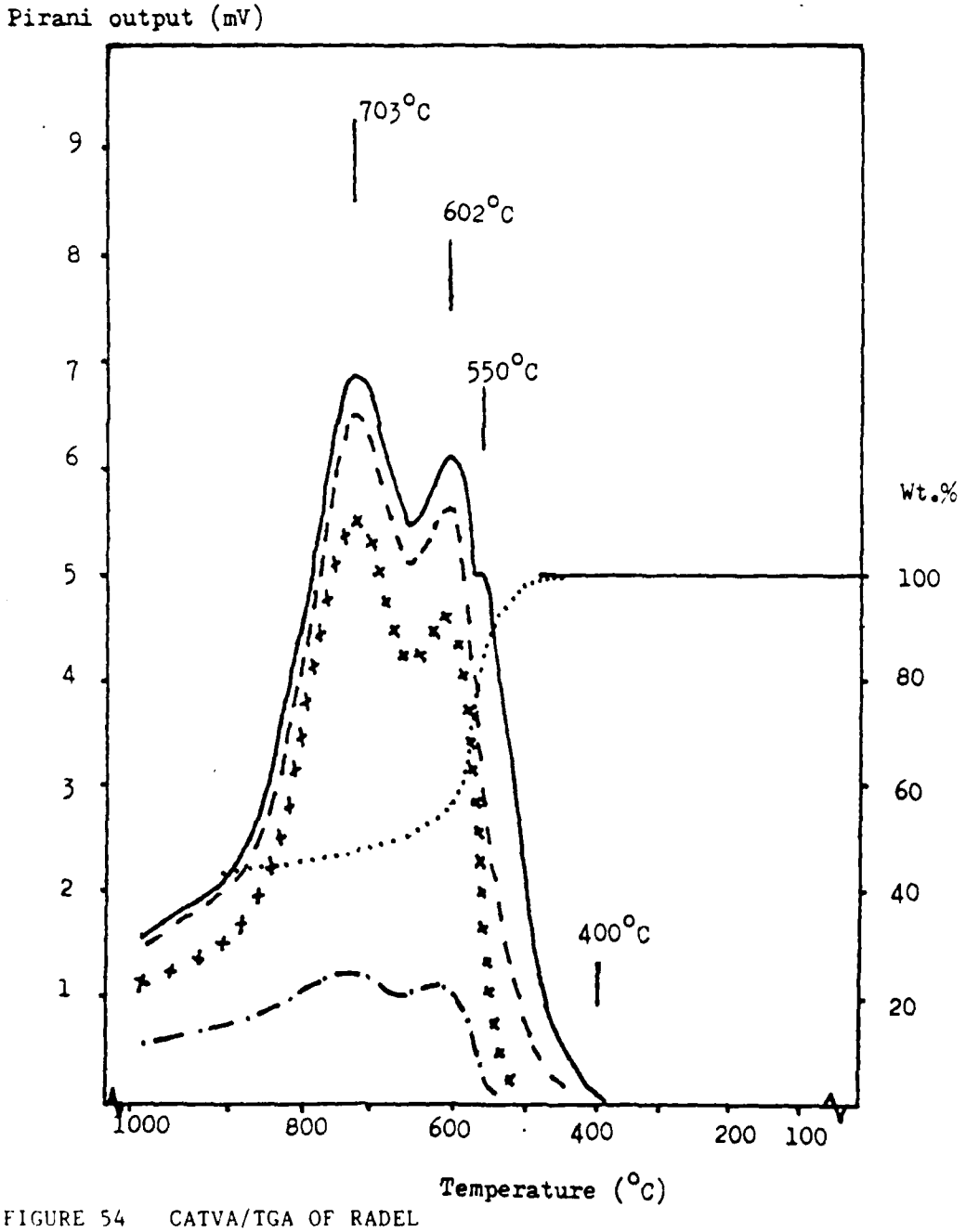

FIGURE 54 CATVA/TGA OF RADEL

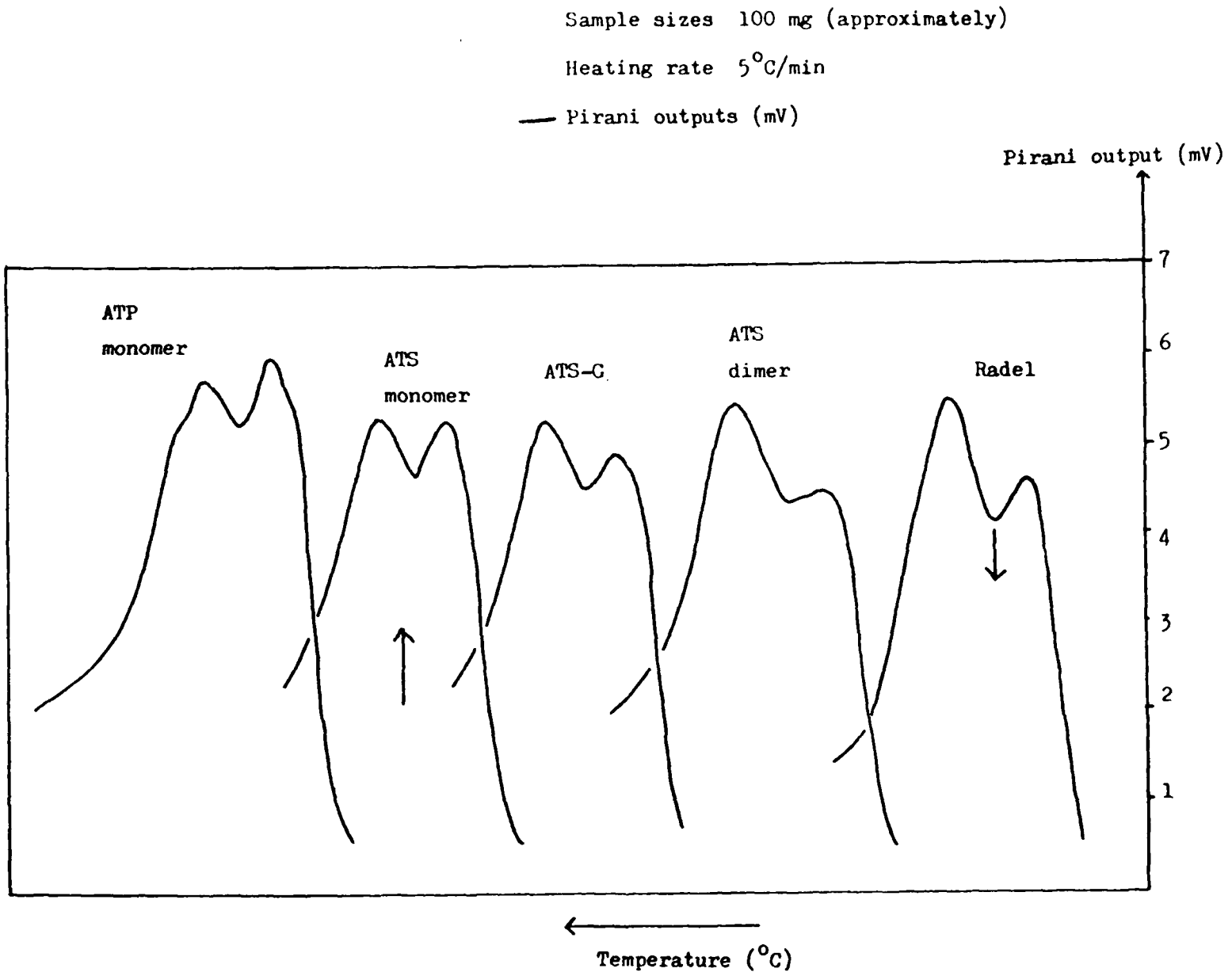

FIGURE 55 NONCONDENSABLE EMISSION CURVES FOR ATS AND RELATED POLYMERS

KEY : 1 Sulfone linkages : 2 Phenylether linkages : 3 Aromatic material

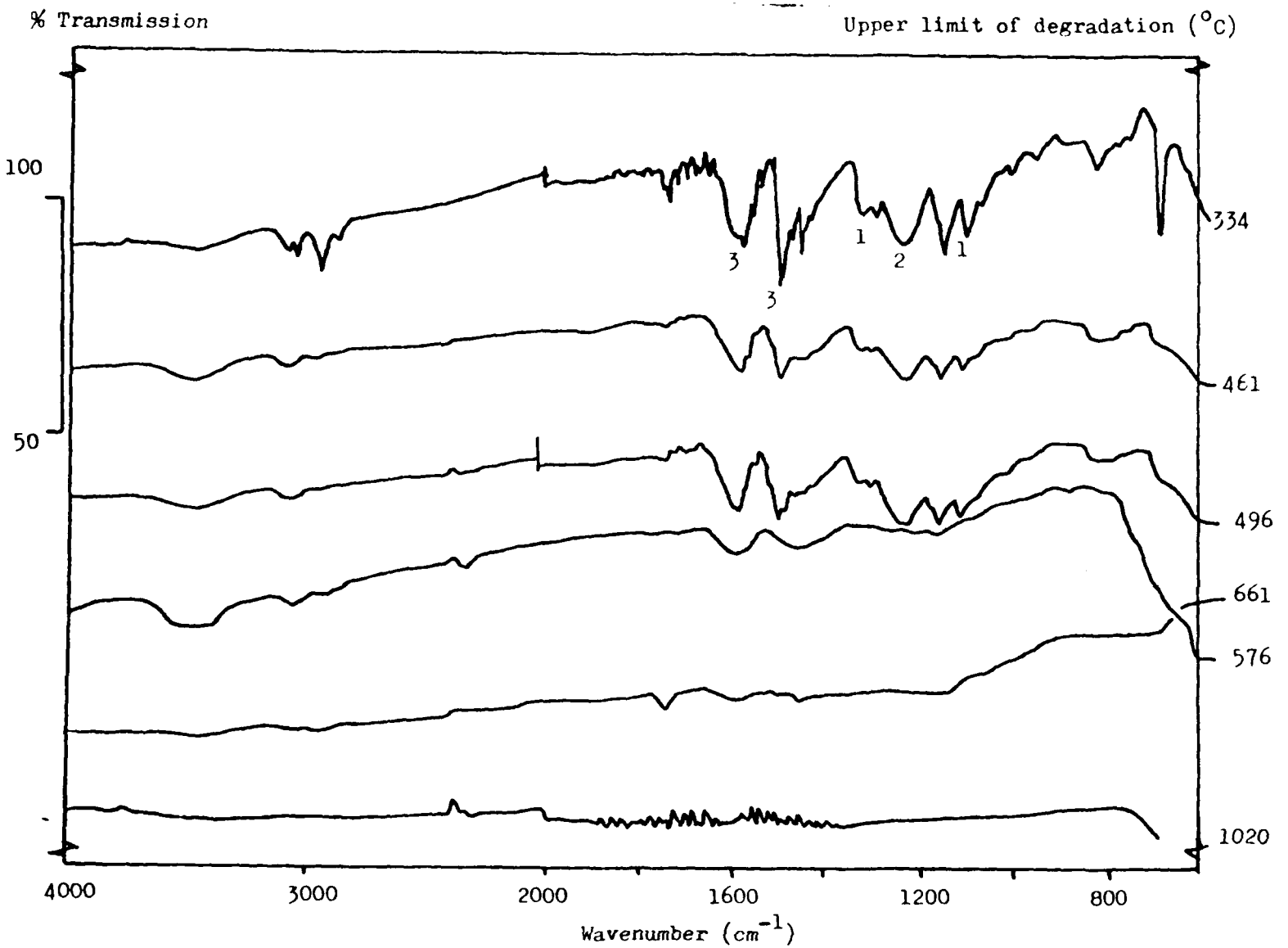

FIGURE 56 I.R. SPECTRA OF RESIDUES OF PARTIAL DEGRADATION OF ATS-G

Heating rate 5°C/min

Sample sizes 100 mg

KEY

carbon

hydrogen

oxygen

sulfur

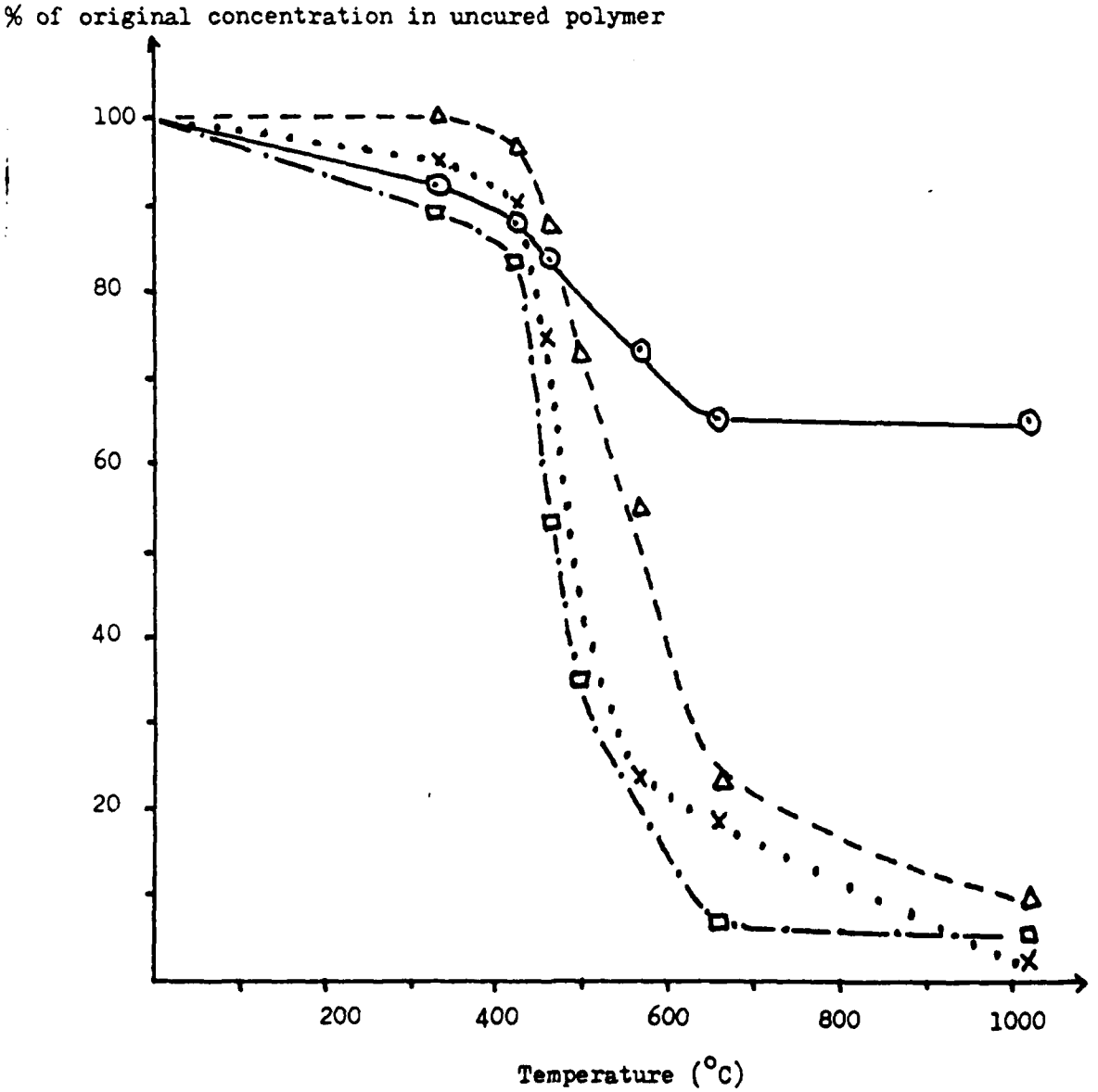

FIGURE 57 ELEMENTAL ANALYSIS OF PARTIALLY DEGRADED ATS-G

KEY

1 Hydroxyl groups
2 Aromatic material
3 Saturated material
4 Phenylether linkages
5 Sulfone linkages

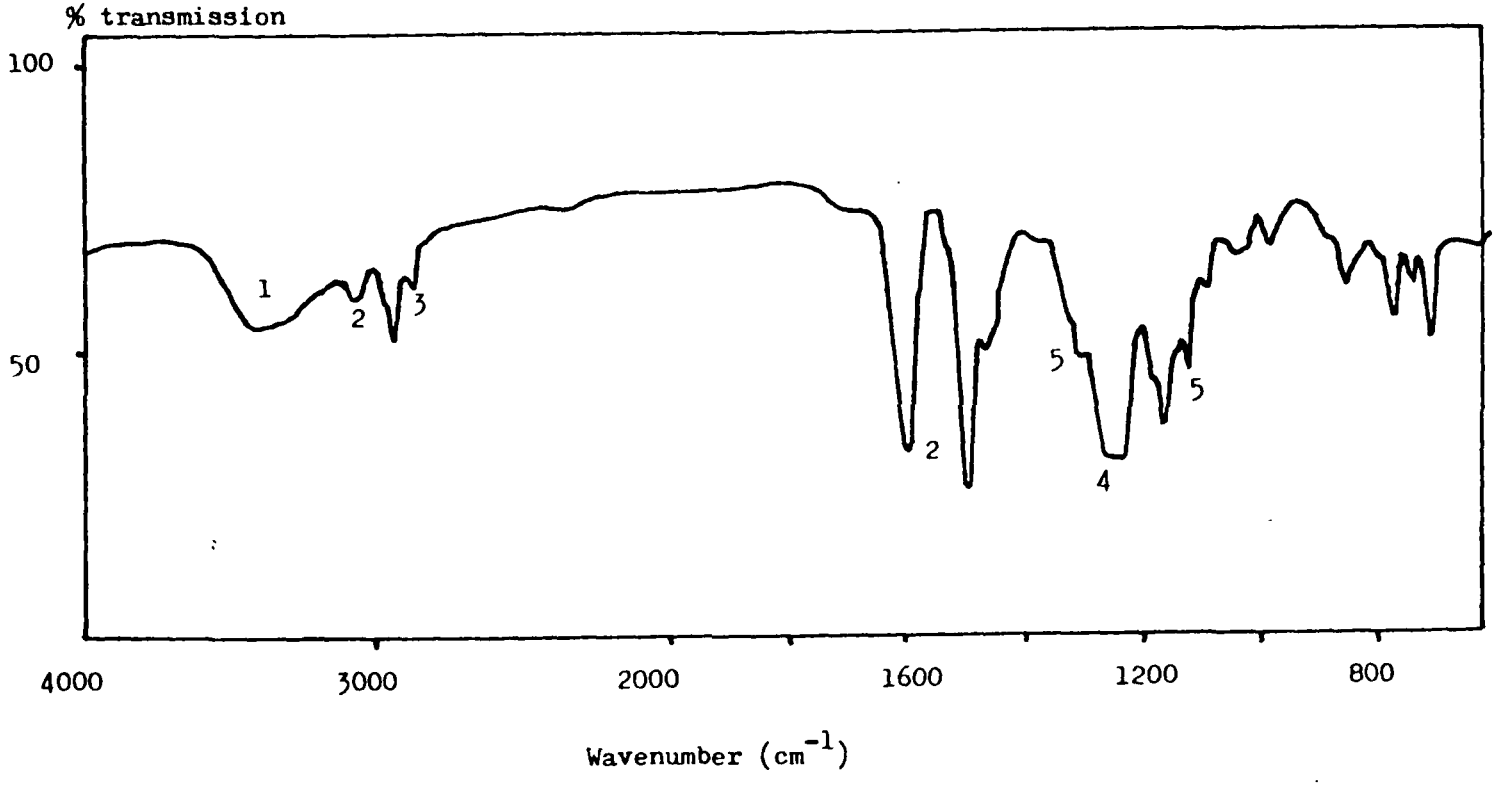

FIGURE 58 I.R. SPECTRUM OF THE OLIGOMERIC PRODUCT FRACTION OF THERMAL DEGRADATION TO 1020°C OF PRECURED ATS-G

KEY

A Aromatic material (3080 cm^{-1})

B Saturated material (2930 cm^{-1})

* Corrected for ATS monomer evaporated in its cure cycle

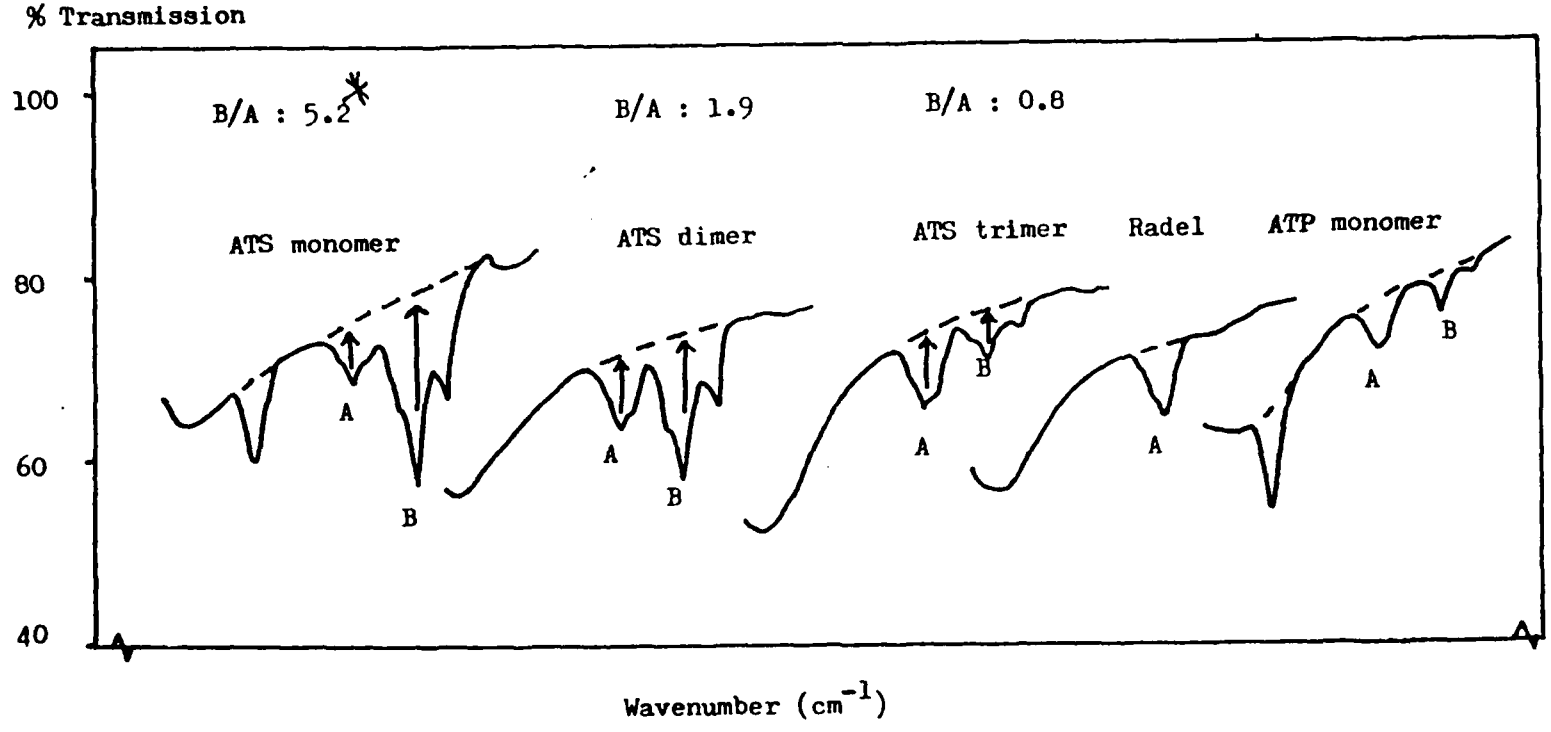

FIGURE 59 I.R. SPECTRA OF THE OLIGOMERIC PRODUCT FRACTIONS OF THERMAL DEGRADATION TO 1020°C OF PRECURED ATS AND RELATED POLYMERS

KEY

1 Hydroxyl groups

2 Aromatic material

3 Saturated material

4 Phenylether linkages

5 Sulfone linkages

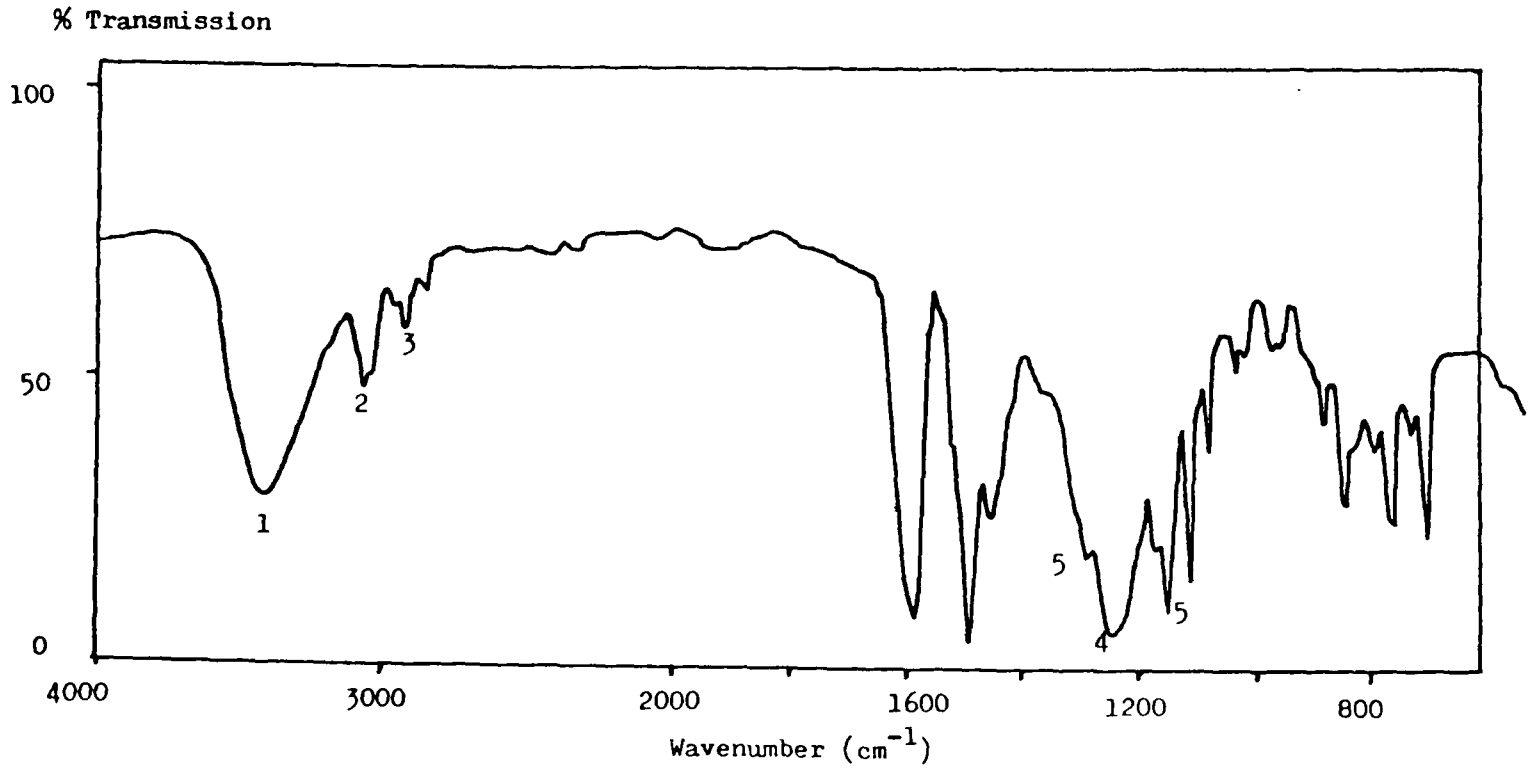

FIGURE 60 I.R. SPECTRUM OF THE OLIGOMERIC PRODUCT FRACTION OF THERMAL DEGRADATION TO 532°C OF PRECURED ATS MONOMER

KEY

1 Hydroxyl groups

2 Aromatic material

3 Saturated material

4 Phenylether linkages

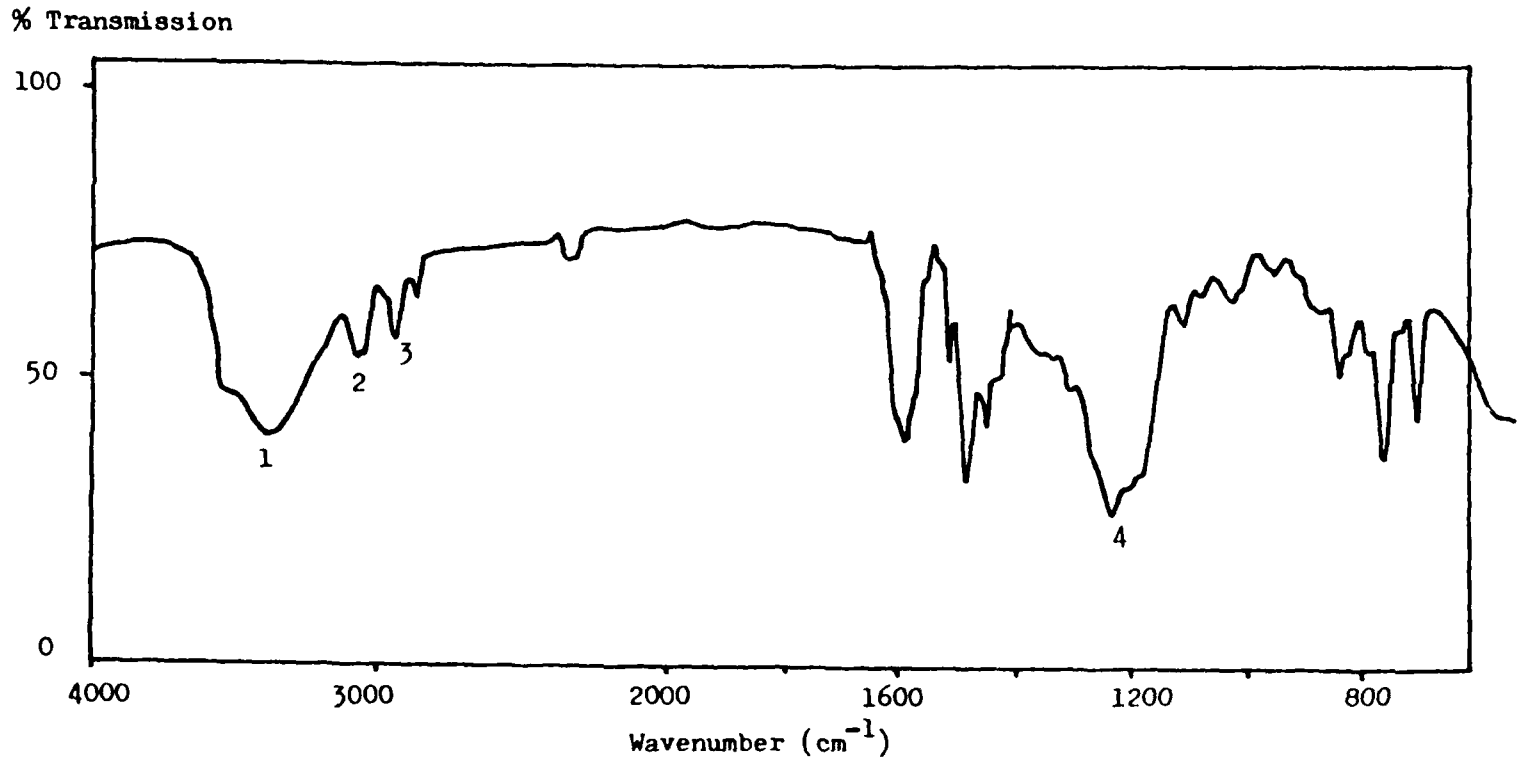

FIGURE 61 I.R. SPECTRUM OF THE OLIGOMERIC PRODUCT FRACTION OF THERMAL DEGRADATION TO 1020°C OF ATS MONOMER, PREDEGRADED TO 532°C

KEY

1 Aromatic material

2 Saturated material

3 Phenylether linkages

* on surface of salt plate

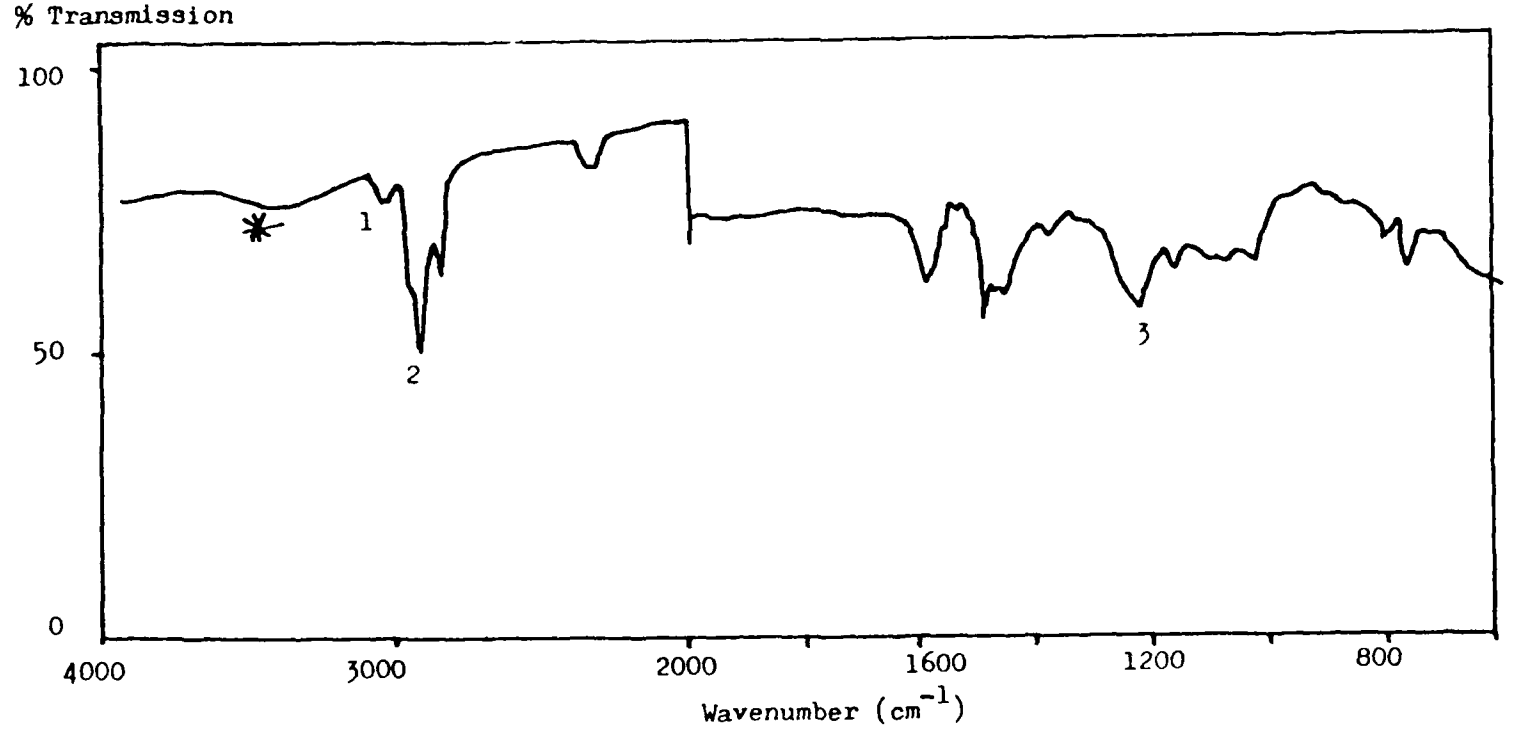

FIGURE 62 I.R. SPECTRUM OF SUB-FRACTION1, ISOLATED BY PREPARATIVE T.L.C. FROM THE HIGH BOILING POINT PRODUCT FRACTION OF DEGRADATION TO 1020°C OF ATS MONOMER

KEY

1 Aromatic material

2 Saturated material

3 Phenylether linkages

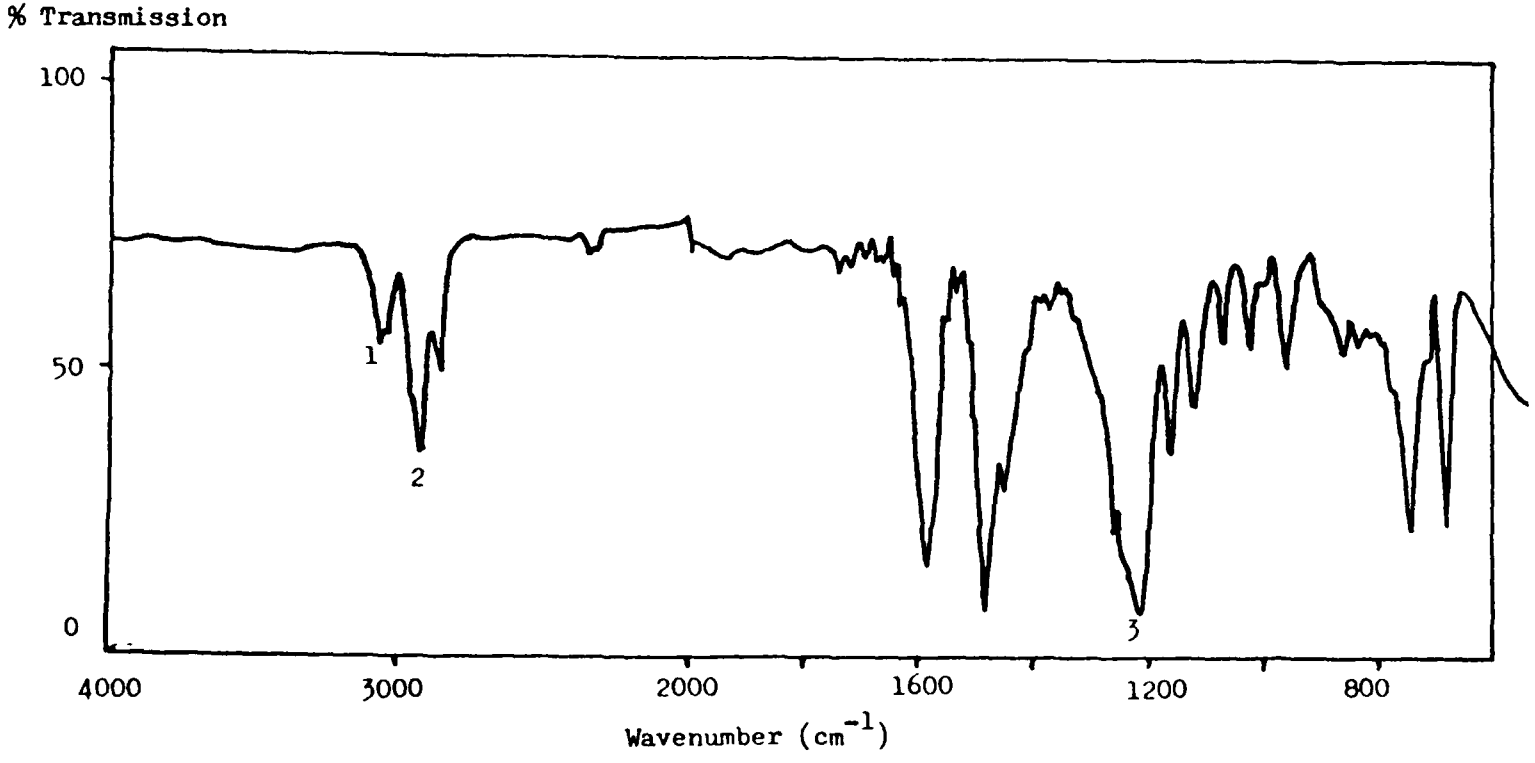

FIGURE 63 I.R. SPECTRUM OF SUB-FRACTION 1, ISOLATED BY PREPARATIVE T.L.C. FROM THE HIGH BOILING POINT PRODUCT FRACTION OF DEGRADATION TO 1020°C OF ATS-G

KEY

1 Aromatic material

2 Saturated material

3 Phenylether linkages

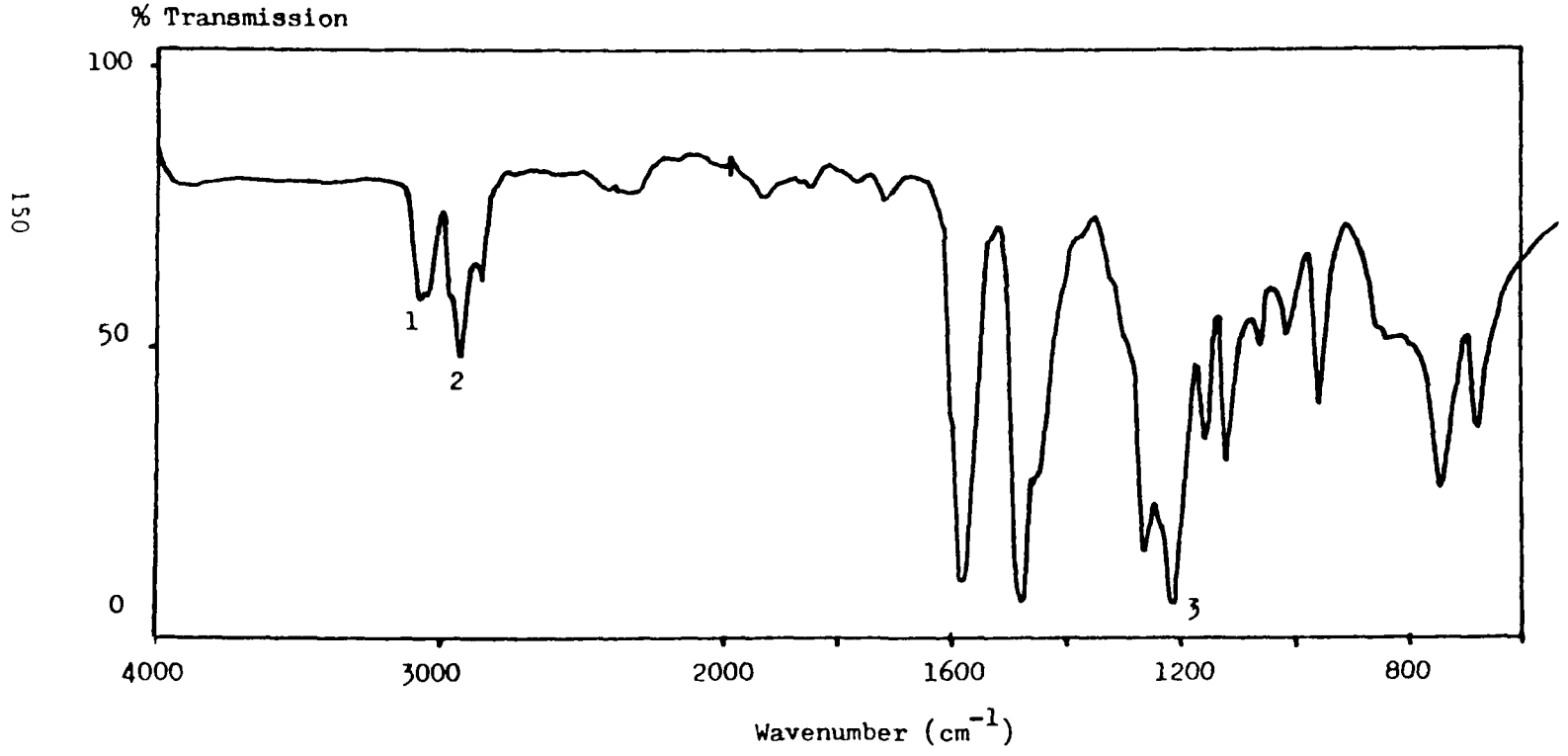

FIGURE 64 I.R. SPECTRUM OF SUB-FRACTION 1, ISOLATED BY PREPARATIVE T.L.C. FROM THE HIGH BOILING POINT PRODUCT FRACTION OF DEGRADATION TO 1020°C OF ATS DIMER

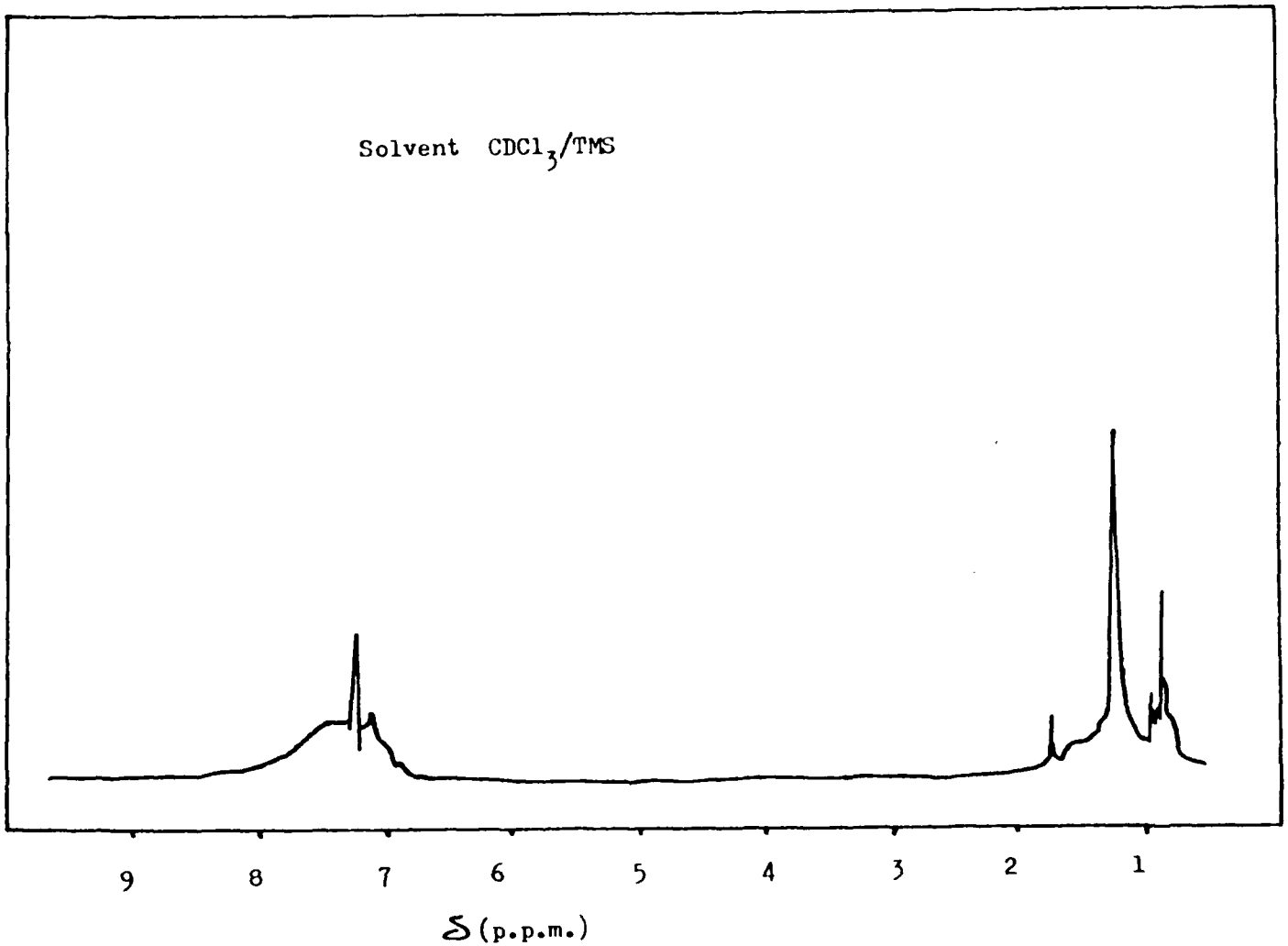

FIGURE 65 PROTON N.M.R. SPECTRUM OF SUB-FRACTION I, ISOLATED BY PREPARATIVE T.L.C. FROM THE HIGH BOILING POINT PRODUCT FRACTION OF DEGRADATION TO 1020°C OF ATS MONOMER

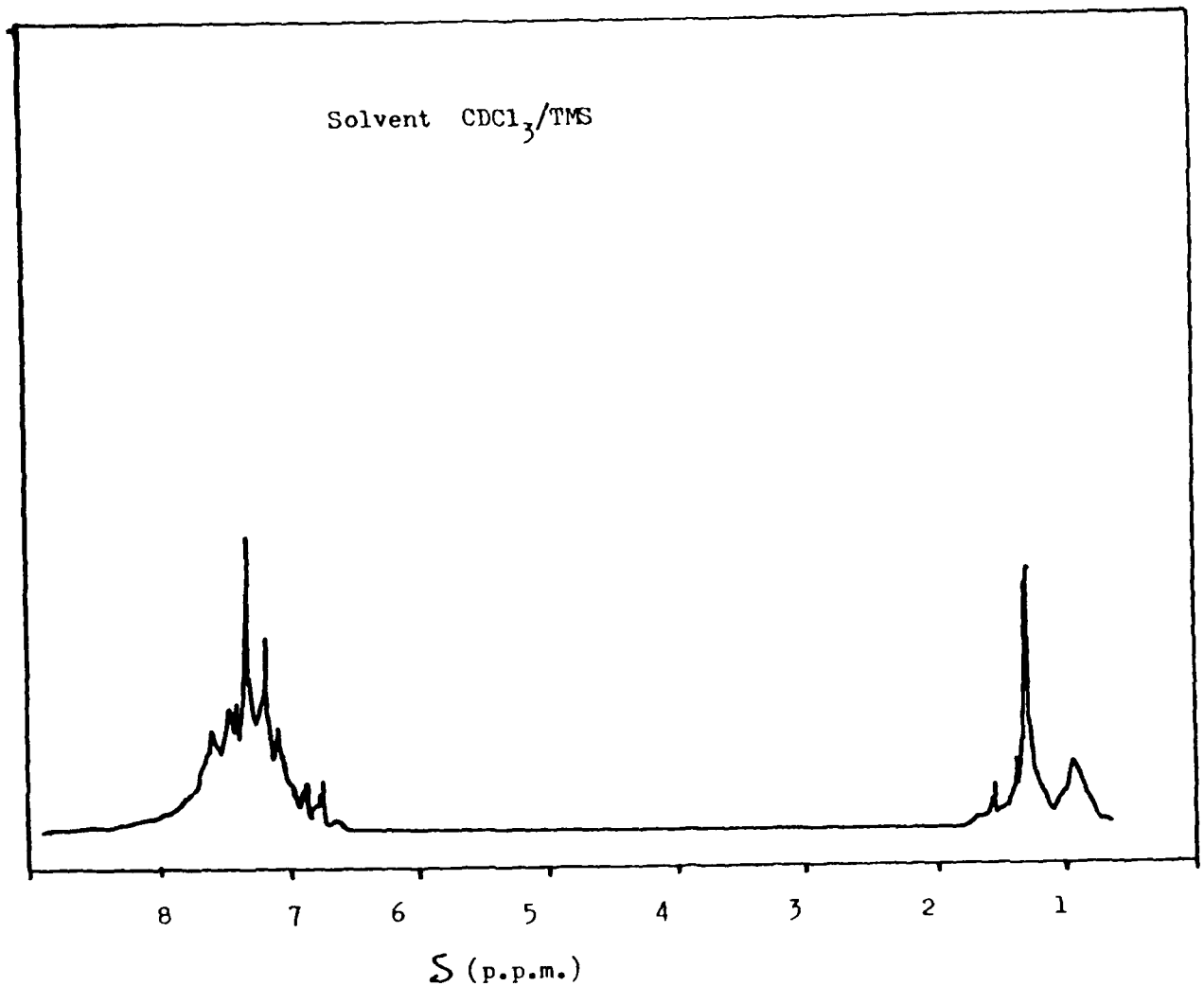

FIGURE 66 PROTON N.M.R. SPECTRUM OF SUB-FRACTION 1, ISOLATED BY PREPARATIVE T.L.C. FROM THE HIGH BOILING POINT PRODUCT FRACTION OF DEGRADATION TO 1020°C OF ATS-G

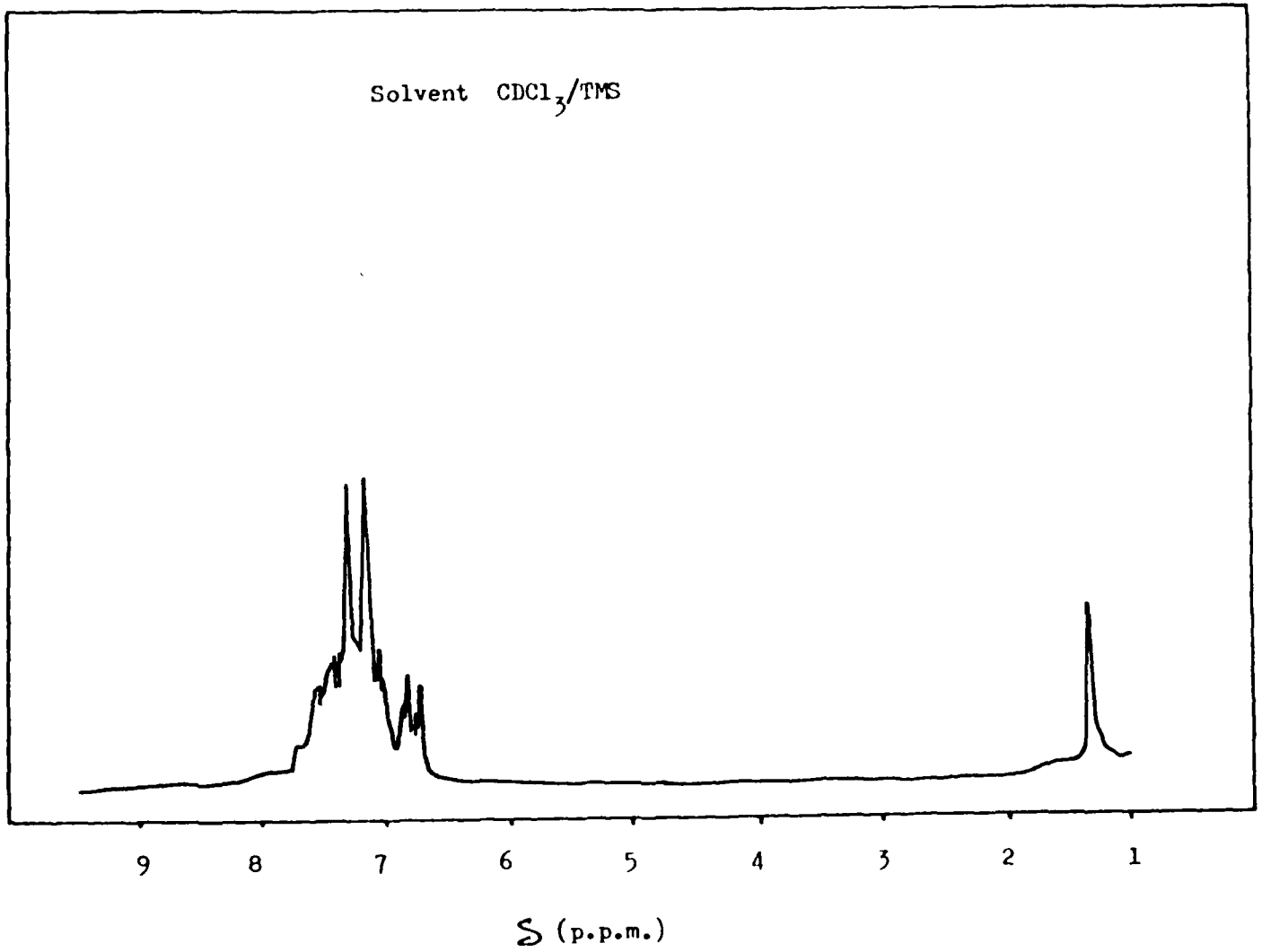

FIGURE 67 PROTON N.M.R. SPECTRUM OF SUB-FRACTION 1, ISOLATED BY PREPARATIVE T.L.C. FROM THE HIGH BOILING POINT PRODUCT FRACTION OF DEGRADATION TO 1020°C OF ATS DIMER

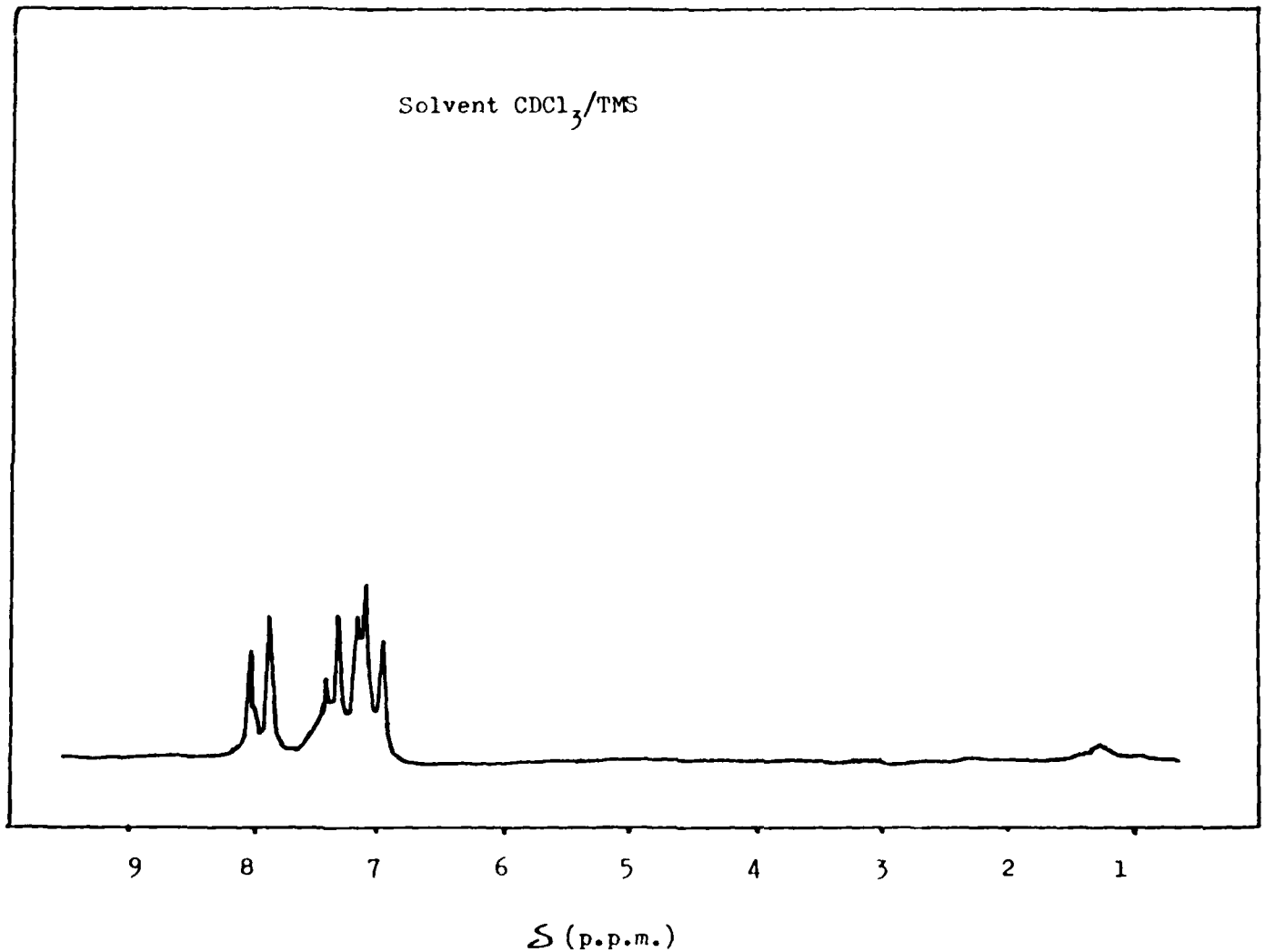

FIGURE 68 PROTON N.M.R. SPECTRUM OF SUB-FRACTION 2, ISOLATED BY PREPARATIVE T.L.C. FROM THE HIGH BOILING POINT PRODUCT FRACTION OF DEGRADATION TO 1020°C OF ATS MONOMER

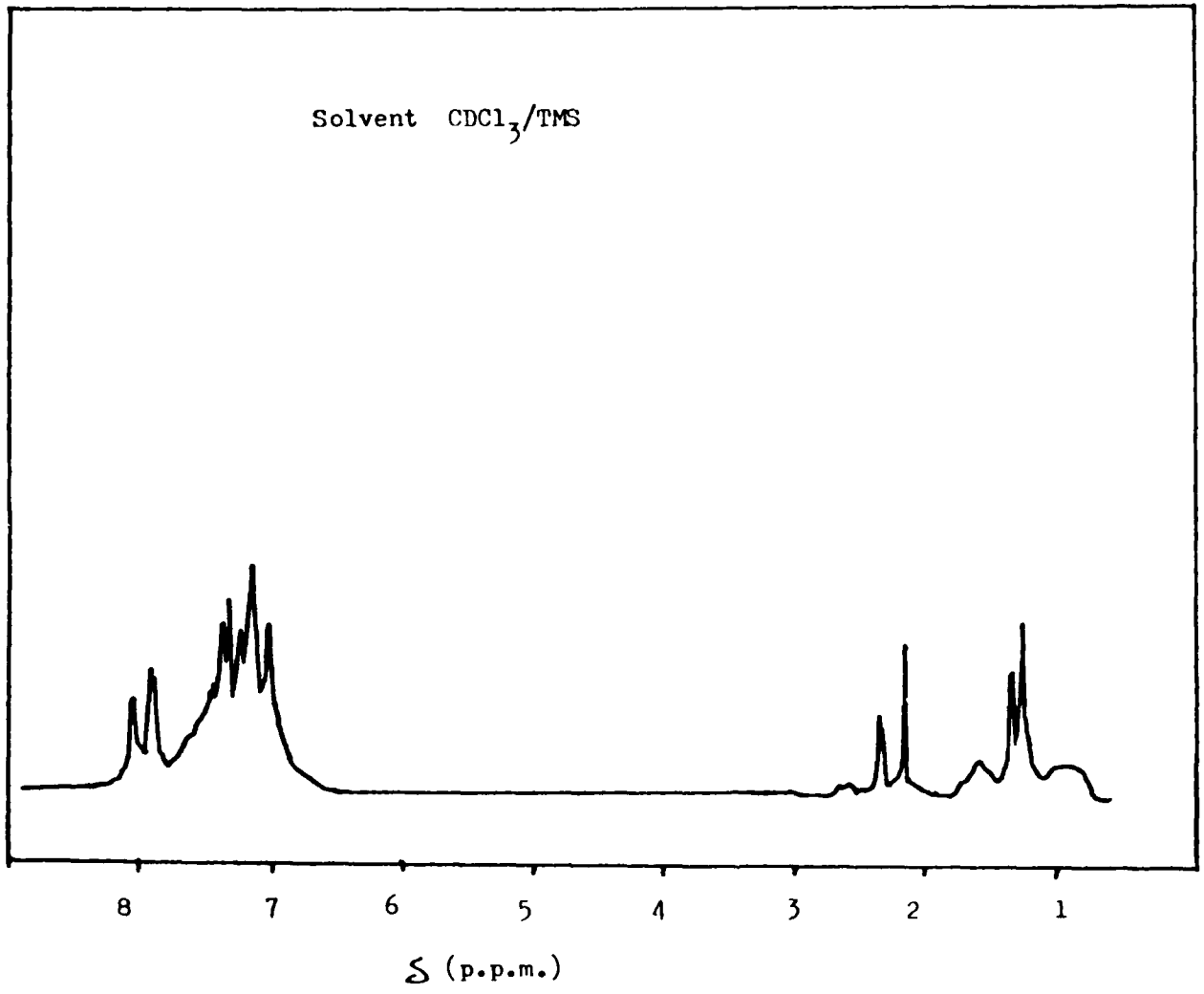

FIGURE 69 PROTON N.M.R. SPECTRUM OF SUB-FRACTION 2, ISOLATED BY PREPARATIVE T.L.C. FROM THE HIGH BOILING POINT PRODUCT FRACTION OF DEGRADATION TO 1020°C OF ATS-G

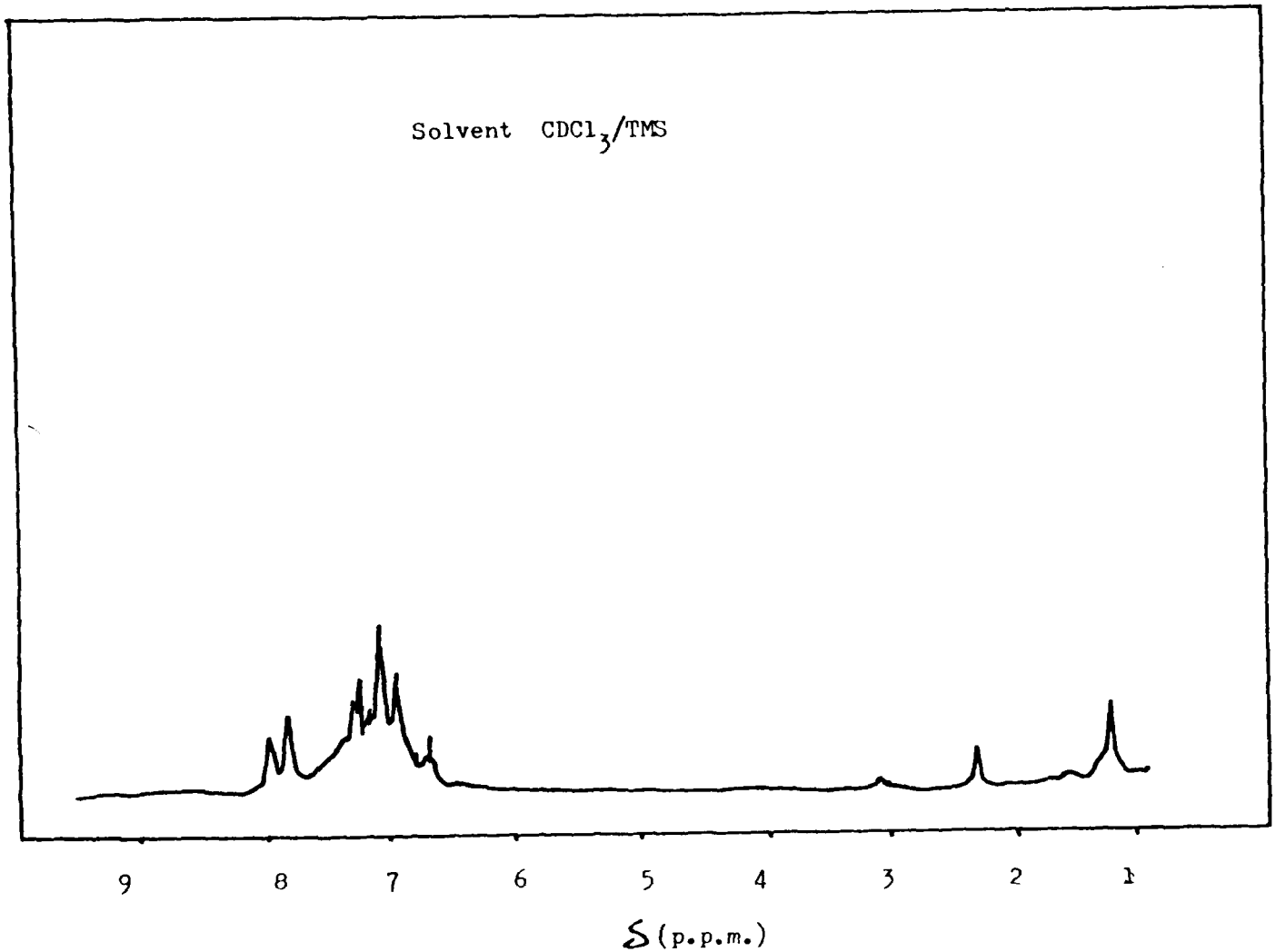

FIGURE 70 PROTON N.M.R. SPECTRUM OF SUB-FRACTION 2, ISOLATED BY PREPARATIVE T.L.C. FROM THE HIGH BOILING POINT PRODUCT FRACTION OF DEGRADATION TO 1020°C OF ATS DIMER

KEY

1 Hydroxyl groups

2 Aromatic material

3 Saturated material

4 Phenylether groups

5 Sulfone linkages

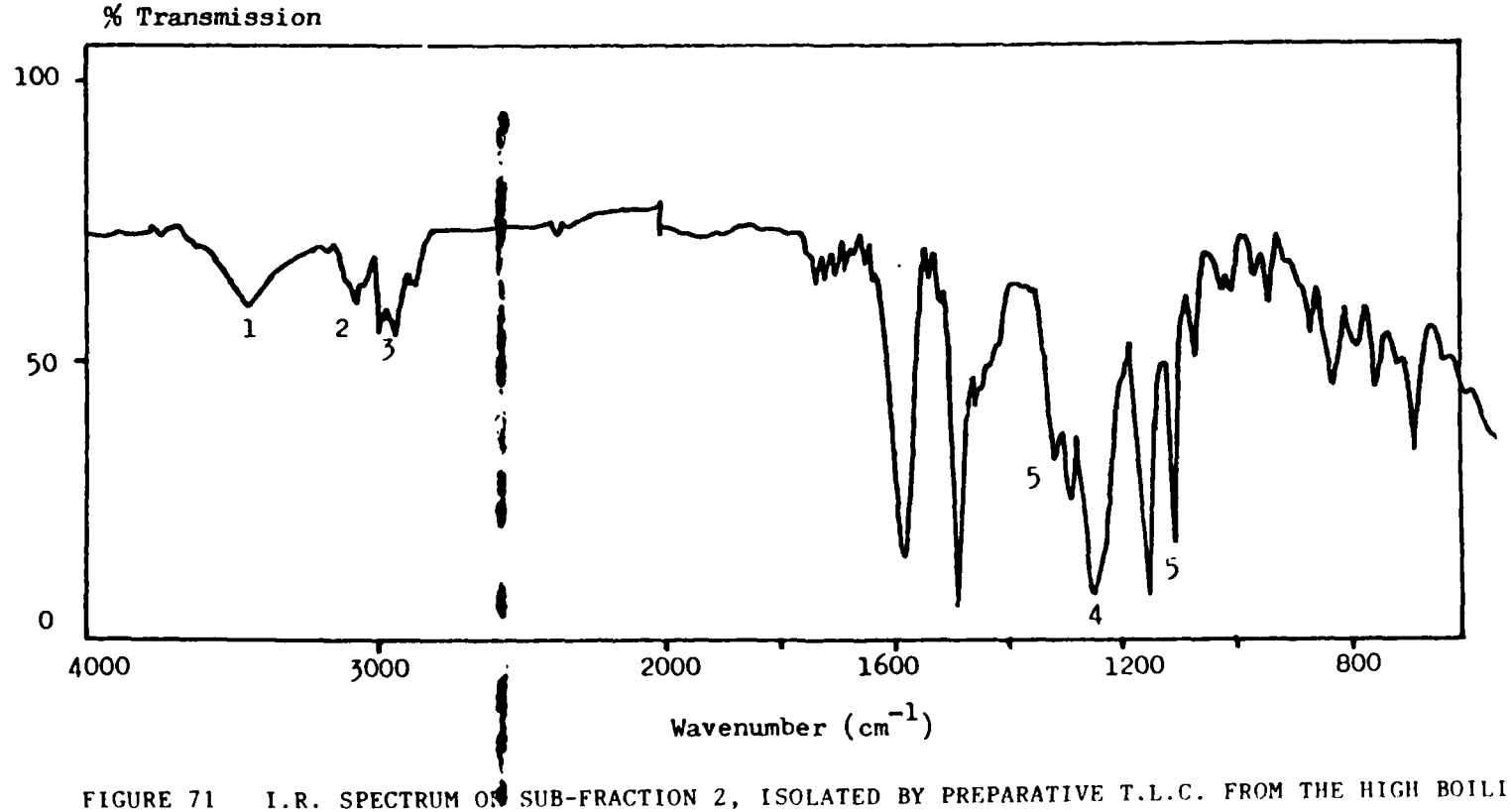

FIGURE 71 I.R. SPECTRUM OF SUB-FRACTION 2, ISOLATED BY PREPARATIVE T.L.C. FROM THE HIGH BOILING POINT PRODUCT FRACTION OF DEGRADATION TO 1020°C OF ATS-G

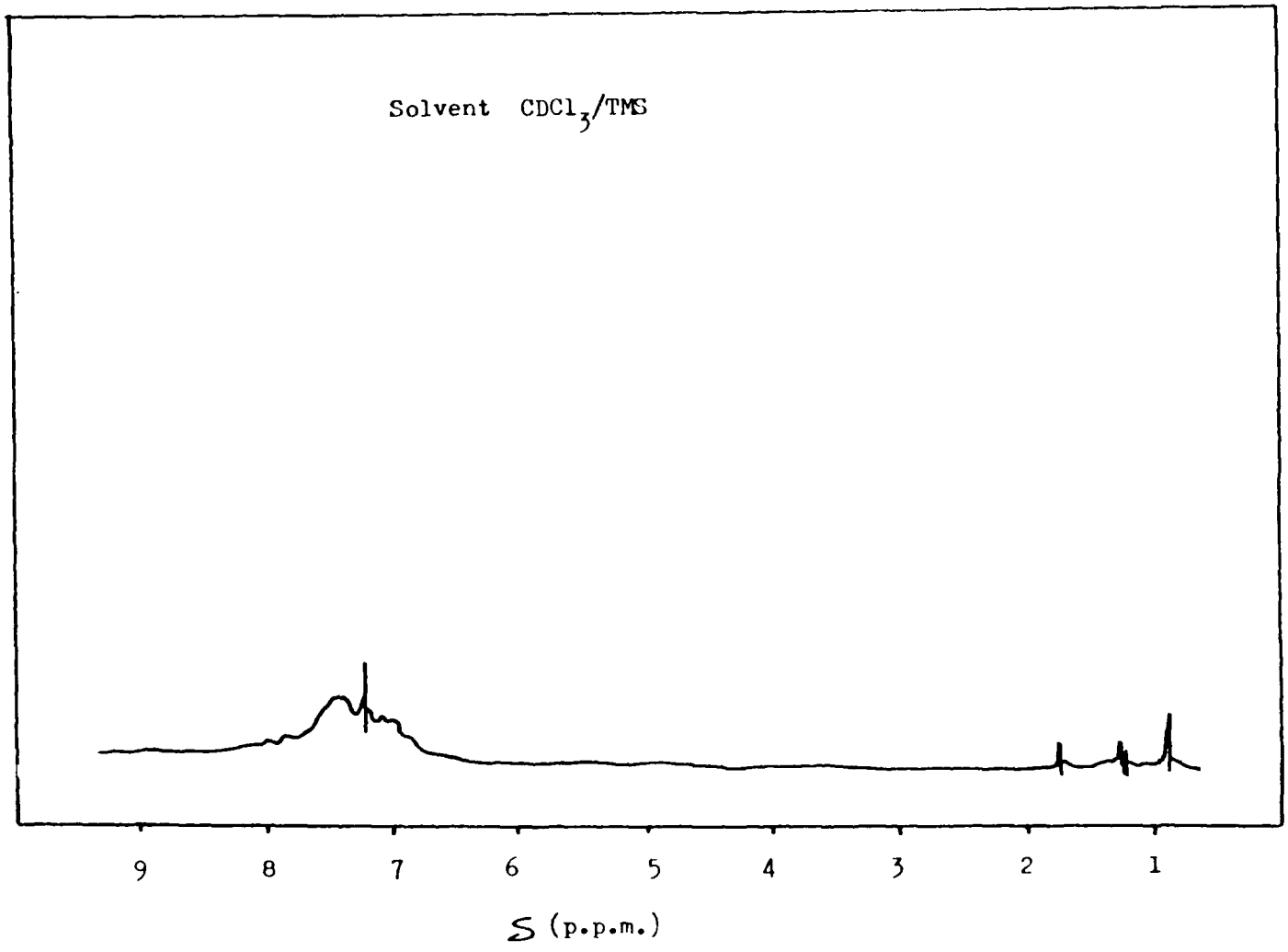

FIGURE 72 PROTON N.M.R. SPECTRUM OF SUB-FRACTION 3, ISOLATED BY PREPARATIVE T.L.C. FROM THE HIGH BOILING POINT PRODUCT FRACTION OF DEGRADATION TO 1020°C OF ATS MONOMER

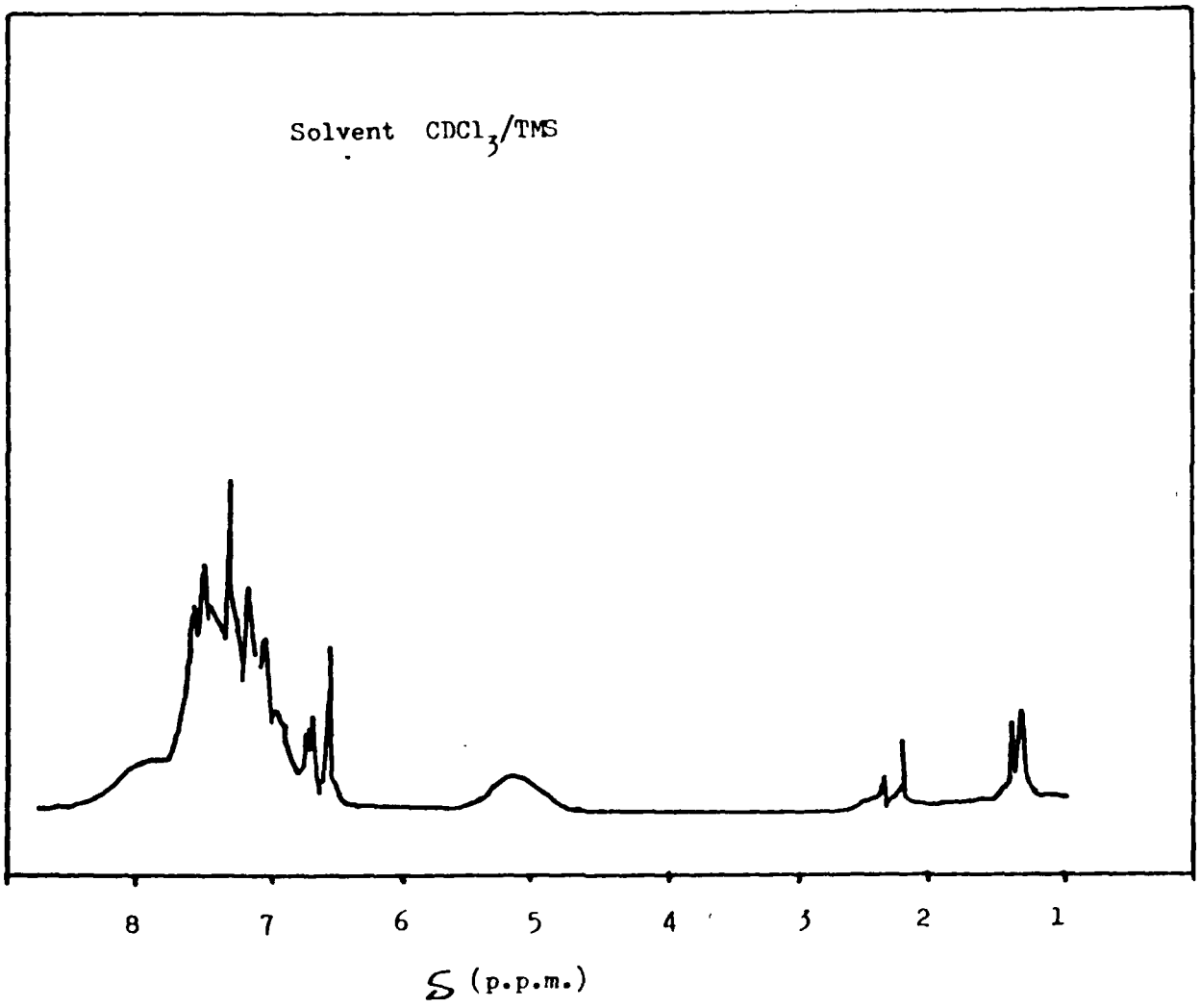

FIGURE 73 PROTON N.M.R. SPECTRUM OF SUB-FRACTION 3, ISOLATED BY PREPARATIVE T.L.C. FROM THE HIGH BOILING POINT PRODUCT FRACTION OF DEGRADATION TO 1020°C OF ATS-G

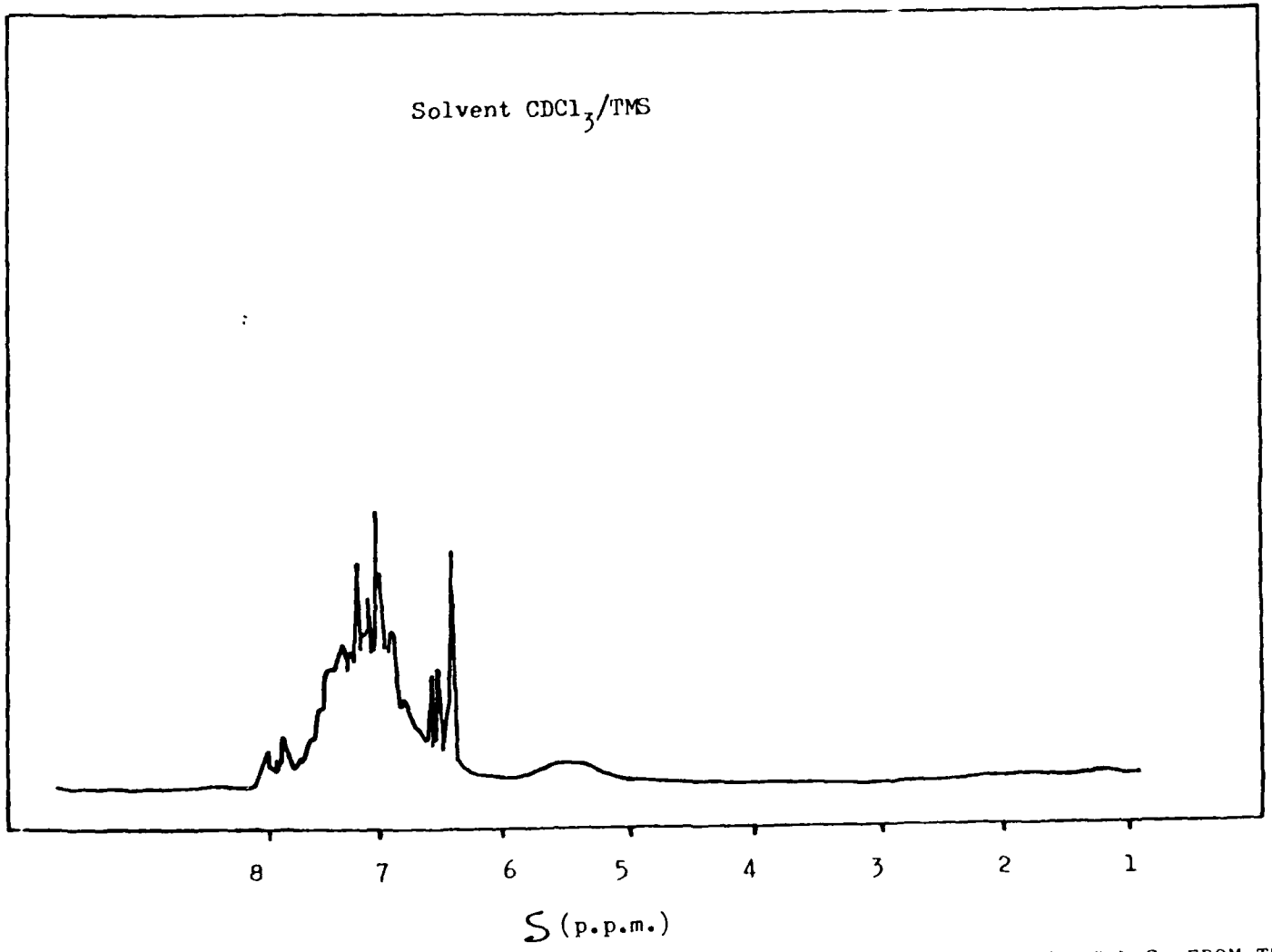

FIGURE 74 PROTON N.M.R. SPECTRUM OF SUB-FRACTION 3, ISOLATED BY PREPARATIVE T.L.C. FROM THE HIGH BOILING POINT PRODUCT FRACTION OF DEGRADATION TO 1020°C OF ATS DIMER

KEY

1 Hydroxyl groups

2 Aromatic material

3 Saturated material (trace)

4 Phenylether linkages

5 Sulfone linkages (trace)

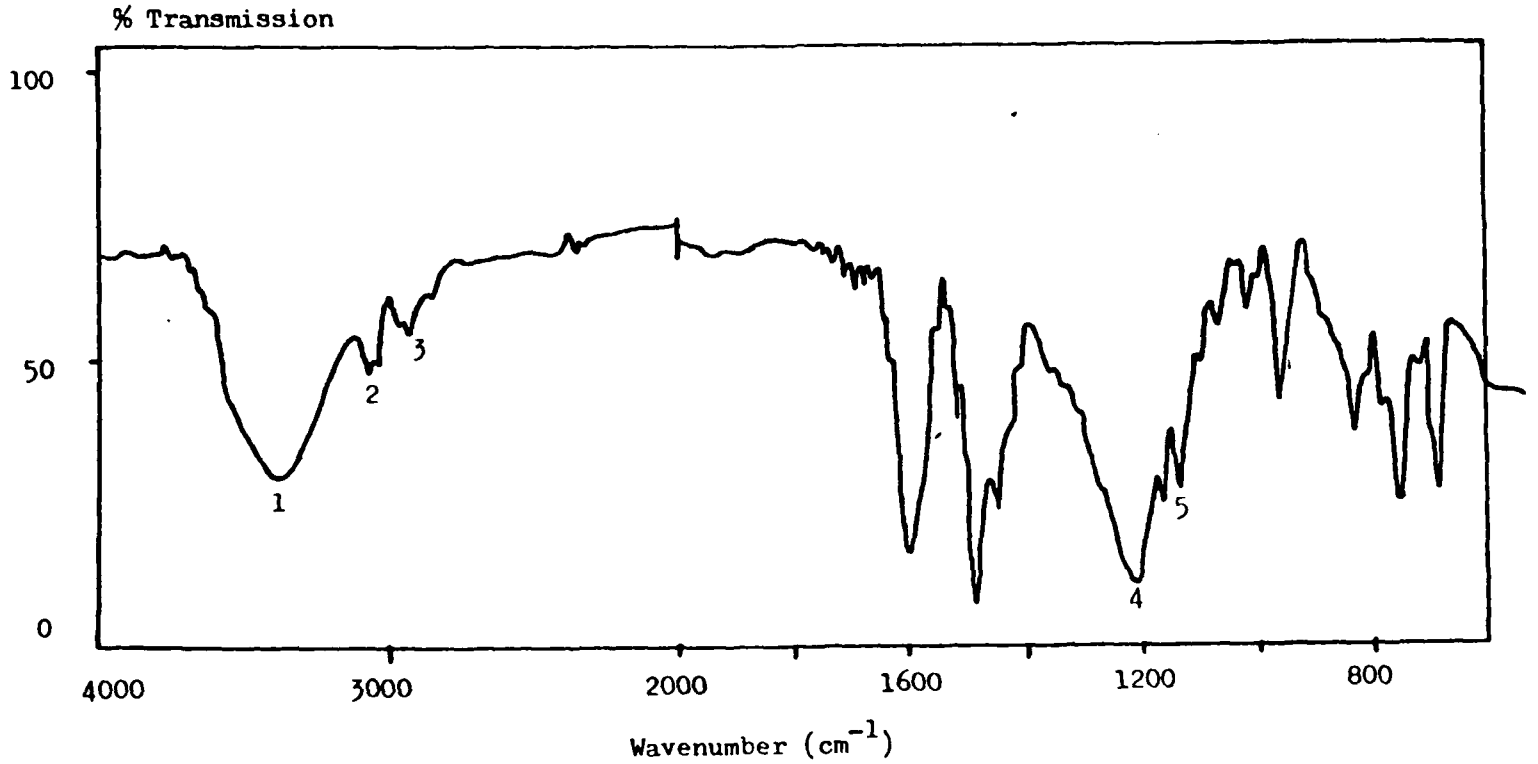

FIGURE 75 I.R. SPECTRUM OF SUB-FRACTION 3, ISOLATED BY PREPARATIVE T.L.C. FROM THE HIGH BOILING POINT PRODUCT FRACTION OF DEGRADATION TO 1020°C OF ATS-G

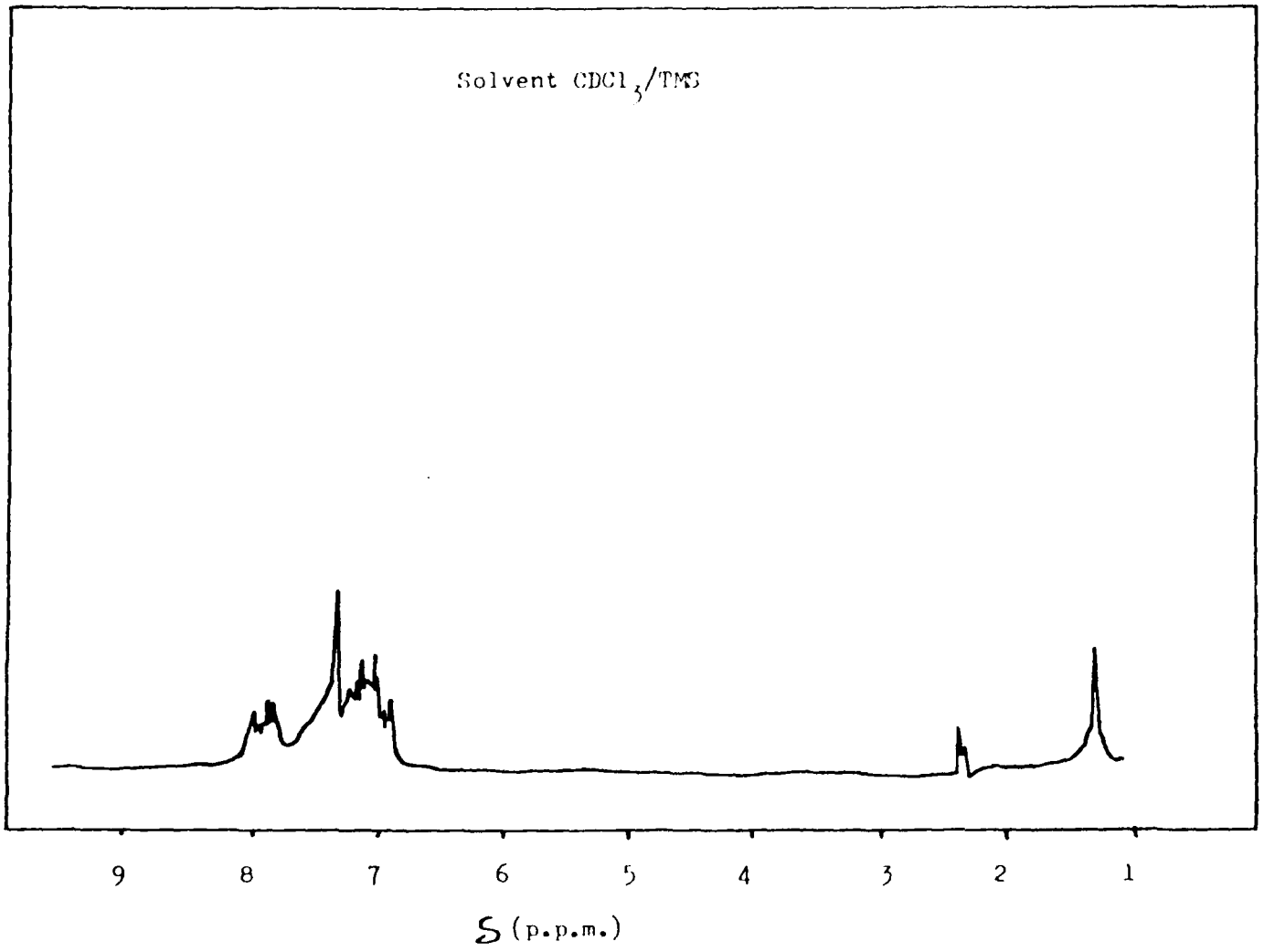

FIGURE 76 PROTON N.M.R. SPECTRUM OF SUB-FRACTION 4, ISOLATED BY PREPARATIVE T.L.C. FROM THE HIGH BOILING POINT PRODUCT FRACTION OF DEGRADATION TO 1020°C OF ATS MONOMER

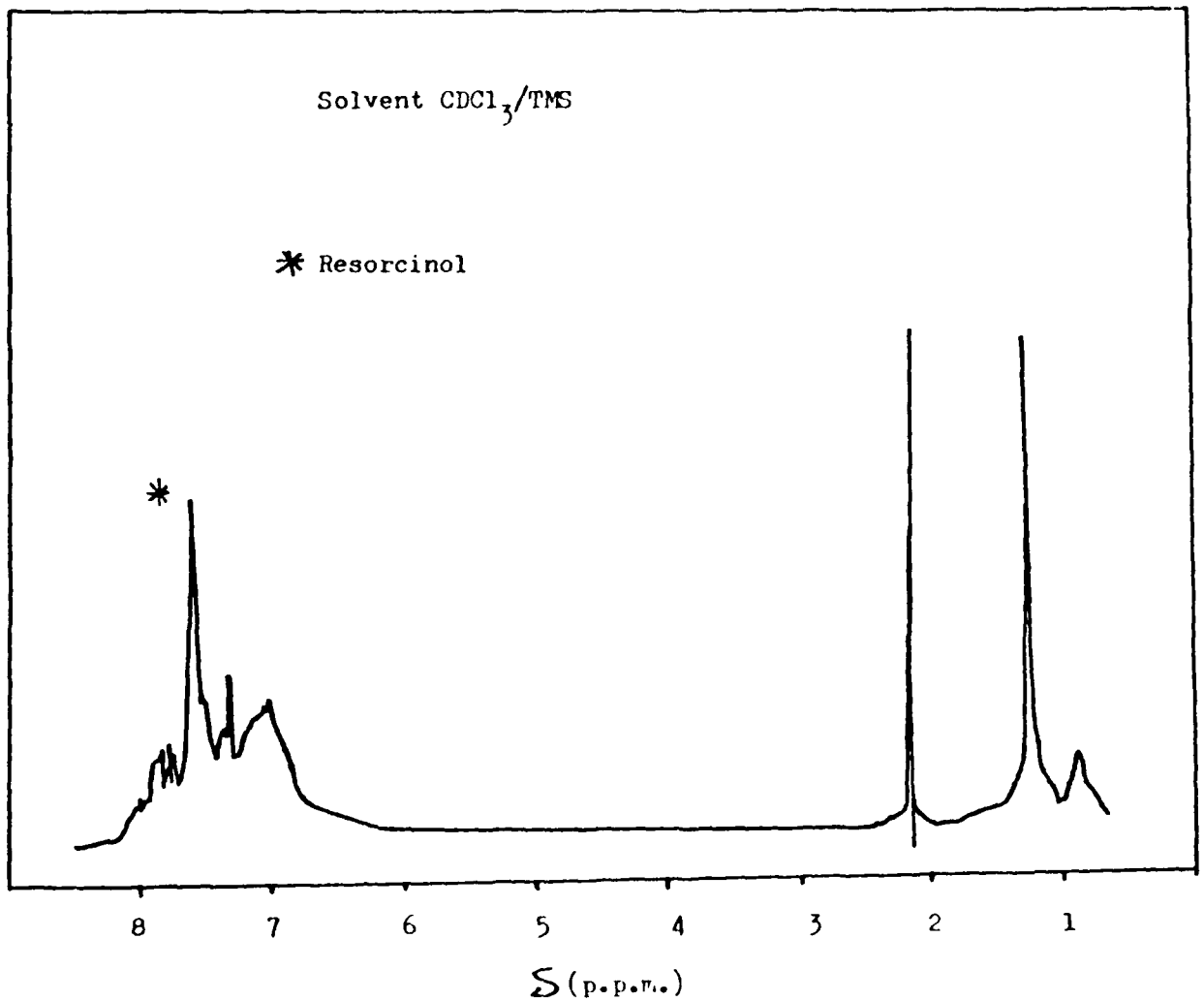

FIGURE 77 PROTON N.M.R. SPECTRUM OF SUB-FRACTION 4, ISOLATED BY PREPARATIVE T.L.C. FROM THE HIGH BOILING POINT PRODUCT FRACTION OF DEGRADATION TO 1020°C OF ATS-G

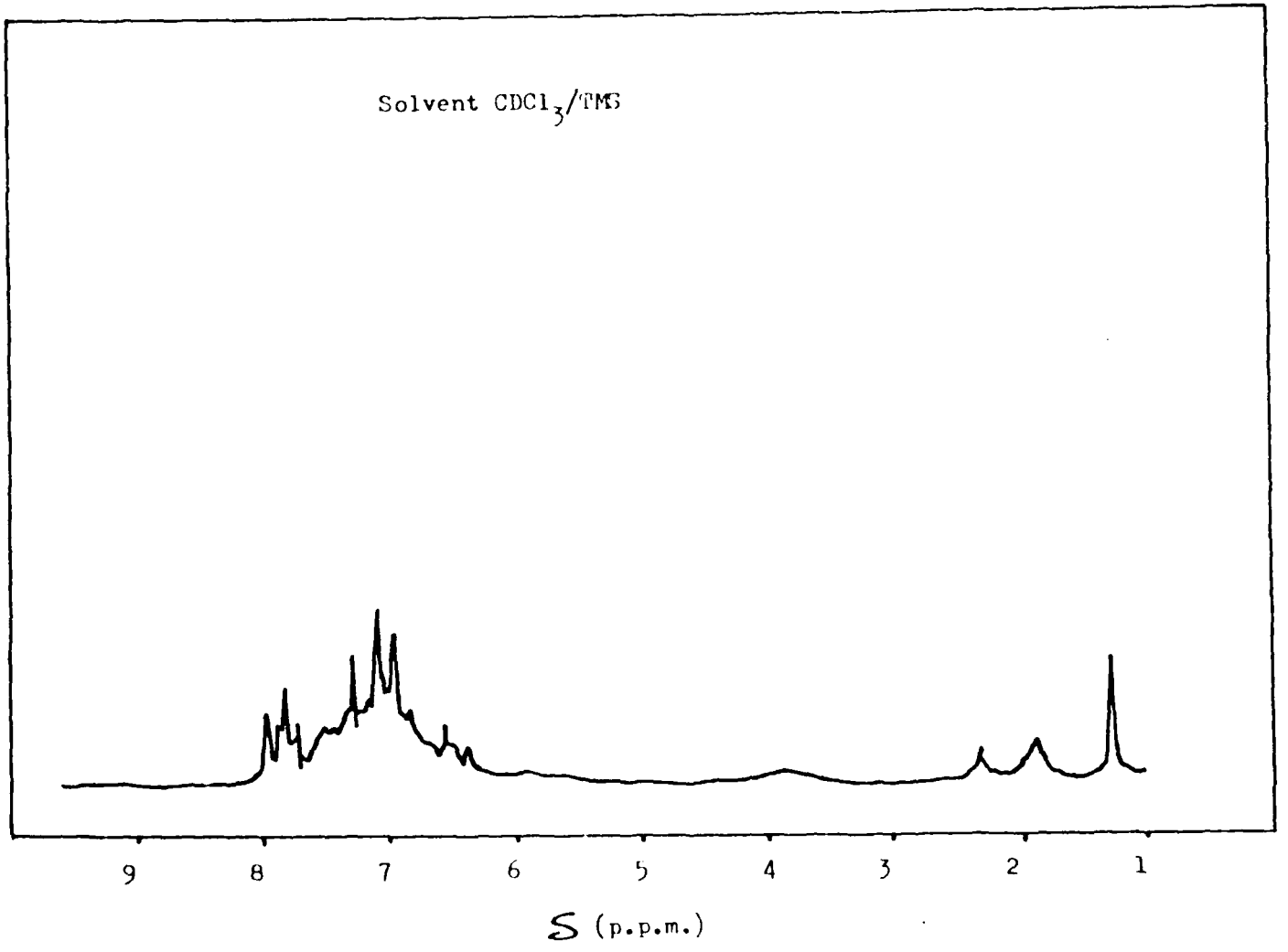

FIGURE 78 PROTON N.M.R. SPECTRUM OF SUB-FRACTION 4, ISOLATED BY PREPARATIVE T.L.C. FROM THE HIGH BOILING POINT PRODUCT FRACTION OF DEGRADATION TO 1020°C OF ATS DIMER

KEY

1 Hydroxyl groups

2 Aromatic material

3 Saturated material

4 Phenylether linkages

5 Sulfone linkages

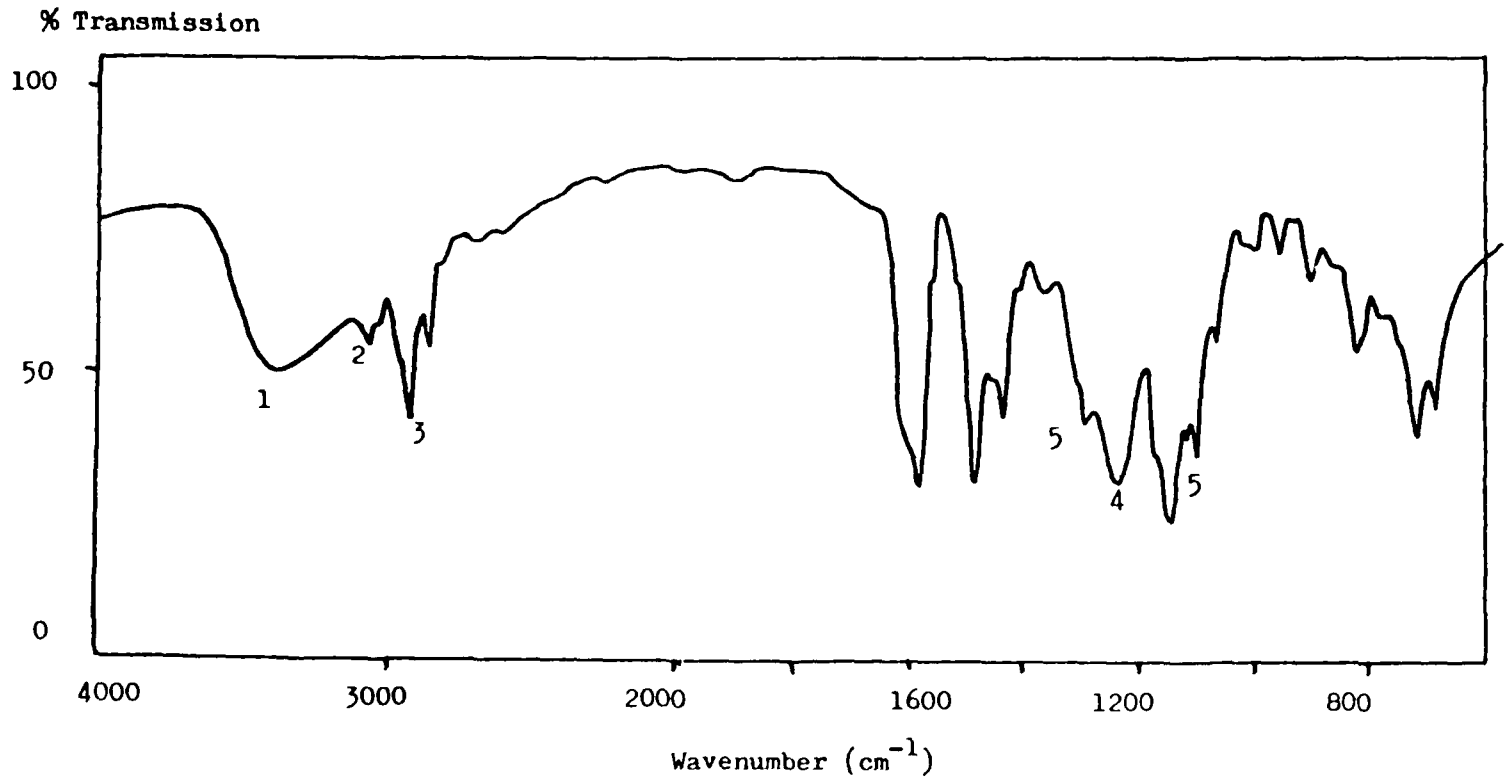

FIGURE 79 I.R. SPECTRUM OF SUB-FRACTION 4, ISOLATED BY PREPARATIVE T.L.C. FROM THE HIGH BOILING POINT PRODUCT FRACTION OF DEGRADATION TO 1020°C OF ATS-G

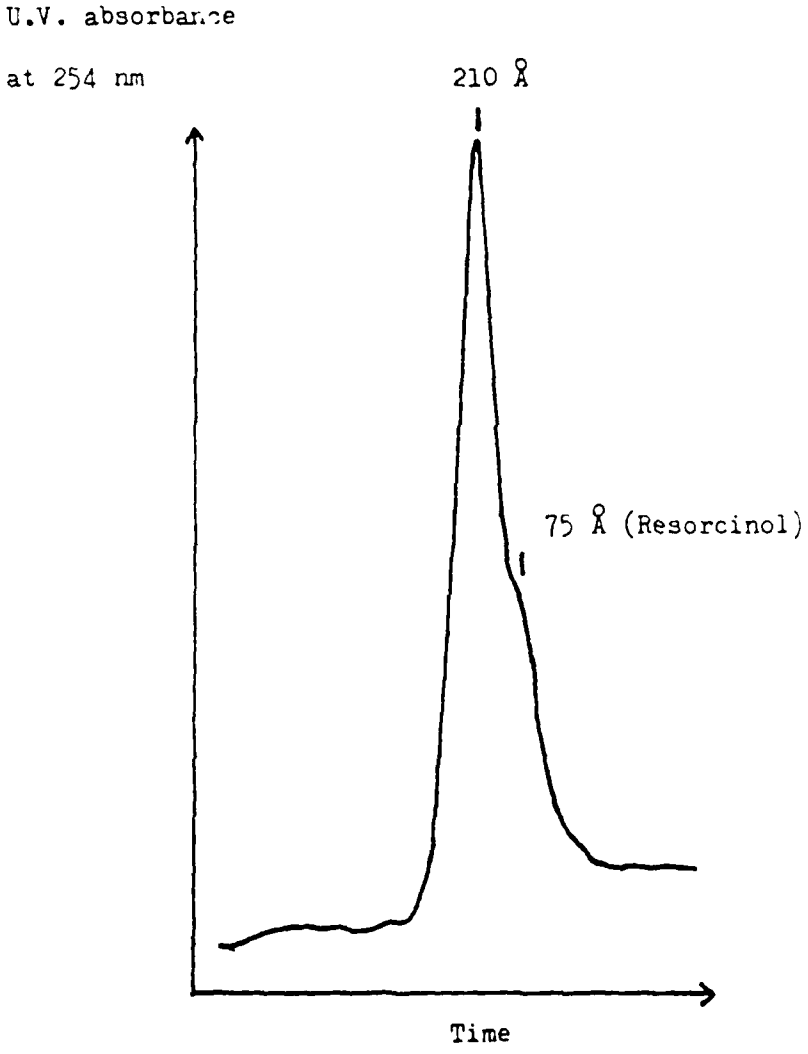

FIGURE 80 G.P.C. OF SUB-FRACTION 4, ISOLATED BY PREPARATIVE T.L.C. FROM THE HIGH BOILING POINT PRODUCT FRACTION OF DEGRADATION TO 1020°C OF ATS-G

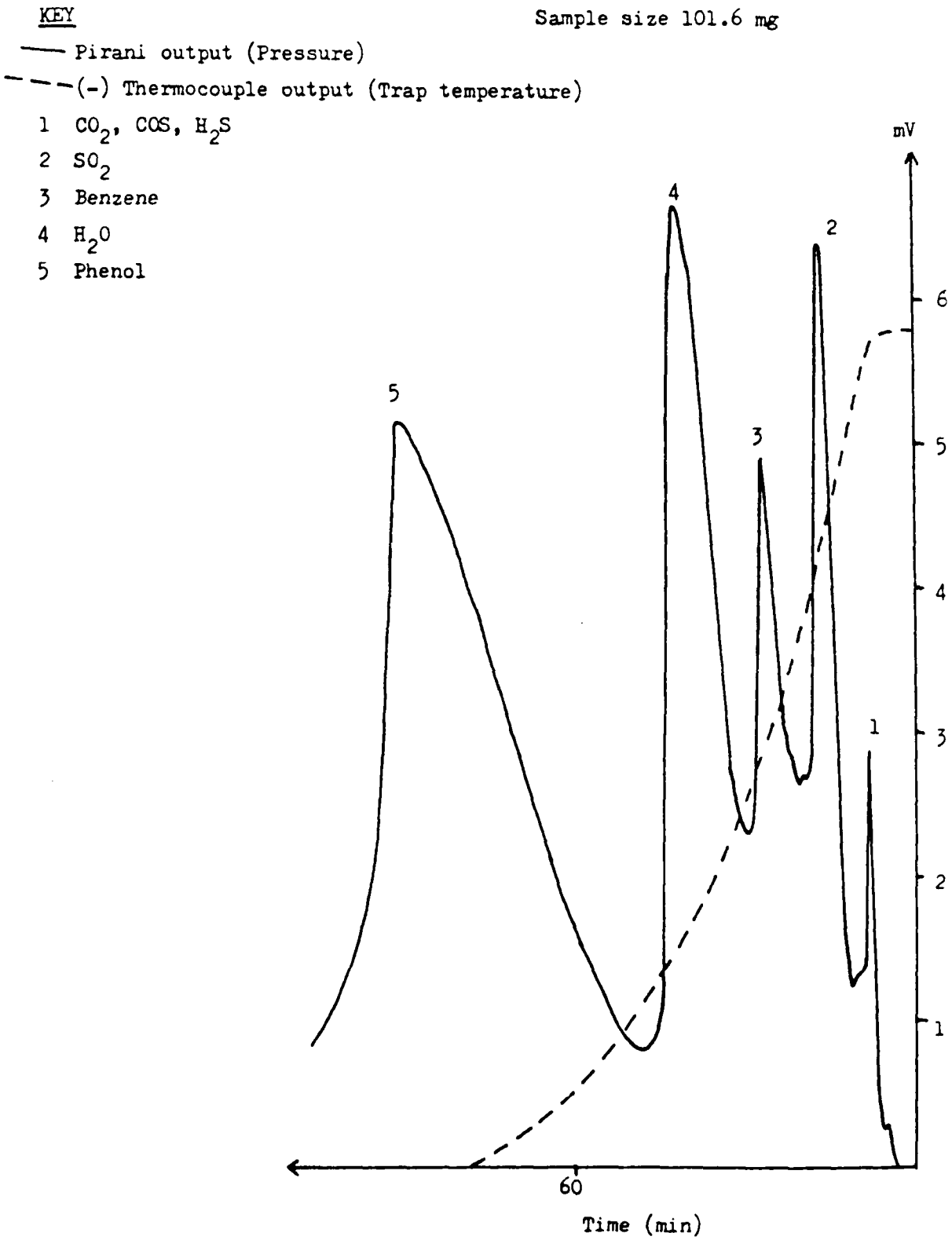

FIGURE 81 SATVA OF THE CONDENSABLE VOLATILE PRODUCT FRACTION OF DEGRADATION TO 1020°C OF ATS-G

Sample size 1 g

KEY

1 CO_2

2 COS

3 SO_2 (SATVA Fraction 2)

4 COS/Glue

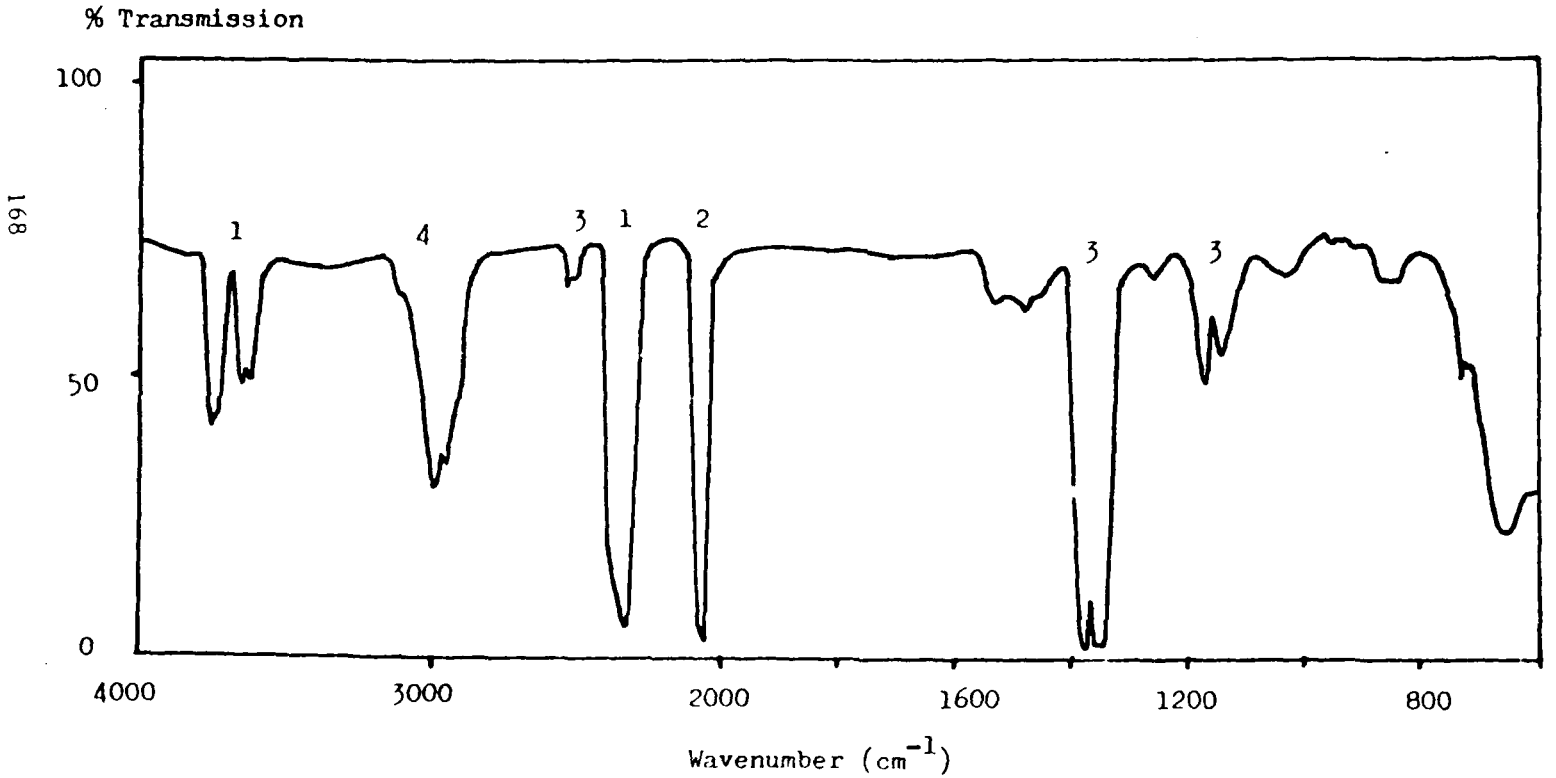

FIGURE 82 GAS PHASE I.R. SPECTRUM OF SATVA FRACTION 1 (ATS-G)

Sample size 500 mg

1 SO_2

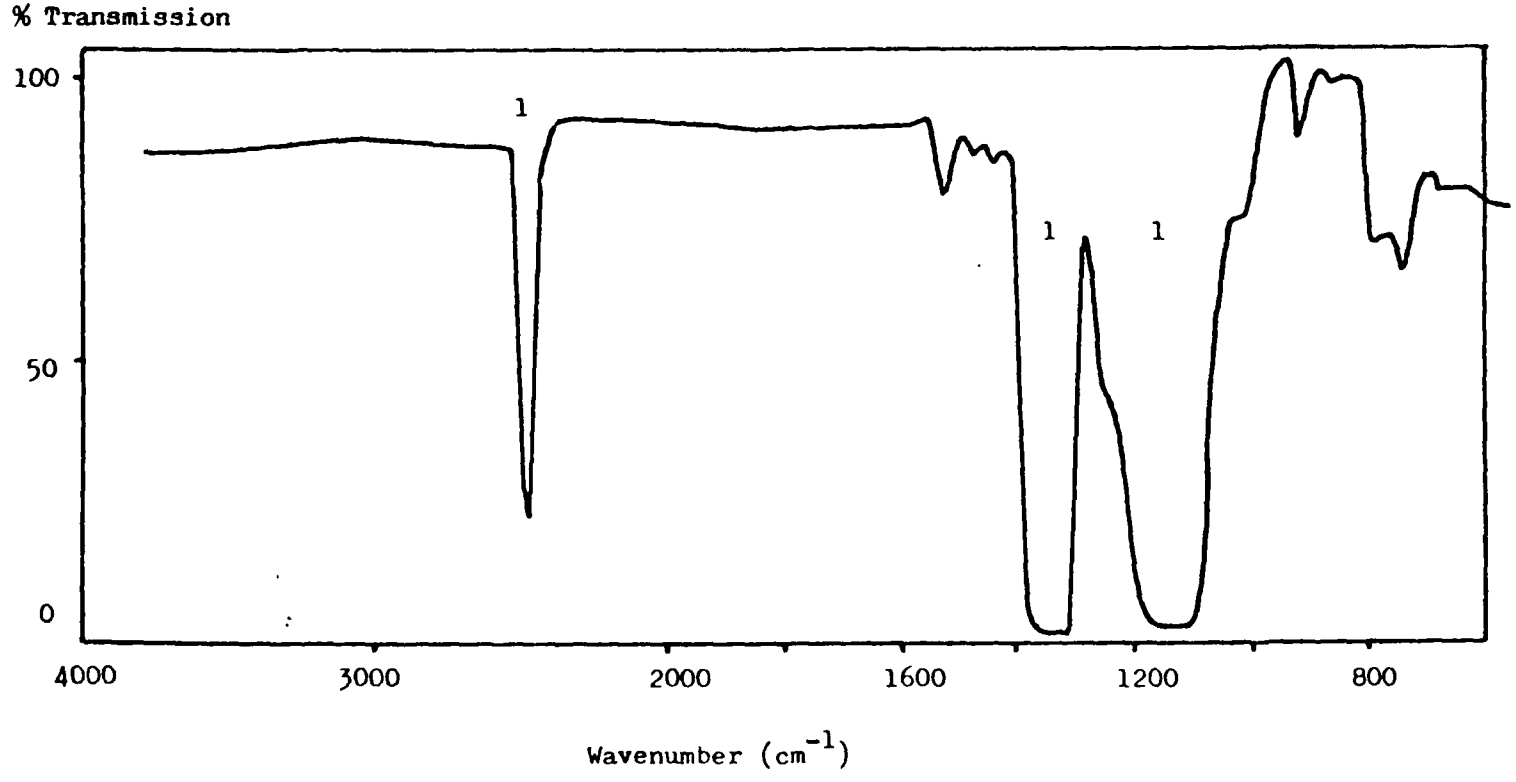

FIGURE 83 GAS PHASE I.R. SPECTRUM OF SATVA FRACTION 2 (AFT-G)

KEY

Sample size 500 mg

1 H_2O (SATVA fraction 4)

2 Benzene

3 SO_2 (SATVA fraction 2)

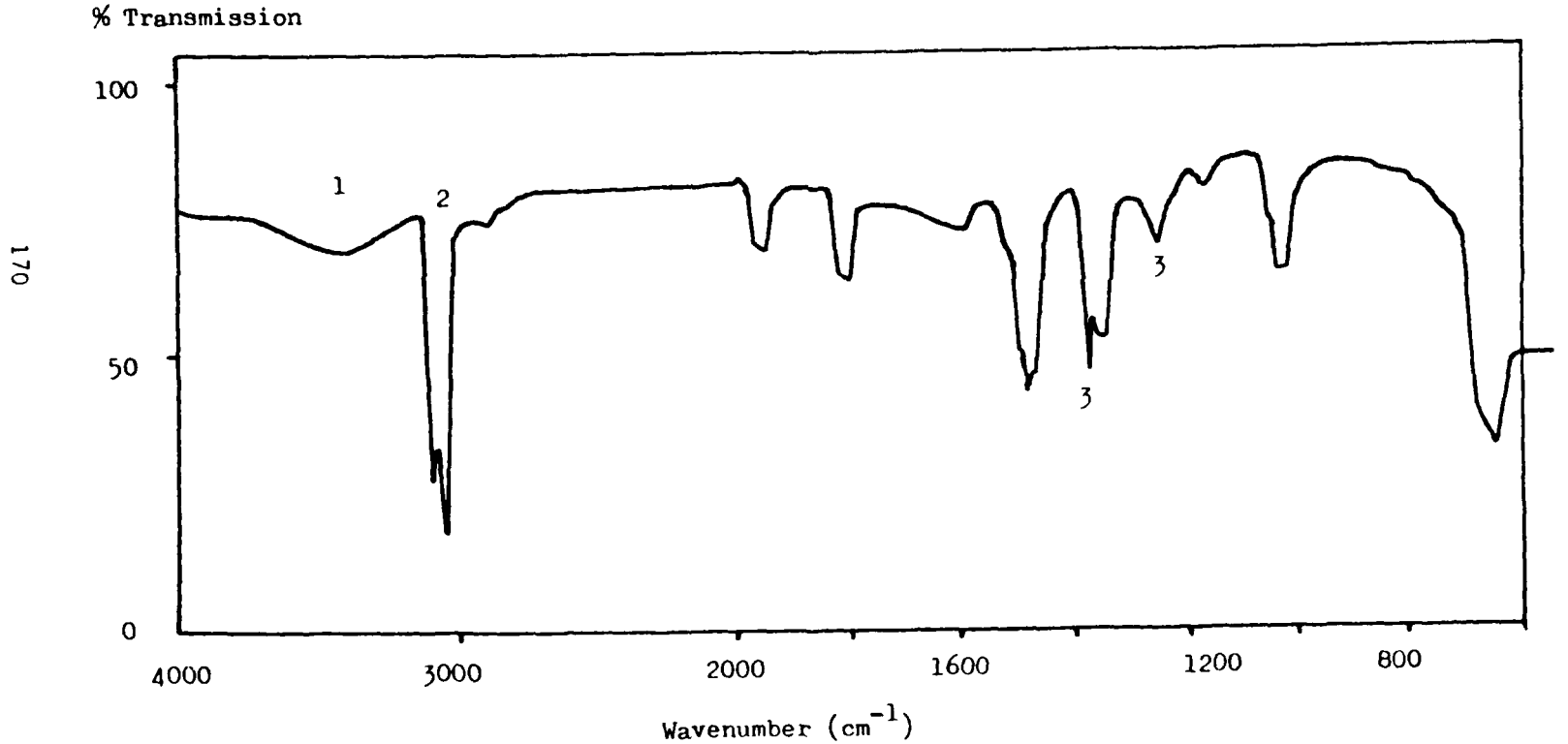

FIGURE 84 GAS PHASE I.R. SPECTRUM OF SATVA FRACTION 3 (ATS-G)

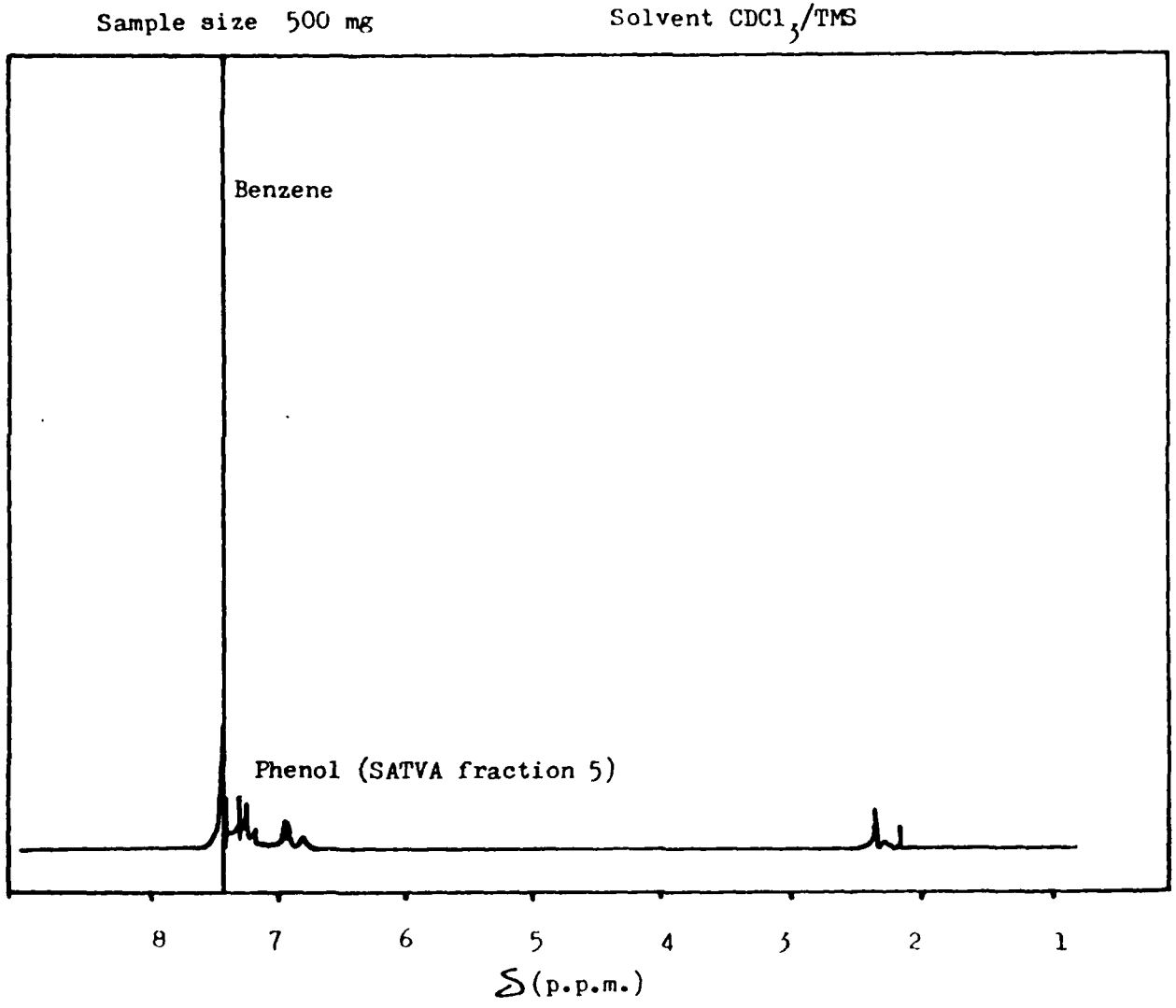

FIGURE 85 PROTON N.M.R. SPECTRUM OF SATVA FRACTION 3 (ATS-G)

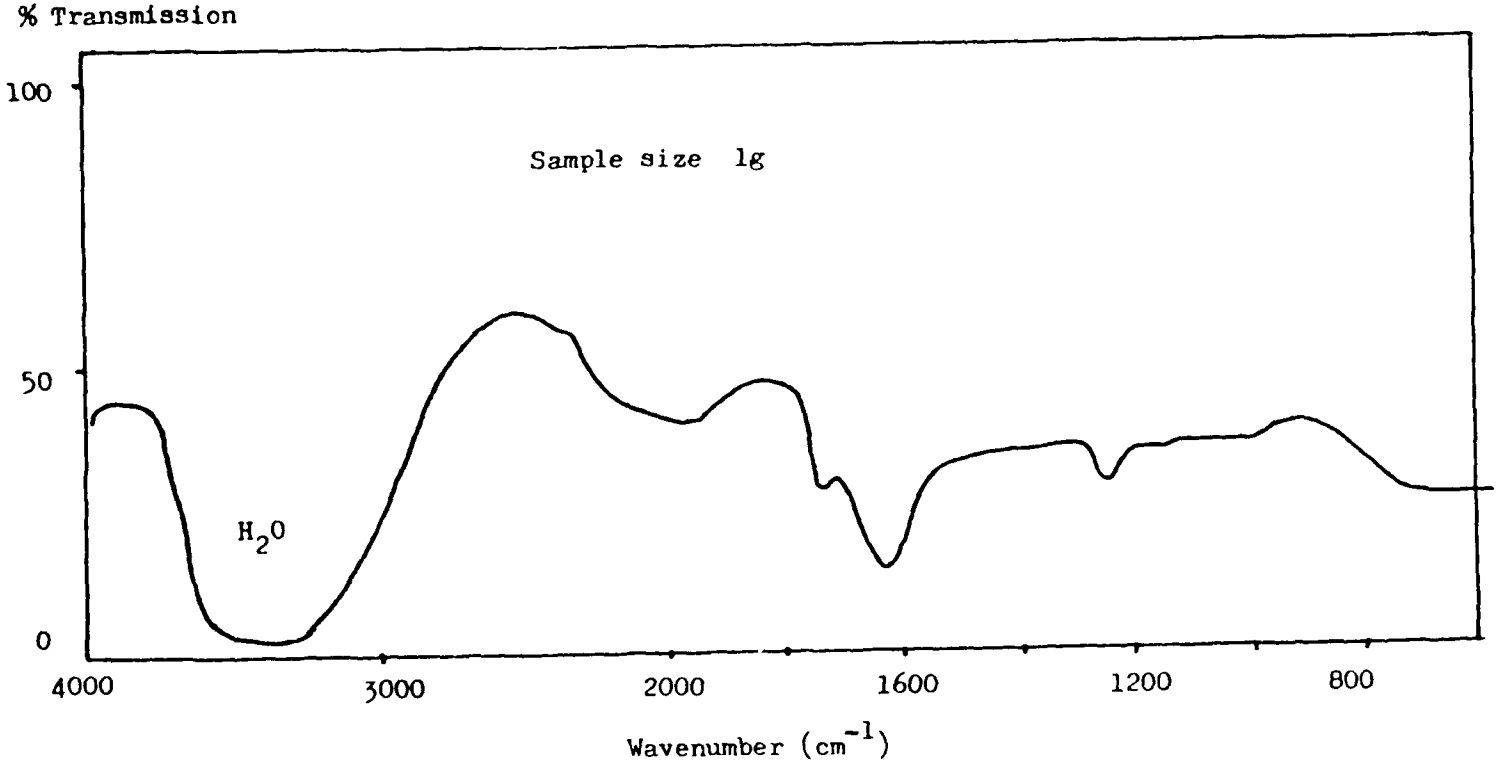

FIGURE 86 GAS PHASE I.R. SPECTRUM OF SATVA FRACTION 4 (ATS-G)

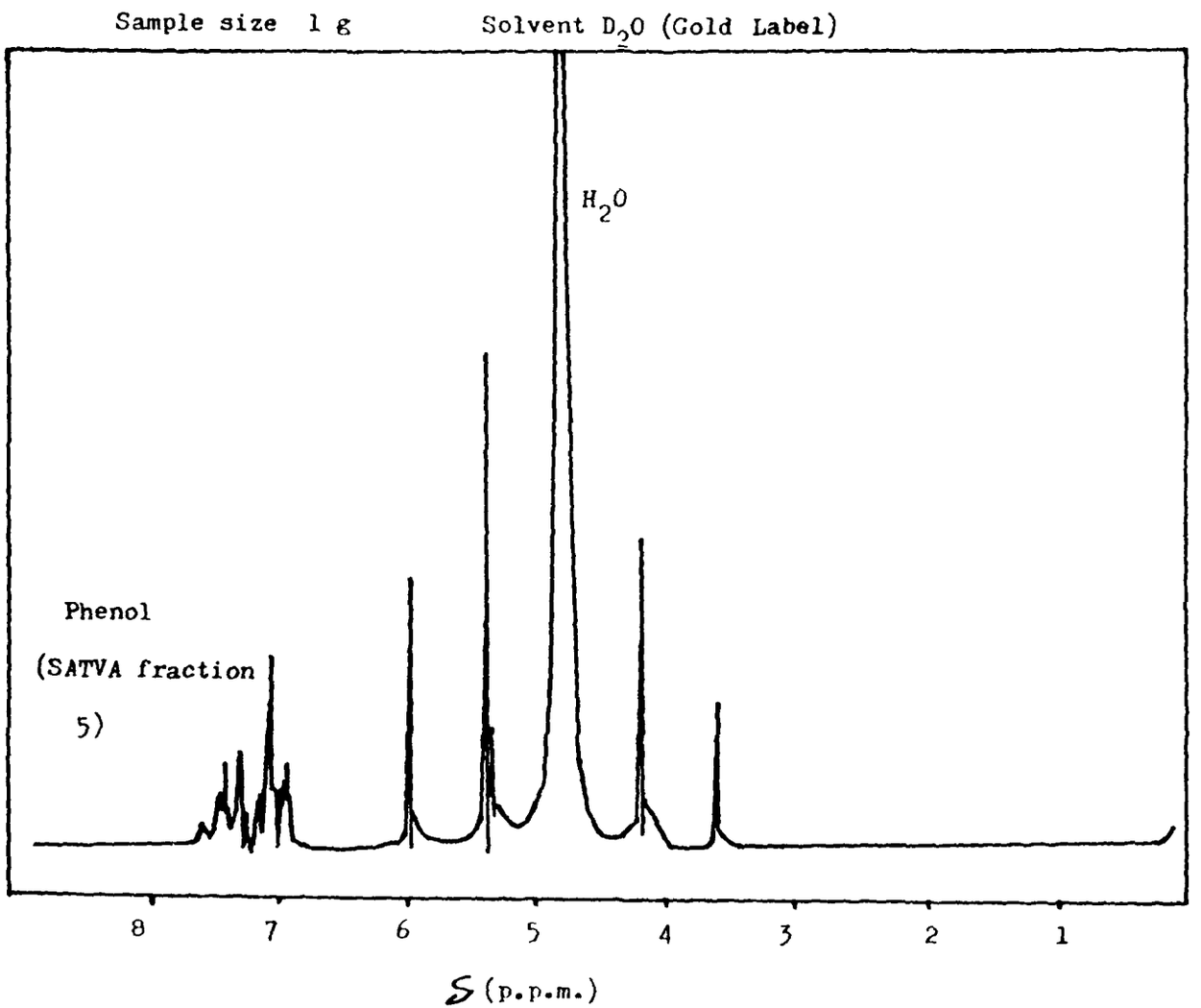

FIGURE 87 PROTON N.M.R. SPECTRUM OF SATVA FRACTION 4 (ATS-G)

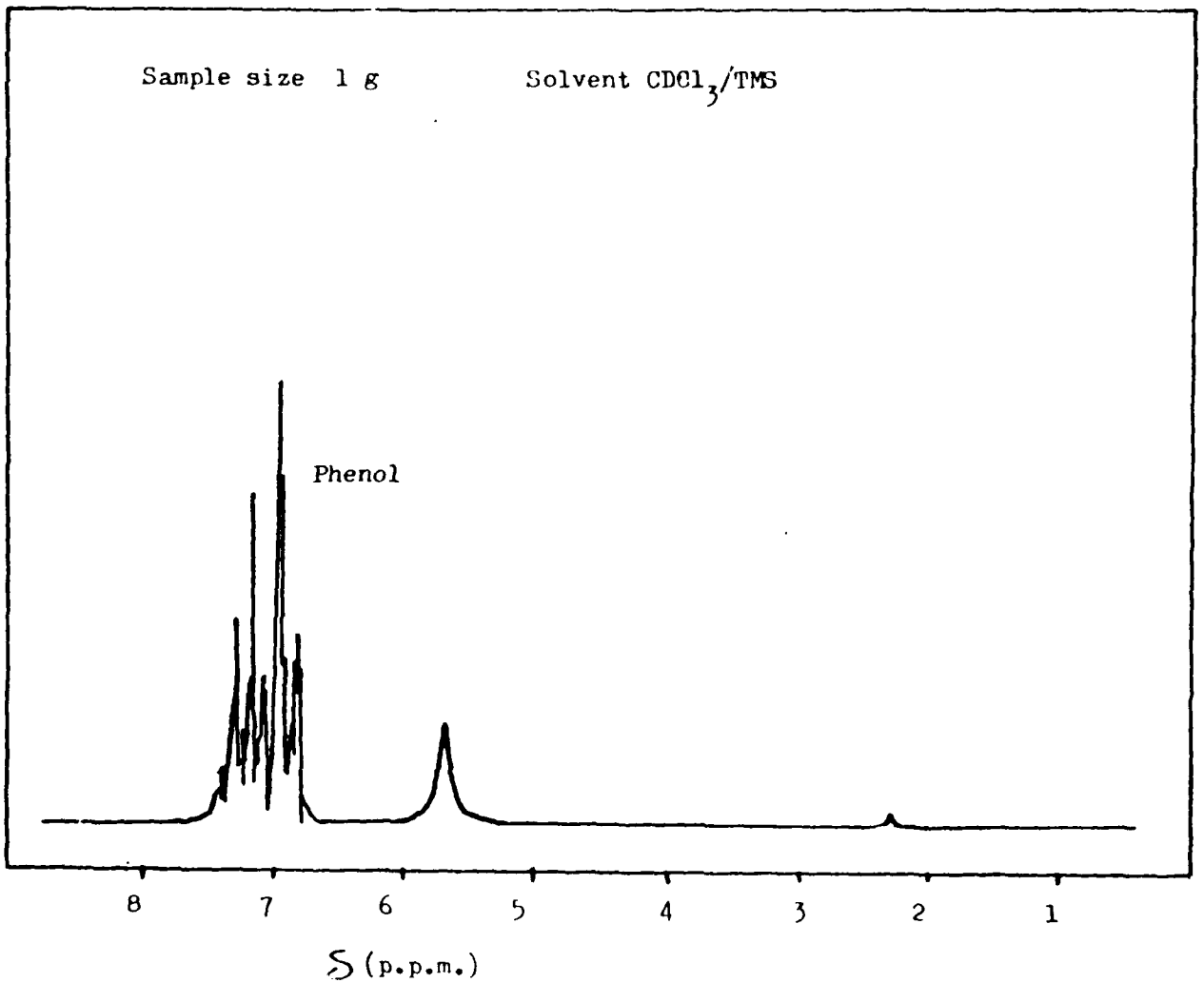

FIGURE 88 PROTON N.M.R. SPECTRUM OF SATVA FRACTION 5 (ATS-G)

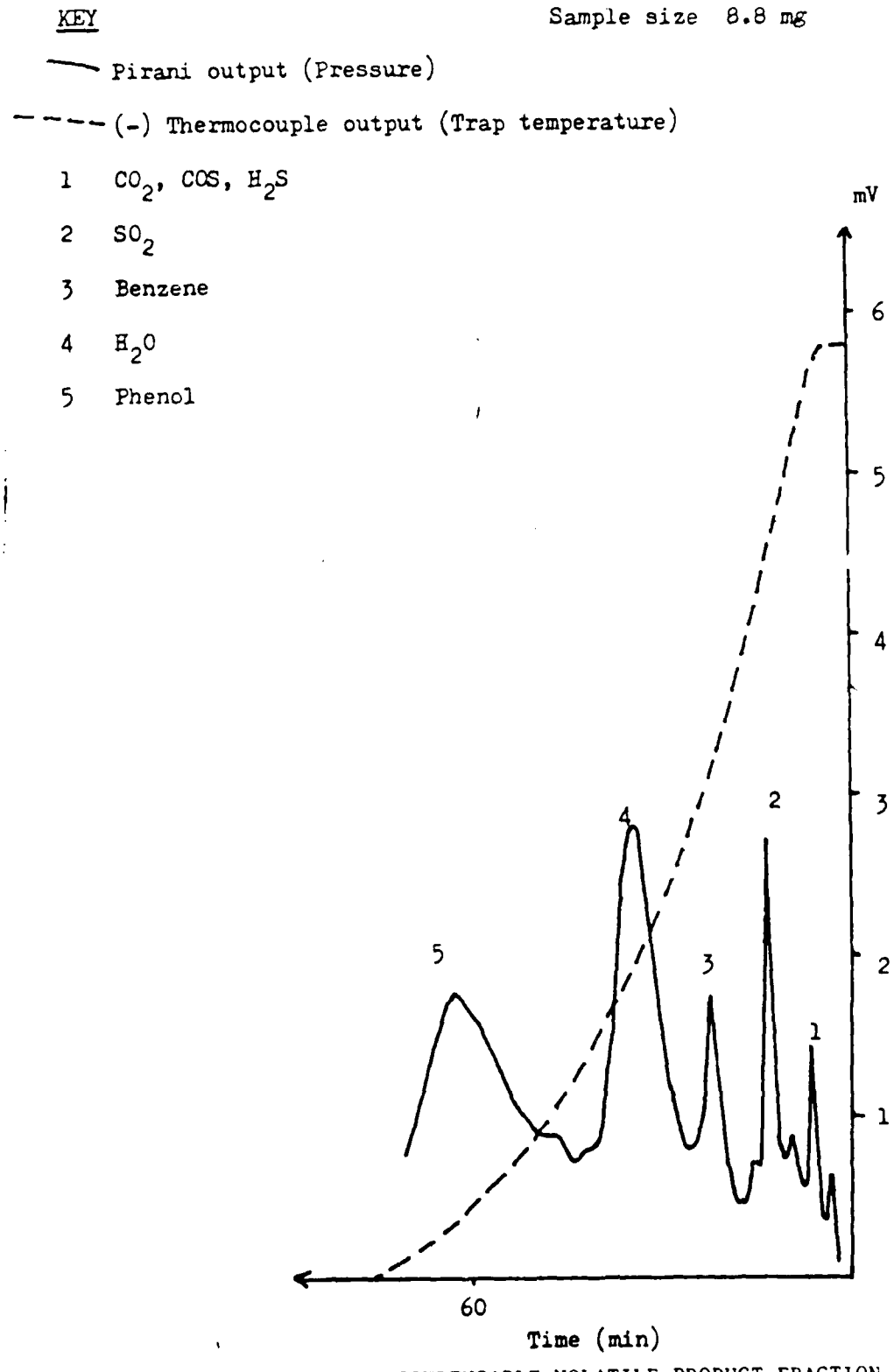

FIGURE 89 SATVA OF THE CONDENSABLE VOLATILE PRODUCT FRACTION OF DEGRADATION TO 1020°C OF F5

KEY

Pirani output (Pressure)

(-) Thermocouple output (Trap temperature)

Sample size 103.5 mg

1 CO_2, COS, H_2S

2 SO_2

3 Benzene

4 H_2O

5 Phenol

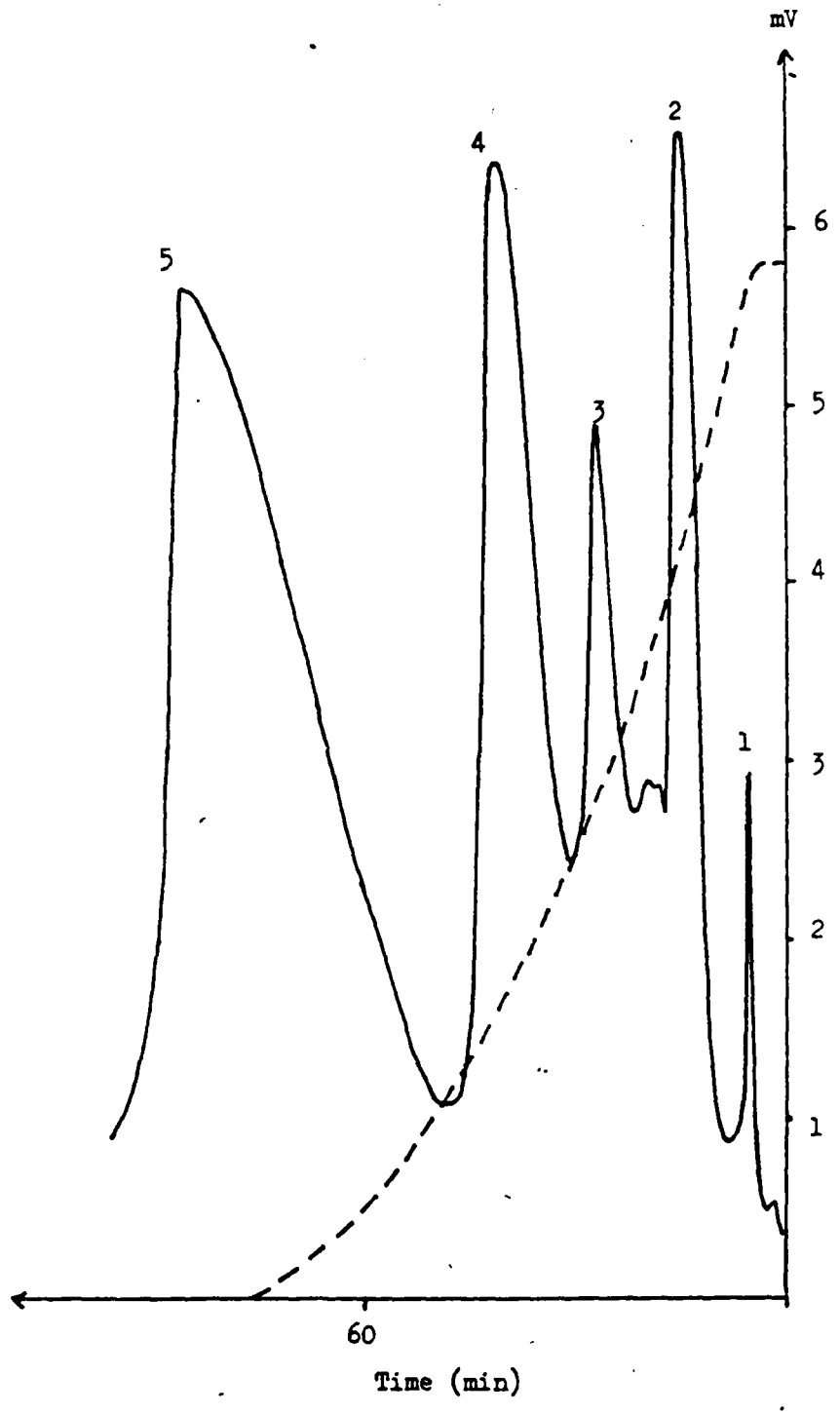

FIGURE 90 SATVA OF THE CONDENSABLE VOLATILE PRODUCT FRACTION OF DEGRADATION TO 1020°C OF ATS MONOMER

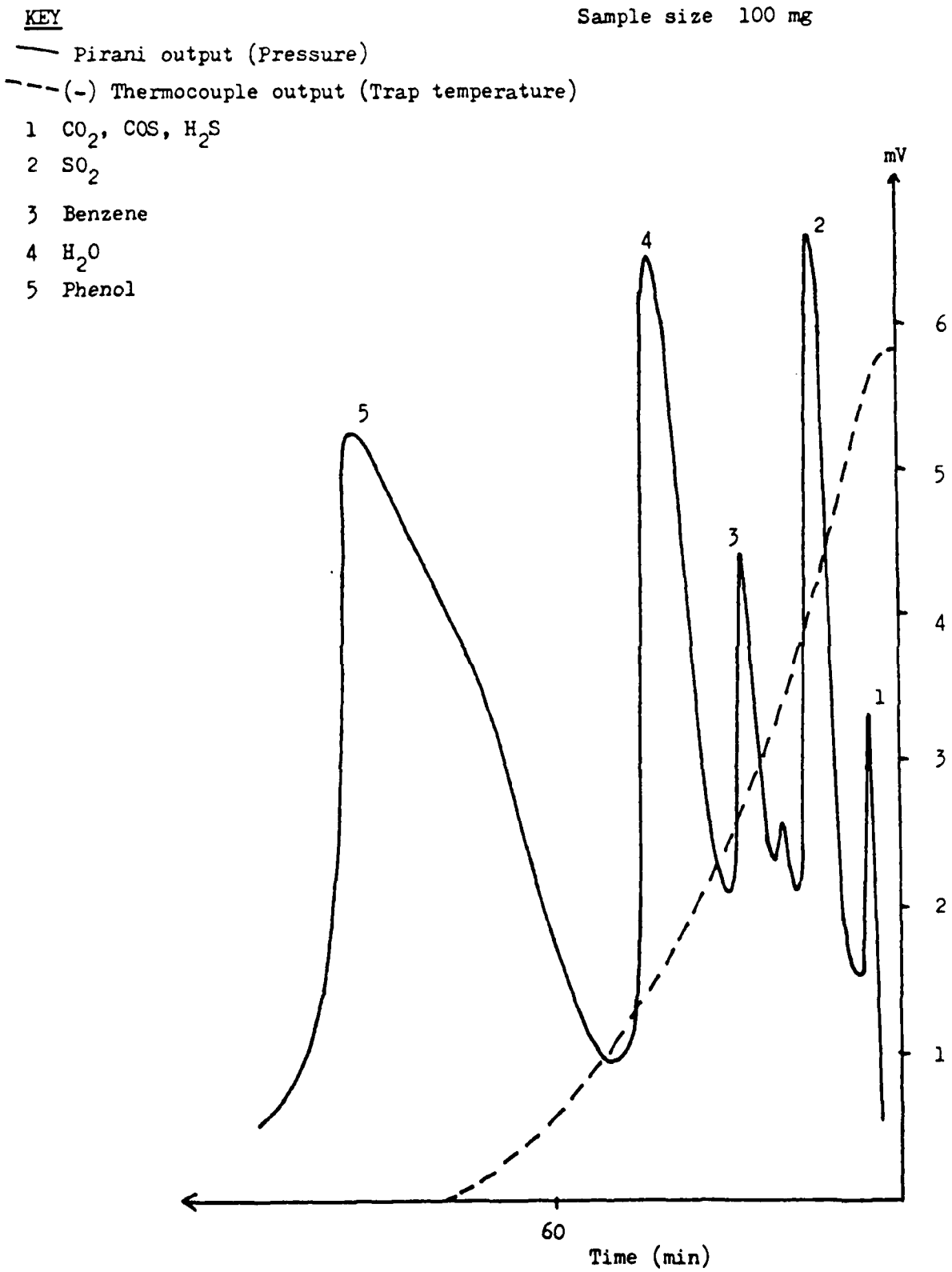

FIGURE 91 SATVA OF THE CONDENSABLE VOLATILE PRODUCT FRACTION OF DEGRADATION TO 1020°C OF ATS DIMER

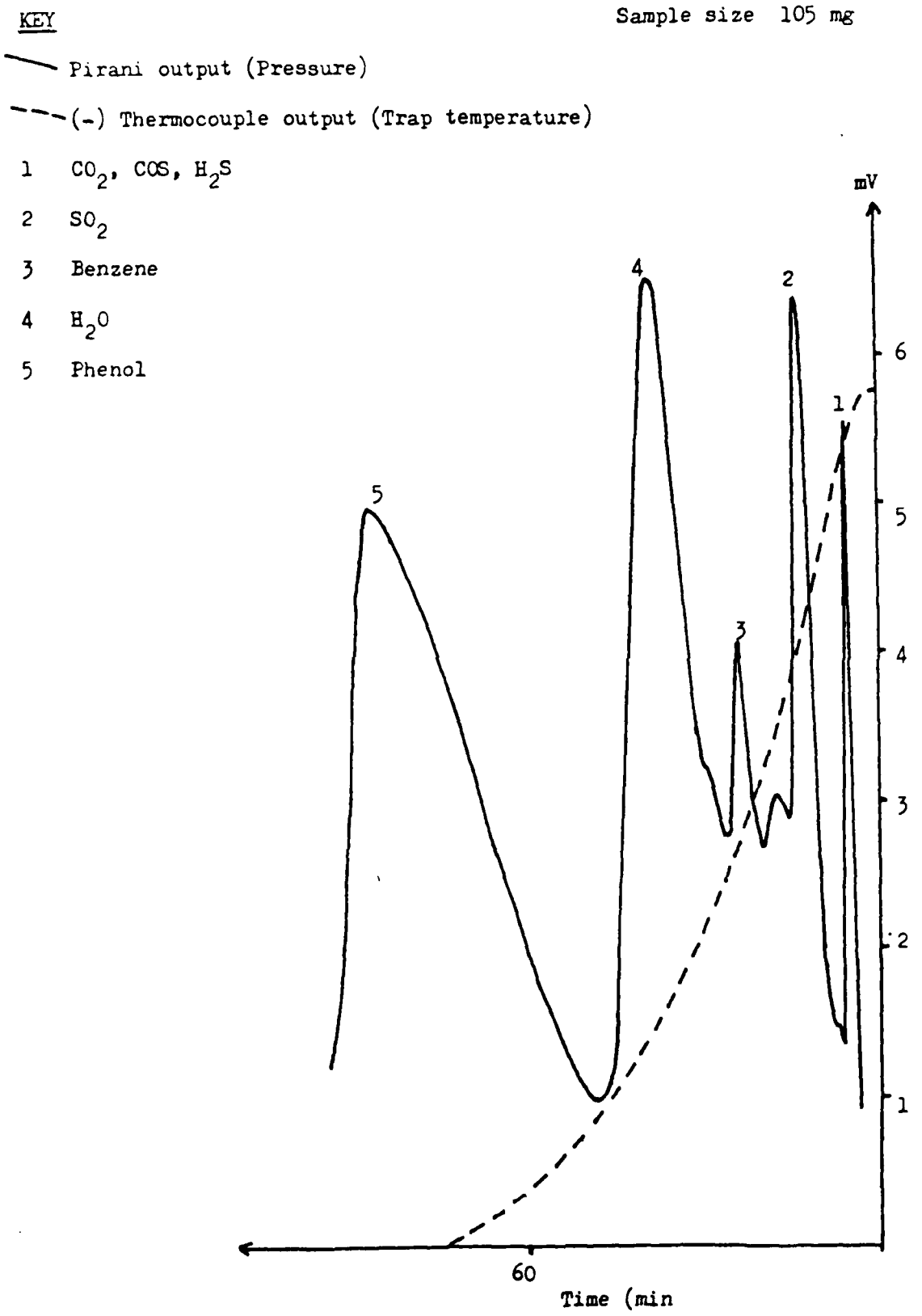

FIGURE 92 SATVA OF THE CONDENSABLE VOLATILE PRODUCT FRACTION OF DEGRADATION TO 1020°C OF ATS TRIMER

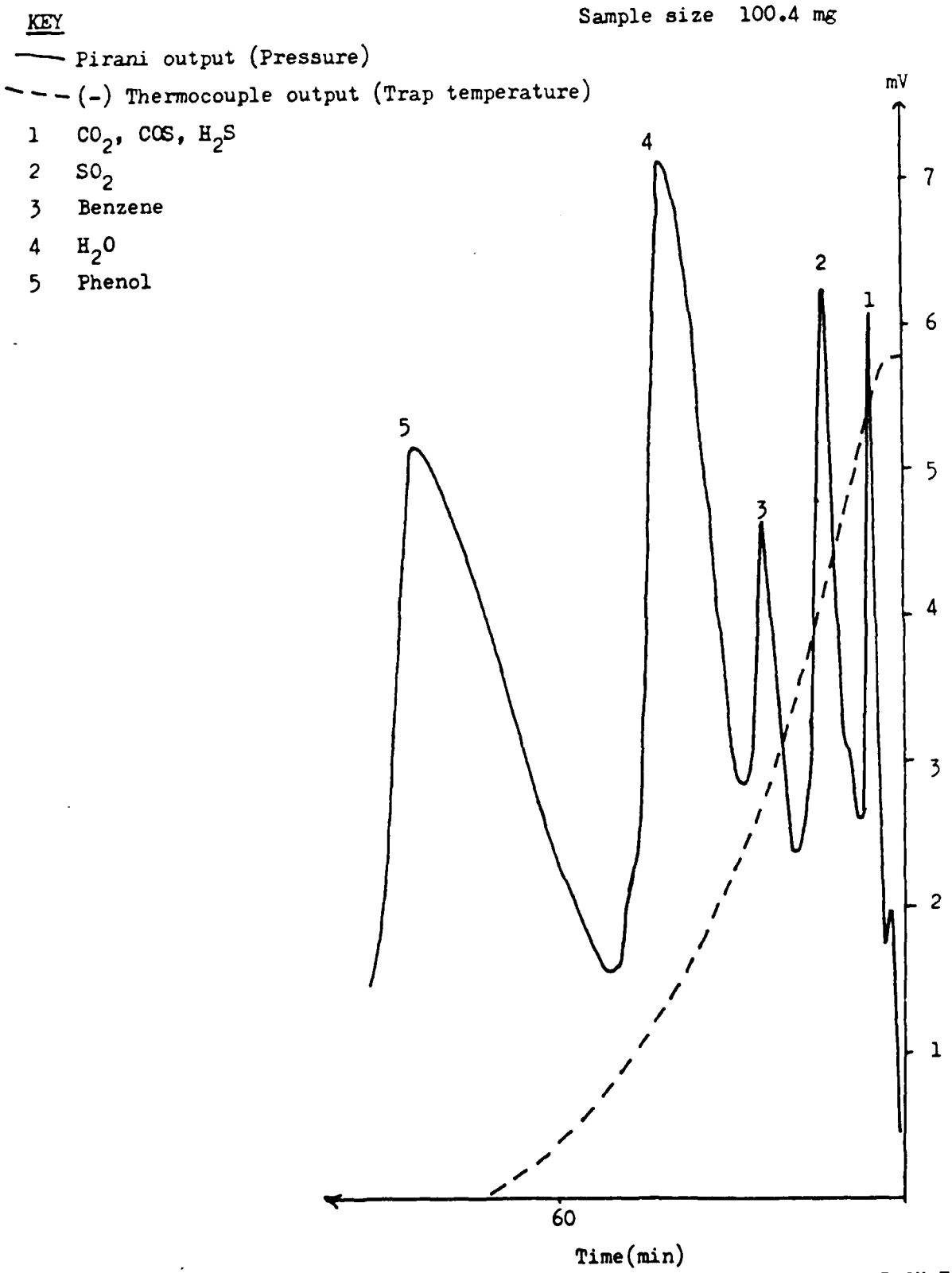

FIGURE 93 SATVA OF THE CONDENSABLE VOLATILE PRODUCT FRACTION OF DEGRADATION TO 1020°C OF F4

KEY

Sample size 108.4 mg

—— Pirani output (pressure)

– – – (-) Thermocouple output (Trap temperature)

1 CO_2, COS, H_2S

2 SO_2

3 Benzene

4 H_2O

5 Phenol

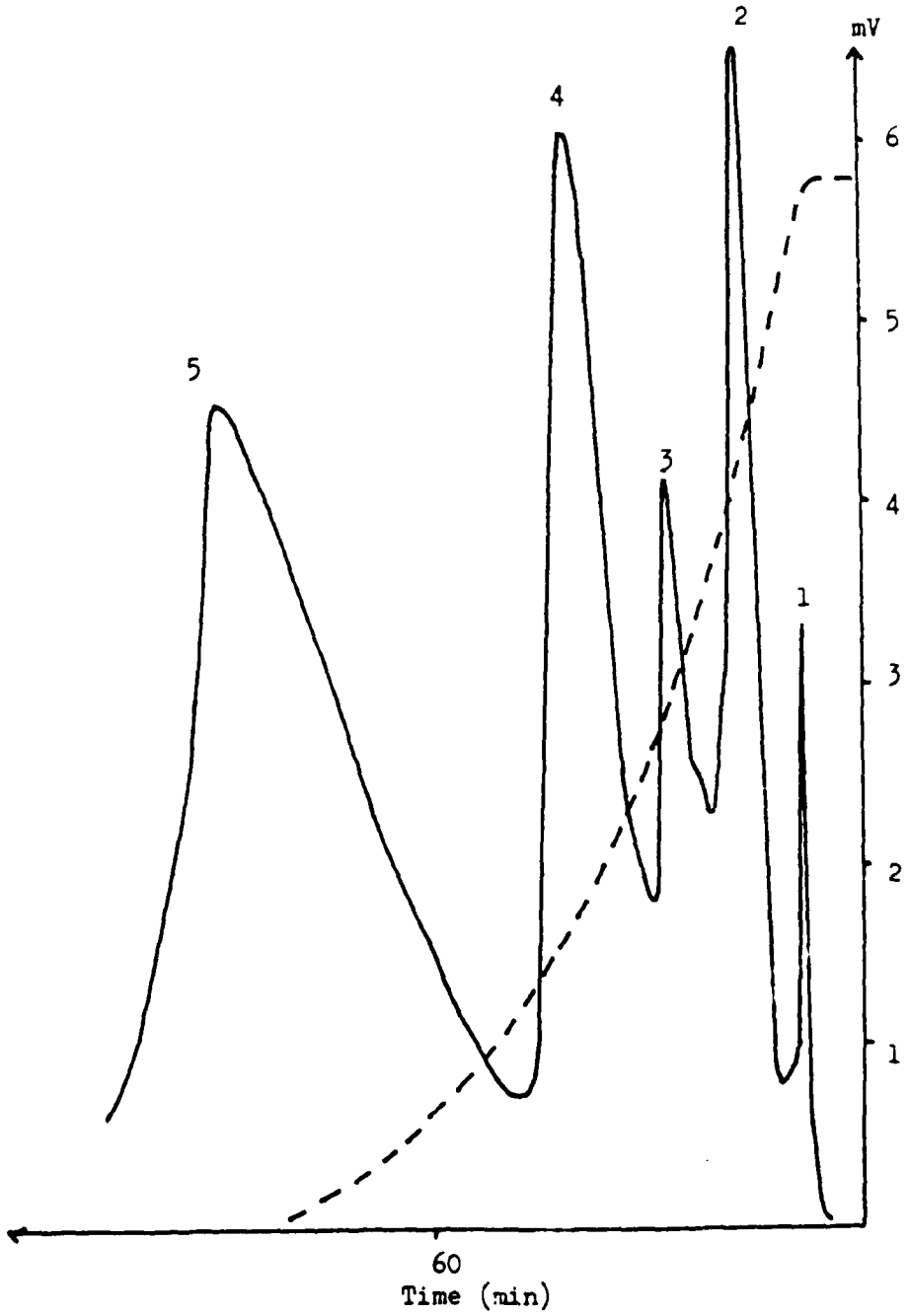

FIGURE 94 SATVA OF THE CONDENSABLE VOLATILE PRODUCT FRACTION OF DEGRADATION TO 1020°C OF RADEL

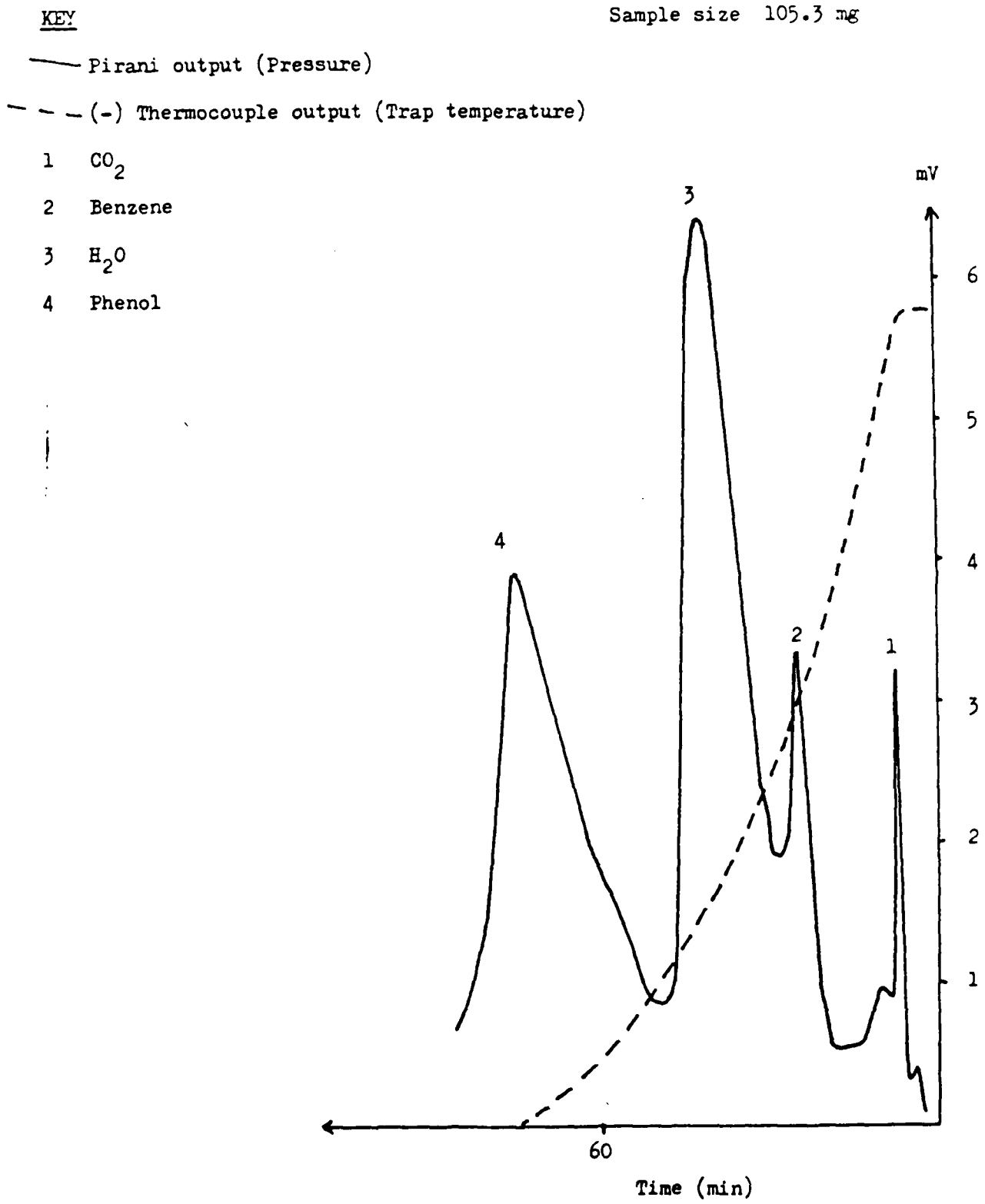

FIGURE 95 SATVA OF THE CONDENSABLE VOLATILE PRODUCT FRACTION OF DEGRADATION TO 1020°C OF ATP MONOMER

Sample size 101 mg

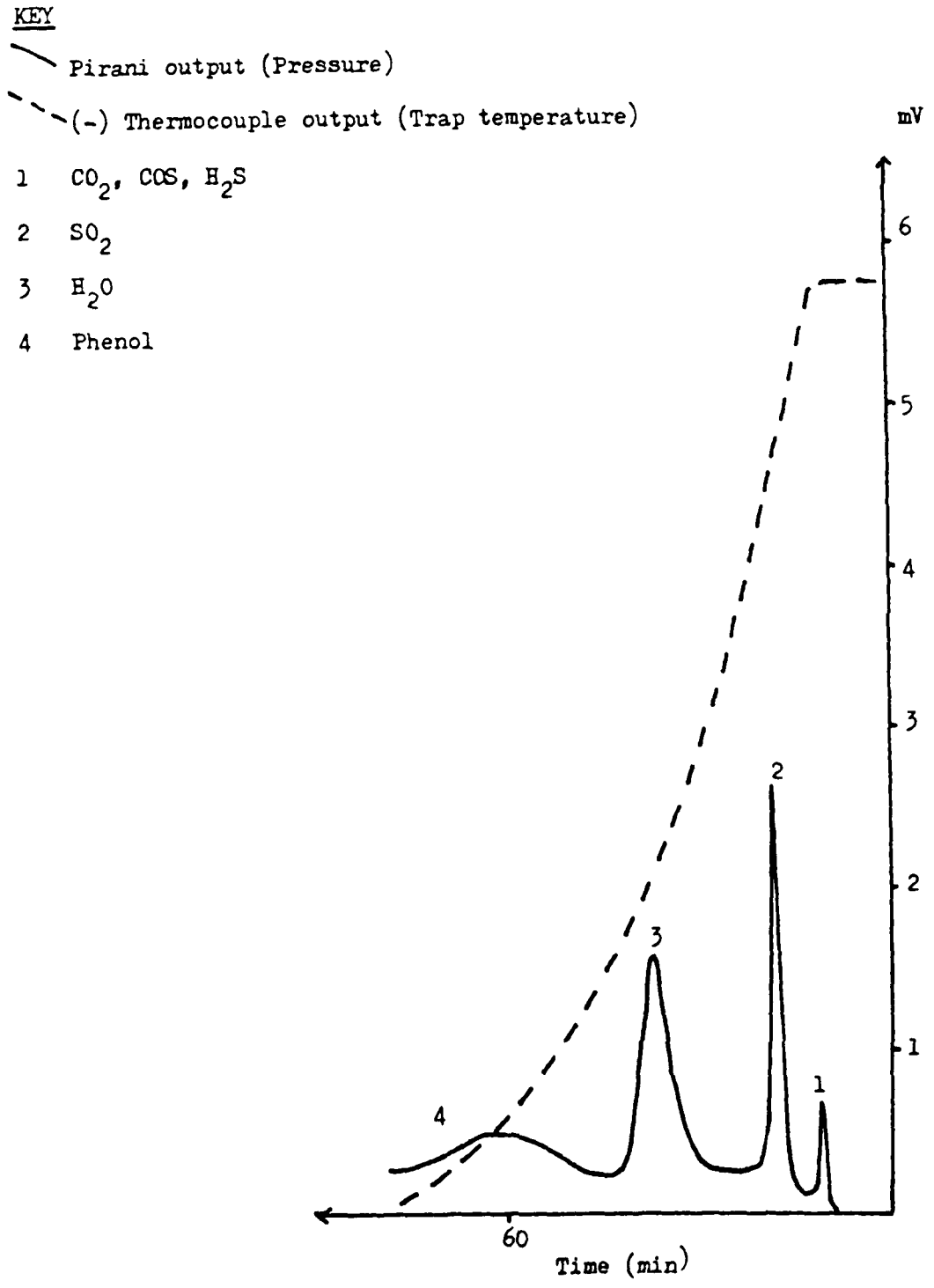

FIGURE 96 SATVA OF THE CONDENSABLE VOLATILE PRODUCTS OF THERMAL DEGRADATION OF ATS-G IN THE TEMPERATURE INTERVAL (283-424)°C

Sample size 104.5 mg

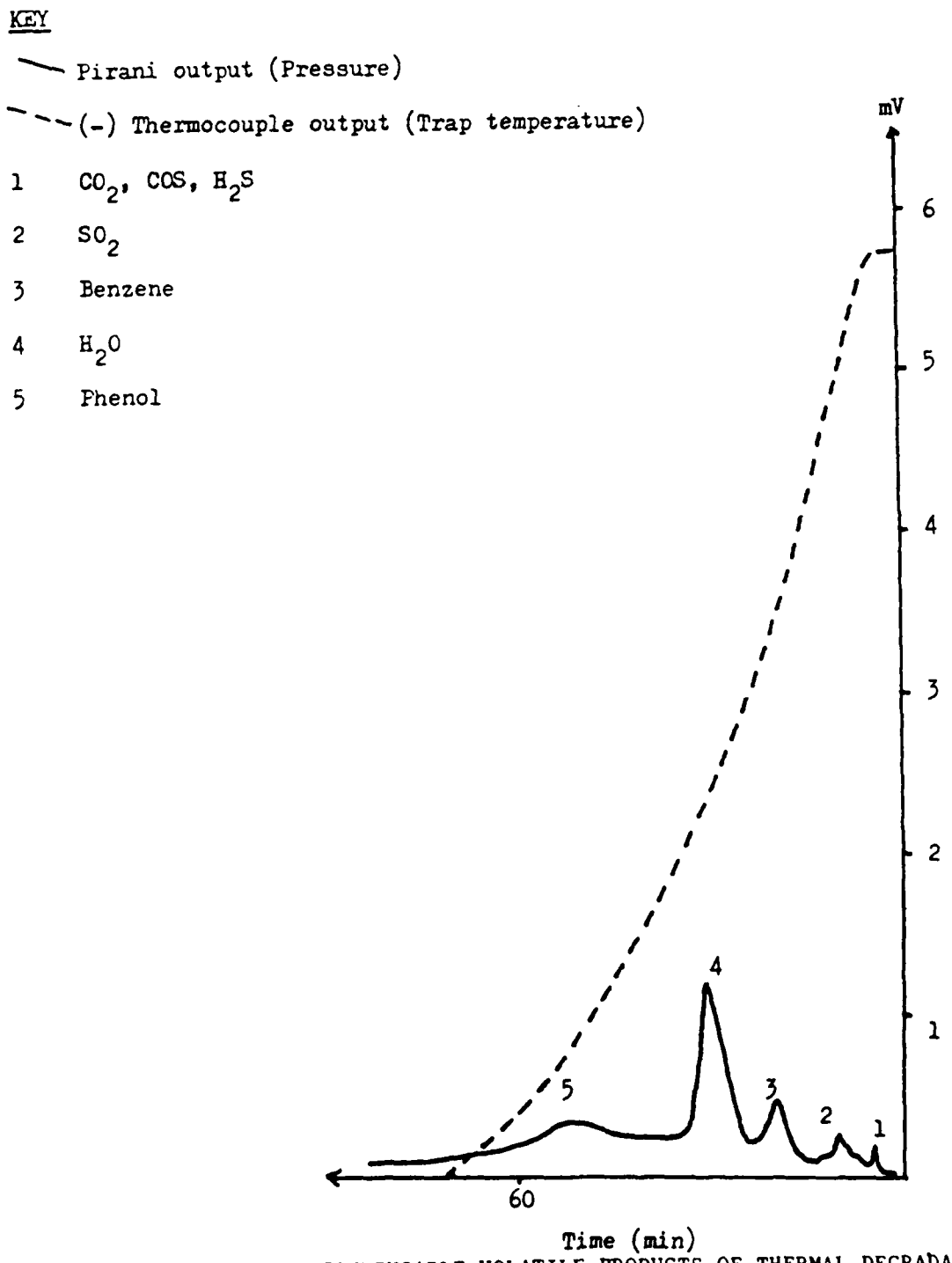

FIGURE 97 SATVA OF THE CONDENSABLE VOLATILE PRODUCTS OF THERMAL DEGRADATION OF ATS DIMER IN THE TEMPERATURE INTERVAL (283-355)°C

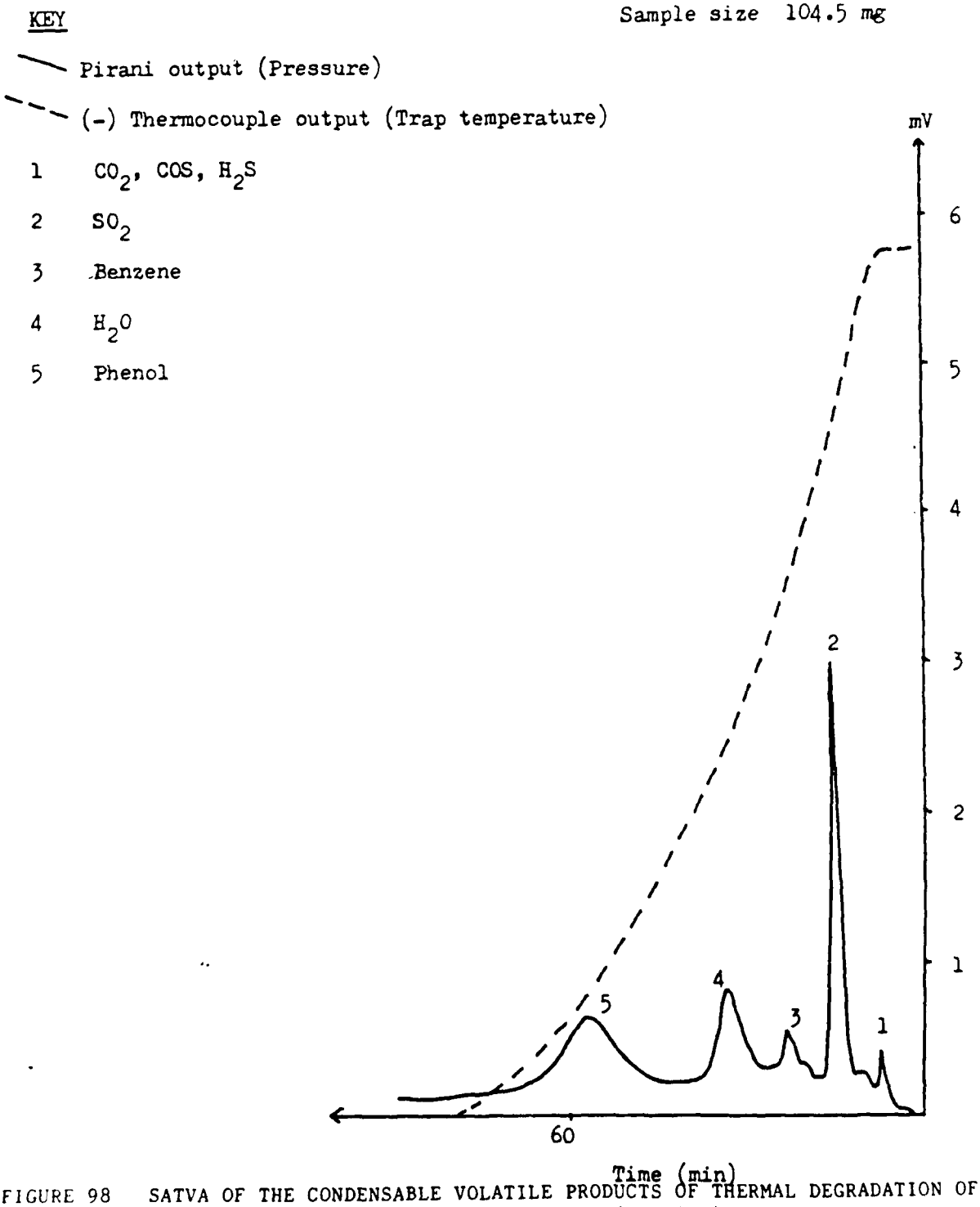

FIGURE 98 SATVA OF THE CONDENSABLE VOLATILE PRODUCTS OF THERMAL DEGRADATION OF ATS DIMER IN THE TEMPERATURE INTERVAL (355-424)°C

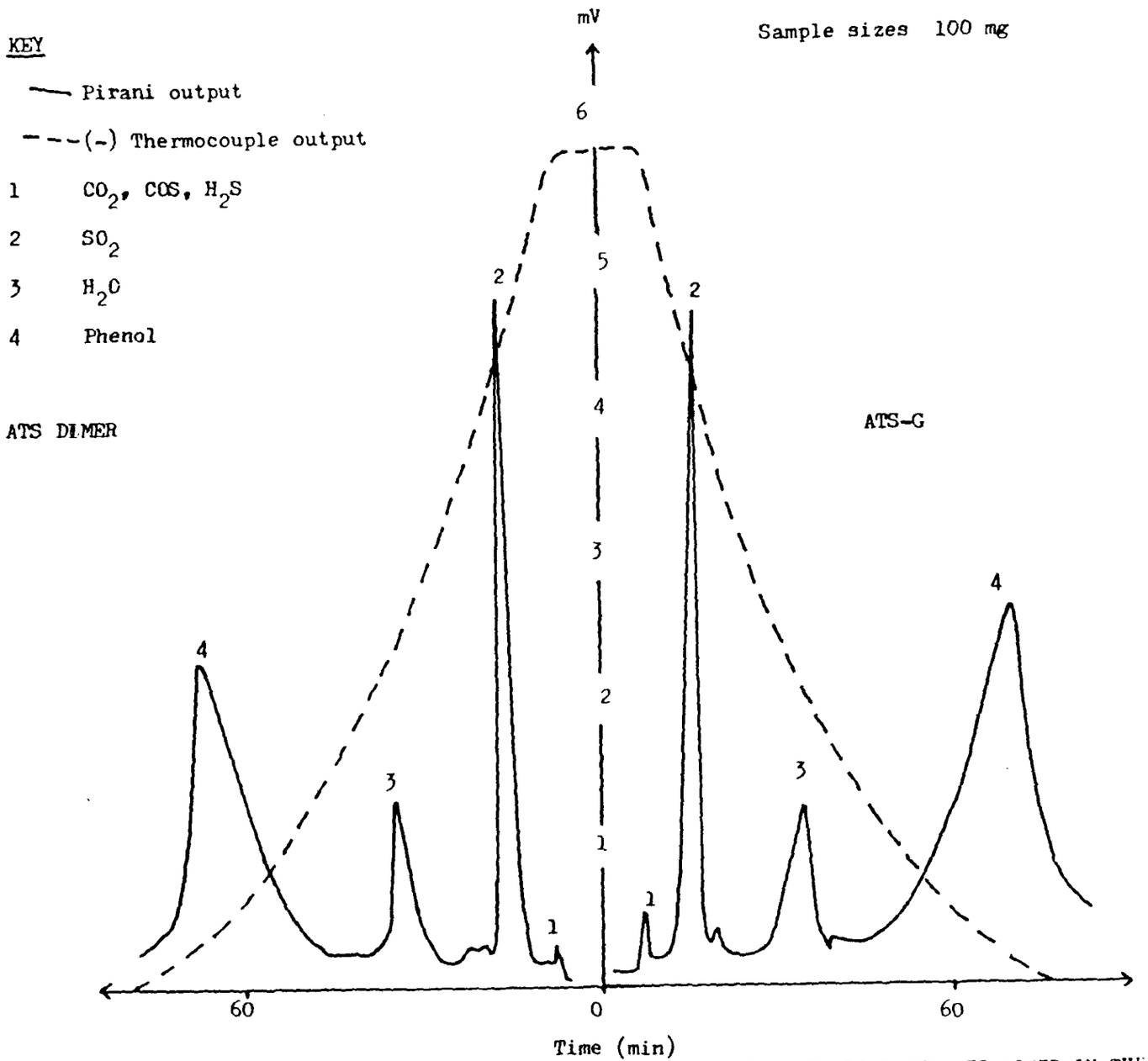

FIGURE 99 SATVA OF THE CONDENSABLE VOLATILE PRODUCTS OF THERMAL DEGRADATIONOF ATS-G AND ATS DIMER IN THE TEMPERATURE INTERVAL (426-461)°C

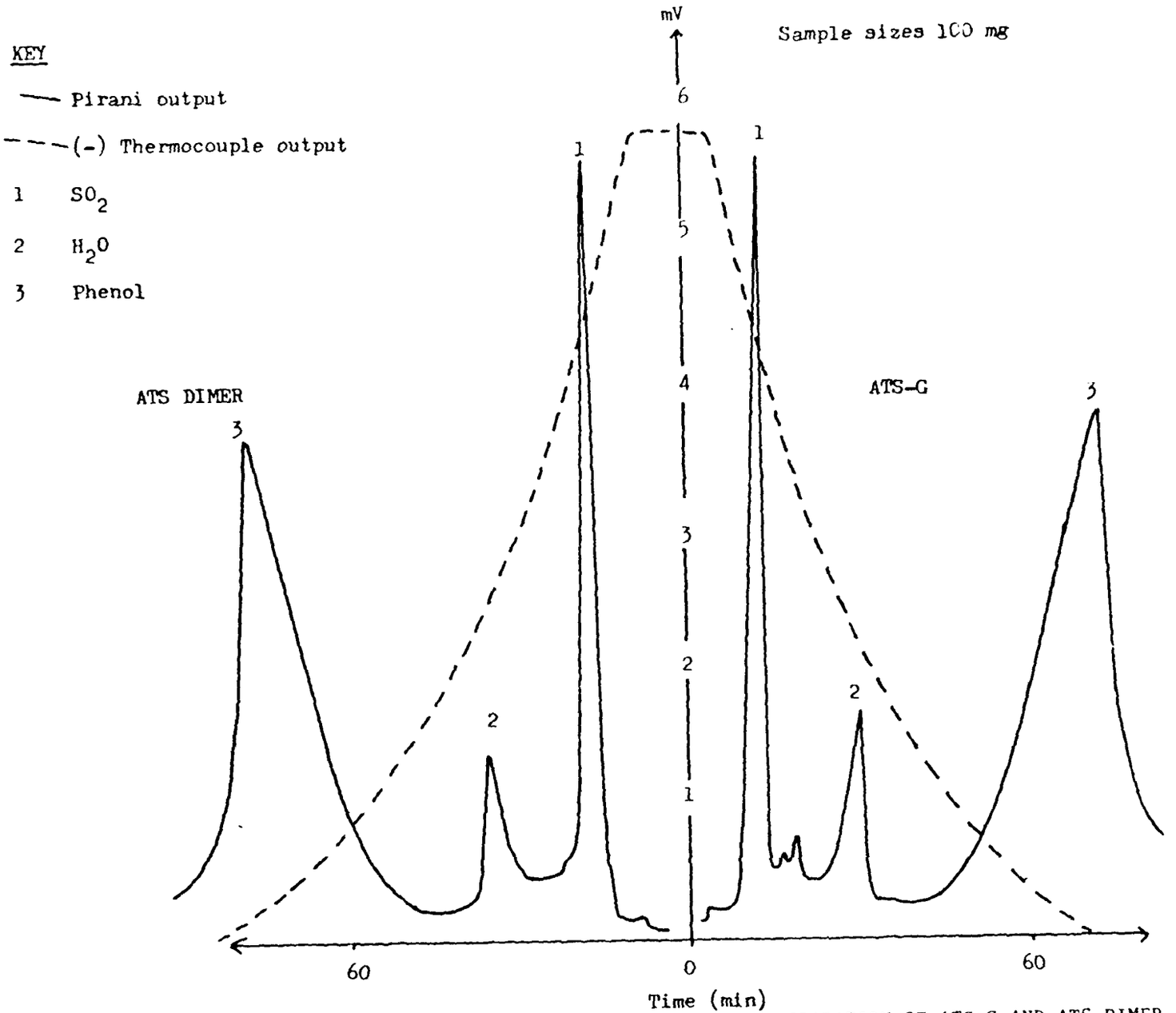

FIGURE 100 SATVA OF THE CONDENSABLE VOLATILE PRODUCTS OF THERMAL DEGRADATION OF ATS-G AND ATS DIMER IN THE TEMPERATURE INTERVAL (461-496)°C

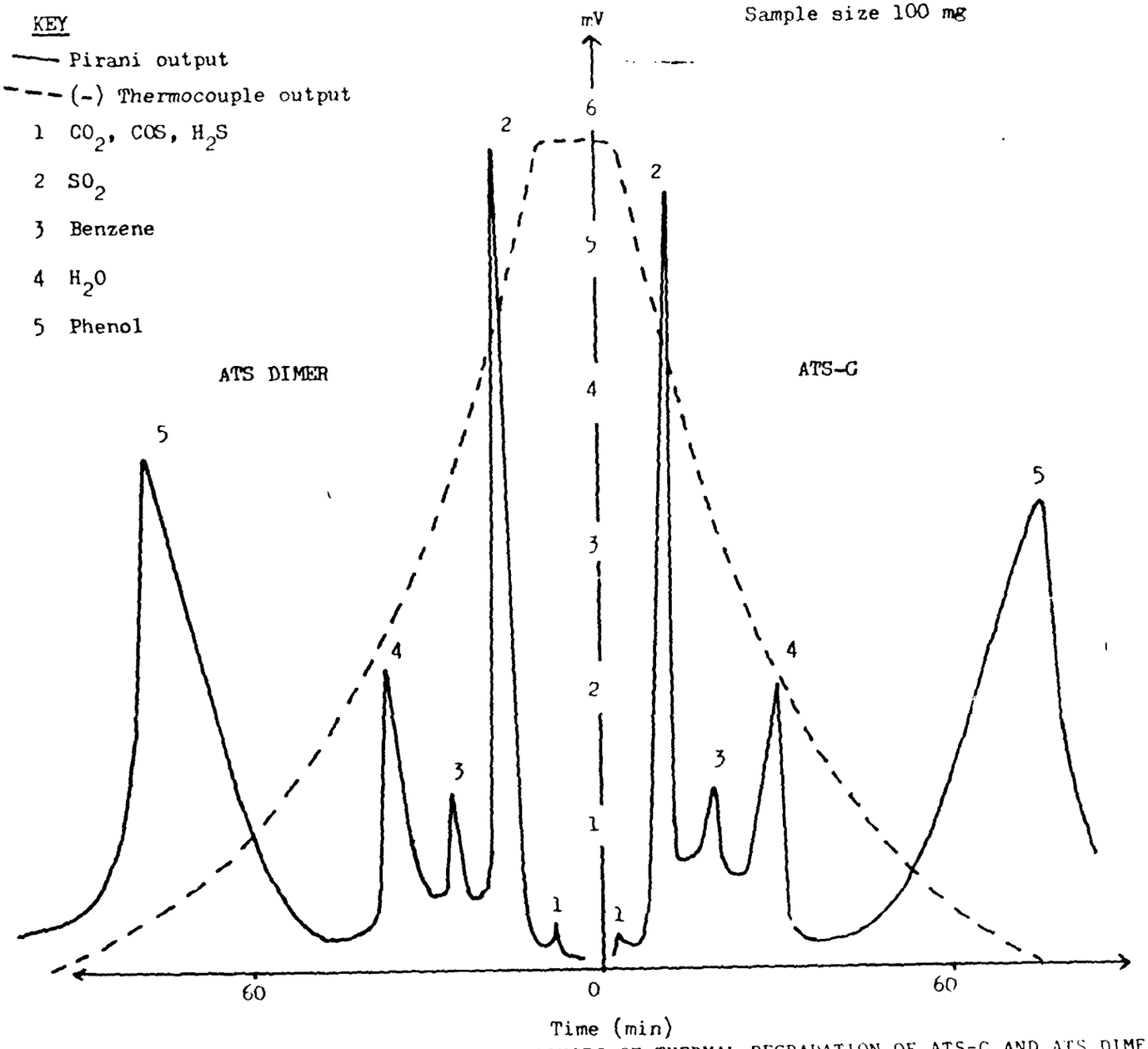

FIGURE 101 SATVA OF THE CONDENSABLE VOLATILE PRODUCTS OF THERMAL DEGRADATION OF ATS-G AND ATS DIMER IN THE TEMPERATURE INTERVAL (496-532)°C

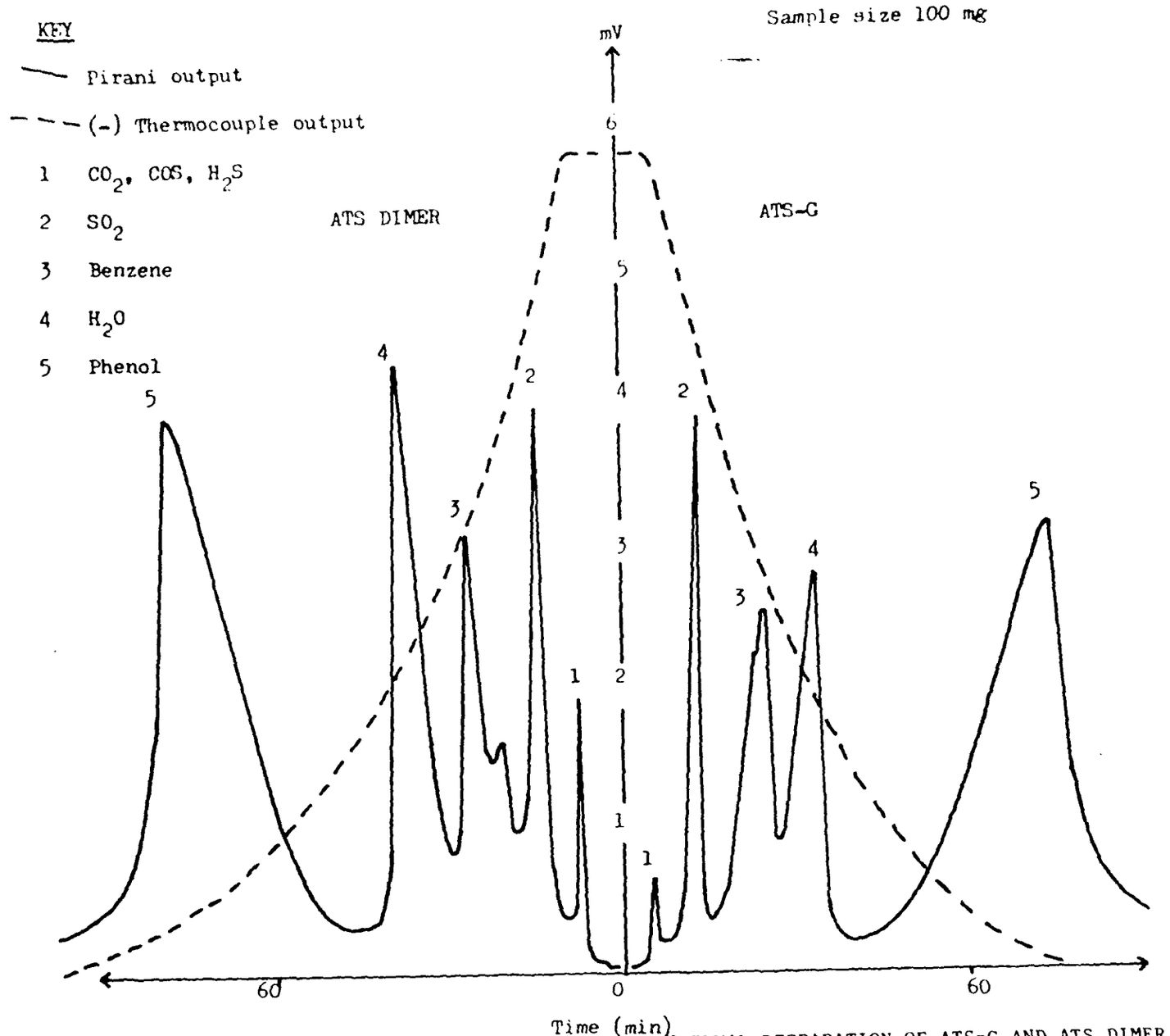

FIGURE 102 SATVA OF THE CONDENSABLE VOLATILE PRODUCTS OF THERMAL DEGRADATION OF ATS-G AND ATS DIMER IN THE TEMPERATURE INTERVAL (532-567)°C

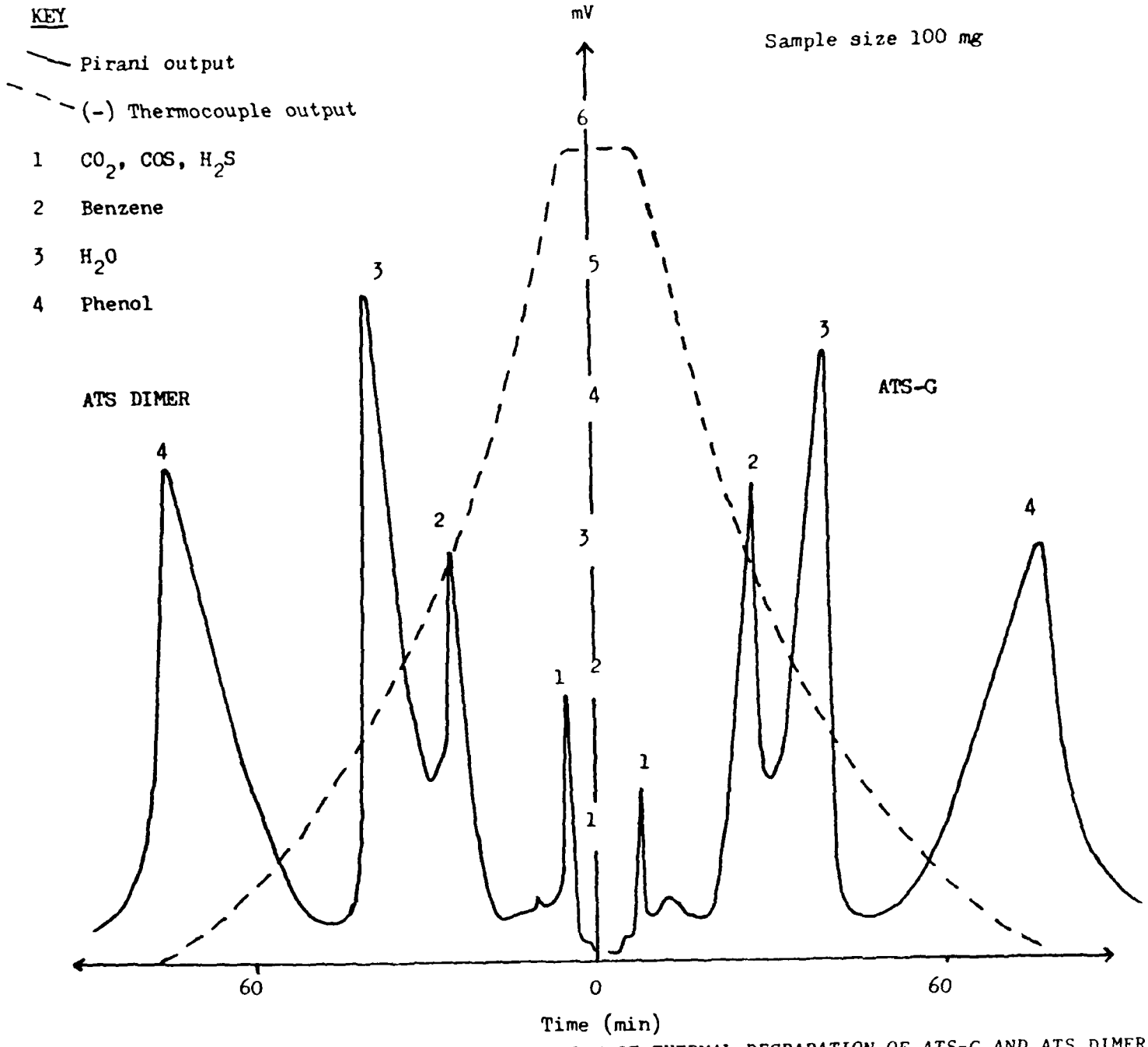

FIGURE 103 SATVA OF THE CONDENSABLE VOLATILE PRODUCTS OF THERMAL DEGRADATION OF ATS-G AND ATS DIMER IN THE

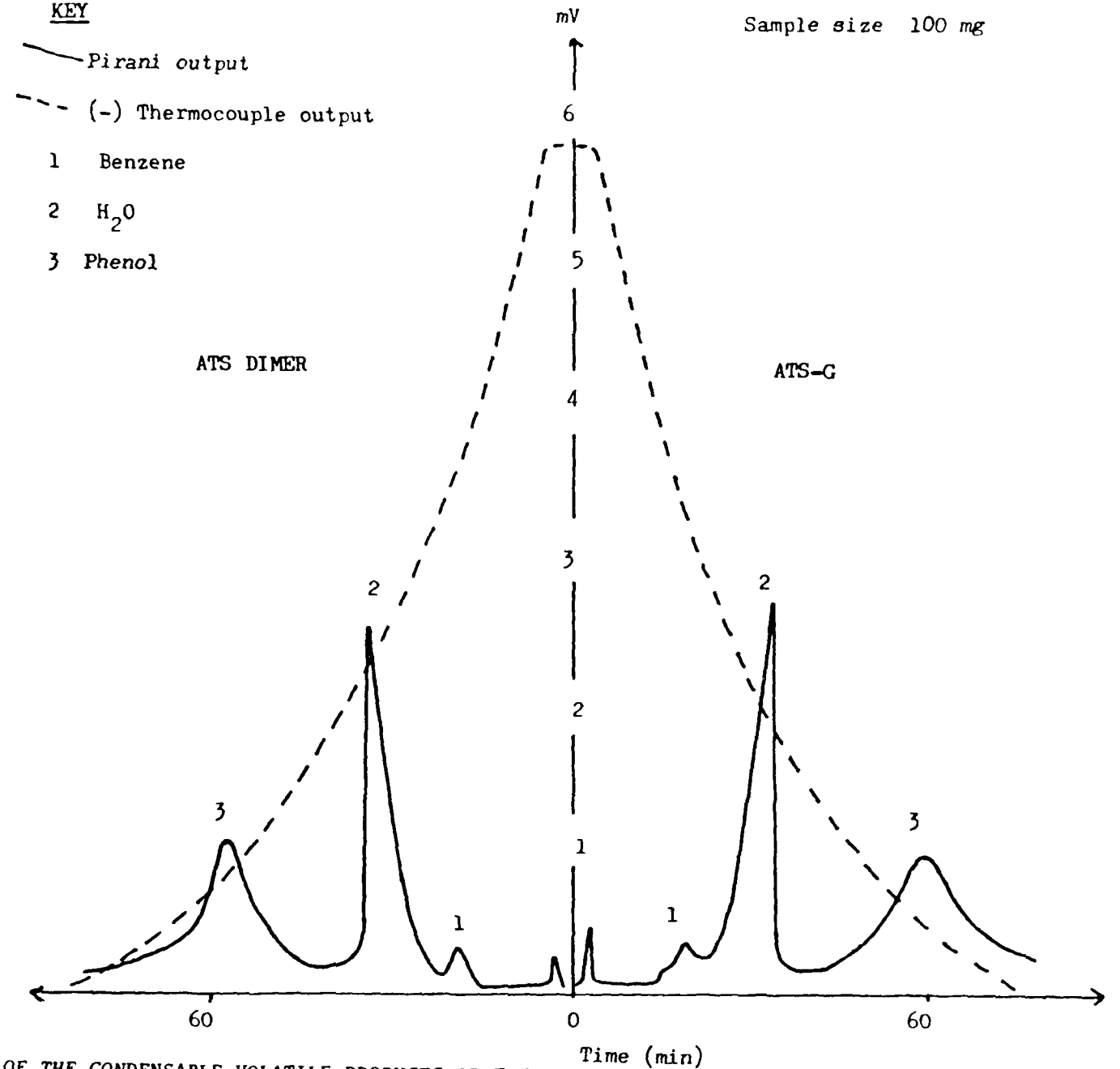

FIGURE 104 SATVA OF THE CONDENSABLE VOLATILE PRODUCTS OF THERMAL DEGRADATION OF ATS-G AND ATS DIMER IN THE TEMPERATURE INTERVAL (625-661)°C

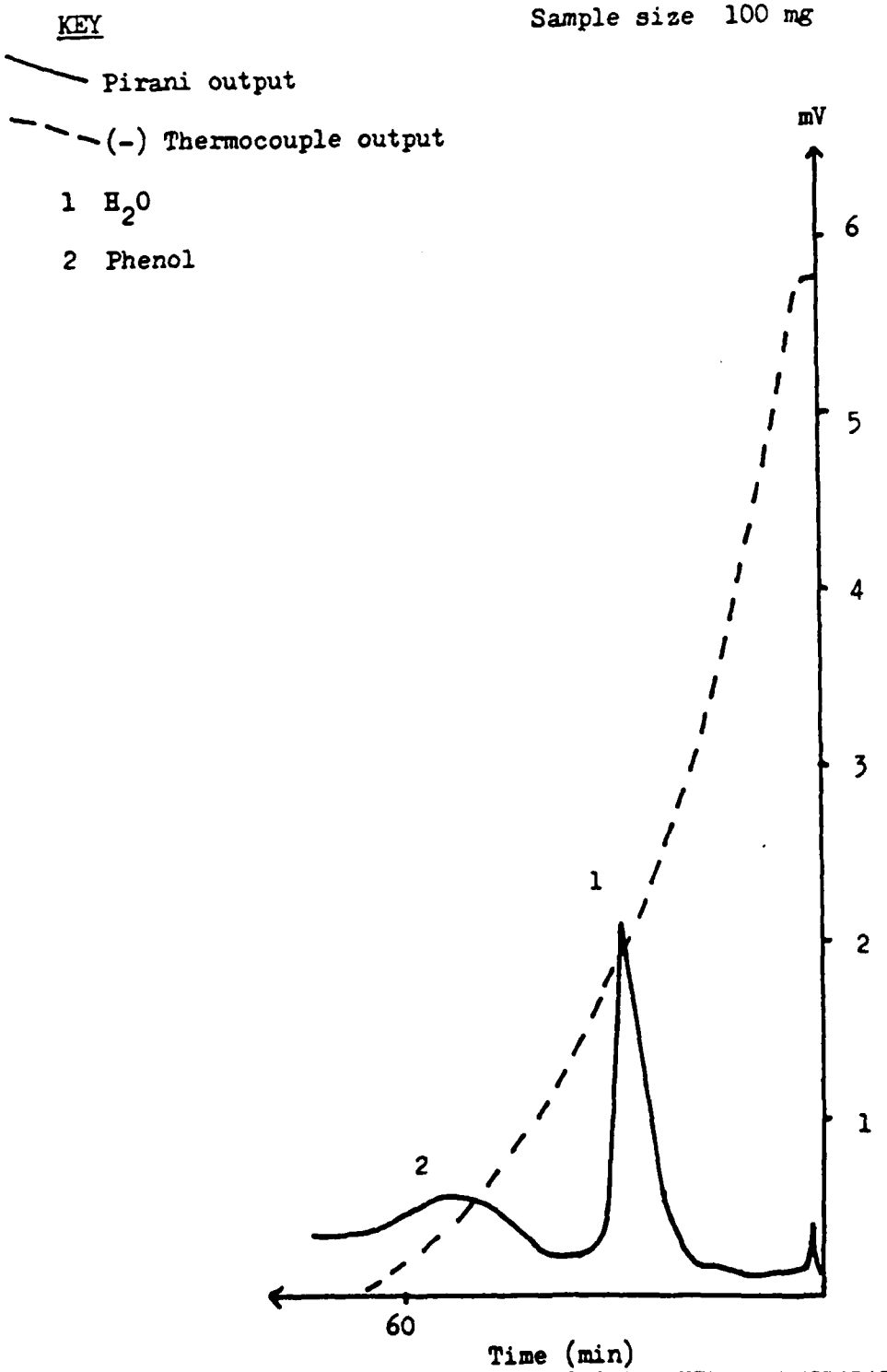

FIGURE 105 SATVA OF CONDENSABLE VOLATILE PRODUCTS OF THERMAL DEGRADATION OF ATS-G IN THE TEMPERATURE INTERVAL (661-851)°C

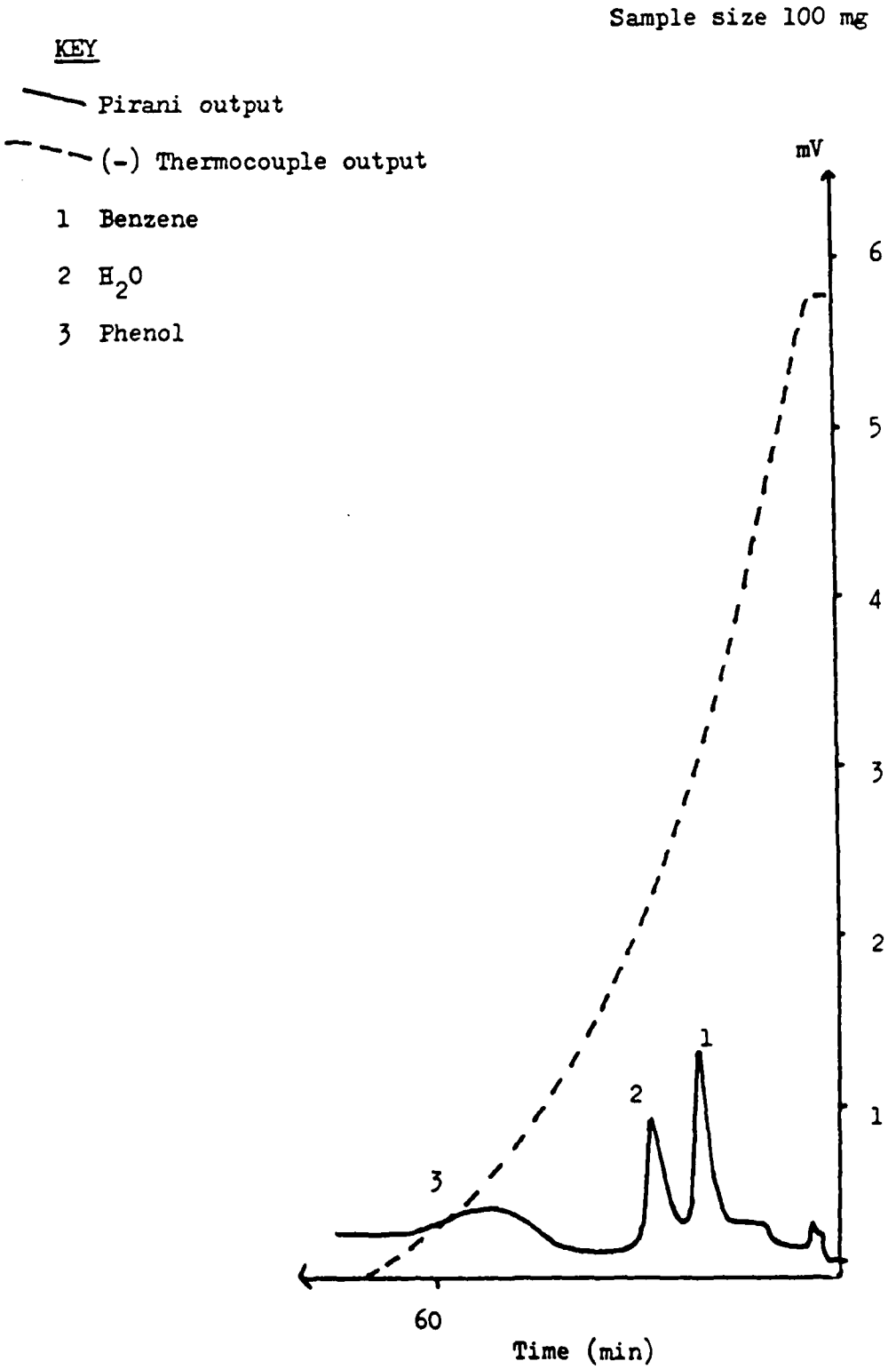

FIGURE 106 SATVA OF THE CONDENSABLE VOLATILE PRODUCTS OF THERMAL DEGRADATION OF ATS-G IN THE TEMPERATURE INTERVAL (851-1020)°C

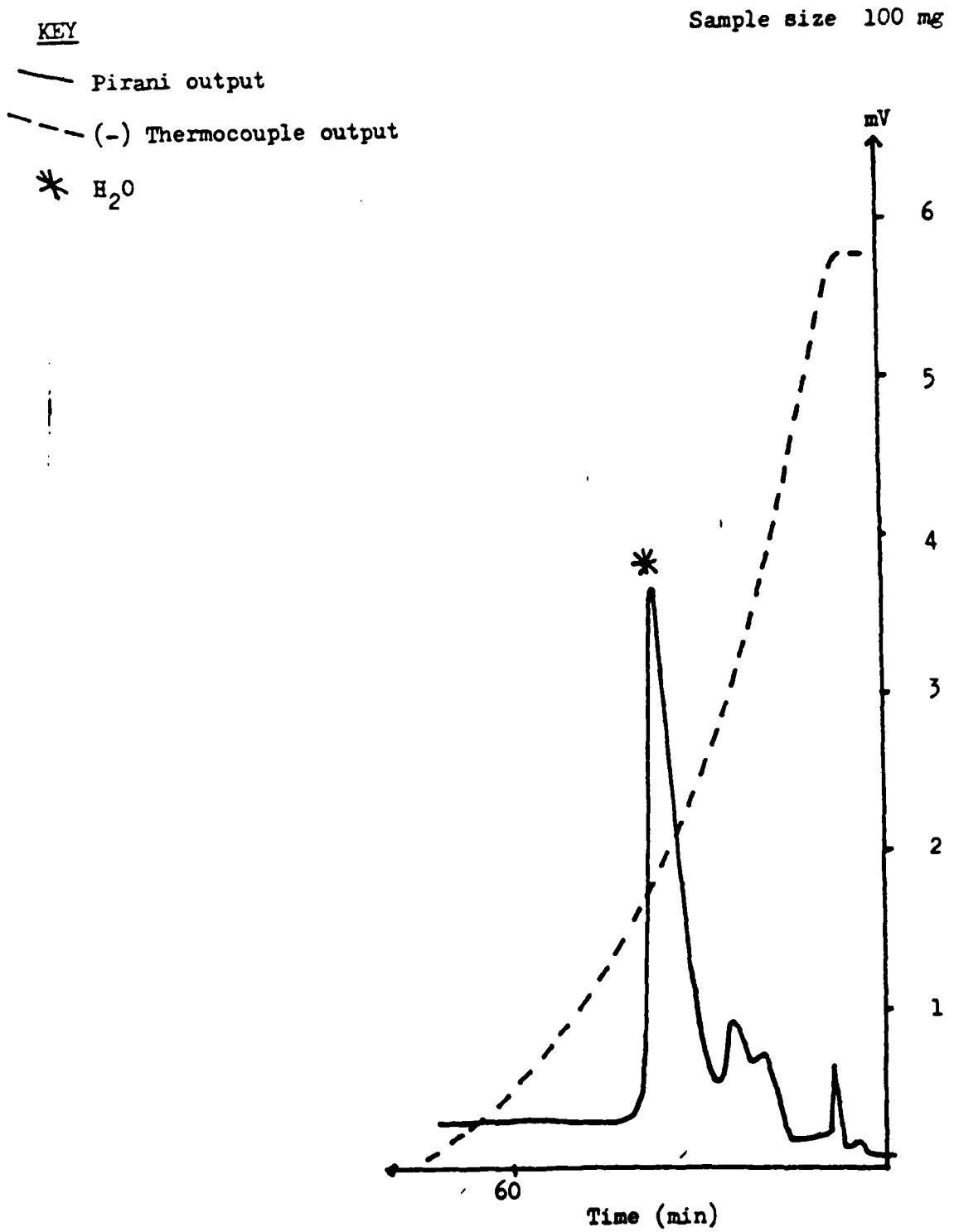

FIGURE 107 SATVA OF THE CONDENSABLE VOLATILE PRODUCTS OF THERMAL DEGRADATION OF F4 IN THE TEMPERATURE INTERVAL (234-307)°C

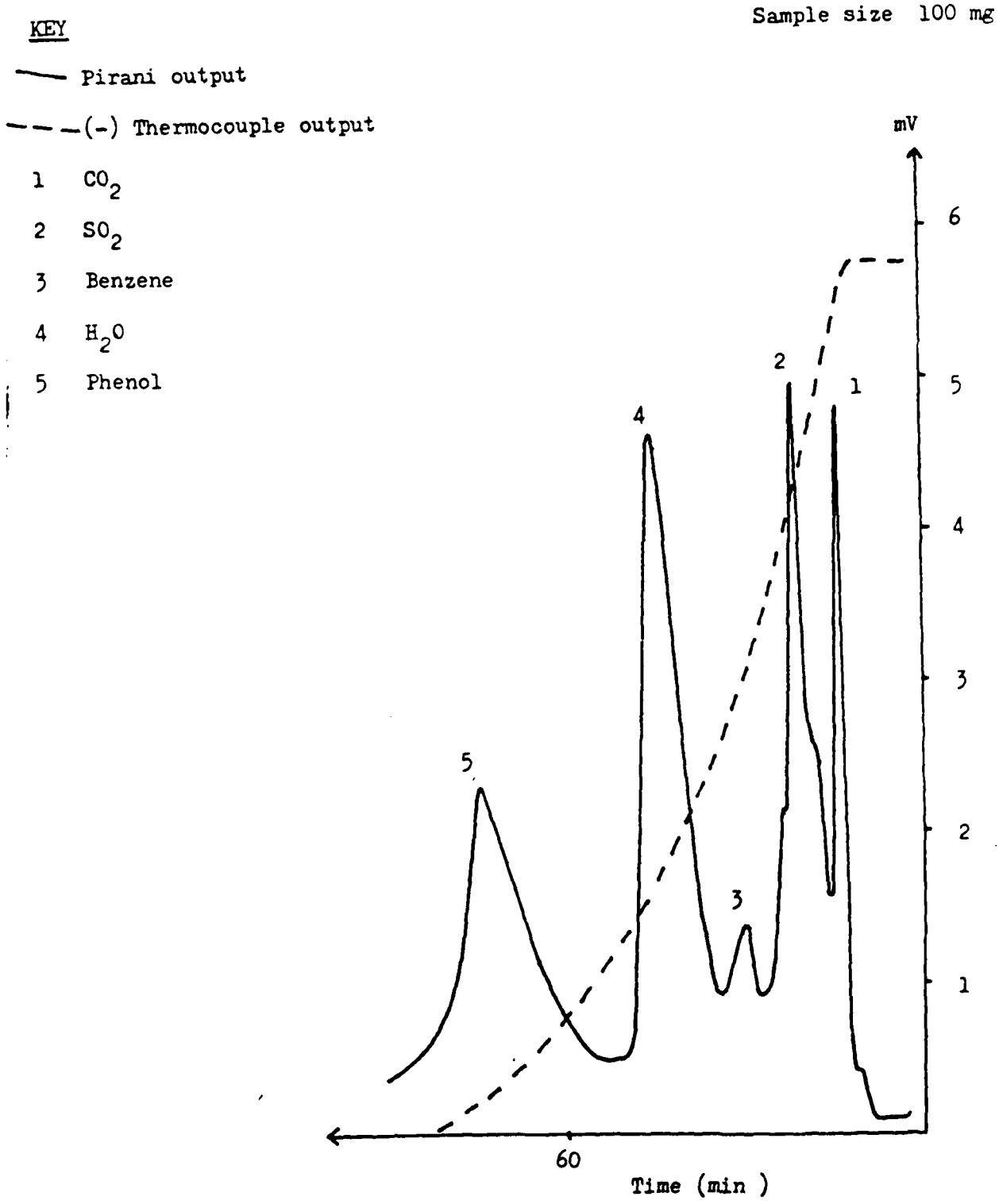

FIGURE 108 SATVA OF THE CONDENSABLE VOLATILE PRODUCTS OF THERMAL DEGRADATION OF F4 IN THE TEMPERATURE INTERVAL (307-450)°C

KEY

Sample size 100 mg

Pirani output

(-) Thermocouple output

1 CO_2, COS, H_2S

2 SO_2

3 Benzene

4 H_2O

5 Phenol

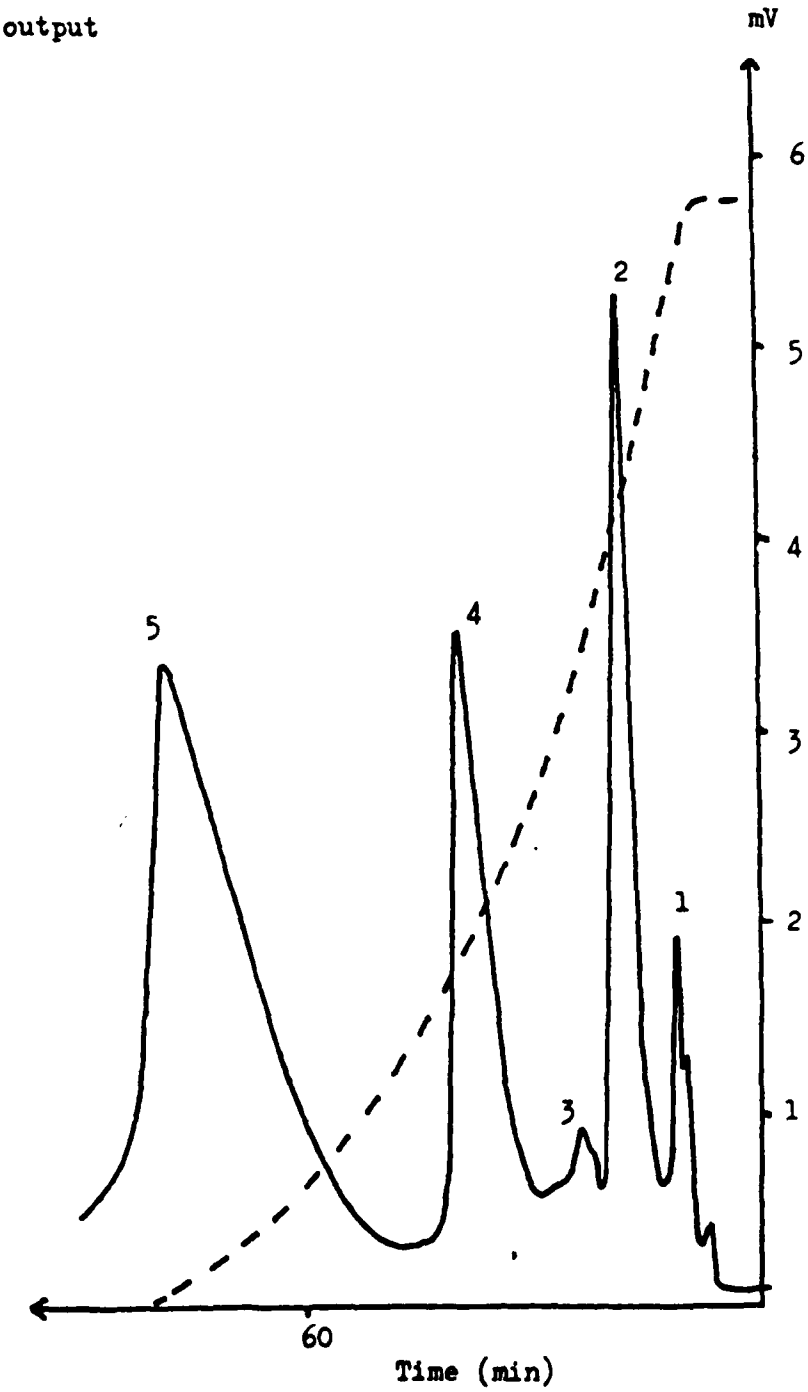

FIGURE 109 SATVA OF THE CONDENSABLE VOLATILE PRODUCTS OF THERMAL DEGRADATION OF F4 IN THE TEMPERATURE INTERVAL (450-485)°C

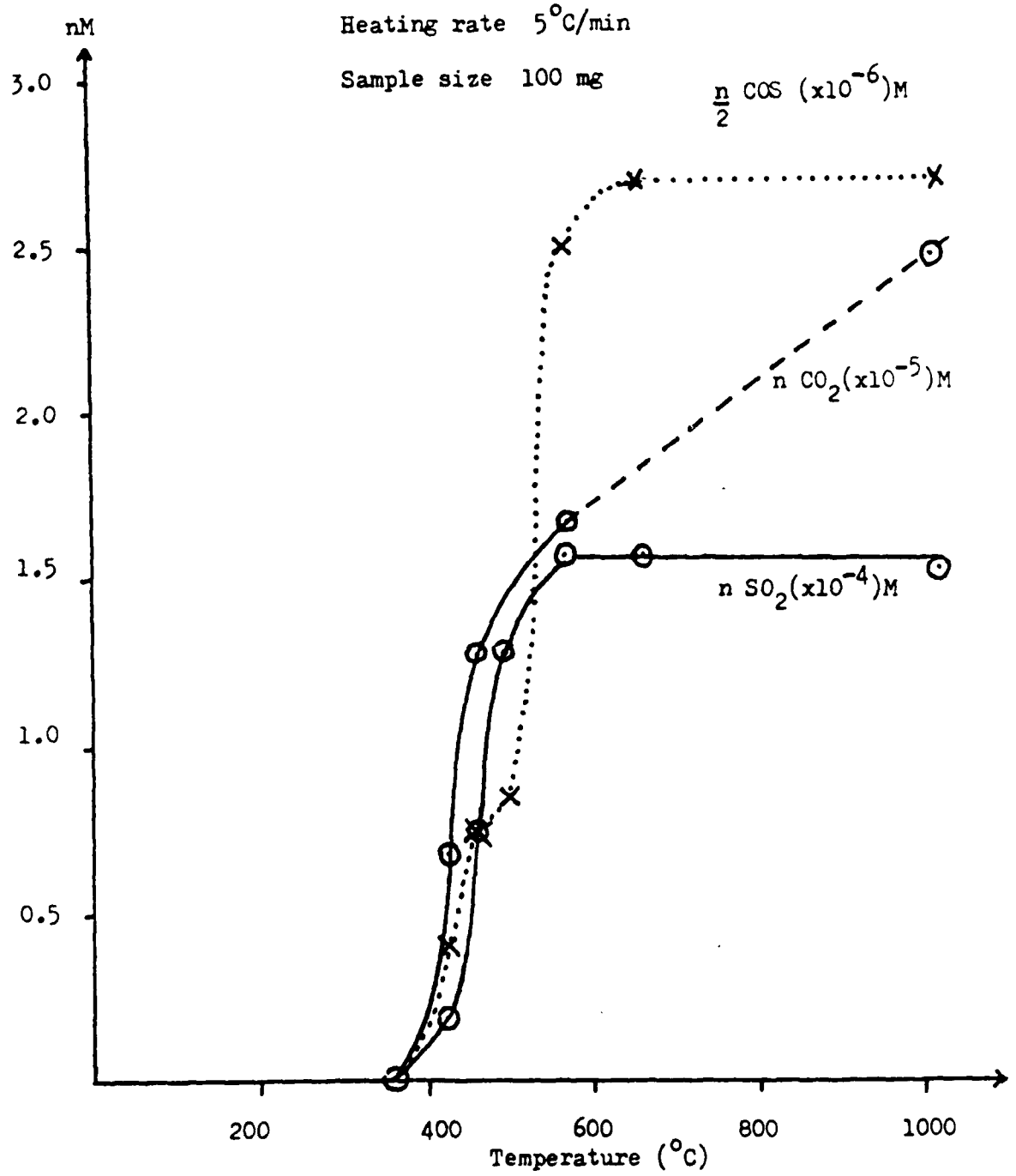

FIGURE 110 CONDENSABLE VOLATILE GAS EVOLUTION CURVES FOR UNCURED ATS-G

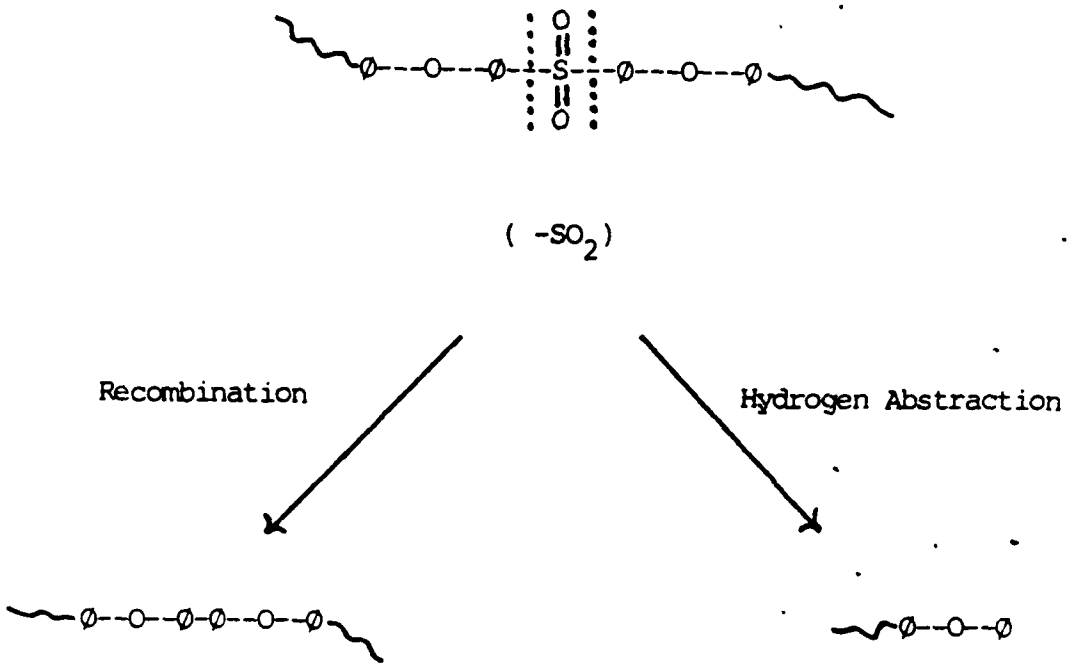

FIGURE 111 PRODUCTION OF SULFUR DIOXIDE IN PROCESS I of DEGRADATION

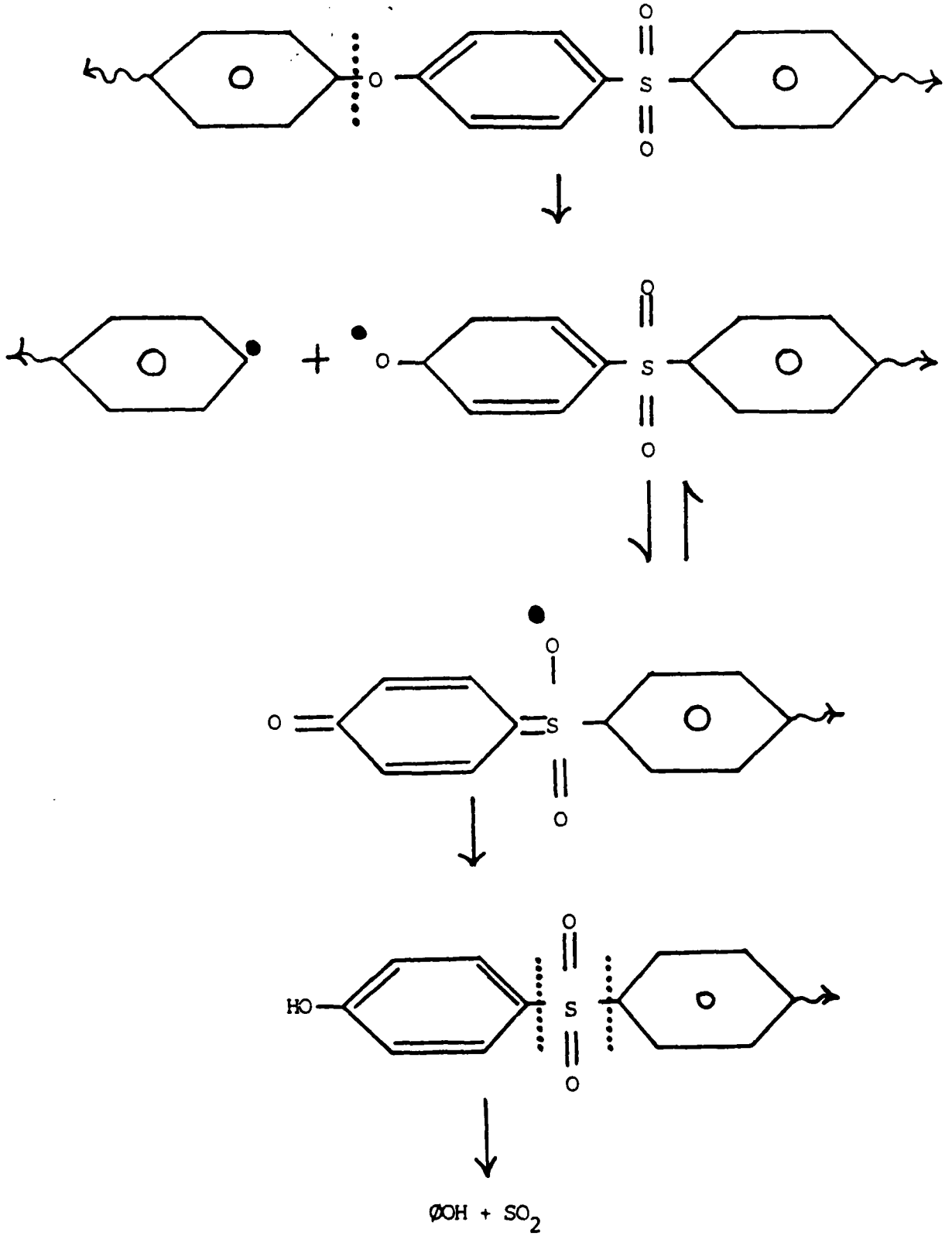

FIGURE 112 CONCERTED PRODUCTION OF SULFUR DIOXIDE AND PHENOL IN PROCESS I OF DEGRADATION

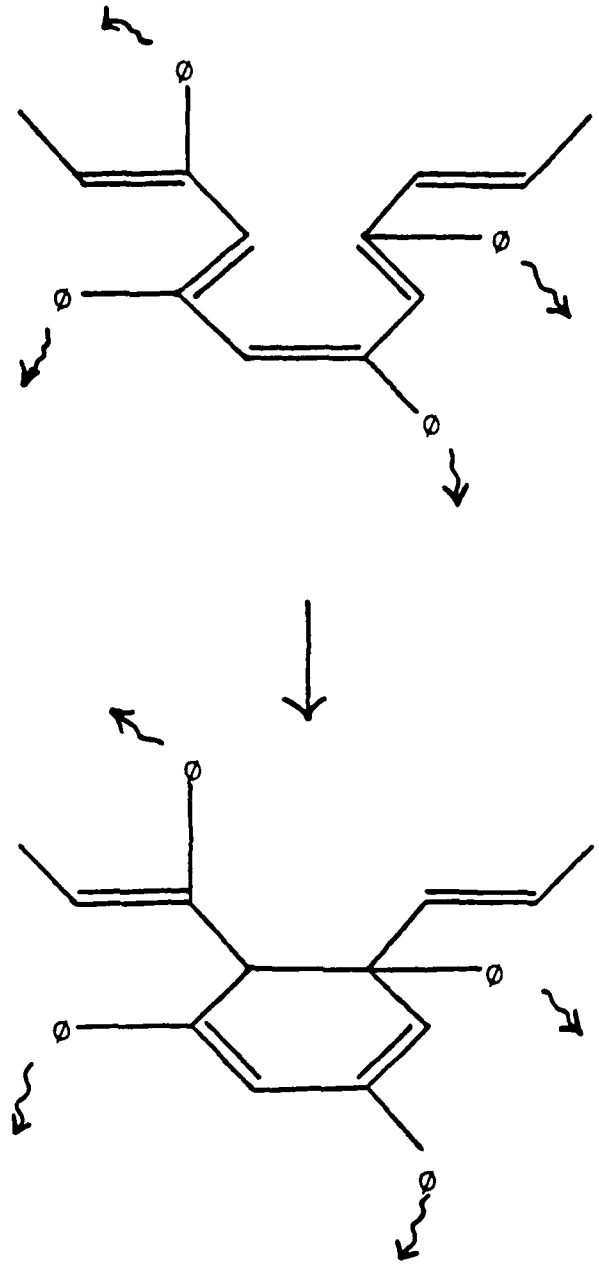

FIGURE 113 LOW TEMPERATURE THERMAL CYCLIZATIONS OF THE POLYENE CROSS-LINK

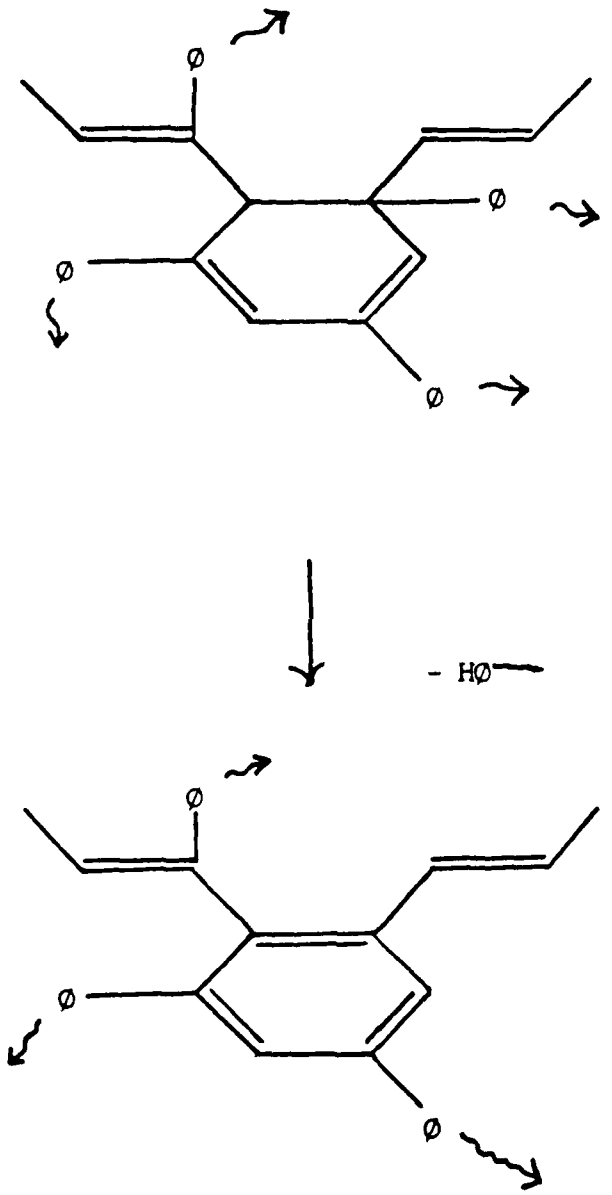

FIGURE 114 REMOVAL OF R-H FROM THE POLYENE CROSS-LINK ("REACTION I OF THE POLYENE CROSS-LINK)

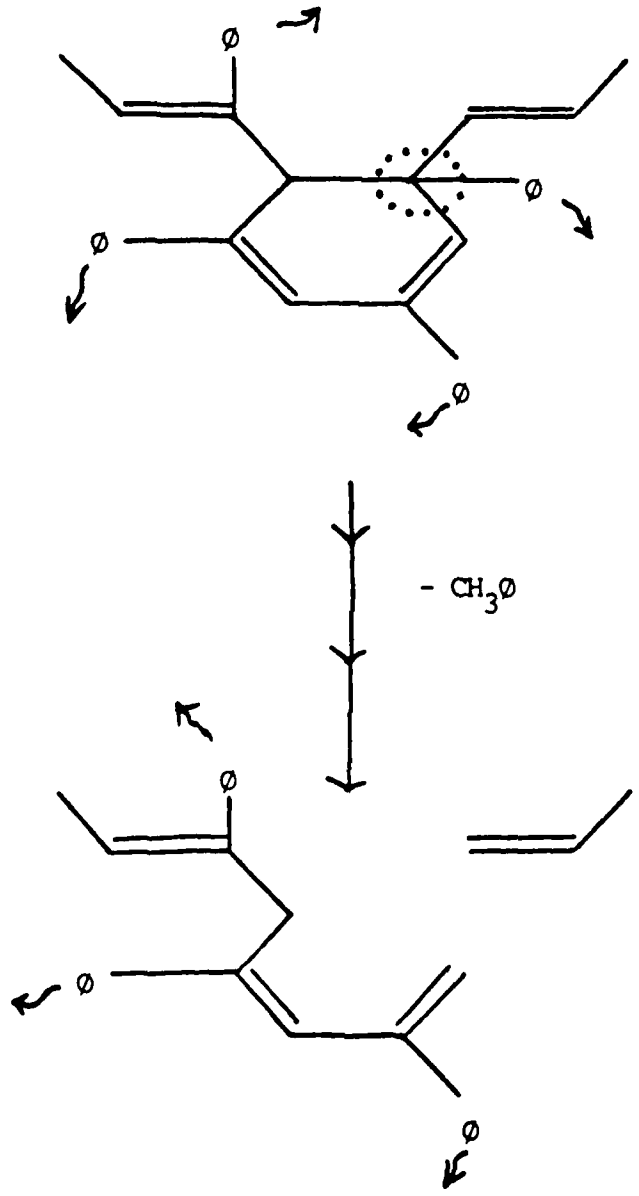

FIGURE 115 REMOVAL OF R-CH_3 FROM THE POLYENE CROSS-LINK ("REACTION II" OF THE POLYENE CROSS-LINK)

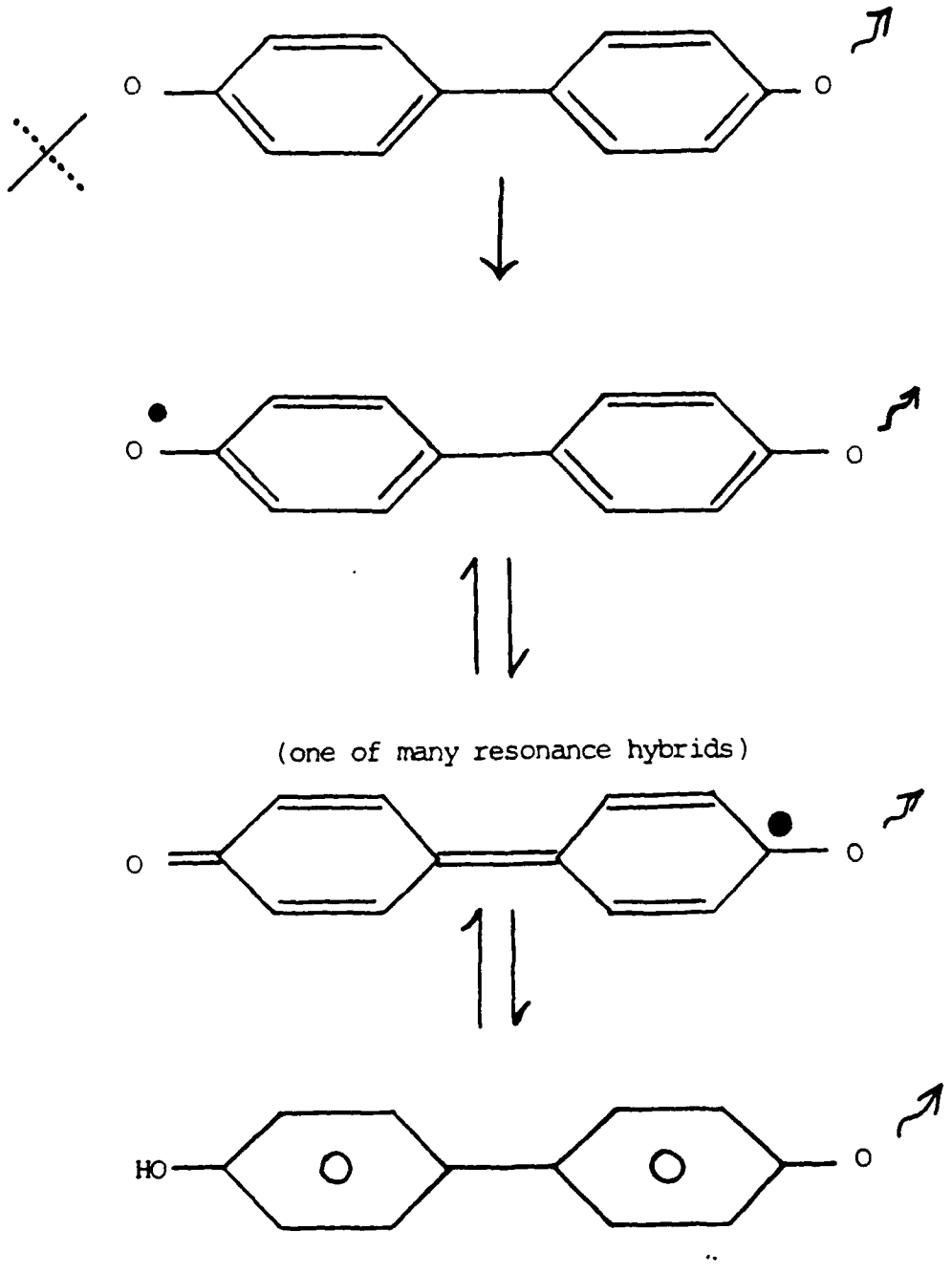

FIGURE 116 DIPHENYL PROMOTED PHENOXY BOND SCISSIONS IN ATS POLYMERS

(a). By Random Chain End Scissions

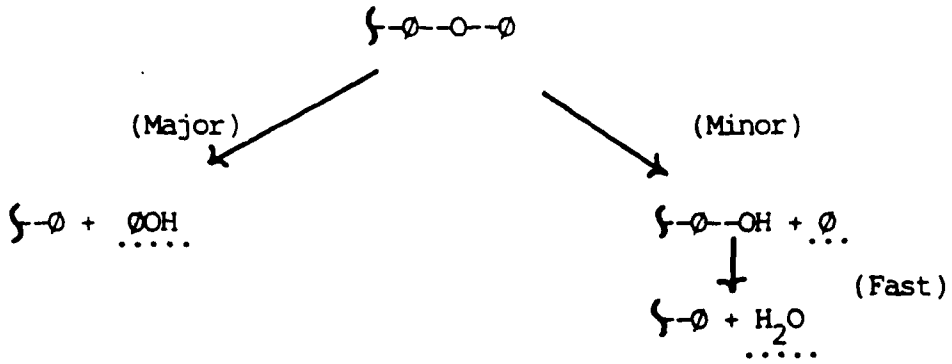

(b). Diphenyl Promoted Bond Scissions

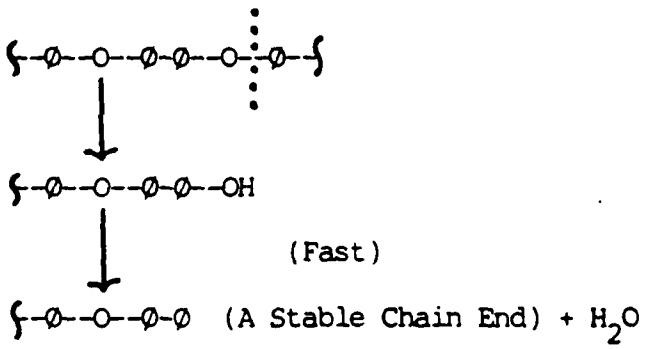

FIGURE 117 PRODUCTION OF BENZENE, WATER, AND PHENOL IN PROCESS 2 OF DEGRADATION

(a). Production

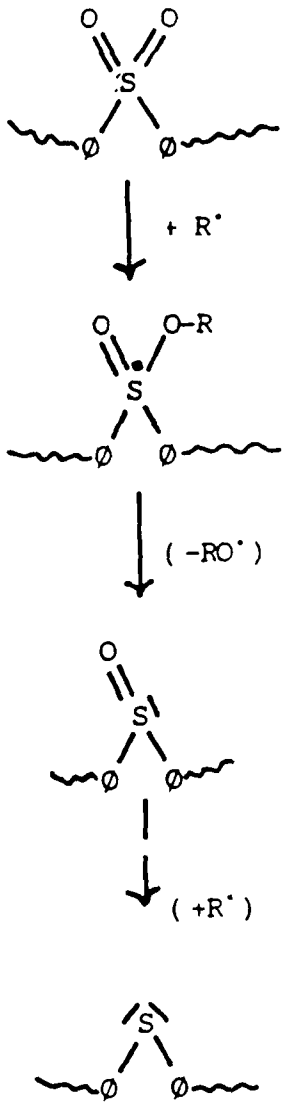

(b). Decomposition

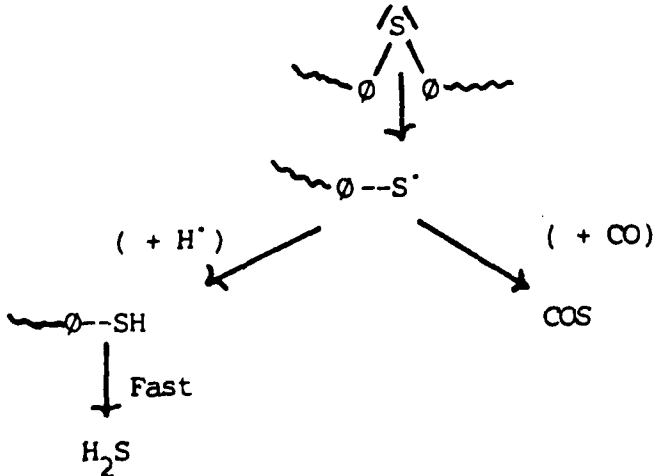

FIGURE 118 PRODUCTION AND DECOMPOSITION OF SULFIDE LINKAGES IN ATS POLYMERS

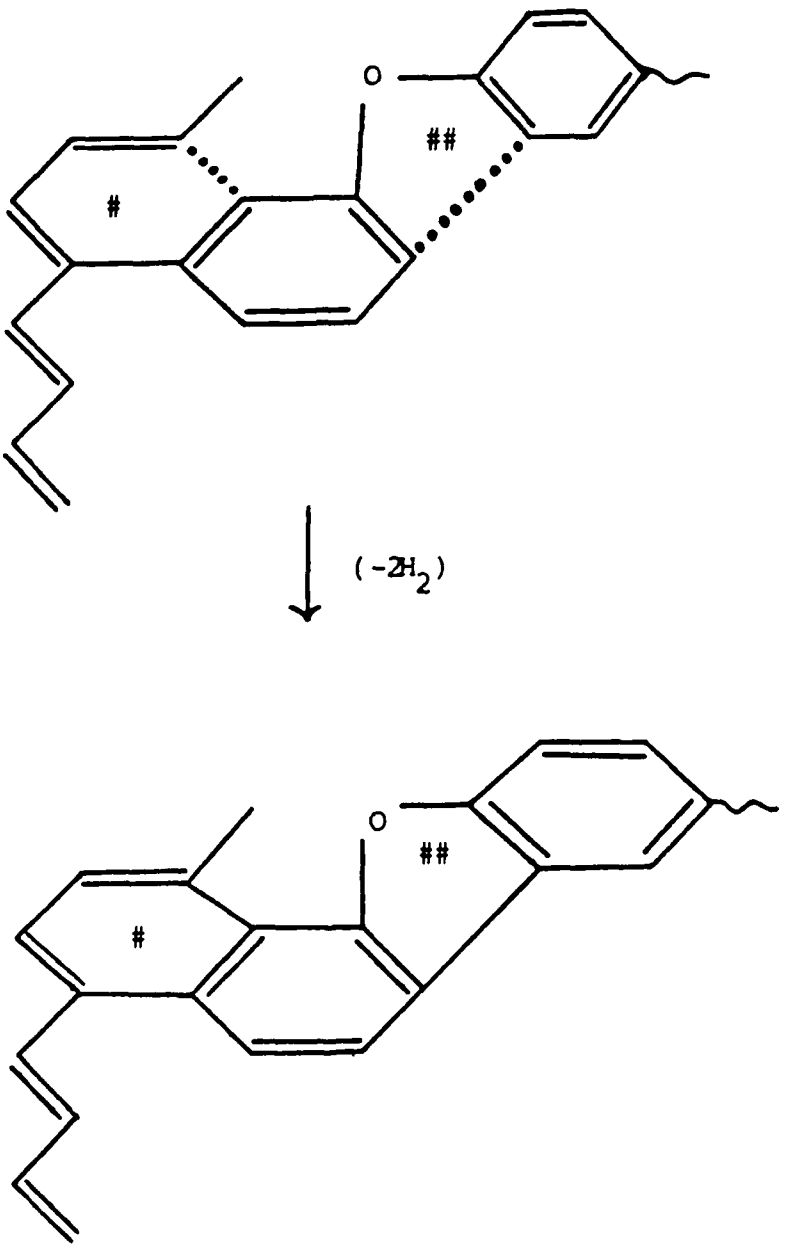

Key :

Step 1

Step 2

FIGURE 119 POLYENE PROMOTED RING FUSIONS IN ATS POLYMERS

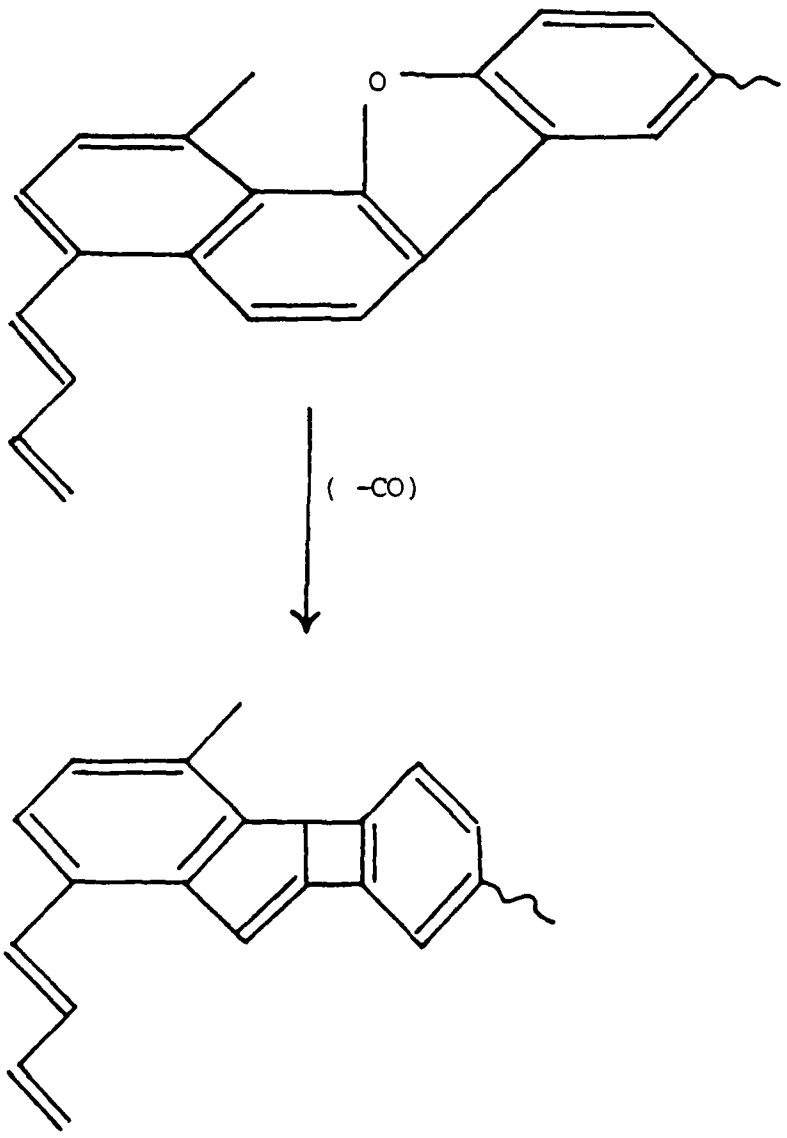

FIGURE 120 DECOMPOSITION AND REARRANGEMENT OF OXYGEN CONTAINING HETEROCYCLES FUSED TO THE POLYENE

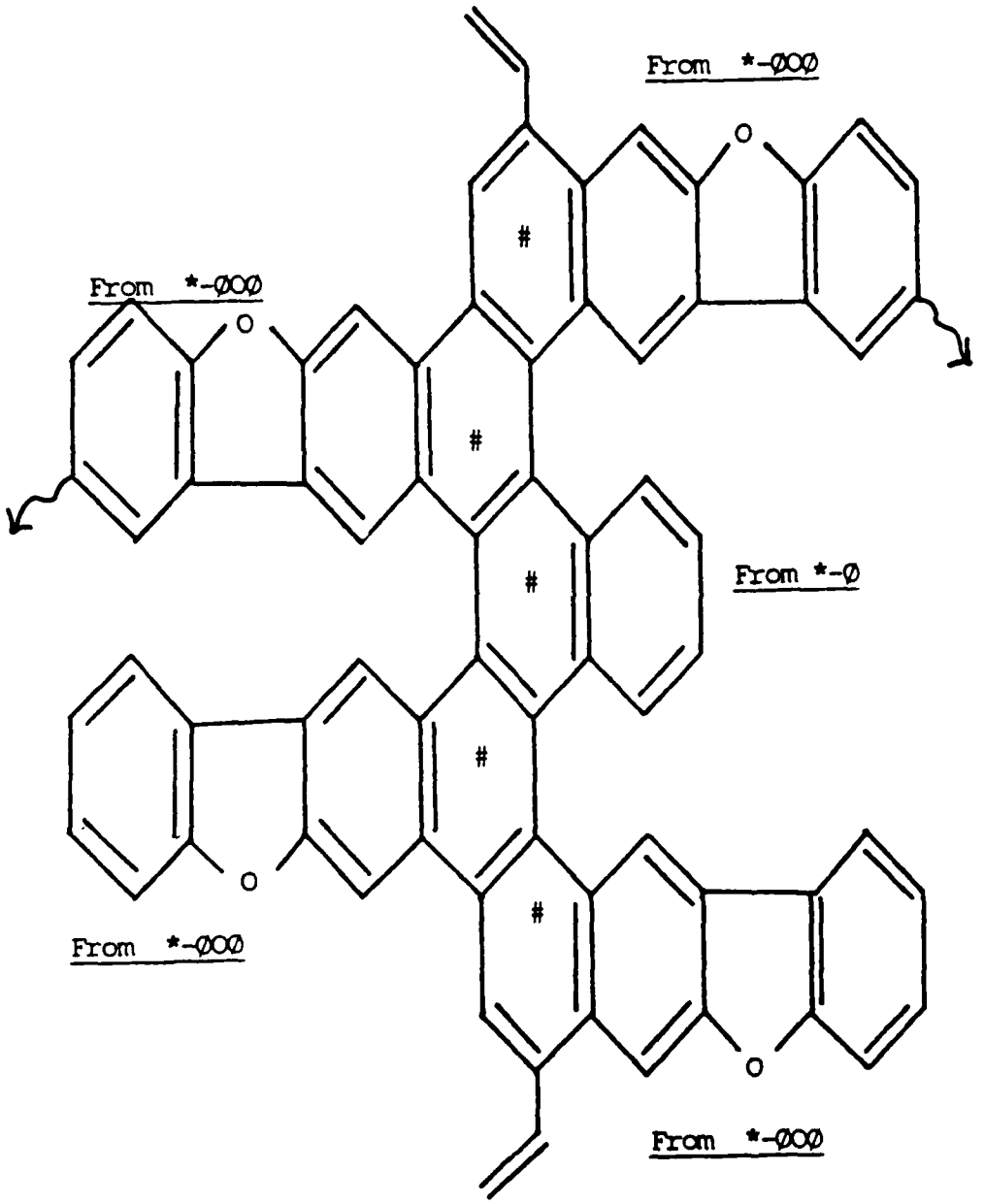

Key :

*- Original Polyene Chain

Derivative of Original Polyene Chain

FIGURE 121 SOME POSSIBLE PRODUCTS OF PROCESS 3 OF DEGRADATION

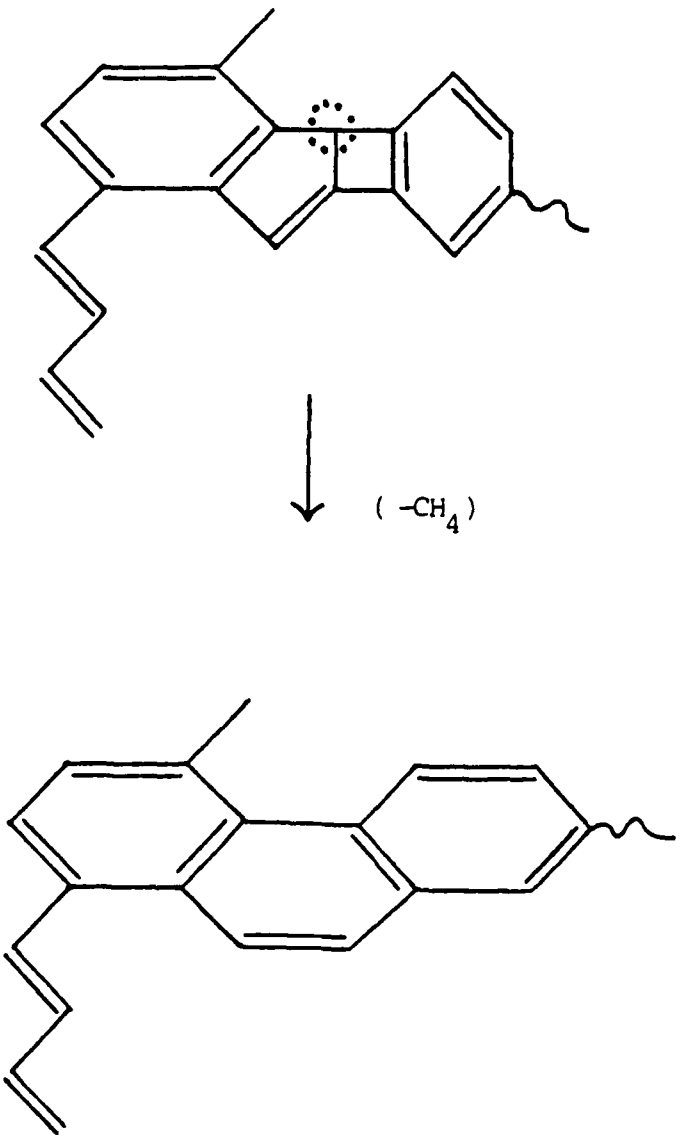

FIGURE 122 A PROMINENT REACTION OF PROCESS 4 OF DEGRADATION OF ATS POLYMERS

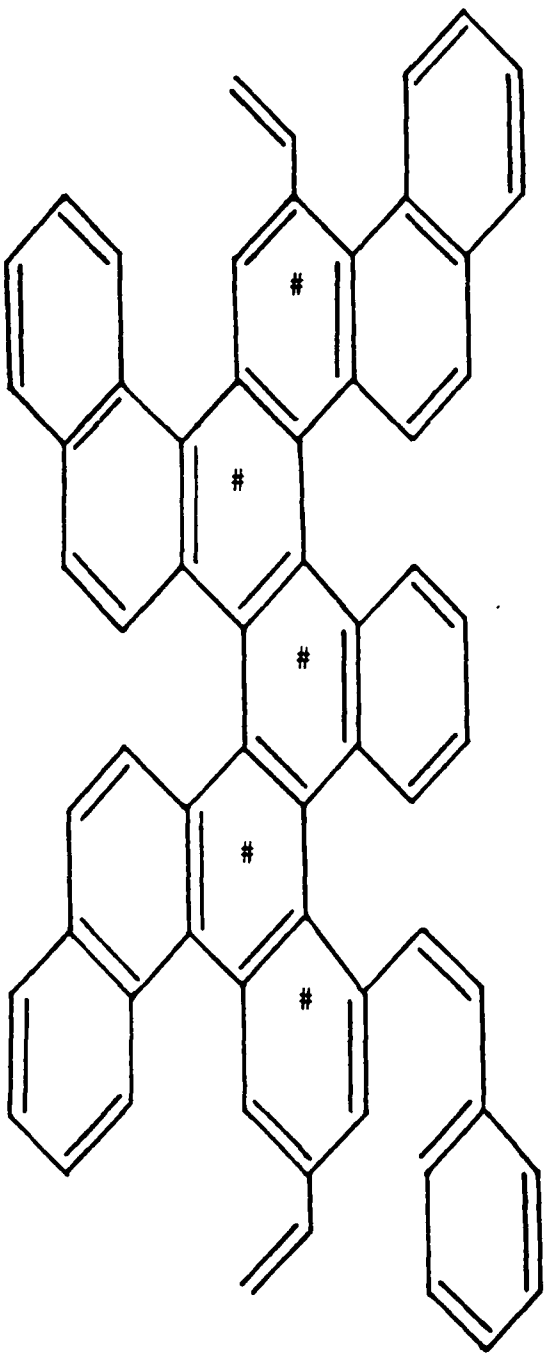

: Thermal Derivative of Polyene Chain

FIGURE 123 SOME POSSIBLE PRODUCTS OF PROCESS 4 OF DEGRADATION

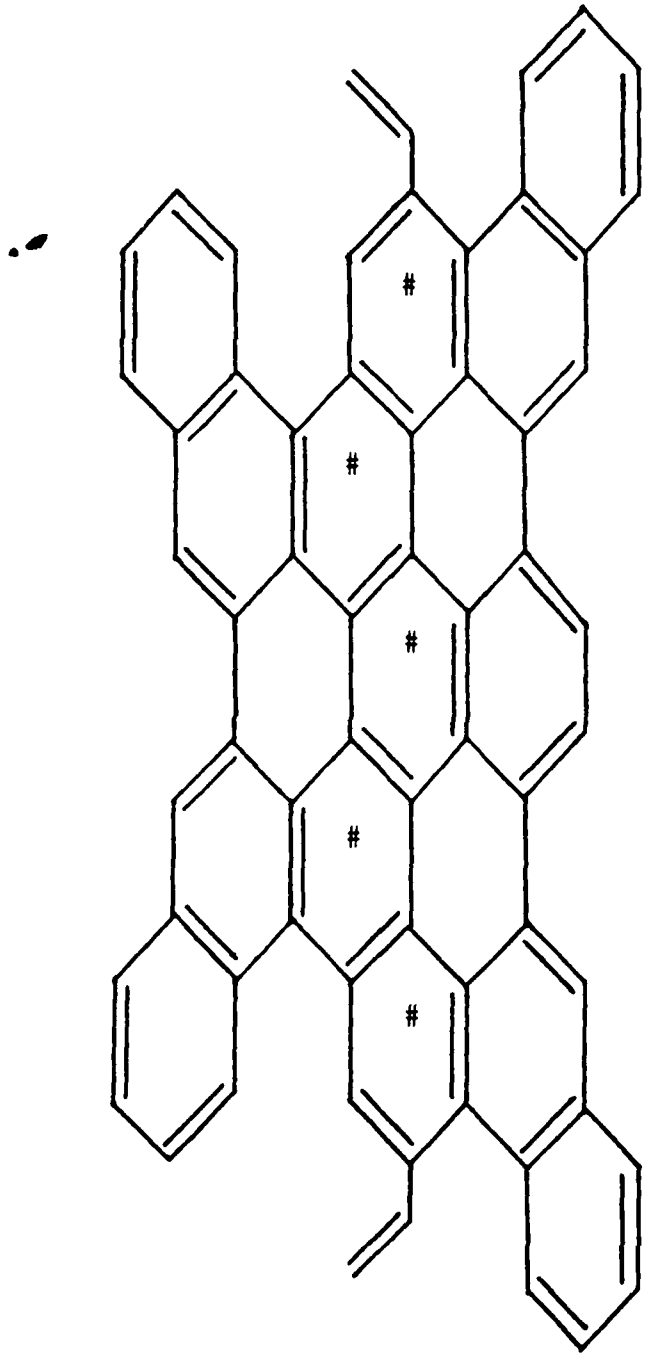

: Thermal Derivative of The Original Polyene Chain

FIGURE 124 POLYCONDENSATION OF THE PRODUCTS OF PROCESS 4 OF DEGRADATION TO FORM GRAPHITIC CLUSTERS

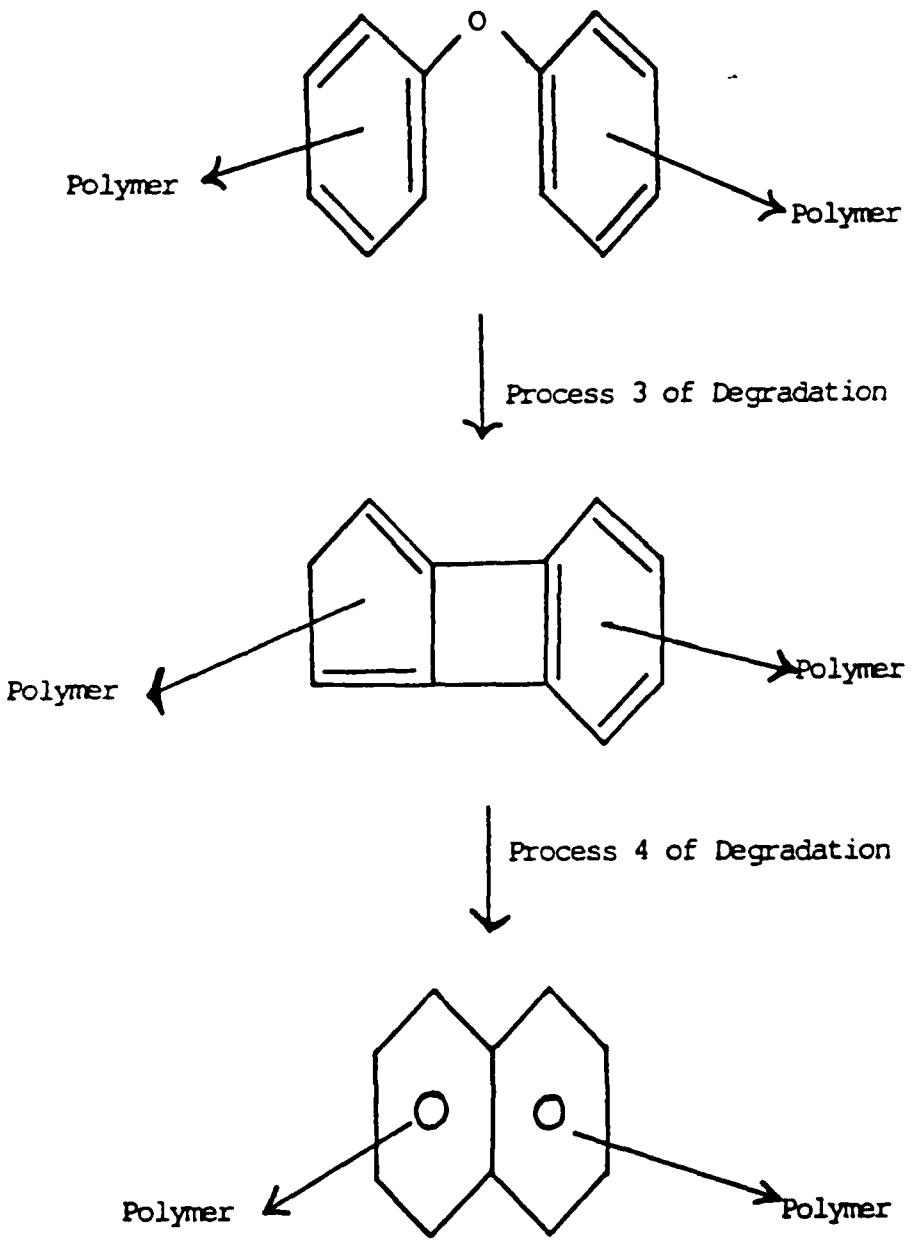

FIGURE 125 A POSSIBLE ROUTE TO THE FORMATION OF AROMATIC RING CONDENSATES IN RADEL THERMOPLASTIC

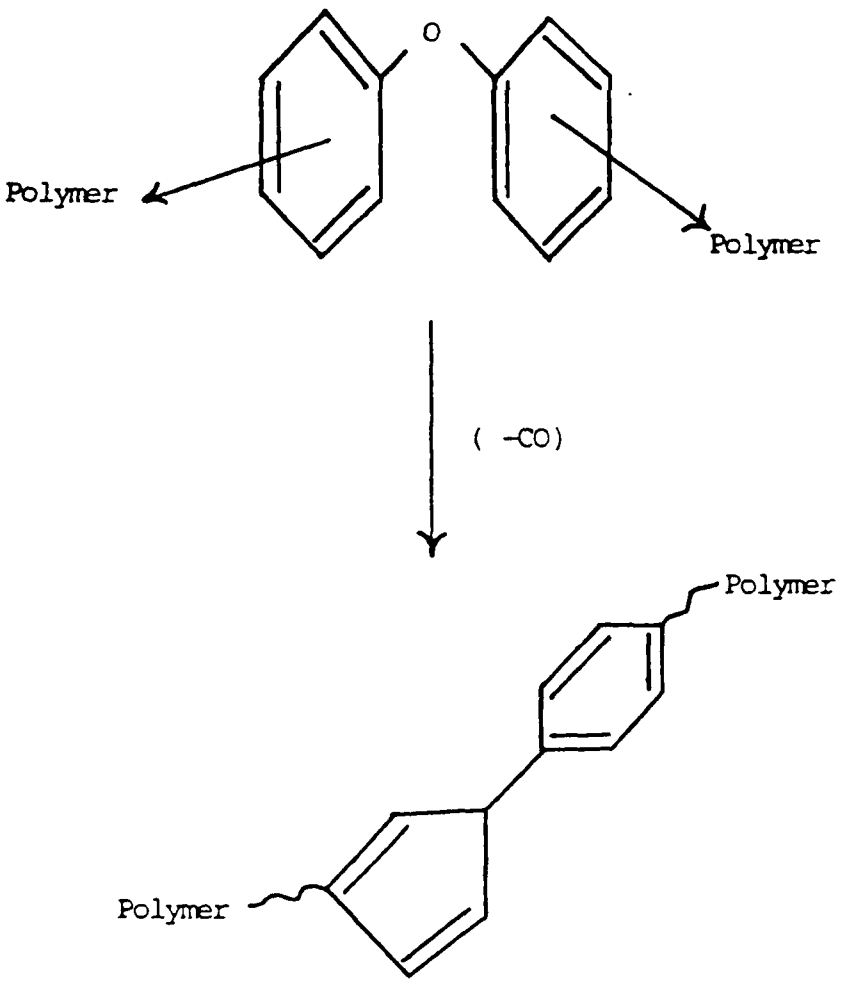

FIGURE 126 A POSSIBLE MECHANISM FOR THE PRODUCTION OF CARBON MONOXIDE IN RADEL THERMOPLASTIC AT ELEVATED TEMPERATURES

* U.S.Government Printing Office: 1990 748-056/24280